DESIGN AND CHARACTERIZATION OF ASPHALT MIXTURES BASED ON PARTICLE PACKING AND MECHANICAL MODELING

By

HUANAN YU

A dissertation submitted in partial fulfillment of
the requirements for the degree of

Doctor of Philosophy

WASHINGTON STATE UNIVERSITY
Department of Civil and Environmental Engineering

AUGUST 2012

To the Faculty of Washington State University:

The members of the Committee appointed to examine the dissertation of HUANAN YU find it satisfactory and recommend that it be accepted.

_____
Shihui Shen, Ph.D., Chair

_____
Haifang Wen, Ph.D.

_____
Balasingam Muhunthan, Ph.D.

_____
Pizhong Qiao, Ph.D.

ACKNOWLEDGMENT

I wish to express my sincere appreciation to those who have contributed to this thesis and supported me in one way or the other during this amazing journey. The experience with hardship, frustration, encouragement, trust, and then step by step towards accomplishment and applause has made it a great treasure in my life.

First and foremost, I would like to gratefully thank my advisor Dr. Shihui Shen for her guidance, understanding, patience, and most importantly, her friendship during my graduate studies at WSU. The thesis would not be possible without her work and passion. The joy and enthusiasm she has for research was contagious and motivational for me, and her advices from both theoretical and experimental aspects have turned out to be fruitful. She has been a tremendous mentor to me and it has been a great honor for me to be her first PhD student.

I would also like to thank Dr Haifang Wen for his service as a committee member. His lectures and insights to pavement materials have inspired me a lot during my study and research. They have become an essential part of this thesis.

In particular, I would like to thank Dr. Balasingam Muhunthan. A great thank to you for his instruction in classes and especially during the period of theoretical modeling

development. His instruction, comments, and suggestions on my research for the past several years have helped me develop my understanding of the mechanical behavior of pavement materials.

Dr. Pizhong Qiao deserves a very special thank for many aspects. Thanks to Dr. Qiao for introducing me to WSU and it is always a delight to interact with him during those years. Thank to him for sharing his knowledge with me. His attitude towards study and research would greatly benefit me for a long time.

In my daily work I have been blessed with a friendly and cheerful group of fellow friends and students. Xin Lu, thanks for our long-term friendship which have brought me a great pleasure. All following buddies, Xiaojun Li, Jingan Wang, Bhusal Sushanta, Thiyagarajah, Sutharsan, Weiguang Zhang, Shenghua Wu, Nathan Bower, Maria Burton, Joseph Westergreen, Mengqi Wu, Junyan Yi, etc. have inspired me in research and life through our interactions during the long hours in the lab. I will never forget friendship from you all!

I would like to acknowledge the academic and technical support from the faculty and staff of the Department of Civil Engineering of Washington State University. Joining WSU was not only a turning point of my life, but also a wonderful experience. I treasured all precious moments here and would really like to thank them. A special thank goes to Dr.

David Mclean, chair of the Department of Civil and Environmental Engineering.

Thanks for the funding support by the Transportation Northwest (TransNow) through the USDOT and the Washington State Department of Transportation (WSDOT). Special thank goes to Dr. Zhanping You at Michigan Tech University who shared the Michigan HMA mix design data for the verification of this study. Thanks Dr. Tutumluer at the University of Illinois at Urbana-Champaign for assisting on the aggregate image scanning and the University of Illinois Aggregate Image Analyzer (UIAIA) analysis.

Always, the deepest gratitude goes to my family members. My father Shufu Yu, mother Xiangying Qiu, father-in-law Zhijun Yang, mother-in-law Xueling Li, sisters Shulan Yu and Guanglan Yu. Your unwavering loves are always with me. My beloved wife Rong Yang and the upcoming baby, your smile and happiness made all my efforts deserved. Thanks, my cousins Anna Shi and Tony Chen**. I LOVE ALL OF YOU**.

DESIGN AND CHARACTERIZATION OF ASPHALT MIXTURES BASED ON PARTICLE PACKING AND MECHANICAL MODELING

ABSTRACT

By Huanan Yu, PhD
Washington State University
August 2012

Chair: Shihui Shen

Existing asphalt mixture design approaches are mainly empirical based "trial-and-error" methods. Based purely on volumetrics, such design methods have little consideration of the mechanical performance of the mixtures. With the trend of moving the pavement research into more mechanistic based methods and targeting the ultimate goal to good field performance, it is necessary to develop a sophisticated mix design and characterization methodology which can help the designer understand the expected engineering performance of the mix at the early stages, at the same time, to have a more efficient tool to evaluate the quality of the mixtures. This research develops a comprehensive aggregate gradation and asphalt mixture design method that estimates the mechanical properties of the mix at early stage. In this method, strong correlations between aggregate properties, volumetrics, and mechanical properties are identified,

making the VMA (Voids in Mineral Aggregate) an excellent media to link the properties of aggregates and asphalt binder to their engineering performance. The concept of the design procedure, especially the aggregate gradation design procedure, is largely based on an analysis of aggregate packing and interlocking. As a fast and convenient design method that emphasizes more on the mechanical performance of the mix, the new design method can be used to evaluate the quality of an existing gradation and mix design, and adjust the gradation of a new mix to satisfy both volumetrics and mechanical properties. In addition, the characteristics of asphalt mixture are studied using micromechanical based discrete element method (DEM) and macromechanical modeling. In DEM simulation, an image based ball clumping technique is used for simulating the angularity properties of aggregate particles. The DEM model is established and calibrated to describe the viscoelastic (dynamic modulus and phase angle) and viscoelastic plastic (strength) properties of asphalt mixtures with or without damage involved. As for macromechanical modeling, a constitutive model for characterizing the permanent deformation of asphalt mixture is explored by taking consideration of the directional distribution of aggregates (anisotropy), and the damage induced by plasticity.

TABLE OF CONTENTS

LIST OF TABLES

LIST OF FIGURES

Dedication

This dissertation is lovingly dedicated to my father Shufu Yu and mother Xiangying Qiu. Your constant love, support and encouragement has sustained me throughout my life.

CHAPTER 1 INTRODUCTION

Roadway infrastructure has grown immensely over the past decades in most parts of the world due to the fast growth of economy and human activities, and hence, the increased capacity and number of vehicles. In order to build a cost effective and high quality roadway infrastructure for a given traffic and environmental condition, it is crucial to have a stable and reasonable design methodology as well as a thorough understanding of the mechanical performance of the pavement structure under external loading. Over decades, pavement researchers and engineers have devoted significant efforts on exploring an efficient asphalt mixture design method to guide design. However, the current widely used asphalt mixture design approaches are still empirical based "trial-and-error" methods. Moreover, the mechanical performance of the mixtures is not warranted as the design is purely based on volumetrics. Therefore, with the trend of moving the pavement research into more mechanistic based methods and targeting the ultimate goal to good field performance, it is necessary to develop a sophisticated mix design and characterization methodology which can help the designer to understand the expected engineering performance of the mix at early stage, at the same time, to have a more fundamental and accurate tool to evaluate the quality of the asphalt mixtures.

Asphalt mixture is a complex composite consisting of aggregate, binder, and air

voids. The mechanical behavior of this composite is drastically different because of the wide variety of the material component in nature. This chapter starts with introducing the composition of asphalt concrete (AC) mixture. The skeleton effect of aggregate structure for AC as a particulate system is described, and the methods to study the characteristics of asphalt mixtures are stated, followed by a statement of the problems. Finally, research objectives are proposed based on the concerns and existing knowledge gap on mix design methods and mixture property characterization.

1.1 BACKGROUND

1.1.1 *Aggregates in AC*

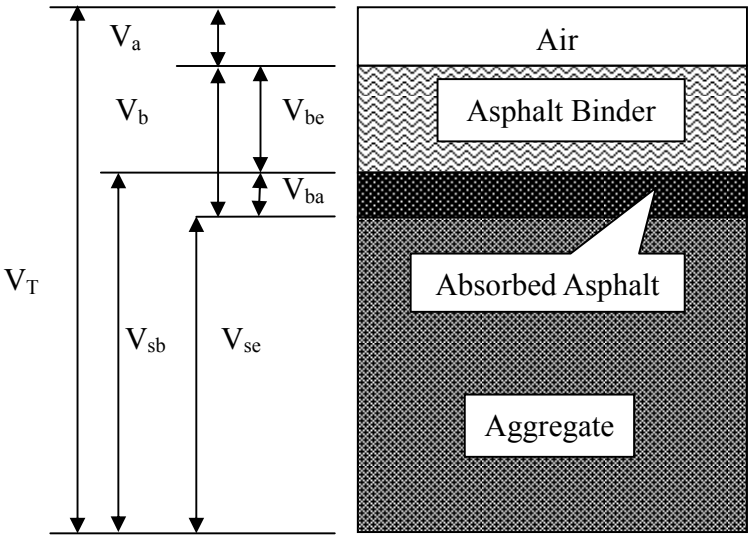

Figure 1-1. Three phase diagram for an AC mixture

Asphalt mixture is a composite material consisting of aggregates, asphalt binder and air voids, in which aggregates occupy the major volume of the mix (around 85% by volume and 95% by weight for a dense-graded AC). The three phase diagram for a

typical AC mixture is shown in Figure 1-1.

The aggregate skeleton determines the load carrying capability of the mix, whose effect becomes more prominent at higher temperatures when asphalt binder is softer. A comprehensive understanding of the mechanical behavior of aggregate particles in an aggregate-binder system is critical to the design of a high performance asphalt mixtures with good resistance to traffic loads and environmental changes.

In 1905, Richardson published his book "The Modern Asphalt Pavement" (Richardson 1905) and pointed out that the role of aggregate is significant in the asphalt mixture. Later, as the study of aggregate moved forward, the aggregate structure and characteristics, particularly aggregate gradation, shape (angularity), and coarse aggregate surface texture, have been considered as primary factors that influence the development of aggregate skeleton, and thus rut susceptibility of an AC mixture (Lottman and Goetz 1956; Button et al. 1990; Gaudette and Welke 1997; Authony and Bahis 2003). Dukatz (1989) specifically stated in his research that rut resistance is "highly dependent upon aggregate grading" and that mixes made with the best possible materials will fail without a proper gradation. Aggregate gradation and properties also have great impact on the strength, stability and fatigue performance of AC mixtures. Vallerga et al (1957) proposed that aggregate shape will have major impact on material strength depending on how different materials are compacted. Holubec and Appolonia (1973) conducted triaxial

tests and observed particle angularity to positively influence strength of granular materials. Monismith (1970) concluded that aggregate shape and surface texture characteristics had an influence on the fatigue and stiffness characteristics of asphalt mixtures. Shen and Carpenter (2007) developed a fatigue prediction model by relating gradation parameters with fatigue life of AC. Laboratory studies based on the Marshall Mixture design procedure suggested that the use of crushed gravel over natural gravel significantly improved the stability of the asphalt concrete. Further, it was also concluded that the use of crushed stone instead of gravel could increase the stability of the mix by as much as 45 percent (Benson 1970).

Researchers have realized that aggregate plays an important role in asphalt mixture. However, in current Superpave mix design system, the selection of gradation is only restricted by means of broad control points. Hudson and Davis (1962) pointed out that those gradation specification control points are determined based on experience. These gradation control points are not necessarily related to the performance of the mixture.

1.1.2 *Volumetric properties of AC*

A basic understanding of weight-volume relationships of AC is important from both a mixture design standpoint and from a field construction standpoint. In order to ensure the performance of AC, it is important to understand that mix design is a volumetric

process whose purpose is to determine the proportion of asphalt binder and aggregates required to produce a mixture with the desired properties (Roberts et al. 1996). The asphalt concrete (AC) mixture volumetric properties including asphalt content, voids in mineral aggregate (VMA), and voids filled with asphalt (VFA) have been identified as important parameters for the durability and performance of AC (Roberts, et al. 1996).

VMA is considered as one of the most important parameters of volumetric properties and is used in the Superpave mixture design specifications to eliminate the use of potentially poor-performing mixtures (Prowell et al. 2005). Its value will directly relate to the amount of asphalt binder required in the mix. Because the VMA is mainly a function of aggregate gradation and properties, large amounts of time and effort will have to be spent on the selection of appropriate aggregate gradation in order to reach the target VMA. Traditional aggregate gradation design methods are based on the maximum density line but with some deviations. This is to provide a mix with the highest density (or lowest VMA) for a strong aggregate structure, at the same time with adequate voids (VMA) for air and asphalt binder to ensure a durable mix. Consequently, a minimum VMA is typically required in the AC mix design methods such as Marshall (1994), and Superpave (2001). The VMA requirements used in the current Superpave system were initially developed by McLeod (1959) in the 1960s. As shown in Table 1-1, those VMA requirements are only function of the nominal maximum aggregate size (NMAS)

regardless of gradation of the aggregate. However, Coree and Hislop (2000) have pointed out other aggregate factors such as aggregate gradation, aggregate surface texture and shape also affect VMA. Of these aggregate factors, gradation can be easily obtained by sieving analysis, but surface texture and shape are not so easy to measure and quantify.

Table 1-1. VMA Requirements in Superpave design method (Superpave 2001)

Aggregate NMAS (mm)	Minimum VMA (%)
4.75	16.0
9.5	15.0
12.5	14.0
19	13.0
25	12.0
37.5	11.0

1.1.3 *AC design methods*

The design of asphalt mixtures is a process to determine the type and optimum combination of aggregate and binder. By carefully choosing the variables of aggregate, asphalt binder and the proportions of the two, a successful mix design should ultimately achieve the field performance in resistance to deformation, fatigue, low temperature

cracking, moisture damage and compactability, etc. (Freddy et al. 1996). Although aggregates and their packing characteristics play an important role in asphalt mixtures, current Superpave mix design system is volumetric guided in nature, that is, the design combines aggregate and asphalt binder together based on requirement of volumetric information, rather than performance. The selection of gradation blend is only restricted by means of broad control points. As pointed by Hudson and Davis (1962), the current gradation specification control points were determined based on experience, and were not necessarily related to the performance of the mixture. The Power Law Method introduced a concept on how to categorize coarse-graded and fine-graded aggregates and mathematically describe gradation curves. It provided insight into aggregate gradation effects on tensile strength, fracture energy and failure strain parameters derived from the SHRP indirect tension test. However, this approach is still an empirical based approach which relies heavily on data regression analysis and requires a "trial and error" process to establish good prediction. The Power Law Method has difficulty in analyzing the gradations with smaller maximum size, particularly if it is gap-graded. Research findings suggested that the Bailey Method seemed to be a useful and practical tool to help mix designers and quality control personnel better understand volumetrics and the compactability of HMA mixtures. It provided some good guidelines in terms of evaluating existing gradations and selecting new aggregate blends. However, researches

also suggested the difficulty in relating Bailey principles to performance (such as rutting) (Aurilio et al., 2005), and the recommended Bailey ratios were worth further investigation (Shamsi et al., 2006). Significant effort has been put forward by the NCHRP 9-33 project (Christensen et al. 2009) to improve the design procedure for HMA mixtures (including dense-graded, open graded and gap-graded mixes). This new design manual emphasized the significance of controlling an appropriate void in mineral aggregate (VMA) value to HMA performance. Target VMA and asphalt content were suggested being selected at the early stage of the mix design process to ensure mixture properties. Suggestion on gradation design was proposed to help achieve the VMA requirement. A narrower VMA control range was proposed which further increased the challenge of selecting appropriate aggregate gradation blend. A graphical approach, called continuous maximum density (CMD) plot, was developed to adjust aggregate gradation. Based on packing theory, the CMD method provided a simple and flexible method to adjust aggregate gradation. However, the application of this procedure required some experience with the mix design process and with a wide range of materials. In addition, different portions of aggregate gradation will have different sensitivities to the changes of VMA.

1.1.4 *Methods to study the characteristics of asphalt mixture*

Researchers have proposed different methodologies to study the mechanical behavior of asphalt mixtures. Normally, the mechanical behavior of the asphalt mixture has been studied using two main approaches, a macro-mechanical based approach and a micro-mechanical based approach. In a macro-mechanical approach, the model parameters are obtained through experimental measures and fit to a constitutive model. There are a wide range of constitutive relationships utilized for this purpose ranging from the simple elastic to the viscoelastic and viscoplastic modeling. Eisenmann and Hilmer (1987) proposed a model for rutting in asphalt mixture, however, this model assumed that rutting is caused by a reduction of air voids and with little consideration of the lateral movement of material. Sousa et al (1993) developed a nonlinear elastic-viscous model with damage parameters incorporated to predict rutting. Subsequently, Sousa and Weissman (1994) revised the elastic-viscous formulas by adding a plastic component. Lytton et al. (1993) developed a permanent deformation model for HMA using the associated plasticity model of Vermeer (1984). All those modeling provided a meaningful understanding of the visco properties of the asphalt mixture. However, the properties of asphalt mixture highly depend on the spatial distribution of the granular particles, which caused an anisotropic microstructure distribution of asphalt mixture. The macromechanical modeling may have some deficiency in characterize those anisotropic

microstructures.

The micro-mechanical modeling, on the other hand, is based on the asphalt mixture microstructure to model the properties and interactions of the AC constituents. The advantage of this approach is that it accounts for the material anisotropy and heterogeneity resulting from the aggregate shape and distribution within the asphalt mixture. Discrete element method (DEM), as a typical micromechanical based computational modeling method, is gaining more and more interest recently given its unique advantages in characterizing discrete particulate system like asphalt concrete and granular material. Zeghal (2004) presented the results of numerical simulations to characterize the resilient modulus of aggregate base/subbase materials. Chang et al. (1995) used the normal contact law to simulate the elastic moduli of granular material with anisotropic random packing structure. Huang et al. (2007) applied an image based micromechanical DEM approach to simulate the effect of particle size, shape, and angularity on the stability of railroad ballast. Matsushima and Saomoto (2002) simulated the angularity of aggregates using ball clumping technique. The irregular shape of the sand was represented by a set of overlapping circles in 2-D analysis. These procedures were validated using bi-axial simulations and the result indicated higher shear strength for angular particles than circular particles. Although promising, current DEM simulations are still limited to either 2D simulation or round balls in 3D. In addition,

current DEM simulations are not able to characterize dynamic modulus over a large range of time and frequencies and also are not able to characterize the phase angle of asphalt mixture.

In summary, both macromechanical modeling and micromechanical based DEM are found to be promising tools for evaluating the properties of a particulate media like asphalt mixture. However, these methods have not been fully developed and knowledge gap still exists in applying these methods for material characterization. More research is needed to develop appropriate theories and methodologies to understand the mechanical properties of asphalt mixtures and guide design.

1.2 Problem Statement

Based on the discussions above, the current aggregate gradation design and mix design require more studies especially on the evaluation of aggregate packing and the correlation between aggregate structure and performance. Therefore, it is necessary to develop a systematic gradation design and mix design approach that will not only help to achieve the volumetric criteria (i.e. VMA) at the early stage of the design, but also result in a mix with well expected engineering performance.

It is generally accepted that aggregate contact and interlocking are critical to the strength and stability of AC mixtures because they will affect the load bearing capacity

and load transferring capability of a mix (Vavrik et al. 2002). The improvement of the packing characteristics of particulate aggregate systems can greatly increase the degree of aggregate interlocking, improve AC fundamental engineering properties such as strength, modulus of elasticity, creep and shrinkage, and enhance the performance of paving materials. Further, it brings valuable savings due to a reduction in the volume of binder. However, current Superpave mix design system lacks specific guidance on the selection of aggregate gradation. It also does not provide a correlation between the selected aggregate gradation and the expected field performance.

In reality, it is very difficult to measure and quantify the degree of aggregate interlocking directly. Some researchers (Sobolev and Amirjanov 2004) have tried to describe the existence of aggregate contact and interlock using image and non-destructive techniques. Shashidhar et al. (2000) used 2-D photo-elastic methods and showed that the stress is transferred from particle to particle through the aggregate skeleton. He also showed that the stress patterns and aggregate structures are different for different aggregate gradations. Bernal et al. (1970) studied the aggregate-aggregate contact with paint and optical method. Bailey's Method (Vavrik et al. 2002) proposed to design the aggregate gradation with certain degree of aggregate interlocking by selecting an appropriate "chosen unit weight", which is suggested to be between 95% and 105% of loose unit weight. With all these efforts of trying to detect the contact and describe

qualitatively the aggregate interlocking, the existing methods are not able to provide a direct and quantitative identification of aggregate interlocking. Many approaches are confined in two dimensional assemblies or have problems in distinguishing between contacts and near-contacts. And the fundamental theories of packing for the aggregate particles are still not fully clear. Therefore, it is important to develop thorough understanding of the packing characteristics of the aggregate particles and their roles to achieve ultimate performance of the mixtures. Specifically, it is essential to investigate the effect of individual aggregate sizes to the stability of the entire aggregate structure, thereby to provide suggestions to the mix design of asphalt mixtures.

In other aspects, the mechanical properties of asphalt mixture captured the stress and strain responses of asphalt mixtures with respect to temperature and loading time. Appropriate determination of the mechanical properties at early stage of the design process will contribute to a more reasonable material design and pavement design. The mechanical properties can be obtained either by laboratory experiments, by empirical regression equations, or by numerical simulations. Experimental testing provides the most straightforward method which can measure the mechanical properties over a wide range of temperature and frequency. However, it is costly and time-consuming due to the material preparation process and requiring of skilled manpower. The availability of the equipment can also limit the wide usage of the mechanical properties for pavement

design and evaluation. Most importantly, it is difficult to determine the correlation between properties of specific component and the overall bulk properties of the mixtures based on pure experimental testing. The regression prediction equations such as the Witczak's semi-empirical model (Witczak et al. 2002; Bari and Witczak2006) and the Hirsch model (Christensen et al. 2003) have related some material properties to the dynamic modulus. However, it is not an easy task to understanding the fundamental nature of asphalt mixtures through regression method.

Researchers have proposed to use numerical models to characterize the mechanical properties of asphalt mixtures because it gives a convenient way to assess the fundamental mechanical properties of asphalt mixture. Numerical simulation based on fundamental material mechanics and theories, including macro constitutive modeling and the micromechanical based discrete element method (DEM), have been found to be promising to simulate the material properties. It can conveniently study the influence of individual material component on the performance of asphalt mixture, at the same time minimize the influence of experimental error.

1.3 Research Objectives

There are two central objectives for this study: (1)develop a performance based asphalt mixture design method to help the selection and proportion of aggregates,

producing mixtures with appropriate volumetric properties and good performance; and (2) characterize the mechanical properties of asphalt mixtures using both macromechanical modeling and micromechanical based DEM simulation.

i. In order to achieve the first central objective, an integrated approach consisting of packing analysis, DEM modeling and material performance model evaluation will be used so that the following specific goals can be met: Evaluate aggregate gradation and packing characteristics of AC mixture, and develop linkage between the aggregate gradation and the volumetric properties of the AC mixture. Identify an approach to describe and classify gradations, and gradations classified as the same group will share many similar properties such as packing characteristics and particle contact behavior, a new definition will proposed for characterizing traditional aggregate gradations into three types: coarse-graded, medium-graded, and fine-graded. The particle packing theory and DEM will help to provide linkage between material components with volumetrics of asphalt mixture.

ii. Conduct experimental testing to evaluate the effect of aggregate properties (size distributions and shape properties) and volumetrics of asphalt mixture on the mechanical performance including compactability, rutting resistance, and dynamic modulus.

iii. Evaluate the dynamic modulus and flow number properties of asphalt mixtures, and compare the traditional Witczak E* model, the new Witczak E* model, and the Hirsch model for the tested samples, and prepare locally calibrated prediction model for the dynamic modulus and flow number prediction. Based on the experimental findings and the dynamic modulus prediction models, the effect of aggregate gradation, with respect to individual sieve size and the whole gradation, is evaluated, which will provide insight to the asphalt mixture and gradation design to achieve high performance mixtures.

iv. Propose a new asphalt mixture design and mix design method based on the relation between aggregate gradation, volumetric properties, and engineering performance. The developed method should help to achieve the volumetric criteria, and ensure high aggregate interlocking and adequate resistance to permanent deformation and other pavement premature distresses.

To achieve the second central objective, the following specific goals will be met:

i. Explore the feasibility of using DEM simulation to characterize asphalt mixture properties, and extend the DEM simulation from 2-D analysis to 3-D analysis. Develop a methodology to study the effect of aggregate angularity and shape effect on packing, dynamic modulus and strength of asphalt mixture. Different

contact laws will be studied to characterize the complex modulus over a large range of temperatures and frequencies of asphalt mixture.

ii. The construction of a successful constitutive model for characterizing the mechanical properties of asphalt mixtures must account for the microstructural features of the mixes such as the directional distribution of aggregates (anisotropy), and the damage induced by plasticity. Hence, it is necessary to develop a nonlinear viscoelastic macromechanical model which is able to taking consideration of initial damage, cumulative damage and anisotropic properties of asphalt mixtures.

There are different types of asphalt mixtures such as dense-graded, gap-graded, and open-graded. This research will focus on the conventional dense graded asphalt mixtures. The developed methodologies and the concept presented in this study can be extended to other type of gradations (gap graded and open graded) and mixtures (warm mix asphalt, asphalt mixtures with recycled asphalt pavement, etc.) to realize a more rationalized mix design and material characterization.

1.4 Thesis Organization

This dissertation has 11 chapters and is organized as follows. Chapter 1 describes the

introduction, problem statement, and the research objectives of this study. Chapter 2 highlights the most relevant literature related to this research work. The research methodologies and scope are described in Chapter 3. Chapter 4 presents the overview of Discrete Element Method and DEM simulation techniques. Chapter 5 conducts an analysis of aggregate packing to derive theoretical correlations between aggregate gradation properties and volumetric properties. Chapter 6 presents the experimental results about the effect of aggregate properties and volumetrics on the performance of asphalt mixture.Chapter7 highlights the evaluation and development of asphalt mixture performance prediction models. Chapter 8 provides a detailed performance based asphalt mixture design guideline and a design example is provided in Appendix C. Moreover, details about DEM simulation models and sensitivity analysis are provided in Chapter 9. Then, Chapter 10 emphasizes on the development of the macromechanical model with microstructural features. The conclusions of the study and recommendations for future research work are given in Chapter 11. And finally, this dissertation is ended with Appendix and references.

CHAPTER 2 LITERATURE REVIEW

This chapter presents a comprehensive literature review on the development of aggregate gradation design method, the effect of aggregate properties on AC performance, a historical background of minimal VMA requirement, and the significance of asphalt film thickness to AC performance. In addition, the fundamentals and existing applications of the packing theory will be provided. A comprehensive review on the methodology and application of Discrete Element Modeling method will be given in Chapter 4 and the background of mechanical modeling will be provided in Chapter 10.

2.1 AGGREGATE GRADATION DESIGN METHOD

The development of aggregate gradation design methods has experienced mainly three steps: (1) method of Maximum Density Line; (2) modified Maximum Density Line with some deviations for volumetric considerations; and (3) recent improvements considering aggregate packing and mixture performance.

2.1.1 *Traditional design method – Maximum Density Line (MDL)*

In the gradation design, the modification of gradations to achieve the densest packing with desired volumetric properties are dominated in the earlier design method.

The maximum density line design method was widely used before 1940's.

Green developed a method on how to obtain the densest gradation for large stone mixtures based on maximum density line (Roberts et al. 1996). Fuller and Thompson (1907) developed ideal gradation for concrete based on experiments, and they found that these ideal gradation curves could be approximated with a parabola, where $n = 0.5$, as given below:

$$p = 100\left(\frac{d}{D}\right)^{n} \tag{2.1}$$

Andreasen and Anderson (1929) found that the voids content is reduced as the exponent *n* is reduced. In practice, engineers follow the criteria that the ideal gradation for maximum packing of aggregate solids occurred when the slope of the log-log gradation chart was 0.45. This agrees with the later work by Goode and Lufsey (1962) in their establishment of the "0.45 chart."

$$p = 100\left(\frac{d}{D}\right)^{0.45} \tag{2.2}$$

Although popularly used, this traditional gradation design method has the following disadvantages:

1. The maximum density of asphalt mixtures generally will result in low asphalt contents,

2. Some Job Mix Formulas (JMF) were established in close conformance to n=0.45 resulting in poor pavement performance,
3. Problem occurs when the aggregate blend contains aggregates with large difference in density. Unless volumetric corrections are applied, it can result in excessive amounts of the lower density aggregate being incorporated into the asphalt concrete mixture
4. The designed aggregate gradation has little correlation with mixture performance.

2.1.2 *Modified MDL method with some deviations for volumetric considerations*

Realizing the mixes produced following the MDL method could experience stability problem due to the low voids and asphalt contents, the Marshall mix design method modified its design procedure and established minimum VMA requirements which resulted in gradations slightly deviate from the MDL. This method was later improved and adopted by the Asphalt Institute and Superpave.

In 1956, McLeod (1956) proposed that the basic design criteria for asphalt paving mixtures should be based on volume instead of on weight. McLeod also illustrated the volumetric relationship between the total asphalt binder, VMA, and the total aggregate. In 1959, McLeod in his another paper (McLeod 1959) suggested using bulk specific gravity of the aggregate to calculate the VMA and the air voids. Relationships between

the minimum VMA and the nominal maximum particle size (NMPS) of the aggregate were developed, which was adopted by the Asphalt Institute (MS-2 1984). Though suggested the relationship between minimum VMA and NMPS, the background data to support the minimum VMA were not given in this paper.

During a long period, many designers and researchers did not realize that these minimum VMA requirements were based on 5% air void content rather than 4% which was usually used in mix design (Kandhal et al. 1998). The minimum VMA requirements for 4% air void content is 1% lower than the recommended value in earlier editions of Asphalt Institute MS-2 (1993). The later 1993 version of Asphalt Institute MS-2 gives minimum VMA requirements corresponding to 3, 4, and 5% air void contents.

These revised minimum VMA requirements have also been incorporated in the Superpave mix design (McGennis et al. 1995; Kennedy et al. 1994) procedures. The Superpave is an abbreviation of **Su**perior **PER**forming Asphalt **PAVE**ments and which is designed to give engineers the tools necessary to design mixtures for different climate and loading conditions. The basic principal for the selection of aggregate gradation is to achieve desired mixture volumetric information. The goal for the aggregate gradation to achieve is a loose control band based on the NMPS of the mixture. The procedure for determining the optimum aggregate blend is a trial and error procedure. It is desirable for the Superpave mix design method to evaluate 2 to 3 aggregate gradations prior to

performing a mix design. If the volumetric properties of those blends do not meet the criteria, more blends should be evaluated. There is no guidance for the selection of gradation, those trial and error procedures is time-consuming and costly.

2.1.3 *New advancements in gradation design*

2.1.3.1 *Power Law Method*

Ruth (2000) in his study developed a Power Law Method for aggregate gradation design. This method determines the slope and intercept of the coarse and fine aggregate gradation curves using power law regression analysis. The equations of the power law regression are given as below.

$$P_{CA} = a_{CA} d^{n_{CA}} \qquad P_{FA} = a_{FA} d^{n_{FA}} \tag{2.3}$$

It is suggested that improved, continuous, and "well-balanced" gradation of the coarse aggregate in combination with an increased volume of coarse aggregate will lead to improved mixtures. The Power Law Method introduced a concept on how to categorize coarse-graded and fine-graded aggregates. It provided insight into aggregate gradation effects on tensile strength (σ_{IDT}), fracture energy (FE) and failure strain ($\mu\varepsilon$) parameters derived from the SHRP indirect tension test, and linked the aggregate gradation design to mixture performance to prevent premature failure of asphalt pavements.

However, this approach is still an empirical based approach which relies heavily on data regression analysis and requires a "trial and error" process to establish good prediction. The Power Law Method has difficulty in analyzing the gradations with smaller maximum size, particularly if it is gap-graded.

2.1.3.2 *Bailey's Method*

The Bailey's Method was originally developed by Mr. Robert Bailey of the Illinois Department of Transportation (DOT) and was later refined by Vavrik and Pine (Vavrik et al. 2002). This method is a tool for developing and analyzing blend gradations in the lab and field based on practical experiences and some consideration of aggregate packing. It provides the concept in helping to choose appropriate gradation with good aggregate interlocking (if desired) and good aggregate packing, giving resistance to permanent deformation, while maintaining volumetric properties that provide resistance to environmental distress. The method includes guidelines for evaluating aggregates and the aggregate blend by volume, as well as by weight, and makes provision for the use of Reclaimed Asphalt Pavement (RAP). Below are some key improvements in the Bailey's Method.

Definition of coarse and fine aggregate

The Bailey's Method re-defined the coarse aggregates and fine aggregates based on the theory of packing. Instead of using a fixed sieve of 4.75mm (No.4) to separate coarse and fine aggregates as used in the conventional method, this method defines coarse aggregate as the large aggregate particles that when placed in a unit volume, create voids; while fine aggregates are aggregate particles that can fill the voids created by the coarse aggregates. The sieve that separates the coarse and fine aggregates is called the primary control sieve (PCS), which is dependent on the nominal maximum aggregate size (NMAS) of the aggregate blend. Mathematically a diameter ratio of 0.22 between the PCS and the NMAS is selected by Vavrik et al. (2002) based on a comprehensive review of two and three dimensional analysis of the packing of different shaped particles done by various researchers. Furthermore, the aggregate blend below the PCS is divided into coarse and fine portions, and each portion is evaluated.

Evaluation of aggregate interlock by volume

The Bailey's Method evaluates the degree of aggregate interlock based on volume. Loose unit weight (LUW) is the amount of aggregate that fills a unit volume without any compactive effort applied, which represents the lower limit of the coarse aggregate interlock. Rodded unit weight (RUW) is the amount of aggregate that fills a unit volume with compactive effort applied, which usually represents the upper limit of the coarse

aggregate interlock. The LUW and RUW can be determined by following the procedure outlined in the AASHTO T-19 Unit Weight and Voids in Aggregate.

The Bailey's Method suggests the designer selecting appropriate Chosen Unit Weight (CUW) to achieve certain degree of coarse aggregate interlock. For fine-graded mixtures (with less coarse aggregates to form a skeleton and loads are carried mostly by fine aggregates), the CUW should be less than 90% of the LUW. For coarse-graded mixtures (coarse aggregates form the skeleton), a CUW between 95% and 105% of the LUW can be used.

Analysis of the design blend

The Bailey's Method defined several parameters to evaluate a design blend.

CA Ratio

CA Ration is used to evaluate packing of the coarse portion of the aggregate gradation and to analyze the resulting void structure.

$$\text{CA Ratio} = \frac{(\%\text{Passing Half Sieve} - \%\text{Passing PCS})}{(100\% - \%\text{Passing Half Sieve})} \tag{2.4}$$

FA_c Ratio

FA_c Ratio describe the ratio of coarse portion in the fine aggregate

$$FA_c = \frac{\%\text{Passing SCS}}{\%\text{Passing PCS}} \quad (2.5)$$

FA_f Ratio

FA_f Ratio describe the fine portion of the fine aggregate fills the voids created by the coarse portion in the fine aggregate.

$$FA_f = \frac{\%\text{Passing TCS}}{\%\text{Passing SCS}} \quad (2.6)$$

In order to ensure the mixtures have a good performance, the Bailey's Method suggested target ranges of the CA ratio, FAc ratio, and FAf ratio.

Summary of Bailey's Method

The Bailey's Method provides a systematic approach to aggregate blending that is applicable to all dense-graded asphalt mixtures, regardless of the maximum aggregate size in the mixture. The parameters in the method are related directly to voids in the mineral aggregate (VMA), air voids, and compaction properties. It provides a means to design the degree of coarse aggregate interlock as well as evaluate the aggregate blends. Although mainly based on experience, the Bailey's Method has been validated with laboratory analysis and field trials. It has been considered as a promising aggregate gradation design method and has gained more and more popularity in the pavement industry.

However, because this method is mainly based on experience, it needs detailed calibration for local materials and conditions. For example, the selection of chosen unit weight may be different depending on different aggregate types and shape properties. The Bailey's Method also appears to be sensitive to certain proportion values. A change from 89 to 91 percentages passing can shift the classification of the aggregate blend to the next smaller size even though the finer material may conform to the same gradation. Most importantly, the Bailey's Method provides no direct link between aggregate structures and AC mixture performance. Although certain degree of aggregate interlock may lead to stronger aggregate structure and good rutting performance, current study has not successfully used the gradation parameters to correlate with mixture's mechanical properties such as dynamic modulus, moisture susceptibility, and rutting potential. All of these indicated that it is worthwhile to conduct further researches to improve the Bailey's Method for a wider application.

2.1.3.3 *The NCHRP 9-33 design manual*

Significant effort has been put forward in the NCHRP 9-33 project (Advanced Asphalt Technologies, LLC. 2011) to improve the design procedure for asphalt concrete asphalt (including dense-graded, open graded and gap-graded mixes). The NCHRP 9-33 design manual clearly indicated the significance of controlling an appropriate VMA value to AC mix performance. Suggestion on gradation design is proposed to help

achieve the VMA requirement. A narrower VMA control range is proposed which further increased the challenge of mix design, especially aggregate gradation design. A graphical approach, called continuous maximum density (CMD) plot, was developed to adjust aggregate gradation. The value on the vertical axis of CMD for a given sieve size shows the difference in the percent of material retained on that sieve for the actual gradation and the continuous maximum density gradation. This method considers that the gradations closer to the maximum density line, which corresponds to the zero line on the CMD plot, will have lower VMA; while those further away will have higher VMA.

Based on packing theory, the CMD method provided a simple and flexible method to adjust aggregate gradation. However, the application of this procedure requires some experience with the mix design process and with a wide range of materials. It is also worth noting that different portions of aggregate gradation will have different sensitivities to the changes of VMA.

Although provided some guidelines on how to adjust gradation to achieve target VMA, there is no clear correlation between gradation and VMA in the NCHRP report 673 (Advanced Asphalt Technologies, LLC. 2011). Given the VMA specification range is becoming narrower; the mix design engineers are facing bigger challenges to satisfy VMA requirements. Therefore, there is an urgent need to develop a simple method to be able to estimate the VMA based on aggregate gradations and properties so that to save

the mix design time and obtain well performing AC mixtures.

2.2 VOLUMETRIC DESIGN AND VMA CRITERIA

2.2.1 *Introduction*

The volumetric properties of AC mixture such as VMA, VFA, and air voids have been identified as important parameters to ensure the good performance of AC. A minimal VMA has to be achieved for a durable AC mixture. Although important, existing VMA requirements are mostly based on the research done in the 1960s. There are increasing reports on the difficulties of meeting the VMA requirements and many suggestions on the VMA criterion have been proposed.

2.2.2 *Development of the minimum VMA criterion*

A minimum VMA requirement was first proposed by McLeod in 1956. It was later improved by many researchers and was adopted by Asphalt Institute and Superpave mix design procedures. In recent years, more and more researchers and engineers have discussed problems about VMA criterion. Hinrichsen and Heggen (1996) pointed out that it was difficult to meet these minimum VMA requirements and those requirements may rule out economical mixes which have acceptable performance properties. Anderson and Bahia (1997) also showed their concerns on difficult and time-consuming steps to

meet the minimal VMA requirement. Some other researchers have suggested that it is not applicable to restrict all of mixture to meet the criterion (Mallick et al. 2000).

In order to derive a predictive relationship relating critical state (e.g., critical VMA) to aggregate related properties such as nominal maximum aggregate size, gradation, shape, and texture, Coree, and Hislop (2000, 2001) conducted a serial of experiments. They identified that three factors—fineness modulus (FM) , coarse aggregate percent crushed (CAPC), and fine aggregate percent crushed (FAPC) and two interactions (FM x CAPC and FM x FAPC)—are significant in predicting the minimal VMA criterion. This paper also suggested replacing the current minimum VMA specification to a durability criterion based on the more robust parameters of VFA or Vbe in designing asphalt mixtures. Or if a minimum VMA is to be specified, it should include FM, CAPC, FAPC, and their interactions.

Kandhal et al. (1996) have argued that the minimum VMA should be based on the minimum desirable asphalt film thickness rather than NMPS or minimum asphalt content. The research point out that NMPS and minimum asphalt content may varies for mixes with different gradations, and mixes with coarse gradation have difficulty meeting the minimum VMA requirement based on minimum asphalt content in spite of thick asphalt films. Unlike the requirement which was based on NMPS, the film thickness approach may represent a more direct, equitable, and appropriate method of ensuring asphalt mix

durability and encompasses various mix gradations.

2.2.3 *Problem of the minimum VMA criterion*

In order to design a gradation to satisfy the minimal VMA and other volumetric properties, a "trial-and-error" process is usually used. It is possible several gradation blends have to be tried and a number of experiments have to be conducted before meeting all design requirements. Clearly, this "trial-and-error" gradation design method is time consuming and has no clear indication of how to achieve the target VMA requirements. Although Bailey's method (Vavrik et al. 2002) has provided some suggestions on how to adjust mix design to achieve the target VMA, the determination of VMA is still a trial-and-error process which relies on initial mix design and requires a large amount of experimental testing.

In the recent improvement of AC mix design method as outlined in the NCHRP 9-33 manual (Advanced Asphalt Technologies, LLC. 2011), VMA specifications have been strongly emphasized considering the importance of having an appropriate VMA to achieve a successful mix. The new design manual suggests the target VMA and air voids values and the resulting target binder content should be determined in the early stage of AC mix design and should be maintained throughout the mix design procedure. In this way, the proper binder content is ensured, and effort is not wasted evaluating mixtures

that don't have the proper VMA and binder content.

Table 2-1. VMA Requirements of NCHRP 9-33 manual (Advanced Asphalt Technologies, LLC. 2011)

Aggregate NMAS (mm)	Minimum VMA[A] (%)	Maximum VMA[A] (%)	Target VMA (%)
4.75	16.0	18.0	17.0
9.5	15.0	17.0	16.0
12.5	14.0	16.0	15.0
19	13.0	15.0	14.0
25	12.0	14.0	13.0
37.5	11.0	13.0	12.0

[A]The specifying agency may increase the minimum and maximum values for VMA by up to 1.0% to obtain mixtures with increased asphalt binder content, which can improve field compaction, fatigue resistance and general durability. Care should be taken to ensure that the resulting AC mixtures maintain adequate rut resistance for their intended application.

Many studies have reported the difficulties of meeting the minimum VMA requirement. The newly added maximum VMA requirements by the NCHRP 9-33 design manual, as given in Table 2-1, bring a more serious challenge to the mix design engineers. Note that a 2.0 % range is specified for allowable VMA, and the target value is in the center of this allowable range. Based on the discussions above, there is an urgent

need to develop a simple method to estimate the VMA based on aggregate gradations and properties so as to save the mix design time, and obtain a more reasonable mix design with appropriate aggregate gradation and volumetric properties.

2.3 ASPHALT BINDER FILM THICKNESS IN MIXTURE PERFORMANCE

Asphalt film thickness is considered as an import factor affecting the durability and performance of the AC mixtures. Campen et al.(1959) in his study pointed out that mixtures with a higher asphalt film thickness are more flexible and endurable, while mixtures with a low film thickness can be brittle and more susceptible to low temperature cracking. Campenet al.(1959) found that average film thickness for most mixtures were ranging from 6 to 8 microns based on data analysis. Kumar and Goetz (1977) suggested using film thickness factor to predict the mixture's resistance to binder hardening. In this study, the film thickness factor was defined as the ratio of the percent asphalt content available for coating the aggregate to the surface area of the aggregate. Kandhal and Chakraborty (1996) studied the relation between the asphalt film thickness and the engineering properties of AC mixtures (such as tensile strength and resilient modulus) after short-term and long-term aging. Their study suggested that there existed an optimum film thickness of 9-10 microns, below which the AC mixture will age at an accelerated rate. This range appeared to concur with the results obtained by Goode and

Lufsey (1965) in terms of air voids-bitumen index ratio. “Bitumen index” was defined as pounds of asphalt cement per square. Goode and Lufsey (1965) suggested that a minimum “bitumen index” of 0.00123 should be used as a design criterion, which was corresponding to 6 microns of average film thickness. They also suggested that in order to ensure reasonable resistance to aging, a maximum value of 4 for voids-bitumen index ratio should be used rather than a maximum value of air voids alone. Wang (2007) studied the effect of the binder film thickness effect on aggregate contact behavior, and concluded that aggregate binder mixture will become stiffer if the film thicknesses decrease.

2.4 PACKING THEORY

The following discussions introduce effects influence aggregate packing and some popular packing theories found in the literatures, which provide thoughtful insights to this study in developing packing models in the Discrete Element Modeling (DEM) simulation.

2.4.1 *Aggregate packing*

The ways how different sizes of aggregates packed to each other can significantly affect the mechanical properties of AC mixtures. In general, the degree of packing

depends on:

1. Type and amount of compactive energy. Different compaction methods such as static pressure, impact Marshall hammer, Gyratory shearing compactor, and California kneading compactor will apply different compaction energy to the materials, thereby, result in different aggregate packing structures.
2. Shape of particles. Research has found that flat and elongated particles tend to rearrange under compaction effort while cubical particles tend to form a denser packing structures.
3. Surface texture of the particles. Comparing with rough surface, smooth surface texture will lead to a relatively denser configuration with aggregates slide against each other.
4. Size distribution. Single sized aggregate structure will not pack as densely as a mixture of particle sizes with continuous gradation.
5. Strength of the particles. Soft aggregates degrade more than strong aggregates, and allow denser aggregate packing to be achieved.

2.4.2 *Analysis of VMA in 2-D model*

Figure 2-1 and Figure 2-2 showed two types of packing in a 2-D model.

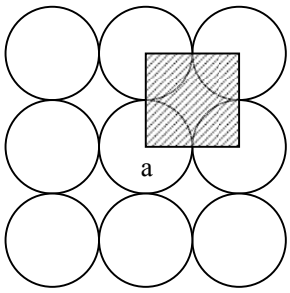

Figure 2-1. Square Array Packing in 2-D Model

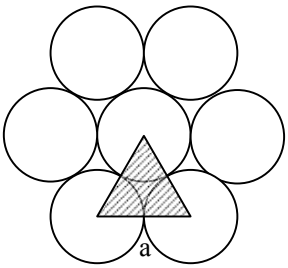

Figure 2-2. Hexagonal Array Packing in 2-D Model

For a square array in Figure 2-1, there is

$$VMA = 1 - \frac{\frac{\pi}{4}a^2}{a^2} = 1 - 0.7854 = 0.2146 \tag{2.7}$$

For a hexagonal array in Figure 2-2, there is

$$VMA = 1 - \frac{\frac{1}{2}\frac{\pi}{4}a^2}{\frac{\sqrt{3}}{4}a^2} = 1 - 0.9069 = 0.0931 \tag{2.8}$$

As results, for a 2-D model, when the aggregates are in unit diameter a, the VMA of the model should be in the range of 0.2146 to 0.0931.

2.4.3 *Particle packing in 2-D model*

In a 2-D model, the size of fine aggregate used to fill the voids created by coarse aggregate is based on different combination of the geometry (Vavrik 2000).

1. All round faced particles, produces a size ratio of 0.155 between final aggregate and coarse aggregate.

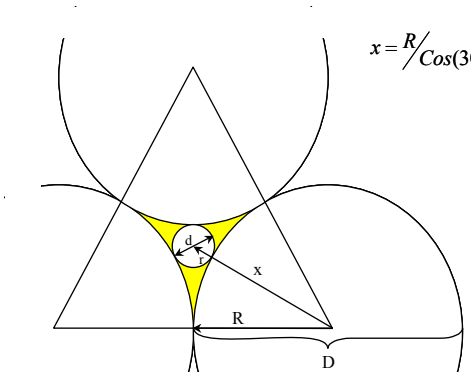

$$x = R/Cos(30)$$

$$d = 2\left(R/Cos(30) - R\right)$$
$$= 2R\left(1/Cos(30) - 1\right)$$
$$= \mathrm{D}\left(1/Cos(30) - 1\right)$$

$$\left.\begin{aligned} r &= x - R \\ d &= 2r \end{aligned}\right\} \; d = 2(x - R)$$

$$d = 0.155\,D$$

2. 2 round faces, 1 flat face, produces a size ratio of 0.20.

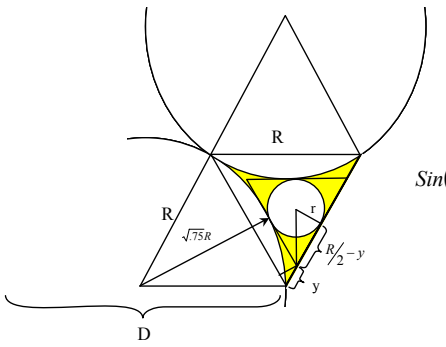

$$Tan(30) = r/0.5\,(\mathrm{R} - 2\,\mathrm{y})$$
$$Tan(30) = r/0.5\,(0.5\,\mathrm{D} - 0.15470\,\mathrm{D})$$
$$Tan(30) = r/0.17265\,\mathrm{D}$$

$$Sin(60) = \frac{\left(1 - \sqrt{.75}\right)R}{y} \qquad y = \frac{\left(1 - \sqrt{.75}\right)R}{Sin(60)}$$

$$y = 0.07735\,D$$

$$r = 0.09968\,D$$

$$d = 0.199\,D$$

3. 1 round face, 2 flat faces, produces a size ratio of 0.24.

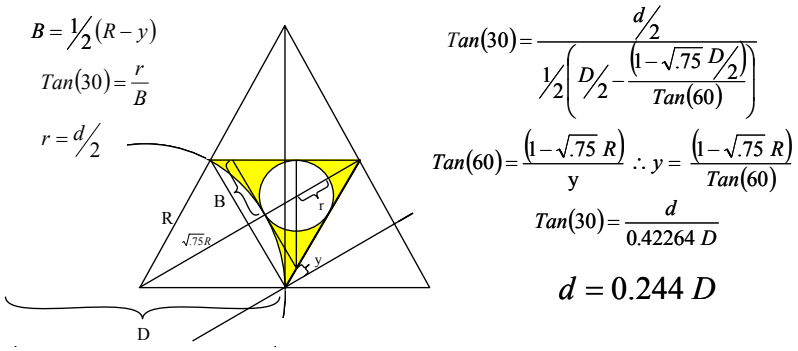

4. All flat faced particles, produces a size ratio of 0.29.

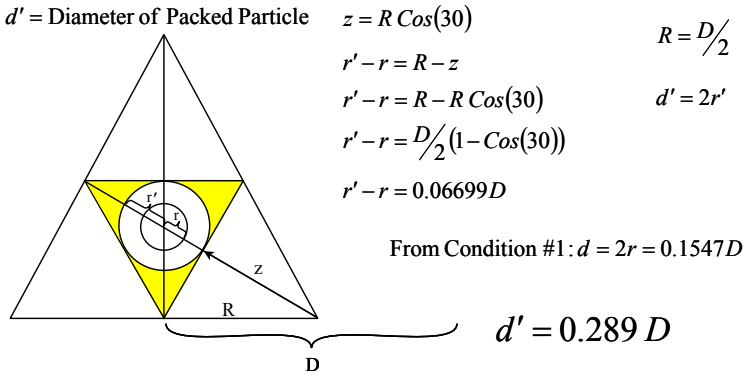

While the actual size ratio of the aggregates varied depending on the gradation, the Bailey's method used the value of 0.22 size ratio which is an average of these four different combinations of two-dimensional particle combinations.

2.5 Mechanical Performance and Gradation Impact

The Superpave mix design method has been adopted by many agencies in the United States. However, unlike the traditional Marshall and Hveem mix design method, the

Superpave method does not have a performance evaluation to complement the volumetric mixture design. Some researchers and designers (Cominsky et al. 1998) have raised the question that whether the volumetric design method alone can provide a sufficient design over a wide range of loading conditions. To address this concern, a set of Asphalt Mixtures Performance Tests (AMPT) have been proposed and evaluated by the National Cooperative Highway Research Program (NCHRP) for estimating the mechanical performance of the mixtures (Witczak et al. 2002). In this study, three key properties that are greatly affected by the aggregate gradation and properties are evaluated, including rutting resistance, dynamic modulus, and compactability.

2.5.1 *Distresses in asphalt mixture*

The principal distresses in asphalt mixture pavement are permanent deformation (rutting), fatigue cracking, and thermal cracking. The appearance of those distresses has a big affects on the durability and long-term performance of an asphalt mixture pavement.

Permanent deformation is the deformation of the pavement layers due to traffic loads, which can be divided in two stages, compactive deformation and plastic deformation (or plastic flow). Compactive deformation corresponds to a deformed surface lower than the initial pavement surface while plastic deformation is when the deformed surface is higher than the original surface. According to Zhou and Scullion (2004), the cumulative

permanent strain curve is generally defined by three zones: primary, secondary, and tertiary. The primary zone is a per-failure period where permanent deformation accumulates rapidly. In this zone there is an increase in total plastic strain because asphalt mixtures will work harden with repeated loading. The physical process that explains this stage is micro-flow motion, or dislocation. The second zone, or steady stage, is where the permanent deformation rate is a constant value. In this stage the occurrence of microcracking causes more space for more dislocation to develop, which further softens the asphalt mixture. Finally, the tertiary or failure zone, with crack formation and propagation occurs when the permanent deformation rate begins to increase due to the formation and growth of micro-cracks. Micro-cracks gradually propagate and coalesce to form macro-cracks. The initiation and propagation of macro-cracks accelerates the rate of work-softening, causing the permanent deformation rate to increase.

Pavement rutting is caused when the underlying layers, subgrade soil, and/or the HMA layers are overstressed and densification or shear failure occurs. The rutting performance of an HMA mixture depends not only on the properties of the aggregates and binder, but also on how these materials interact within the mixture. Tarefder et al. (2003) evaluated factors affecting rutting using Asphalt Pavement Analyzer (APA), the asphalt mixture are designed based on Superpave design method, their research found that the binder type, specimen type, test temperature, and their interactions were the most

significant factors affecting rutting, while moisture, traffic load, binder content were found to be the least significant factors.

The fatigue resistance of asphalt mixture is defined as its ability to withstand repeated bend loading without fracture. The asphalt pavement tend to bend when it is in service and under traffic loading, when the number of loading are reaching to one certain number, the asphalt mixture are begin to express fatigue characteristics. Traditionally, fatigue appears in the forms of cracks following the direction of wheel path. These cracks can result from the shear stresses in the surface of the asphalt mixture layer or the tensile stresses at the bottom of this layer. Possible asphalt mixture properties that contribute to poor fatigue performance may including not enough binder content, high air voids content and inadequate asphalt layer thickness.

2.5.2 ***Flow Number***

2.5.2.1 *Introduction of flow number*

Table 2-2. Approaches for Rutting Resistance from Flow Number Test Data

Method	Air Voids	Temperature	Confining Stress, psi	Deviatoric Stress, psi	Pulse	Criteria
NCHRP9-33 (Christensen, et al. 2009)	7 %	50 % reliability high pavement temperature from LTPPBind at depth of 20 mm for surface courses and top of layer for other layers	0	87	0.1 sec with 0.9 sec dwell	Flow number > critical value as a function of traffic
NCAT(Willis et al. 2009)	7 %	50 % reliability PG grade – 6 °C	10	70	0.1 sec with 0.9 sec dwell	Flow number > critical value as a function of traffic and allowable rut depth
NCHRP 9-30A (Quintus 2010)	Avg.; In Place (Specs.)	Option A: 3 Temps. (50% reliability PG minus 5°C, 20°C, mid-range). Option B: Effective temperature based on rutting (MEPDG).	10	70	0.1 sec with 0.9 sec dwell	Slope and intercept of permanent deformation curve<critical values as a function of traffic (rut depth<threshold value).
UNR (Hajj et al. 2010)	7 %	Effective temperature for rutting	Variable*	Variable*	Variable*	Slope and intercept of permanent deformation curve<critical values as a function of traffic
NCHRP 9-26A	7%	3 temperatures: Binder high PG, PG minus 6°C, PG minus 12°C	0	29	0.1 sec with 0.9 sec dwell	Rutting calculated from Minimum Strain Rate at 3 temperatures, aging index, and pavement temperature frequencies < critical rutting

* using developed predictive equations.

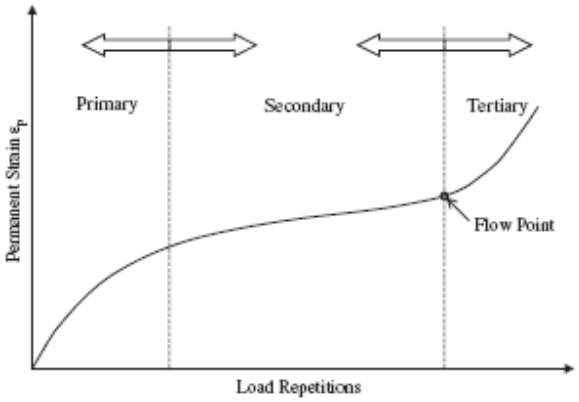

Figure 2-3. Typical repeated load permanent deformation behavior of pavement materials.

The repeated load flow number (Fn) test is a dynamic creep test where a haversine type of loading is applied with rest periods between loadings. As shown Figure 2-3, the typical results between the measured permanent strain and load cycle can be divided into three major zones. In the primary phase, the strain rate (slope of the permanent strain curve) decreases; in the secondary phase, the permanent strain rate is constant; and in the tertiary phase the permanent strain rate dramatically increases. At low stress levels, the material may mainly exhibit primary and/or secondary permanent strain. In this case, the permanent strain rate may approach a value equal to zero as the total strain reaches a certain value. This also suggests that at this very low stress level the tertiary flow region may never appear within a reasonable amount of time. At higher stress levels, the

occurrence of the constant secondary permanent strain rate phase will depend on the stress level applied.

2.5.2.2 *Flow number testing methods*

The flow number test protocol was developed in the NCHRP 9-19 project (Witczak 2007) although the testing procedures and set-ups were not fully standardized. NCHRP Project 9-19 recommended testing the flow numbers at the effective pavement temperature using either unconfined tests with axial stress between 10 and 30 psi or confined tests with confining pressure between 5 and 30 psi and deviatoric stress between 70 and 140 psi. Using the effective pavement temperature and the range of stress levels recommended in the NCHRP 9-19 Project, many mixtures did not exhibit flow within 10,000 cycles (approximately 2.8 hours testing time), the recommended maximum number of load cycles. Therefore, many researchers as listed in Table 2-2 have modified testing conditions such as either increasing the temperature, deviatoric stress or both to ensure that flow would occur in the mixtures within 10,000 load cycles. Table 2-2 provided a summary of the testing conditions and evaluation criteria used for flow number test.

2.5.2.3 *Flow number and rutting*

Ideally, the large increase in permanent strain generally occurs at a constant volume within the tertiary zone. The flow number is therefore defined as the postulated cycle when shear deformation, under constant volume, starts, indicating the start of tertiary flow in the mixture. Practically, the flow number can be determined as the load cycle at which the rate of the change of permanent strain reaches the minimum value.

Permanent deformation (rutting) of the HMA pavement is caused by a combination effect of densification and shear deformation under repetitive loading. Rutting can be categorized into three types: one-dimensional densification or vertical compression, lateral flow or plastic movement, and mechanical deformation. Factors affecting rutting vary since rutting is a complex phenomenon between aggregate, asphalt, and aggregate-asphalt interface, and the properties of those component are changing with the change of time, loading and temperature (Witczak, M.W., 2007).

Several testing methods have been proposed by Witczak et al. (2007) for evaluating the rutting resistance including the dynamic modulus (E*) test, flow number (Fn) test, and flow time (Ft) test. Particularly, the flow number test was found to be able to correlate with field rut depth as verified by field projects at MNRoad (Figure 2-4), Westrack (Figure 2-5), and the FHWA Pavement Testing Facility (Figure 2-6) in the NCHRP project 9-19 (Witczak 2007). During the NCHRP project 9-19, the relationship

between the reduced flow number and field rut depth at a specific traffic level were studied. Temperature-reduced flow numbers were calculated with the following Equation (2.9):

$$\log(F_{nr}) = \frac{\ln\left(\frac{\alpha}{\log(\sigma) - \delta} - 1\right) - \beta}{\gamma} \tag{2.9}$$

σ = applied stress,

tr= Ft or Fn at the reference temperature,

δ = minimum stress that will cause damage,

δ + α = maximum stress that will cause instantaneous damage, and

β, γ = parameters describing the shape of the sigmoidal function.

α will be a linear function of δ.

The parameters in the equation were determined from a global temperature shifted master curve analysis.

Christensen (2008) proposed a resistivity/rutting equation which gives allowable traffic as a function of mixture composition, compaction and air voids based on data regression. Equation (2.10) is expressed as below:

$$TR = 9.85 \times 10^{-5} \left(\mathrm{P} N_{eq} K_s\right)^{1.373} V_d^{1.5185} V_{IP}^{-1.4727} M \tag{2.10}$$

where:

TR = allowable traffic in million ESALs to an average rut depth of 7.2

mm (50 % confidence level)

= allowable traffic in million ESALs to a maximum rut depth of 12 mm (95 % confidence level)

P = resistivity, s/nm

$$= \frac{\left(|G^*|/\sin\delta\right)S_a^2 G_a^2}{49VMA^3}$$

$|G^*|/\sin\delta$ = Estimated *aged* PG grading parameter at high temperatures, determined at 10 rad/s and at the yearly, 7-day average maximum pavement temperature at 20 mm below the pavement surface, as determined using LTPPBind, Version 3.1 (units of Pa/s); aged value can be estimated by multiplying the RTFOT value by 4.0 for long-term projects (10 to 20 year design life), and by 2.5 for short term projects of 1 to 2 years.

S_a = specific surface of aggregate in mixture, m^2/kg

≅ the sum of the percent passing the 75, 150 and 300 micron sieves, divided by 5.0

≅ 2.05 + (0.623 × percent passing the 75 micron sieve)

G_a = the bulk specific gravity of the aggregate blend

VMA = design voids in the mineral aggregate for the mixture, volume

N_{et} = design gyrations

K_s = speed correction

= $(v/70)^{0.8}$, where v is the average traffic speed in km/hr

V_d = design air void content, volume %

V_{IP} = air void content, volume %, in-place

M = 7.13 for mixtures containing typical polymer-modified binders, 1.00 otherwise

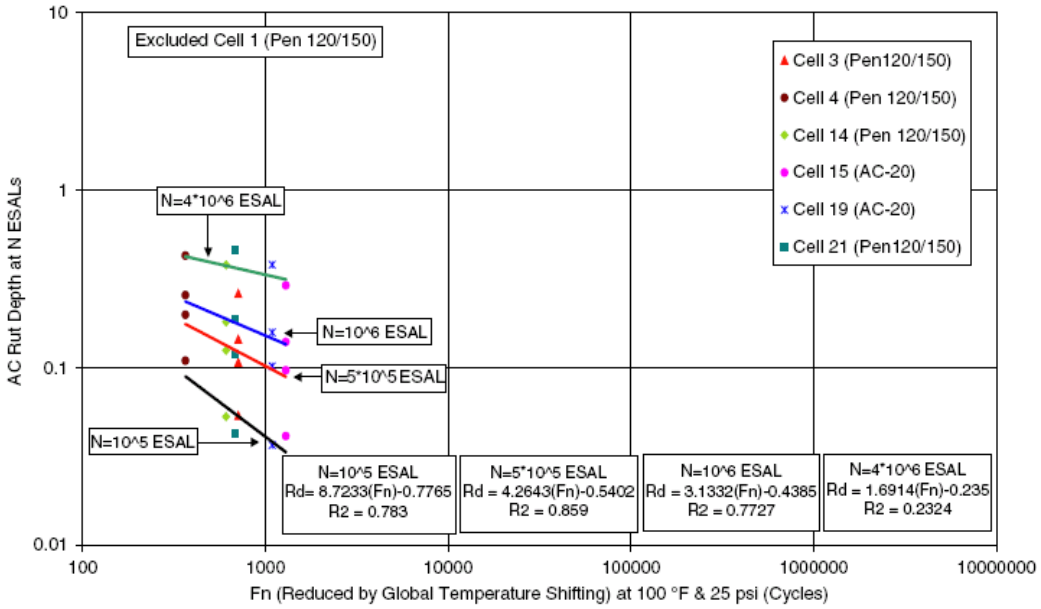

Figure 2-4. Flow number (reduced by global temperature shifting) at 100° F and 150 psi (1034 kPa) V.S. rut depth at N ESALs for MnRoad plant mixes (unconfined).

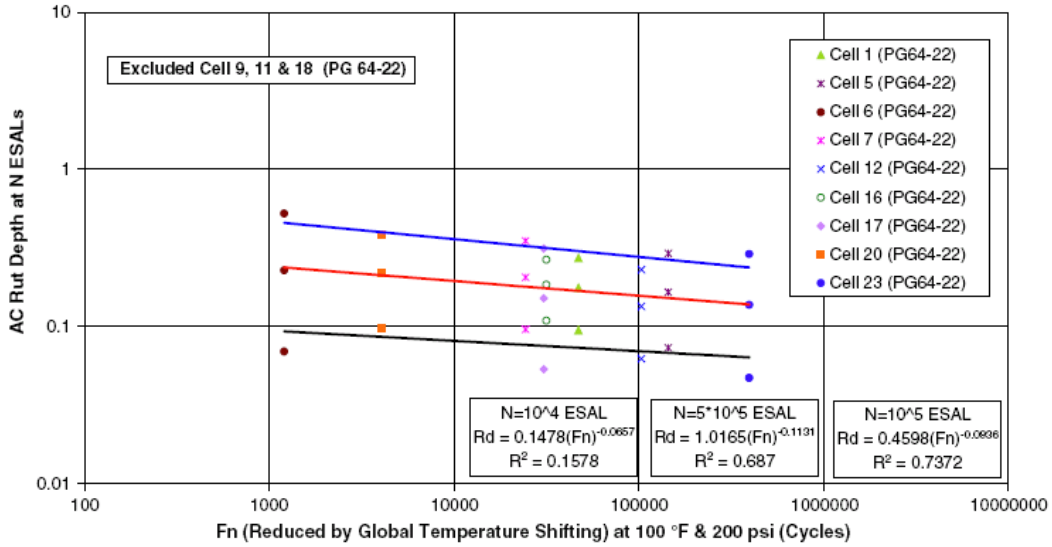

Figure 2-5. Flow number versus rut depth at Westrack

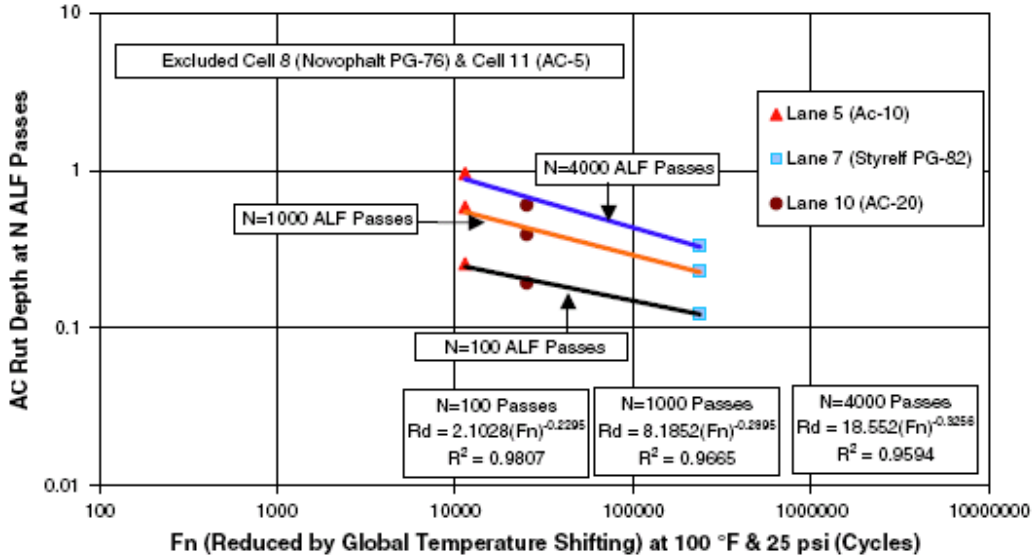

Figure 2-6. Flow number (reduced by global temperature shifting) at 100F and 25psi (172 kPa) versus rut depth at N ALF passes and 136.4F for ALF field

2.5.2.4 *Flow number prediction models*

Over the past few years, there have been significant effects to establish a testing method to evaluate the material properties of asphalt mixture design, such that it would be indicative of field performance. And the majority of interest has centered around dynamic modulus with primary efforts on the predictive models. However, some researchers (Witczak 1996; Bhasin 2004) felt that additional test should be employed in conjunction with dynamic modulus for rutting performance evaluation of mixtures, and the flow number has been proved to be an effective tool as a rutting performance indicator.

Flow number test provides information concerning the three phases of flow (primary, secondary and tertiary) within an asphalt mix with particular emphasis on tertiary flow. Flow number is obtained from the repeated load permanent deformation test to evaluate the resistance of an asphalt mixture to tertiary flow. In order to predict the flow number of asphalt mixture, some researchers have been proposed different prediction models to provide guidance on the understanding of flow characteristics.

Kaloush (2001) provided the first attempt in predicting the Flow Number of an HMA mixture based on mixtures volumetric properties, binder type, and test temperature. The model used 135 unconfined laboratory FN tests and was presented as follows:

$$FN = (432367000)T^{-2.215}Visc^{0.312}V_{beff}{}^{-2.6604}V_a{}^{-0.1525} \quad (2.11)$$

Where,

FN = Flow Number

T = Test Temperature, °F

Visc = Binder Viscosity at 70°F, 106 poise

Vbeff = Effective Asphalt Content, % volume

Va = Air Voids, %

Another study by Kvasnak et al (2007) presented a Flow Number predictive equation based on 17 dense graded mixtures from the State of Wisconsin.

$$\log FN = 2.866 + 0.00613Gyr + 3.86Visc - 0.072VMA + 0.0282P_4 - 0.051P_{16} + 0.075P_{200} \quad (2.12)$$

In this model, the number of gyrations (Gyr) was found to be the most significant factor. The authors pointed out that the model should only be applied within the data ranges used for the dense graded HMA mixes.

Rodezno and Kaloush et al (2010) proposed an equation to predicted flow number as following

$$\log FN = 2.174 + 0.649 Log V_1 + 0.101 P_{200} + 18.465 Log p + 0.0140 R_{04} - 0.084 V_a - 18.901 \log q - 0.872 R_{34} + 0.182 q - 0.193 p - 0.871 \log T$$

(2.13)

In this final model, it can be seen that the variables that are significant in the model are: the viscosity at testing temperature (V_1), the air voids level, the temperature, three variables related with the gradation of the mix: $\%P_{200}$, $\%R_{04}$ and $\%R_{34}$ and the shear and normal stresses (p and q) that contribute to the model in the arithmetic and logarithmic terms. The presence of the p and q variables indicates the importance of the combination of stress levels applied to the samples.

Christensen (2008) applied various statistical techniques to relate the flow number with complex modulus, air void content and applied stress level, and proposed a model based on data regression:

$$N_f = 4.96 \times 10^{-8} \beta_i |E^*|^{2.478} \sigma^{-0.089 VTM - 0.187 |E^*|} \quad (2.14)$$

where,

N_f= flow number

β_i= indicator variable, adjusting regression constant for i_{th} projects/sections

$|E^*|$ = complex modulus (lb/in2) at 10 Hz and same temperature as flow number test

VTM = air voids in flow number test specimen, volume %

σ = deviator stress for flow number stress, lb/in2

2.5.3 *Dynamic Modulus*

Dynamic modulus (E*) is one of the fundamental properties defining the response of HMA mixtures in flexible pavement systems. It is a critical input parameter in the Mechanistic-Empirical Pavement Design Guide (MEPDG) software for determining the stress-strain relationship of the asphalt mixtures at different loading and temperature conditions. It is also considered as one of the most important material properties for evaluating the rutting and fatigue performance of the mixture. The dynamic modulus test has the potential to relate the material properties of the mix to the structural field performance of the pavement through the 2002 Design Guide. Various E* predictive models have been developed over the last several decades to estimate E* as an alternative to laboratory testing, which can require days of specimen preparation, temperature equilibration, and loading. There are mainly three dynamic modulus prediction models that are widely used and evaluated by pavement researchers, Witczak traditional model (MEPDG model), new Witczak model, and the Hirsch model.

2.5.3.1 *Witczak traditional model (Witczak et al. 2002)*

The traditional Witczak E* predictive model was developed based on a database of 2750 dynamic modulus measurements from 205 different asphalt mixtures tested over the last 30 years in the laboratories of the Asphalt Institute, the University of Maryland, and the

Federal Highway Administration. This model can predict the dynamic modulus of mixtures using both modified and conventional asphalt binders. This model is considered as the most popularly used E* prediction model which is also adopted by the MEPDG for correlating mixture material properties with the dynamic modulus. The equation is as follows;

$$\log|E^*| = 3.750063 + 0.02932\rho_{200} - 0.001767(\rho_{200})^2 - 0.002841\rho_4 - 0.058097V_a$$
$$- 0.802208\left(\frac{V_{beff}}{V_{beff} + V_a}\right) + \frac{3.871977 - 0.0021\rho_4 + 0.003958\rho_{38} - 0.000017(\rho_{38})^2 + 0.00547\rho_{34}}{1 + e^{(-0.603313 - 0.313351\log(f) - 0.393532\log(\eta))}} \quad (2.15)$$

Where,

|E*| = dynamic modulus, psi

η= bitumen viscosity, 10^6 Poise

f = loading frequency, Hz

V_a= air void content, %

V_{beff}= effective bitumen content, % by volume

ρ_{34} = cumulative % retained on the 19-mm (3/4) sieve

ρ_{38} = cumulative % retained on the 9.5-mm (3/8) sieve

ρ_4 = cumulative % retained on the 4.76-mm (No. 4) sieve

ρ_{200} = % passing the 0.075-mm (No. 200) sieve

2.5.3.2 *New Witczak model (Bari and Witczak 2006)*

Bari and Witczak in 2006 developed a new Witczak model based on a more comprehensive study and included a larger database with 7400 data points from 346 HMA mixtures. The new model was selected from a number of candidate models based on the tests on rationality, accuracy, precision, bias, trend, sensitivity, and overall performance. The new Witczak model is shown in Equation (2.16).

$$\log(|E^*|) = -0.349 + 0.754\left(|G_b^*|^{-0.0052}\right)\cdot\begin{pmatrix}6.65 - 0.032\rho_{200} + 0.0027\rho_{200}^2 - 0.011\rho_4 - 0.0001\rho_4^2 \\ + 0.006\rho_{38} - 0.00014\rho_{38}^2 - 0.08V_a - 1.06\left(\frac{V_{beff}}{V_a + V_{beff}}\right)\end{pmatrix} + \frac{2.558 + 0.032V_a + 0.713\left(\frac{V_{beff}}{V_a + V_{beff}}\right) + 0.0124\rho_{38} + 0.0001\rho_{38}^2 - 0.0098\rho_{34}}{1 + e^{(-0.7814 - 0.5785\log|G_b^*| + 0.8834\log(\delta_b))}} \quad (2.16)$$

Where,

|E*| = dynamic modulus, psi;

ρ 200 = % (by weight of total aggregate) passing the 0.075-mm (No. 200) sieve;

ρ 4 = cumulative % (by weight) retained on the 4.76-mm (No. 4) sieve;

ρ 34 = cumulative % (by weight) retained on the 19-mm (3/4-in.) sieve;

ρ 38 = cumulative % (by weight) retained on the 9.5-mm (3/8-in.) sieve;

Va = air void content (by volume of the mix), %;

Vbeff = effective binder content (by volume of the mix), %;

|Gb*| = dynamic shear modulus of binder, psi;

δ b = phase angle of binder associated with |Gb*|, degree.

2.5.3.3 *Hirsch Model (Christensen et al. 2003)*

Hirsch model is a rational, though semi-empirical method of predicting asphalt concrete modulus. It is based on the theory of composite material which combines series and parallel elements of the phases. Comparing to the Witczak models, Hirsch model is considered relatively simpler which relates the dynamic modulus of the asphalt concrete (|E*|) with binder modulus (G*), voids in the mineral aggregate (VMA), and voids filled with asphalt (VFA), as shown in Equation (2.17).

$$|E^*| = Pc\left[4{,}200{,}000\left(1-\frac{VMA}{100}\right)+3|G^*|_{binder}\left(\frac{VFA\cdot VMA}{10{,}000}\right)\right]+(1-Pc)\left[\frac{1-\frac{VMA}{100}}{4{,}200{,}000}+\frac{VMA}{VFA\cdot 3|G^*|_{binder}}\right]^{-1} \quad (2.17)$$

Where:

|E*| = dynamic modulus, psi

$|G^*|_{binder}$ = binder dynamic modulus, psi

VMA= voids in the mineral aggregate, %

VFA = voids filled with asphalt, %

Pc = aggregate contact factor, where

$$Pc = \frac{\left(20+\frac{VFA\cdot 3|G^*|_{binder}}{VMA}\right)^{0.58}}{650+\left(\frac{VFA\cdot 3|G^*|_{binder}}{VMA}\right)^{0.58}} \quad (2.18)$$

2.5.4 *Prediction Model of Idaho mixtures (Abdo et al. 2009)*

Abdo et al. (2009) proposed s model to predict E* from the properties of the asphalt mixture constituents. The model parameters were determined by dimensional analysis and s new mix design mechanistic parameter, the Gyratory Stability (GS), was included in the model. The model was shown in Equation (2.19)

$$E^* = 1.08\left(\frac{G^* \cdot GS \cdot \%G_{mm}}{P_b(1-P_b)}\right)^{0.558} \quad (2.19)$$

where,

E*: Dynamic Modulus for Asphalt Mix, MPa,

G*: Dynamic Shear Modulus for RTFO Aged Binder, MPa,

Pb: Percent Binder Content,

GS: Gyratory Stability, kNm,

Gmb: Bulk Specific gravity of Mix, Gmb= Gmm (1-AV%),

Gmm: Maximum Specific gravity of Mix, and

AV%: Air Voids.

2.5.5 *Prediction Model of Florida mixtures (Yang et al. 2011)*

Yang et al (2011) developed a predicting model of dynamic modulus for characterizing

Florida asphalt mixtures based on 20 selected Florida Superpave mixtures. The model including variables related to aggregate gradation, mixture volumetrics, and percent weight of asphalt content, loading frequencies, and temperatures. The model was shown in Equation (2.20)

$$\log|E^*| = 2.312 + 0.01\rho_{200} + 0.01\rho_8 - 0.013\rho_4 - 0.002\rho_{3/8} + 0.024P_b - 0.043VFA + \frac{[-1.34 - 0.019\rho_8 + 0.022\rho_4 + 0.004\rho_{3/8} - 0.055P_b + 0.052VFA]}{1 + e^{(-8.267 - 0.722\log f + 5.397\log T)}} \quad (2.20)$$

where,

$|E^*|$ = dynamic modulus, in 105 psi

T= Test temperature, in °C

f= load frequency, in Hz

VFA= Voids filled with asphalt, % by volume

Pb= Percent weight of asphalt, % by weight

$\rho_{8/3}$ = cumulative percent retained on 3/8 in (9.5mm) sieve, % by weight

ρ_4= cumulative percent retained on No. 4 (4.75mm) sieve, % by weight

ρ_8= cumulative percent retained on No. 8 (2.36mm) sieve, % by weight

ρ_{200}= percent passing on No. 200 (0.075mm) sieve, % by weight

Table 2-3. Comparison of dynamic modulus prediction models

(Bari and Witczak 2006)

Parameters	E* Predictive Models		
	Witczak 1999	Hirsch 2003	New Model 2005
Total Mixes	346	346	346
Mixes with Modified Binders	17	17	17
Data Points	7400	7400	7400
Goodness of Fit in Normal (Arithmetic) Scale			
Se/Sy	0.60	0.88	0.45
R^2	0.65	0.23	0.80
Goodness of Fit in Logarithmic Scale			
Se/Sy	0.35	0.62	0.32
R^2	0.88	0.61	0.90

2.5.5.1 *Comparison of the predictive models*

Bari and Witczak (2006) also compared the three prediction methods. Table 2-3 listed the regression statistics among the models, and Figure 2-7 showed the comparisons between the predicted and the measured E* values.

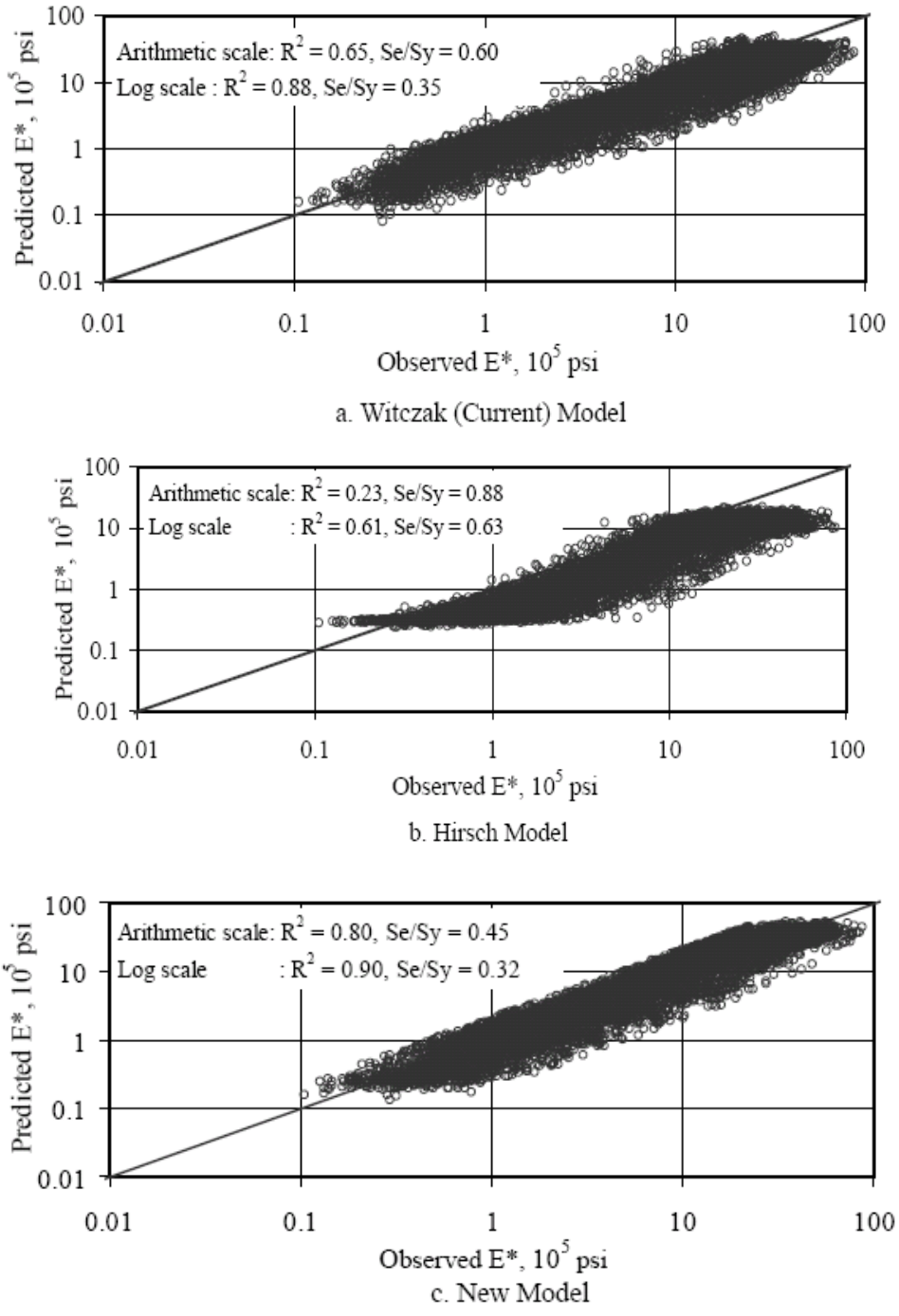

Figure 2-7. Predicted versus measured E* for three models

(Bari and Witczak 2006)

Based on the statistics analysis data, Bari and Witczak concluded that the new Witczak model showed the best predictive strength in comparison with the previous models. It must be noted, however, that the comparison against the Hirsch model was not completely "fair", because an important part of the |Gb*| data included in the "new database" are only "estimates" and not direct measurements from lab tests. A more reliable comparison should be done with "measured" data (Garcia and Thompson, 2007).

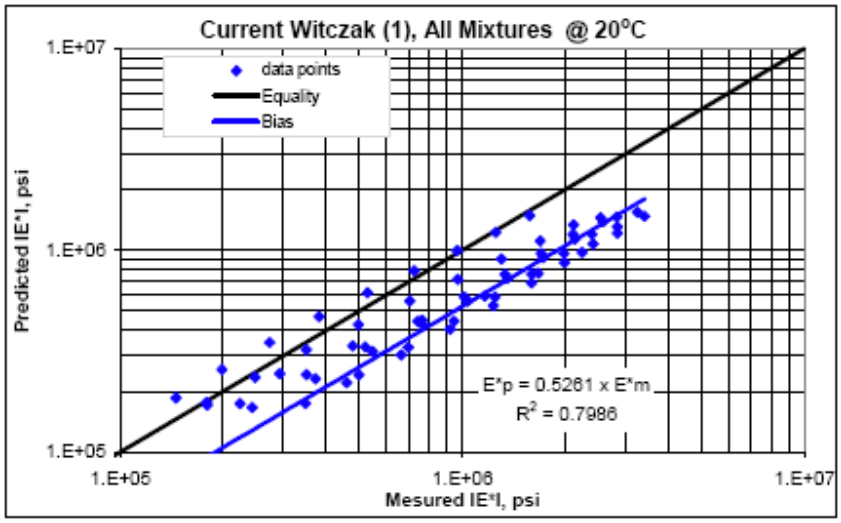

(a)Results for All Mixtures, Applying Current Witczak Model.

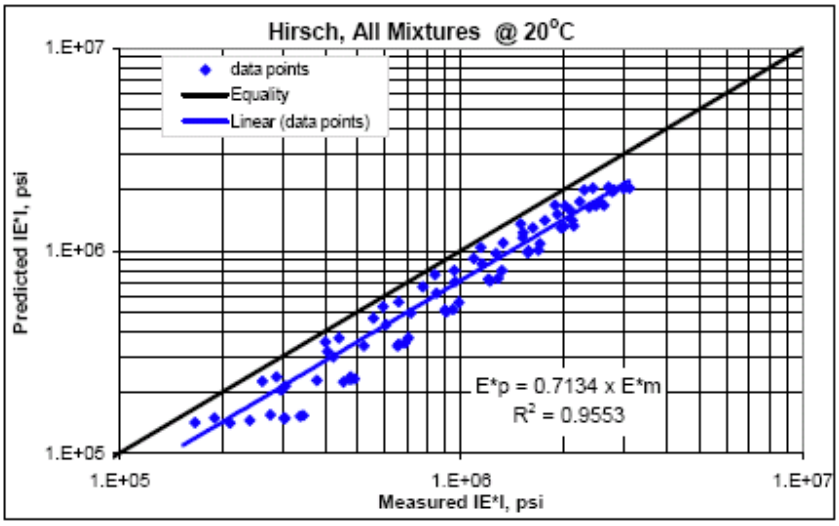

(b) Results for All Mixtures, Applying Hirsch Model.

Figure 2-8. Predicted Versus Observed E*(Garcia and Thompson, 2007)

Garcia and Thompson (2007) also compared the three models based on their E* data for Illinois mixtures (Figure 2-8). They found that the most promising model was the Hirsch model which showed the highest precision and the lowest bias. However in general, the model "under predicted" the E*. In a study conducted by Abdo et al. (2009), both the traditional and the new Witczak models were found to significantly over-estimated the dynamic modulus, as shown in Figure 2-9.

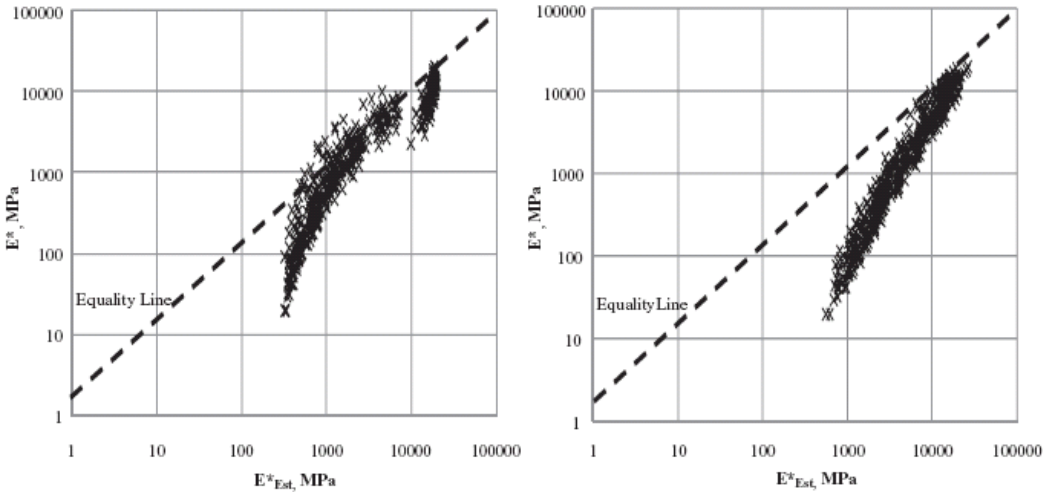

(a) Traditional Witczak model.(b)New Witczak Model

Figure 2-9. Predicted versus measured E* (Abdo et al. 2009)

The simplicity of the prediction models are another important criterion for evaluating the models as it will directly affect the easiness of obtaining input information and the required time/cost for achieving a reasonable prediction. Both the traditional and new Witczak predictive equation requires eight input parameters, which can be obtained through experimental testing, based on mix design information, or based on suggested values. The Hirsch model needs only three input parameters, which are available from the routine Superpave mix design process. Specifically, the Witczak models consider the effect of aggregates by four sieve sizes while the Hirsch model accounts for the overall gradation impact through a volumetric term VMA.

2.5.6 *Compactability*

Compaction is the process by which the volume of air in an HMA mixture is reduced by the application of external forces, which is also associated with the rearrangement of aggregate packing and the increase of the unit weight. There are a lot of factors influencing the compaction ability of the mixture in the field. Some of those factors include: aggregate characteristics, environmental conditions, compaction equipment and roller operation, gradation and lift thickness (Leiva-Villacorta 2007). In order to simulate the compaction behavior in the field, the Superpave mix design method uses the Superpave Gyratory Compactor (SGC) to compact the experimental samples. The SGC is designed to apply a compaction pressure of 600kPa (87psi) on the top of sample. In order to help achieving a particle densification condition like the mixture achieved in the field, the sample is inclined 1.25^{o}C and rotated at a frequency of 30 cycles per minute. The schematic picture of the compactor is shown in Figure 2-10. Researchers (Anderson et al. 2003) have proposed that the densification curve of the gyratory compactor compacting process is related to the aggregate strength and can be viewed as an indication of mixture strength and pavement performance. Different parameters and approaches were used to characterize the compactability of the mixtures, which are discussed below in details.

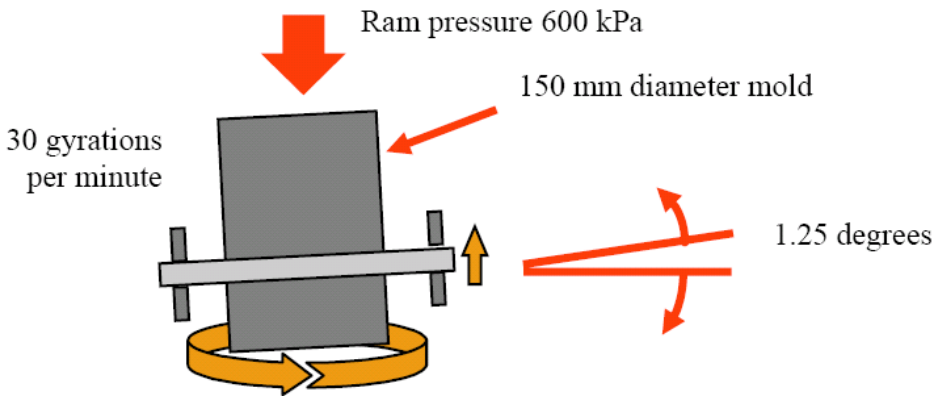

Figure 2-10. Schematic of gyratory compactor (Leiva-Villacorta 2007)

2.5.6.1 *Superpave mix design method (%Gmm@Nini) (Asphalt Institute SP-2 2001)*

The Superpave mix design method suggested using the percentage of maximum theoretical specific gravity at N_{ini} ($\%G_{mm}@N_{ini}$) to indicate the compactability of a mixture. Different from other criteria, this method specified maximum value requirements for $\%G_{mm}@N_{ini}$ based on different design EASLs to exclude the possibility of having tender mix which can be unstable under traffic loading.

2.5.6.2 *N@92%Gmm*

The number of gyration at which the sample reaches 92% relative density (92% Gmm) have been used to compare the compactability of the gyratory specimens (Asphalt Institute SP-2 2001). It is generally believed that a mix with lower gyration numbers at 92% Gmm will have better compactability. For the simplicity of the method,

Solaimanian (2007) in the NCHRP report 589 suggested using it for evaluating the compactability of warm mix asphalt mixtures. However, this method was found usually having greater variation (Leiva-Villacorta 2007).

2.5.6.3 *Compaction Energy Index(CEI)*

The CEI concept was defined by Bahia et al. (1998) as the area beneath the compaction curve from percent of Gmm at the 8th gyration to 92% of Gmm, as shown in Figure 2-11. Bahia reasoned that this index was analogous to the work applied by the roller to compact the mixtures to the required density during construction. A lower CEI value generally indicated that it took less energy to compact the mixtures during construction, while a too low value of CEI could be an indication of a tender mixture and should be avoided.

Bahia et al. (1998) also introduced the Traffic Densification Index (TDI) which is defined as the area beneath the compaction curve from 92% to 98% of Gmm. This index represents the energy required by traffic to density the mixture from 92% Gmm to a terminal density of 98% of Gmm. 98% of Gmm is considered a critical density, at which the mixture is approaching the plastic failure zone. Mixtures with lower values of CEI and higher values of TDI will have better constructability and performance.

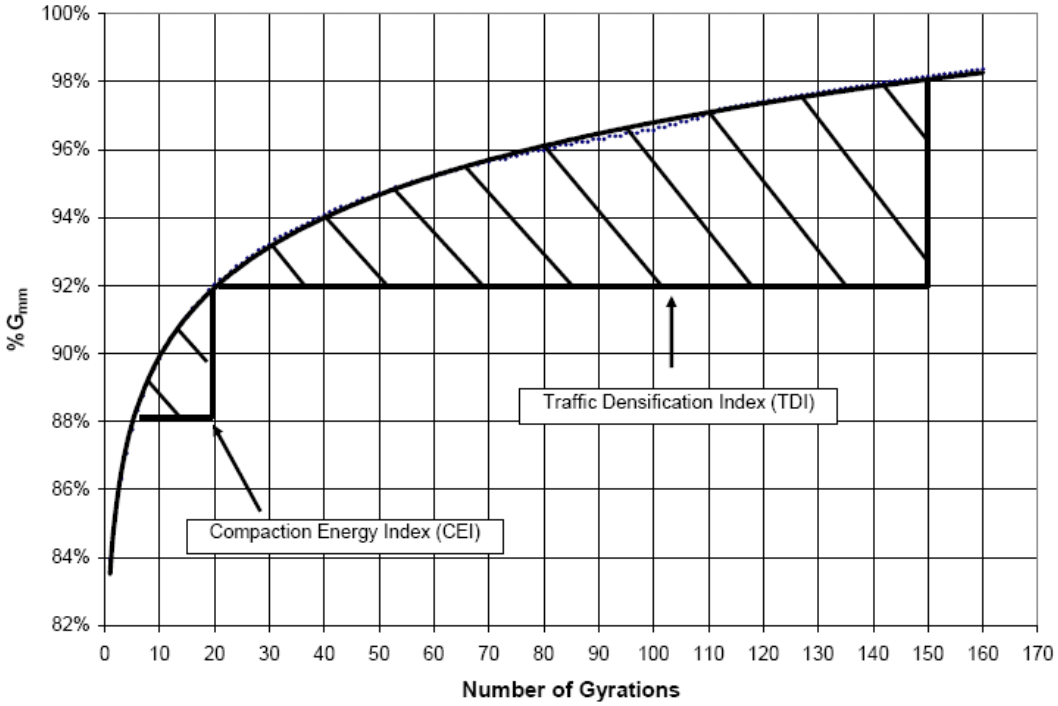

Figure 2-11. Gyration numbers V.S. % Gmm (Bahia et al. 1998)

2.5.6.4 *Compaction slope*

That aggregate characteristics, rather than asphalt binder characteristics, dominate the rate of compaction in the SGC is evident in Strategic Highway Research Program (SHRP) Report A-407 (Cominsky et al. 1994)

$$\text{Compaction slope} = 100 * \frac{C_{des} - C_{ini}}{\log(N_{des}) - \log(N_{ini})} \quad (2.21)$$

Where, C_{des} is the level of compaction achieved (density) at the design number of gyrations (N_{des}), and C_{ini} is the level of compaction achieved (density) at initial number of

gyrations (N_{ini}).

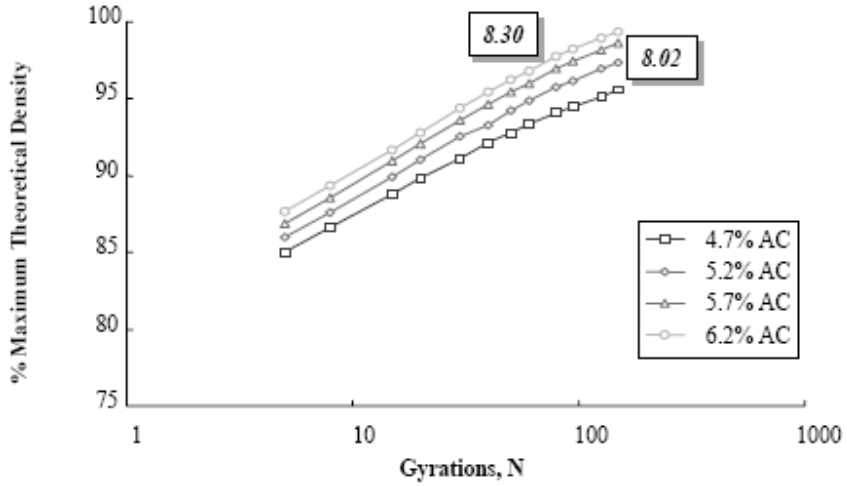

Figure 2-12. Effect of asphalt binder content on compaction slope

(Witczak et al. 2002)

Asphalt binder content was found to have little impact on the compaction slope when aggregate gradation was the same. Figure 2-12 showed that the compaction curves were almost parallel to each other for mixtures with different AC content but the same gradation when plotted on a semi-logarithmic graph. So the main problem in relating compaction slope to mixture performance properties is that the compaction slope, unlike mixture performance, is not sensitive to asphalt binder content. This was verified in the NCHRP 9-7 experiment, "Sensitivity of Superpave Mixture Tests to Changes in Mixture Components" (Anderson et al. 1998). From another point of view, the compaction slope

is mainly an aggregate structural issue.

It is generally accepted that finer gradations tend to have lower compaction slopes, and more rounded aggregates or those with less internal friction also tend to produce lower compaction slopes (Cominsky et al. 1994). Some previous researches (Anderson and Bahia 1997) found that higher compaction slope mixtures had higher shear stiffness and lower permanent shear strain. However, the differences between the mixture properties were not as great as expected for the wide range in compaction slopes. NCHRP 9-7 project also indicated the higher shear stiffness with higher compaction slope for project - Mississippi US-61, 12.5 mm mixture. Repeated shear testing performed by the Asphalt Institute on several asphalt mixtures from Northeast Texas (McGennis 1997) also indicates that a general trend to higher permanent shear strain as the percentage of sand is increased or as the compaction slope becomes smaller. These data are not conclusive, given that there are some outliers, but the general trend supports conventional expectations from experience.

2.5.6.5 *Locking points*

The locking point is defined as the gyration at which the aggregate skeleton "locks" together and further compaction will result in aggregate degradation and very little additional compaction. It was used to simulate the maximum number of roller passes in

the field before the increase in in-place density leveled off or decreased. This locking point is determined as the first gyration of three consecutive gyrations with the same height. Gyrations beyond this point exhibit a deviation from a uniform densification curve. Vavrik (2000) found that the locking point increased with the increase of design unit weight of the mixture. In addition, the increase in coarse aggregate volume resulted in an increase in the locking point, indicating reduced compactability. Reviewed based on the concept of Bailey's Method, Vavrik (2000) suggested that the locking point will only have little change when the design unit weight is below the loose unit weight, while it will change considerably when the design unit weight is above the loose unit weight. The advantage of the concept of locking point is that it captured the development of coarse aggregate interlock, however, some specimens may not able to find locking point before it reached the design volumetric state.

2.6 Summary of Literature Review

Aggregate gradation and properties were important properties of the HMA mixtures which could influence every aspect of the mix including volumetrics, stiffness, stability, durability, permeability, workability, fatigue resistance, frictional resistance and resistance to moisture damage. Based on a comprehensive literature review, this chapter summarized the development of aggregate gradation design methods and the VMA

requirement for mix design, with special focus on the correlations between aggregate gradation, volumetric properties, and mechanical performance (dynamic modulus, rutting resistance, and compactability). Although different efforts have been conducted to rationalize the aggregate gradation design and to develop gradations and mix designs based on field performance, it is found that none of existing methods have successfully correlated the aggregate gradation with performance. The packing theory and the discrete element method were considered as promising tools for the evaluation of aggregate gradations and to analyze the packing characteristics of aggregate structures.

As illustrated by literatures, dynamic Modulus (|E*|) is one of the key elements of a mechanistic-empirical based flexible pavement design procedure. It is used to characterize the material properties of asphalt mixtures and determine the stress strain responses of a pavement at different loading conditions, and is a direct input parameter in several pavement performance models to estimate the field fatigue cracking and rutting performance. As part of the asphalt mixture performance tests, the flow number has been found to be able to correlate well with the field rutting depth by a number of projects. Also, it is also concluded that the compactability analysis of experimental results can provide valuable guidance on the evaluation of the compactability of asphalt mixture in the field. In this chapter of literature review, the Witczak traditional model, New Witczak model and Hirsch model with some other prediction models were evaluated and

compared for their suitability to be used to correlate aggregate gradation with performance. Literature also revealed that those prediction models are still need local calibration if the engineers want to get a more accurate prediction of local asphalt mixture. As stated before, previous effects on the prediction of mechanical properties of asphalt mixture have been put on the dynamic modulus, and there is no widely applied flow number prediction model available at this moment. Some researchers Kaloush (2001) suggested flow number prediction models but are based on limited database. Hence, it will be a great value if a model capable of predicting or providing general guidance on the Flow Number characteristics based on a wider database.

CHAPTER 3 RESEARCH METHODOLOGY AND SCOPE

3.1 INTRODUCTION

This research aims to study the design and characterization of the viscoelastic asphalt mixtures based on particle packing theories, discrete element modeling method and mechanical modeling. The first portion of this research is to explore the feasibility of using discrete element method and packing theory to evaluate the packing characteristics of the asphalt mixture. Based on the findings, a new aggregate gradation design and mix design approach is proposed to help the selection and proportion of aggregates, producing mixtures with appropriate volumetric properties and good performance.

The other important portion of this study is to characterize the properties of asphalt mixture through DEM and macromechanical modeling. For DEM simulation, different contact models are studied to characterize the mechanical properties of asphalt mixture, and a proper model is established, calibrated and validated by experimental results. Different loading conditions are applied to study different traffic conditions. Also, the sensitivity analyses of model parameters are studied. As for macromechanical modeling, a constitutive model for characterizing the permanent deformation of asphalt mixture is explored by taking consideration of the directional distribution of aggregates (anisotropy), and the damage induced by plasticity. A commercial software PFC3D is used in this study for DEM simulation.

The scheme of research methodology is shown in Figure 3-1, separated by two central research objectives. To achieve the first central objective, this research will first conduct an analysis of packing theory to theoretically derive correlations between aggregate particle packing and volumetric properties. The discrete element method (DEM) will be used to simulate the characteristics of aggregate packing and investigate the degree of aggregate contact and interlocking, also a lot of collected data will be used to validate the findings from DEM. Secondly, the findings from the DEM modeling and packing analysis will be implemented into the experimental work to establish correlations between gradation parameters and laboratory performances of the mixes. Finally, a performance based aggregate gradation design method will be proposed and validated based on experimental and DEM simulation results. To achieve the second central objective, this research will first establish a micromechanical based 3D DEM model to capture the viscoelastic properties (dynamic modulus and phase angle) of asphalt mixture over a wide range of temperatures and frequencies. This model will further be extended to describe the strength properties of asphalt mixtures when damage is involved. Finally, a macromechanical based nonlinear elasto-visco-plastic constitutive model is developed to systematically describe the viscoelastic plastic behavior of asphalt mixtures. Such model has the unique advantages of considering anisotropic behavior and particle orientation for particulate asphalt mixture when both plastic deformation and fracture damage are

involved.

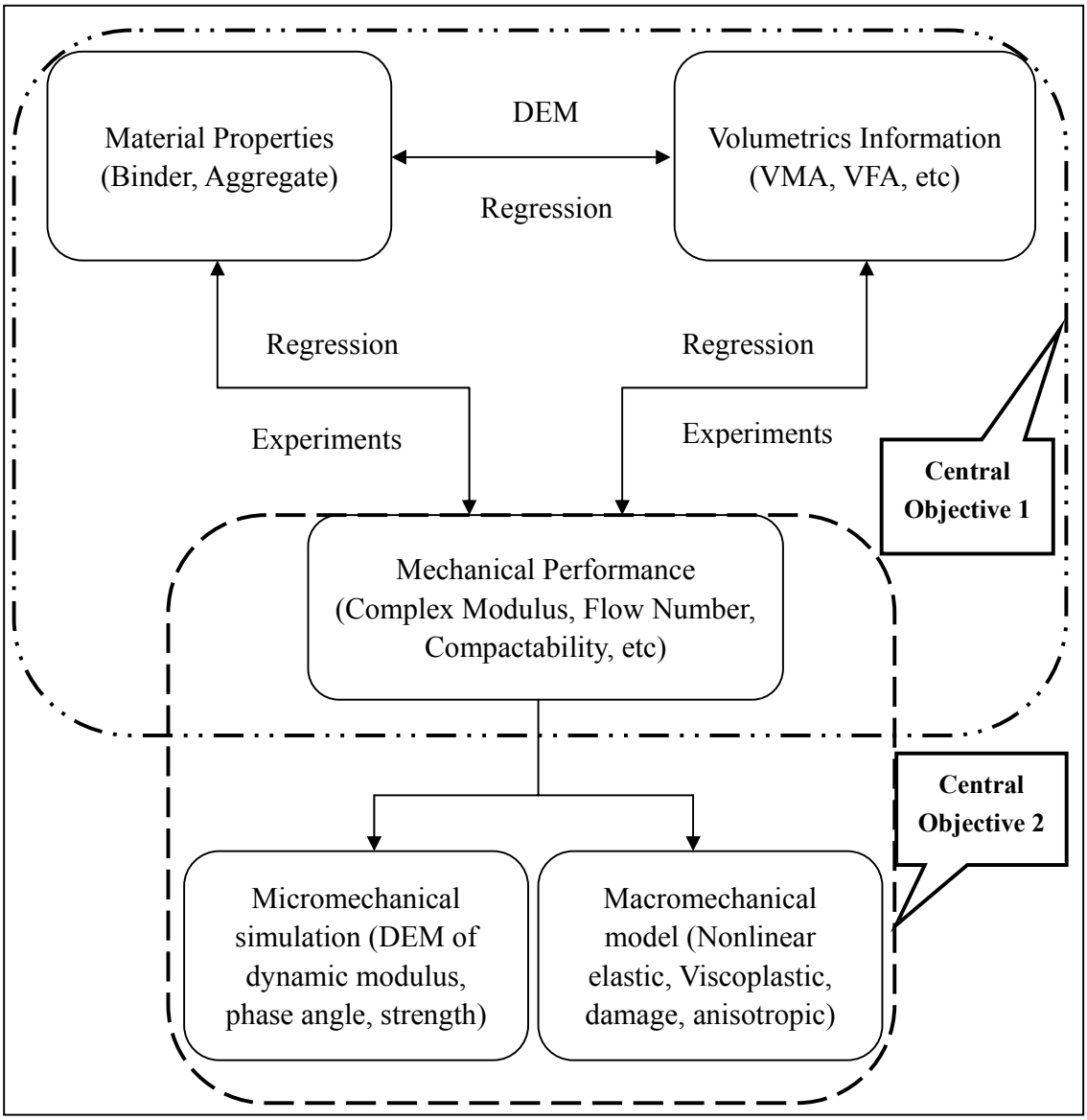

Figure 3-1. Scheme of research methodology

In summary, the key components of this study include the following six tasks.

Task 1: Explore the relation between aggregate properties and volumetrics based on aggregate packing and DEM simulation.

Task 2: Study the impact of aggregate gradation on the mechanical performance of asphalt mixture.

Task 3: Develop dynamic modulus and flow number prediction models.

Task 4: Develop an asphalt mixture design method to provide guidance with solid performance, at the same time, with convenience.

Task 5: Explore DEM simulation models which are capable of simulate the mechanical properties of asphalt mixture within a large range of temperatures, frequencies, and loading rates.

Task 6: Develop a macroscopic constitutive model which is able to capture the microscopic properties of asphalt mixture.

3.2 Relation Between Aggregate Properties and Volumetrics

The research approach of this section is based on packing theory to theoretically derive a correlation between aggregate structures and volumetric properties. A gradation weighing factor, f_v, which is the percent of voids change by volume due to the addition of unit aggregate, is developed to link the gradation information directly to the VMA. The

determination of f_v values involves two approaches, either from direct data regression when large numbers of mix designs with the same nominal maximum aggregate size are available; or from the discrete element modeling (DEM) simulation, and then mix design data from different states are used to verify the applicability of the proposed VMA prediction method to a wide aggregate sources and gradation distributions. Finally, the influence on the aggregate contact and interlocking are studied.

The research details and findings on this task is given in Chapter 5.

3.3 RELATION OF AGGREGATE PROPERTIES OF ASPHALT MIXTURE

This section will conduct a set of comprehensive experiments to evaluate the effect of aggregate properties and volumetrics on the mechanical performance of asphalt mixture. The research process including data analysis of experimental testing to establishes correlations between gradation parameters and laboratory mechanical performances of the mixes. The effect of aggregate gradation, with respect to individual sieve size and the whole gradation is evaluated. The performance evaluation parameters including dynamic modulus, compactability, and flow number, etc. The findings from experiments and data analysis will provide insight to the asphalt mixture and gradation design to achieve high performance mixtures.

The research details and findings on this task is given in Chapter 6.

3.4 DEVELOPMENT OF ASPHALT MIXTURE PERFORMANCE PREDICTION MODELING

Given the strong correlations among aggregate gradation, optimum asphalt content and volumetric properties, this section aims to develop a predictive model for mechanical properties of asphalt mixture based on aggregate degree of contact, aggregate gradation parameters and binder film thickness. This work is schematically shown in Figure 3-2.

To ensure the mixture have sound performance and high resistance to permanent deformation, low temperature cracking, and fatigue, a desired volumetric properties with appropriate VMA, air voids and asphalt content should be guaranteed. The volumetric information can be easily determined once the aggregate gradation and packing characteristics are known. This is because that VMA, which can be estimated by aggregate gradation and packing, is the sum of air voids and asphalt content by volume. For standard Superpave mixtures designed for 4% air voids, the design optimum asphalt content can then be obtained given the aggregate absorption rate is known. Since the surface area of aggregate particles has been found to be related to the gradation, the average asphalt film thickness can be estimated. Combining the effect of aggregates (aggregate contact and interlocking) and asphalt binder (binder type, viscoelastic

properties, and film thickness), it is hypothesized that a predictive model for AC mechanical performance (dynamic modulus as selected property for this study) can be developed. Based on DEM simulation, this prediction model can serve two functions: performance prediction and mix design optimization.

The research details and findings on this task are given in Chapter 7.

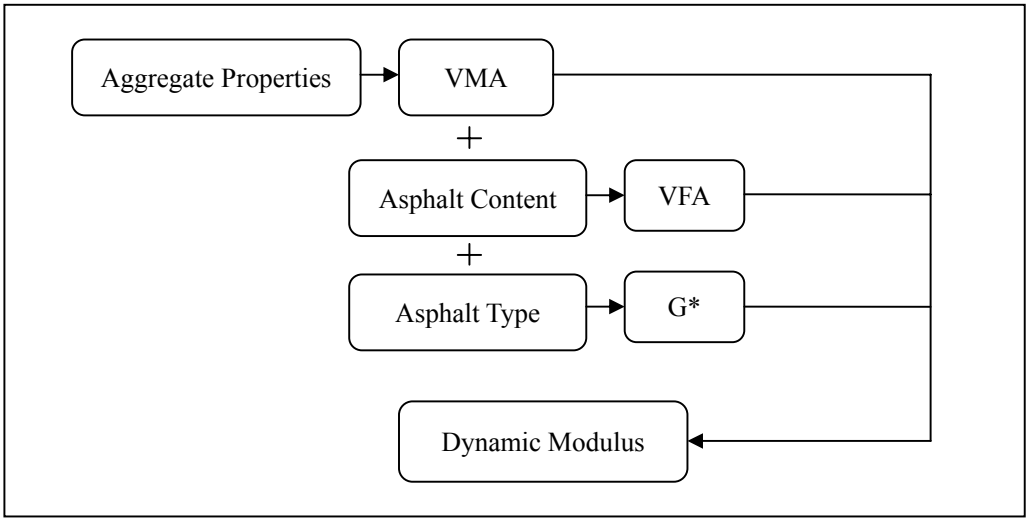

Figure 3-2. Methodology of the performance modeling

3.5 DEVELOPMENT OF MIXTURE DESIGN GUIDELINE

Based on the results of computational modeling and experimental validation, a new gradation design procedure will be developed. This guideline will introduce the parameters that are found can reasonably describe a gradation, and indicate the recommended control ranges of these parameters. A step by step guideline on how to use

the design method to design a gradation with more knowledge of aggregate structure and interlocking, and mixture volumetric properties, thereby, with more knowledge of expected performance, will be explained in great detail. This proposed gradation design guideline will also help the optimization of mix designs to achieve the most economical design with good field performance. In the end of the guideline, a design example will be attached which should help designer at different levels to quickly understand and apply this new method to practice.

The research details and findings on this task is given in Chapter 8.

3.6 CHARACTERIZATION OF ASPHALT MIXTURE WITH DEM

Asphalt mixture is a typical particulate system whose mechanical performance can be modeled based on the particle interactions (contacts) at microscale. Once calibrated microscopically, the model can be used to predict the macroscopic properties based on the same contact mechanisms. The effect of individual component on the performance of the mixture can also be captured by the calibrated micromechanical model.

In this study, firstly a three-dimensional DEM approach will be developed to model the complex modulus of asphalt mixtures. Complex modulus is a crucial viscoelastic material property which describes the stress and strain responses of asphalt mixtures and has been incorporated into the DARWin-ME mechanistic empirical pavement design

program to guide pavement design. The accurate information of volume, angularity, shape and texture are needed in order to reconstruct 3-D model of an aggregate particle in the computer. The University of Illinois Aggregate Image Analyzer (UIAIA) developed by Tutumluer and Carpenter. (2005) can provide accurate and automated measurement of individual particles. This research considers the effect of shape and angularity by combining tens of balls together in PFC3D to match the 3-D image of the individual particles obtained from the UIAIA. The effect of surface roughness is taken into account through model parameter assignment such as contact friction angle. The simulation results are calibrated based on experimental results to establish a reasonable DEM model for further evaluation. The details about generating particles and conducting DEM simulations are discussed in the later chapters.

Secondly, heavy traffic loading and large number of load repetitions can cause tremendous damage and premature failure to asphalt pavements that were designed for standard loads. Although there are many ways to assess the adequacy of a mix design to support heavy traffic loads, computational modeling is one of the promising approach because it provides convenience to evaluate the interaction and contribution of individual mixture component to the overall mix performance. In this study, a micromechanical three-dimensional discrete element method will be used to model the resistance of asphalt mixture to heavy loads; a displacement softening contact model will be

implemented for describing the damage of mixture under heavy load. The same aggregate clumping techniques are applied here to study the strength tests. After calibrated by constant rate uniaxial compression test, this model will be further used to evaluate the effect of particle angularity and loading rates on mix strength performance.

The research details and findings on this task is given in Chapter 9.

3.7 CHARACTERIZATION OF ASPHALT MIXTURE WITH MACROMECHANICAL MODELING

Rutting, one of the primary distresses in asphalt mixtures, is influenced by the nonlinear deformation of mixture constituents, the microstructural features of the mixes such as the directional distribution of aggregates (anisotropy), and the damage induced by plasticity. The construction of a successful constitutive model for characterizing the permanent deformation of asphalt mixtures must account for these features and their interactions. This study develops a nonlinear elasto-visco plastic model to systematically account for the aggregate directional distribution and damage propagation during the accumulation of permanent deformation. This is accomplished by incorporating a fabric tensor for aggregates and a direction dependent damage parameter into the yield and potential functions and by the use of Perzyna's viscoplastic formulation. The comparison of indirect tensile test results with the predictions from the model show that the model is

adequate in capturing the permanent deformation performance of asphalt mixtures.

The research details and findings on this task are given in Chapter 10.

CHAPTER 4 OVERVIEW OF DISCRETE ELEMENT METHOD

This chapter provides a brief overview of the methodology of the discrete element method and its applications in the pavement engineering. The key components of the DEM simulations are also provided.

4.1 INTRODUCTION OF DISCRETE ELEMENT METHOD

The discrete element method (DEM) can be used to simulate the movement and interaction of stressed assemblies of rigid spherical particles. In 1971, Cundall (1971) firstly introduced the DEM method and used it in the analysis of rock-mechanics problems. Later Cundall and Strack (1979) applied this method to soils.

PFC^{3D} is an abbreviation of *Particle Flow Code in Three-Dimensions*. It is a commercial DEM model software developed by Itasca Consulting Group, Inc. *PFC*^{3D} is classified as a *discrete element* code based on the definition in the review by Cundall and Hart (1992). Since it allows finite displacements and rotations of discrete bodies including complete detachment, and recognizes new contacts automatically as the calculation progresses, *PFC3D* has been viewed as a simplified implementation of the DEM because of the restriction to rigid spherical particles.

In the DEM, the interaction of the particles is treated as a dynamic process with

states of equilibrium developing whenever the internal forces balance. The contact forces and displacements of a stressed assembly of particles are found by tracing the movements of the individual particles. Movements result from the propagation through the particle system of disturbances caused by specified wall and particle motion and/or body forces. This is a dynamic process in which the speed of propagation depends on the physical properties of the discrete system.

The dynamic behavior is represented numerically by a timestepping algorithm in which it is assumed that the velocities and accelerations are constant within each timestep. The solution scheme is identical to that used by the explicit finite-difference method for continuum analysis. The DEM is based upon the idea that the timestep chosen may be so small that, during a single time step, disturbances cannot propagate further from any particle than its immediate neighbors. Then, at all times, the forces acting on any particle are determined exclusively by its interaction with the particles with which it is in contact. Since the speed at which a disturbance can propagate is a function of the physical properties of the discrete system, the timestep can be chosen to satisfy the above constraint. The use of an explicit, as opposed to an implicit, numerical scheme makes it possible to simulate the nonlinear interaction of a large number of particles without excessive memory requirements or the need for an iterative procedure.

The calculations performed in the DEM alternate between the application of

Newton's second law to the particles and a force-displacement law at the contacts. Newton's second law is used to determine the motion of each particle arising from the contact and body forces acting upon it, while the force-displacement law is used to update the contact forces arising from the relative motion at each contact. The presence of walls in PFC3D requires only that the force-displacement law account for ball-wall contacts. Newton's second law is not applied to walls, since the wall motion is specified by the user.

There are three critical components for a DEM simulation: (a) calculation cycle and algorithm, (b) particle generation and properties, and (c) contact detection and models.

4.2 Calculation Cycle and Algorithm

The calculation cycle in PFC3D is a timestepping algorithm that requires the repeated application of the law of motion to each particle, a force-displacement law to each contact, and a constant updating of wall positions. Contacts, which may exist between two balls, or between a ball and a wall, are formed and broken automatically during the course of a simulation. The calculation cycle is illustrated in Figure 4-1. At the start of each timestep, the set of contacts is updated from the known particle and wall positions. The force-displacement law is then applied to each contact to update the contact forces based on the relative motion between the two entities at the contact and the

contact constitutive model. Next, the law of motion is applied to each particle to update its velocity and position based on the resultant force and moment arising from the contact forces and anybody forces acting on the particle. Also, the wall positions are updated based on the specified wall velocities. The calculations performed in each of the two boxes of Figure 4-1 can be done effectively in parallel. The force-displacement law is described first, followed by a description of the law of motion. The development is for the three-dimensional case.

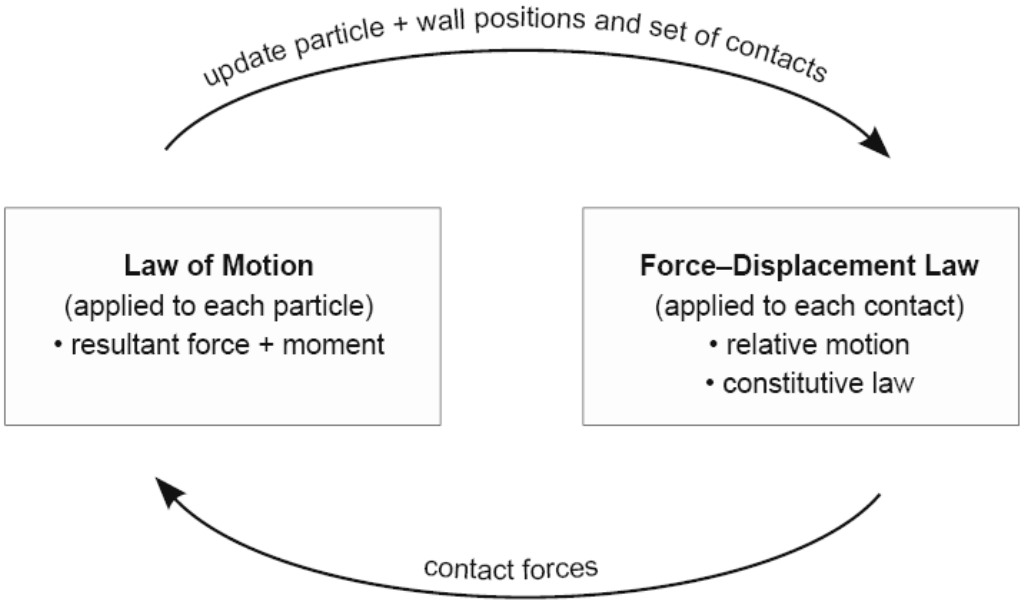

Figure 4-1. Calculation cycle in PFC3D(PFC3D manual)

4.3 Particle Generation and Clump

There are two commands that can be used to create particles: BALL and GENERATE. Clumps can be created by using the CLUMP replace command to replace particles. There are two main categories of particle assemblies: regular and irregular. A regular assembly is one that contains repeating patterns of particles. This type of packing may be used to represent structural members such as beams. Initial contact forces may be prescribed exactly when setting up a regular assembly, because normal contact forces are determined solely from the relative positions of the particles in contact. The second type of packing (irregular) has no discernible pattern in the arrangement of particles. Usually, this type of assembly is used to represent a solid or granular material with an internal structure that is not ordered (e.g. asphalt concrete that consists of aggregate particles). In DEM, the clump technique provides a methodology to simulate very complex physical properties of the material. Aggregate shape and angularity can be similarly represented and modeled using clusters of particles forming particle clumps. The clump technique is made a group of round balls clumping together to behaves as one rigid body, and the motion of a clump is determined by the resultant force and moment vectors acting upon it. The contact forces only exist between clumps and the contacts internal to the clump are skipped during the calculation to save computer time. However, contacts with particles external to the clump are not affected. Particles within a clump may overlap to any extent;

and it will not generate internal contact forces, and any contact forces that exist when the clump is created will be preserved unchanged during cycling. Thus, a clump is unbreakable regardless of the forces acting upon it. In this sense, a clump differs from a group of particles that are bonded to one another.

4.4 Contact Detection and Models

The overall constitutive behavior of a material is simulated in PFC3D by associating a simple constitutive model with each contact. The constitutive model acting at a particular contact consists of three parts: a stiffness model; a slip model; and a bonding model. The stiffness model provides an elastic relation between the contact force and relative displacement. The slip model enforces a relation between shear and normal contact forces such that the two contacting balls may slip relative to one another. The bonding model serves to limit the total normal and shear forces that the contact can carry by enforcing bond-strength limits.

4.4.1 *Contact Detection*

The force-displacement law is described for both ball-ball and ball-wall contacts. For ball-ball contact, the relevant equations are presented for the case of two spherical particles, labeled A and B in Figure 4-2(a). For ball-wall contact, the relevant equations

are presented for the case of a spherical particle and a wall, labeled b and w, respectively, in Figure 4-2(b) . In both cases, U^n defined to be the relative contact displacement in the normal direction, is given by:

$$U^n = \begin{cases} R^{[\mathrm{A}]} + R^{[\mathrm{B}]} - d, & \text{(ball-ball)} \\ R^{[\mathrm{b}]} - d, & \text{(ball-wall)} \end{cases} \tag{4.1}$$

where

$$d = \left| x_i^{[\mathrm{B}]} - x_i^{[\mathrm{A}]} \right| = \sqrt{\left(x_i^{[\mathrm{B}]} - x_i^{[\mathrm{A}]} \right) \left(x_i^{[\mathrm{B}]} - x_i^{[\mathrm{A}]} \right)} \qquad \text{(ball-ball)} \tag{4.2}$$

And for ball-wall contact, d equals to the distance between the ball center and the wall. $x_i^{[A]}$ and $x_i^{[B]}$ are the position vectors of the centers of balls A and B, and $R^{[\Phi]}$ is the radius of ball Φ.

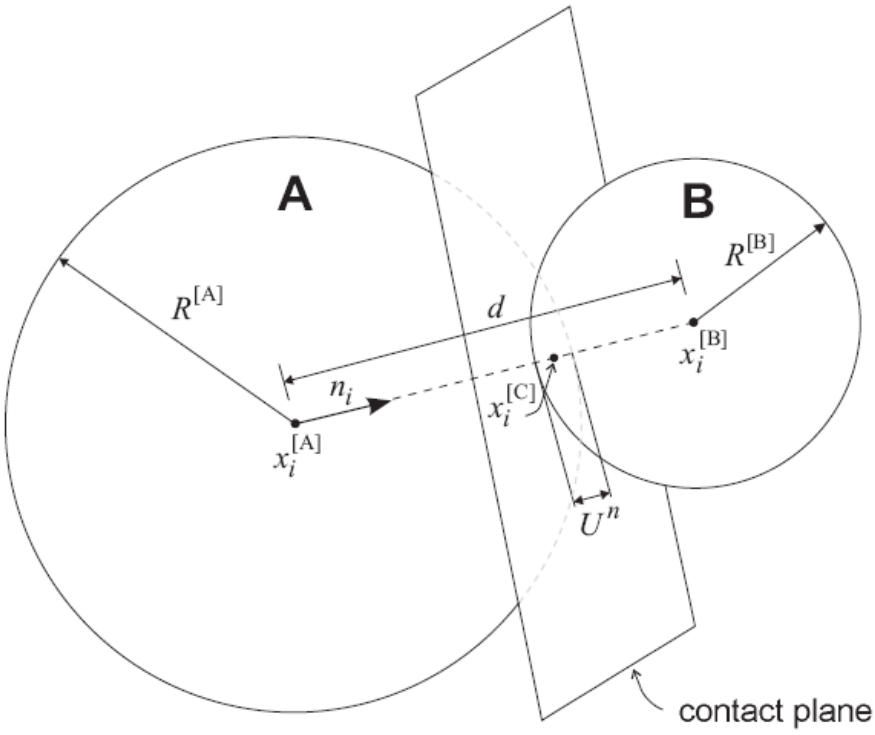

(a) ball-ball contact

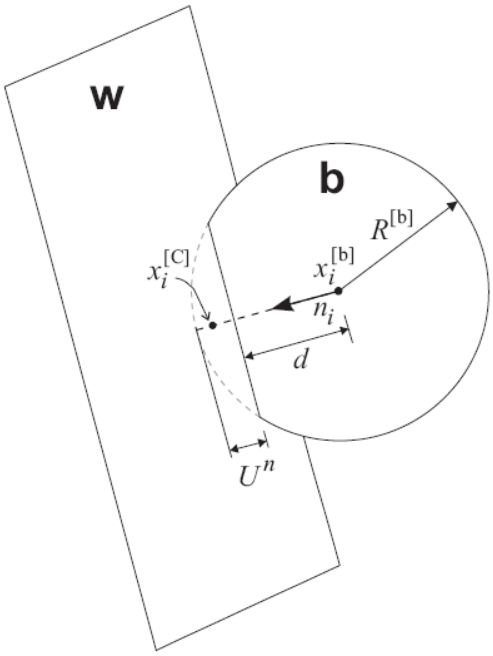

(b) ball-wall contact

Figure 4-2. Notation used to describe contact(PFC3D manual)

As given in Equation (4.3) is the criterion for determinate whether a contact occurs or not.

$$\begin{cases} U^n < 0 & \text{No contact} \\ U^n \geq 0 & \text{Contact occurs} \end{cases} \tag{4.3}$$

If contact occurs, the position of contact point is given by

$$x_i^{[C]} = \begin{cases} x_i^{[A]} + \left(R^{[A]} - \frac{1}{2}U^n\right) n_i, & \text{(ball-ball)} \\ x_i^{[b]} + \left(R^{[b]} - \frac{1}{2}U^n\right) n_i, & \text{(ball-wall)} \end{cases} \tag{4.4}$$

4.4.2 *Contact-Stiffness Models*

The contact stiffnesses relate the contact forces and relative displacements in the

normal and shear directions are shown here.

The normal stiffness is secant stiffness,

$$F_i^n = K^n U^n n_i \tag{4.5}$$

since it relates the total normal force to the total normal displacement.

The shear stiffness is a tangent stiffness,

$$\Delta F_i^s = -k^s \Delta U_i^s \tag{4.6}$$

since it relates the increment of shear force to the increment of shear displacement.

The contact stiffnesses used in the above equations are assigned different values depending upon the contact-stiffness model employed. PFC3D provides two contact-stiffness models: a linear model and a simplified Hertz-Mindlin model. Contact between a ball with the linear model and a ball with the Hertz model is not allowed, since the behavior is undefined. Also, the Hertz model is incompatible with any type of bonding, since the Hertz model is not defined for tensile forces.

The linear contact model is defined by the normal and shear stiffnesses kn and ks [force/displacement] of the two contacting entities (ball-to-ball or ball-to-wall). The contact stiffnesses for the linear contact model are computed assuming that the stiffnesses of the two contacting entities act in series. The contact normal secant stiffness is given by

$$K^n = \frac{k_n^{[A]} k_n^{[B]}}{k_n^{[A]} + k_n^{[B]}} \tag{4.7}$$

and the contact shear tangent stiffness is given by

$$k^s = \frac{k_s^{[A]} k_s^{[B]}}{k_s^{[A]} + k_s^{[B]}} \tag{4.8}$$

where the superscripts [A] and [B] denote the two entities in contact. For the linear model, the normal secant stiffness k_n is equal to the normal tangent stiffness, since

$$k^n \equiv \frac{dF^n}{dU^n} = \frac{d(K^n U^n)}{dU^n} = K^n \tag{4.9}$$

4.4.3 *The Slip Model*

The slip model is an intrinsic property of the two entities (ball-ball or ball-wall) in contact. It provides no normal strength in tension and allows slip to occur by limiting the shear force. This model is always active, unless a contact bond is present — in which case, the contact bond model behavior supersedes the slip model behavior. These two models describe the constitutive behavior for particle contact occurring at a point. The parallel-bond model, on the other hand, describes the constitutive behavior for cementitious material existing between the two balls. These two behaviors can occur simultaneously; thus, in the absence of a contact bond, the slip model is active in conjunction with the parallel-bond model. The slip model is defined by the friction

coefficient at the contact μ [dimensionless], where μis taken to be the minimum friction coefficient of the two contacting entities.

The criterion of no-normal strength is enforced by checking whether the overlap, given by follow equation, is less than or equal to zero. If it is, then both the normal and shear contact forces are set to zero. The contact is checked for slip conditions by calculating the maximum allowable shear contact force

$$F^s_{\max} = \mu |F^n_i| \tag{4.10}$$

If $|F^s_i| > F^s_{\max}$, then slip is allowed to occur (during the next calculation cycle) by setting the magnitude of F^s_i equal to $F^s_{\max}$ via

$$F^s_i \leftarrow F^s_i \left(F^s_{\max}/|F^s_i|\right) \tag{4.11}$$

4.4.4 *The Bonding Model*

4.4.4.1 *The contact bond*

A contact bond can be envisioned as a pair of elastic springs (or a point of glue) with constant normal and shear stiffnesses acting at the contact point. These two springs have specified shear and tensile normal strengths. The existence of a contact bond precludes the possibility of slip. Instead, the magnitude of the shear contact force is limited by the shear contact bond strength. Contact bonds also allow tensile forces to develop at a contact. These forces arise from when there is no overlapping. In this case, the contact

bond acts to bind the balls together. The magnitude of the tensile normal contact force is limited by the normal contact bond strength.

If the magnitude of the tensile normal contact force equals or exceeds the normal contact bond strength, the bond breaks, and both the normal and shear contact forces are set to zero. If the magnitude of the shear contact force equals or exceeds the shear contact bond strength, the bond breaks, but the contact forces are not altered, provided that the shear force does not exceed the friction limit and provided that the normal force is compressive.

The constitutive behavior relating the normal and shear components of contact force and relative displacement for particle contact occurring at a point is shown in Figure 4-3. At any given time, either the contact-bond model or the slip model is active. In this figure, Fn is the normal contact force, where Fn> 0 indicates tension; Un is the relative normal displacement, where Un > 0indicates overlap; Fs is the magnitude of the total shear contact force; and Us is the magnitude of the total shear displacement measured relative to the location of the contact point when the contact bond was formed. Note that an additional force and moment may also be acting, as well as the force shown in Figure 4-3, if a parallel bond is present.

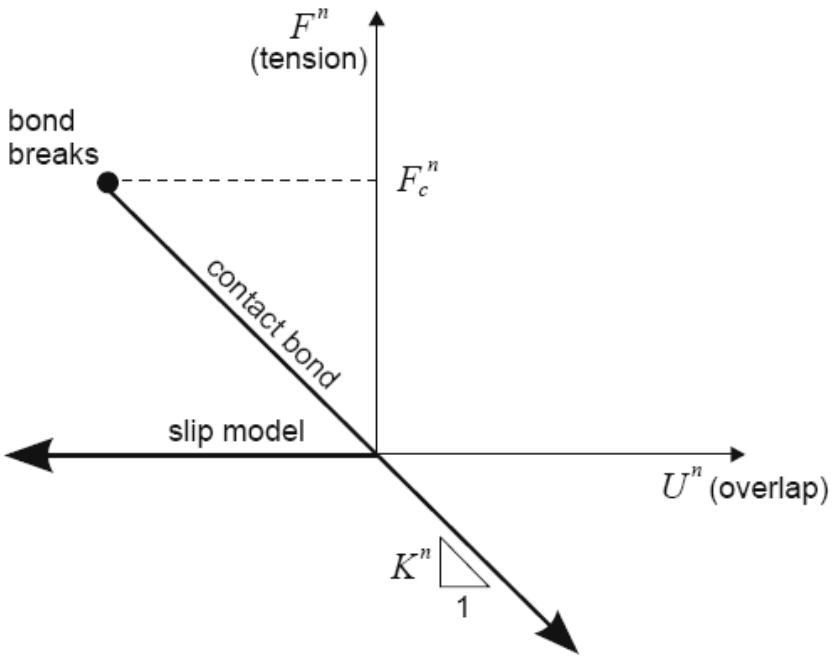

(a) normal component of contact force

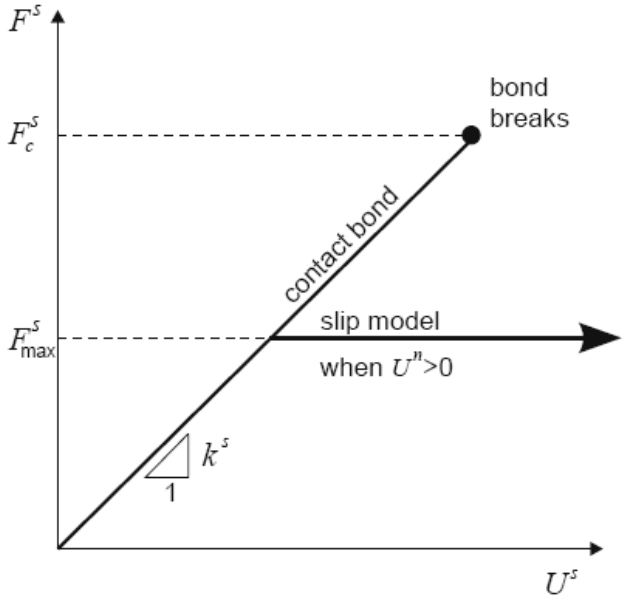

(b) shear component of contact force

Figure 4-3. Constitutive behavior for contact occurring at a point(PFC3D manual)

4.4.4.2 *The parallel bond*

The parallel-bond model describes the constitutive behavior of a finite-sized piece of cementitious material deposited between two balls. These bonds establish an elastic interaction between particles that acts in parallel with the slip or contact-bond models described above. Thus, the existence of a parallel bond does not preclude the possibility of slip. Parallel bonds can transmit both forces and moments between particles, while contact bonds can only transmit forces acting at the contact point. Thus, parallel bonds may contribute to the resultant force and moment acting on the two bonded particles.

A parallel bond can be envisioned as a set of elastic springs with constant normal and shear stiffnesses, uniformly distributed over a circular disk lying on the contact plane and centered at the contact point. These springs act in parallel with the point-contact springs that are used to model particle stiffness at a point. Relative motion at the contact (occurring after the parallel bond has been created) causes a force and a moment to develop within the bond material as a result of the parallel-bond stiffnesses. This force and moment act on the two bonded particles and can be related to maximum normal and shear stresses acting within the bond material at the bond periphery. If either of these maximum stresses exceeds its corresponding bond strength, the parallel bond breaks.

4.4.5 *Burger's Model*

Burger's model is implemented in PFC3D for simulation of more complex contact behavior. The model contains the Kelvin model and the Maxwell model, which are connected in series in both the normal and shear directions, respectively, at a contact point. The Burger's contact model uses eight parameters to describe the contact relations between two microscopic particles, as indicated in Figure 4-4. The eight parameters are:

normal viscosity for Kelvin section (Ckn)

normal viscosity for Maxwell section (Cmn

shear viscosity for Kelvin section (Cks)

shear viscosity for Maxwell section (Cms)

normal stiffness for Kelvin section (Kkn)

normal stiffness for Maxwell section (Kmn)

shear stiffness for Kelvin section (Kks)

shear stiffness for Maxwell section (Kms)

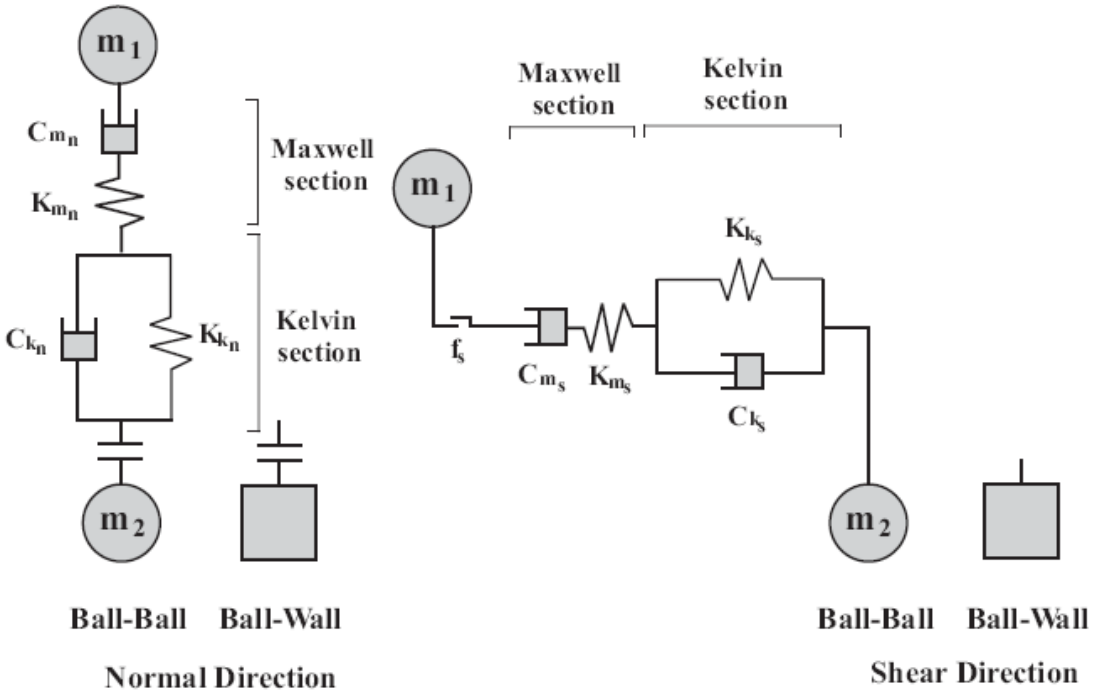

Figure 4-4. Mechanical entities comprising the Burger's model(PFC3D manual)

The total displacement u of Burger's model composed of three components, the displacement of the Kelvin section (u_k) and the Maxwell section (u_{mK} ,u_{mC}).

$$u = u_k + u_{mK} + u_{mC} \tag{4.12}$$

The first and second derivatives of displacement are given by

$$\dot{u} = \dot{u}_k + \dot{u}_{mK} + \dot{u}_{mC} \tag{4.13}$$

$$\ddot{u} = \ddot{u}_k + \ddot{u}_{mK} + \ddot{u}_{mC} \tag{4.14}$$

The contact forces, f, using the Kelvin section and the first derivative, are given by

$$f = \pm K_k u_k \pm C_k \dot{u}_k \tag{4.15}$$

$$\dot{f} = \pm K_k \dot{u}_k \pm C_k \ddot{u}_k \tag{4.16}$$

Note that the symbols $\pm$ and $\mp$ correspond to the cases of normal direction and shear direction, respectively. (For example, $\pm$ means + for normal direction and $-$ for shear direction.)

Also, the contact forces, f, can be expressed using stiffness K_m and viscosity C_m of the Maxwell section,

$$f = \pm K_m u_{mK} \tag{4.17}$$

$$\dot{f} = \pm K_m \dot{u}_{mK} \tag{4.18}$$

$$\ddot{f} = \pm K_m \ddot{u}_{mK} \tag{4.19}$$

$$f = \pm C_m \dot{u}_{mC} \tag{4.20}$$

$$\dot{f} = \pm C_m \ddot{u}_{mC} \tag{4.21}$$

The second-order differential equation for contact force f is given by

$$f + \left[\frac{C_k}{K_k} + C_m\left(\frac{1}{K_k} + \frac{1}{K_m}\right)\right]\dot{f} + \frac{C_k C_m}{K_k K_m}\ddot{f} = \pm C_m \dot{u} \pm \frac{C_k C_m}{K_k}\ddot{u} \tag{4.22}$$

From Equation (4.15), the rate of displacement of the Kelvin section is given by:

$$\dot{u}_k = \frac{-K_k u_k \pm f}{C_k} \tag{4.23}$$

With a central difference approximation of the finite difference scheme, this equation can be expressed as follow:

$$\frac{u_k^{t+1}-u_k^t}{\Delta t}=\frac{1}{C_k}\left[-\frac{K_k\left(u_k^{t+1}+u_k^t\right)}{2}\pm\frac{f^{t+1}+f^t}{2}\right] \tag{4.24}$$

Hence,

$$u_k^{t+1}=\frac{1}{A}\left[Bu_k^t\pm\frac{\Delta t}{2C_k}\left(f^{t+1}+f^t\right)\right] \tag{4.25}$$

Where,

$$A=1+\frac{K_k\Delta t}{2C_k} \tag{4.26}$$

$$B=1-\frac{K_k\Delta t}{2C_k} \tag{4.27}$$

While, for the Maxwell section, the displacement and the first derivative are given by following equations,

$$u_m=u_{mK}+u_{mC} \tag{4.28}$$

$$\dot{u}_m=\dot{u}_{mK}+\dot{u}_{mC} \tag{4.29}$$

Substituting Equation (4.18) and Equation (4.20) into Equation (4.29),

$$\dot{u}_m=\pm\frac{\dot{f}}{K_m}\pm\frac{f}{C_m} \tag{4.30}$$

With a central difference approximation of the finite difference scheme, this equation can be expressed as follow:

$$\frac{u_m^{t+1}-u_m^t}{\Delta t}=\pm\frac{f^{t+1}-f^t}{K_m\Delta t}\pm\frac{f^{t+1}-f^t}{2C_m} \tag{4.31}$$

Therefore,

$$u_m^{t+1} = \pm\frac{f^{t+1} - f^t}{K_m} \pm \frac{\Delta t\left(f^{t+1} - f^t\right)}{2C_m} + u_m^t \tag{4.32}$$

Since the total displacement and first derivative of the Burger's model can be given as,

$$u = u_k + u_m \tag{4.33}$$

$$\dot{u} = \dot{u}_k + \dot{u}_m \tag{4.34}$$

Using the finite difference scheme, the time derivative of displacement can be expressed as,

$$u^{t+1} - u^t = u_k^{t+1} - u_k^t + u_m^{t+1} - u_m^t \tag{4.35}$$

Substitute Equations (4.25) and (4.32) into Equation (4.35), then, the contact force,

$$f^{t+1} = \pm\frac{1}{C}\left[u^{t+1} - u^t + \left(1 - \frac{B}{A}\right)u_k^t \mp Df^t\right] \tag{4.36}$$

Where,

$$C = \frac{\Delta t}{2C_k A} + \frac{1}{K_m} + \frac{\Delta t}{2C_m} \tag{4.37}$$

$$D = \frac{\Delta t}{2C_k A} - \frac{1}{K_m} + \frac{\Delta t}{2C_m} \tag{4.38}$$

So, the contact force f^{t+1} can be calculated from known values of u^{t+1}, u^t u_k^t and f^t.

4.4.6 *The previous application of DEM on asphalt mixture*

A contact model was used to define the physical behaviors between particles or

particle and boundary walls. Different models and material properties should be chosen to take into account various materials before loads were applied to the model.

Figure 4-5 showed different models to represent micromechanics behavior between AC model particles. That is (a) Wall-Mastic (W-M), (b) Mastic-Mastic (M-M), (c) Aggregate-Mastic (A-M), (d) Aggregate-Aggregate (A-A), and (e) Wall-Aggregate (W-A). (Zelelew2007)

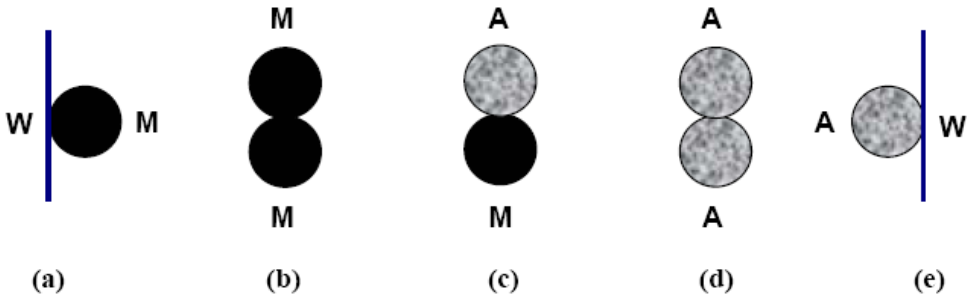

Figure 4-5. Different contact models for particles and walls(Zelelew2007)

Previous studies showed that the aggregate elastic modulus value of 30 GPa would predict satisfactory Simple Performance Test (SPT) parameters (Abbas et al. 2005). Habtamu (2007) used the elastic modulus of 30GPa and assumed that the rigid wall stiffness to be 10 times stiffer than the particles stiffness. Also, he used an aggregate-to-aggregate contact friction coefficient μ=0.5, which corresponds to an angle of internal friction of 27^{o}.In the biaxial test simulation, the axial stress and axial strain of

a rectangular sample were recorded during the PFC-2D run.

Buttlar and You (2001), You and Buttlar (2002) obtained the macro-scale stiffness of the specimen from the stress–strain curve. Sensitivity analysis indicated that the overall specimen modulus was not very sensitive to the aggregate modulus. You and Buttlar therefore used a typical value of 55.5 GPa for their simulation model runs. Figure 4-6 is the model introduced by Hashin (1965) and used by You and Buttlar (2004) in their research.

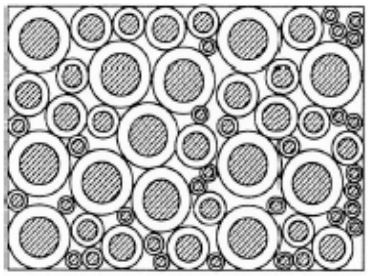

Figure 4-6. Composite spheres model (Hashin 1965)

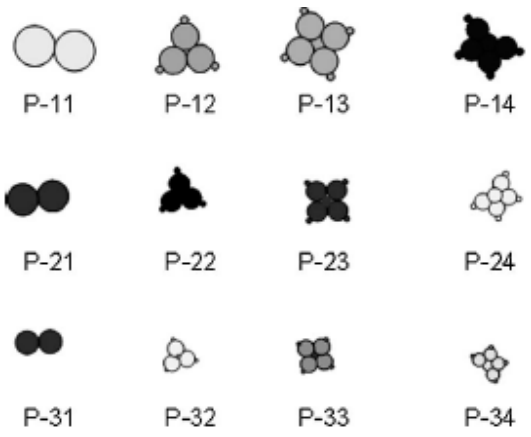

Figure 4-7. Angularity of the particles model (Hossain et al. 2007)

Hossain et al. (2007) analyzed the angular ballast breakage behavior under cyclic loading. Under this research, an assembly of ballast particles of irregular shapes was considered and the angularity of the particles was modeled by clumping two to nine circular particles together to form single particles of twelve different sizes. The models are shown in Figure 4-7. Contact normal stiffness (kn) of the disks was set to 5·109 N/m, and the contact shear stiffness (ks) was set to half of the contact normal stiffness because results are not affected significantly by different ratios of kn/ks.

4.5 SUMMARY

This chapter introduced the key concepts for understanding of DEM simulation, and also described some potential models could be used for model asphalt mixture in details. As the Burger's model can capture the visco properties of asphalt mixture, it can be a good

option for the model of dynamic modulus and phase angle simulations. What's more, in order to accurately reflect the aggregate to aggregate contact and the physical geometry of the aggregate, the concept of clump technique is introduced.

The DEM allows the finite displacement and rotation of aggregate particles to simulate the complex micro-behavior between aggregate within the mixture. It has been proved to be an effective method to model discontinuous material such rocks and granular materials. In this research, the DEM approach will be used to study the characteristics of particulate asphalt mixtures.

PFC3D is considered to be a promising tool for performing DEM simulations. There are several advantages of using PFC^{3D} to simulate the aggregate compaction. First, the balls in PFC^{3D} can effectively represent the aggregate with physical properties implemented. Second, the aggregate-to-aggregate contact and friction can be handled. Third, the contact force within the mixture and the air void can be measured easily and accurately. PFC^{3D} DEM modeling program will therefore be used in this study to model the packing characteristics of aggregates and correlate aggregate packing with mixture performance.

CHAPTER 5 AGGREGATE GRADATION AND VOLUMETRIC PROPERTIES

This chapter conducts an analysis of aggregate packing to derive theoretical correlations between aggregate gradation properties and volumetric properties. The discrete element method (DEM) is used to simulate the characteristics of aggregate packing and investigate the degree of aggregate contact and interlocking. The findings from the DEM modeling and packing analysis will be implemented into the experimental work to establish correlations between gradation parameters and laboratory mechanical performances of the mixes including dynamic modulus, compactability, and flow number, which will be detailed in Chapter 6. And then, dynamic modulus and flow number prediction models will be provided in Chapter 7. Finally, a gradation design guideline that is calibrated for Washington mixtures will be suggested in Chapter 8 to correlate aggregate gradation with target volumetric properties and expected performance.

5.1 Characterization of Aggregate Gradation and Gradation Curves

As a first step for a systematic gradation design, more scientific definitions of gradation types and shapes are needed. Aggregate can play a very different role for different types

of gradations, coarse-graded or fine-graded. Conceptually, coarse and fine graded mixtures are usually categorized depending on whether the gradation curve is passing below or above the maximum density line. Although these different gradations can behave quite differently in terms of particle packing, volumetric properties, and field performance, existing methods have no clear definition to differentiate these different gradation types. Therefore, this study will start with the development of a clear definition to characterize and categorize the different gradation types. Particularly, the new definition will be based on packing theory and can be related to the aggregate contact performance. This study will use 12.5mm NMAS as an example as it is the most popular type of asphalt mixtures in the United States.

5.1.1 *Background*

Based on the different shapes of gradation curves and the packing nature of the mix structures, HMA can be divided into three major types: dense-graded mixtures, gap-graded mixtures and open-graded mixtures. This study will focus on dense-graded gradation for dense-graded mixture is the most commonly used HMA mix type which is designed to have dense structure to prevent moisture infiltration at the same time maintain adequate voids to allow asphalt expansion. The dense-graded gradation can be further categorized into dense/dense graded, dense/coarse-graded (coarse-graded) and

dense/fine-graded (fine-graded) mixtures. Traditionally, coarse-graded gradation is defined as mixtures that are somewhat coarser than the maximum density gradation, while fine-graded gradation is mixtures somewhat finer than the maximum density gradation. The Power Law Method (Ruth 2000) introduced a concept on how to categorize coarse-graded and fine-graded aggregates as shown in Figure 5-1.The equations of the power law regression are given as below.

$$P_{CA} = a_{CA} d^{n_{CA}}, P_{FA} = a_{FA} d^{n_{FA}} \tag{5.1}$$

In this method, coarse-graded gradation is characterized as n_{FA}<0.45, and n_{CA}>0.45, while for fine-graded gradation, we have n_{FA}>0.45,n_{CA}<0.45.In Bailey's Method, the coarse-graded gradation is the mixture has a coarse aggregate skeleton; while the fine-graded gradation is the mixture does not have enough coarse aggregate particles to form a skeleton. The way to reach a coarse-graded mixture is to select an appropriate Chosen Unit Weight which should be in the range from 95% to 105% of the Loose Unit Weight.

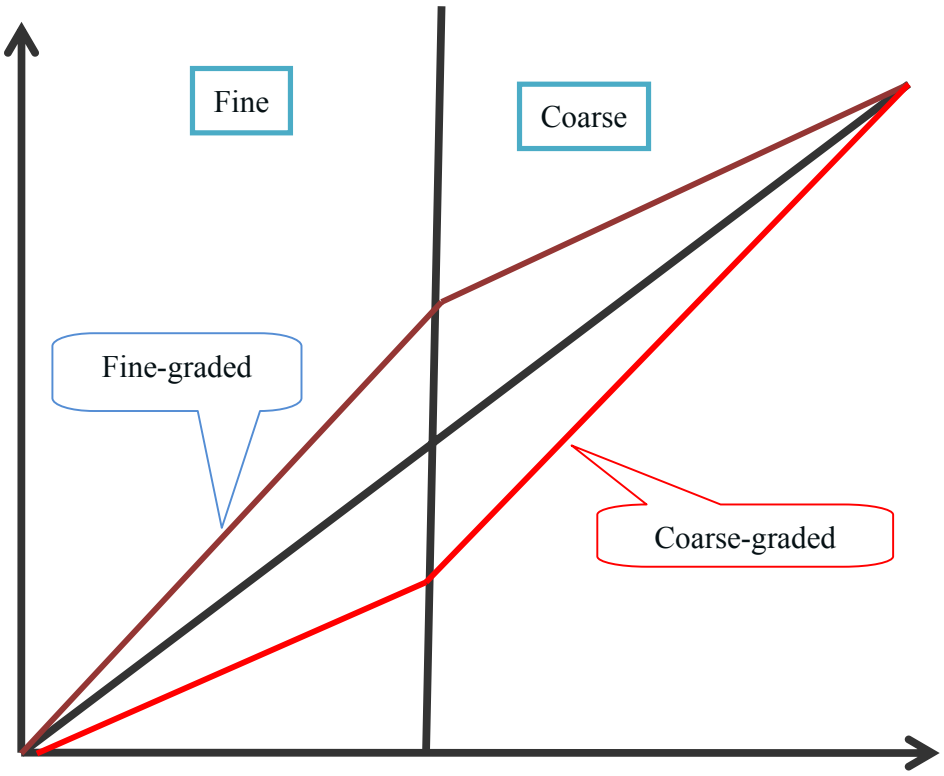

Figure 5-1. Gradation shape definition by Power Law Method (Ruth 2000)

5.1.2 *Categorize Aggregate Gradation Types*

To study different gradation types, 107 aggregate gradations including mix designs from Washington, Illinois, Alabama, Wisconsin, and Michigan State were collected. These gradations represented a wide variety of gradations, as shown in Figure 5-2.

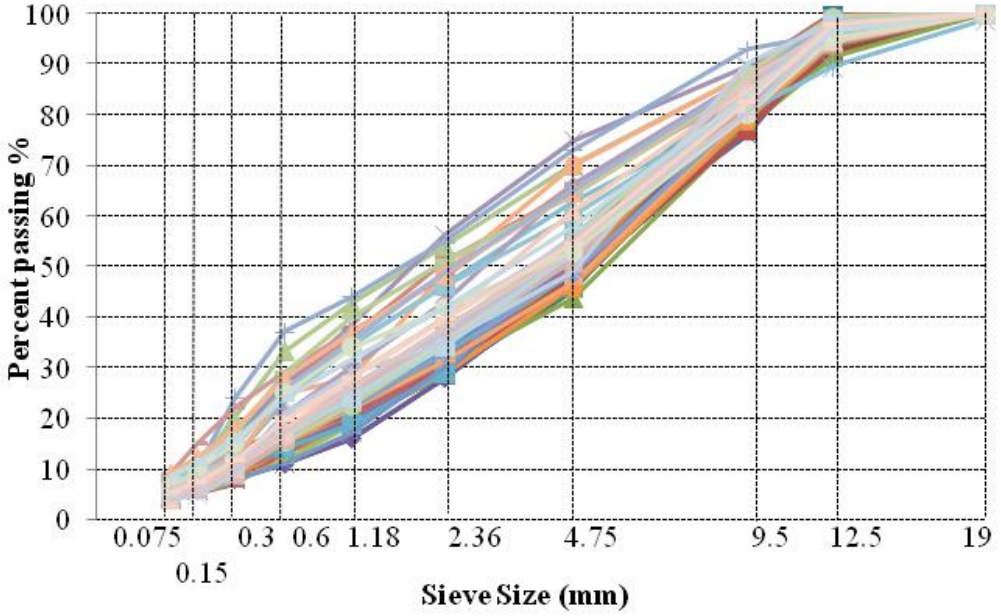

Figure 5-2. Collected gradations chart

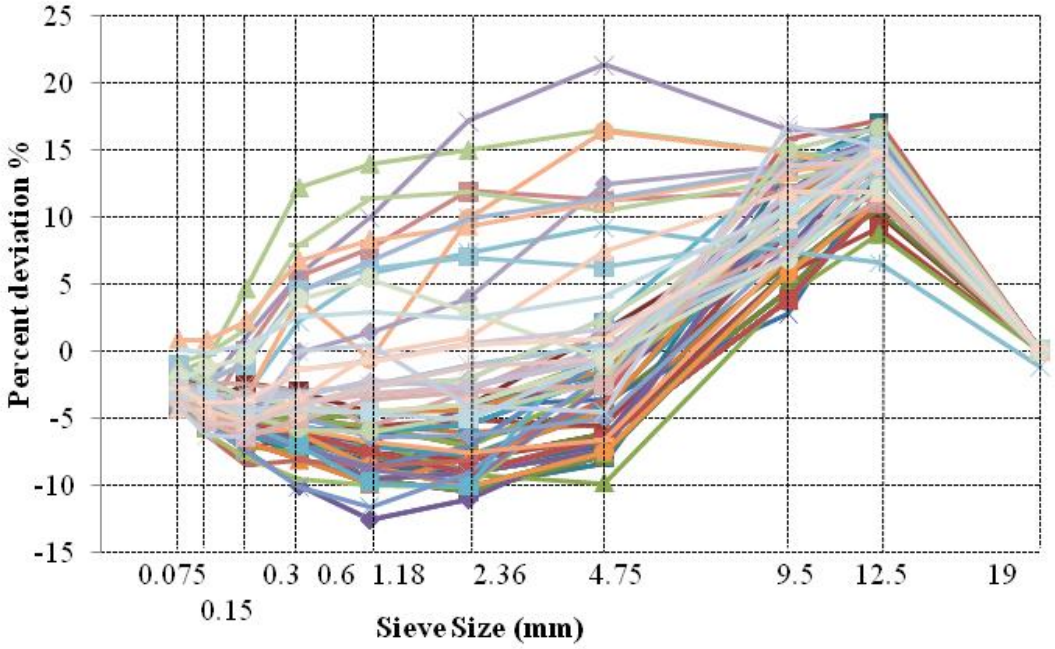

Figure 5-3. Collected gradations in CMD plot method

The continuous maximum density (CMD) plot as proposed in the NCHRP 9-33 report (Advanced Asphalt Technologies, LLC. 2011) was used here for differencing different gradation types according to their deviations from the maximum density line. As shown in Figure 5-3, the CMD plots for all gradations represented a wide range of the gradation types.

Define$P_d(d)$ as the percent of aggregates (size d) deviating from the maximum density line, which can be obtained from Equation (5.2).

$$P_d(d)=P(d)- P_{Dens.} \tag{5.2}$$

Where

$P(d)$: Percent of aggregates passing sieve size d for a specific gradation (%);

$P_{Dens.}$: Percent of aggregates passing the maximum density line (%), which can be calculated from Equation (5.3);

$$P_{Dens.} = \left(\frac{d}{D_{\max}} \right)^{0.45} \times 100\% \tag{5.3}$$

Where

d: sieve size (mm);

D_{max}: maximum sieve size for that gradation (mm).

According to Equations (5.3), the percent of particles passing the maximum density line of 12.5mm NMPS gradation can be calculated, as shown in Table 5-1.

Table 5-1. The percent passing of maximum density line

Sieve size	19	12.5	9.5	4.75	2.36	1.18	0.6	0.3	0.15	0.075
% passing	100	82.8	73.2	53.6	39.1	28.6	21.1	15.5	11.3	8.3

A critical deviation value, *Pdc*, is proposed in this study to classify different gradation types. The *Pdc* is the sum of the deviations of four medium sieve sizes, the sieves that play important roles in determining a gradation curve shape. For a gradation with a NMPS of 12.5mm, a collected gradation CMD plots are shown in Figure 5-3, as shown from the figure, the most varied numbers for $P_d(d)$are four sieve sizes between 9.5mm to 1.18mm for different gradations, so those four sizes between 9.5mm to 1.18mm are recommended to calculate the *Pdc*, and the *Pdc* can be calculated using Equation (5.4).

$$P_{dc} = P_d(9.5) + P_d(4.75) + P_d(2.36) + P_d(1.18) \tag{5.4}$$

Table 5-2 listed the recommended ranges for Pdc to categorize three different gradation types, coarse-graded, medium-graded, and fine-graded gradations. The

selections of the breaking points are to be consistent with the existing gradation type definitions (Advanced Asphalt Technologies, LLC. 2011). The VMA estimation analysis described later in this report also confirmed that such breaking points are appropriate for dividing aggregates into three groups and using three *fv* values for VMA prediction.

Table 5-2. P_{dc} criteria for different gradation types

P_{dc}	Gradation type
$P_{dc} \leq 0$	coarse-graded
$0 < P_{dc} \leq 20$	medium-graded
$P_{dc} > 20$	fine-graded

Using this method, all the collected gradations were divided into three categories, presented in Figure 5-4, Figure 5-5 and Figure 5-6, respectively. This procedure will be followed in this study to categorize all gradations into three gradation types, coarse-graded, medium-graded, and fine-graded gradation.

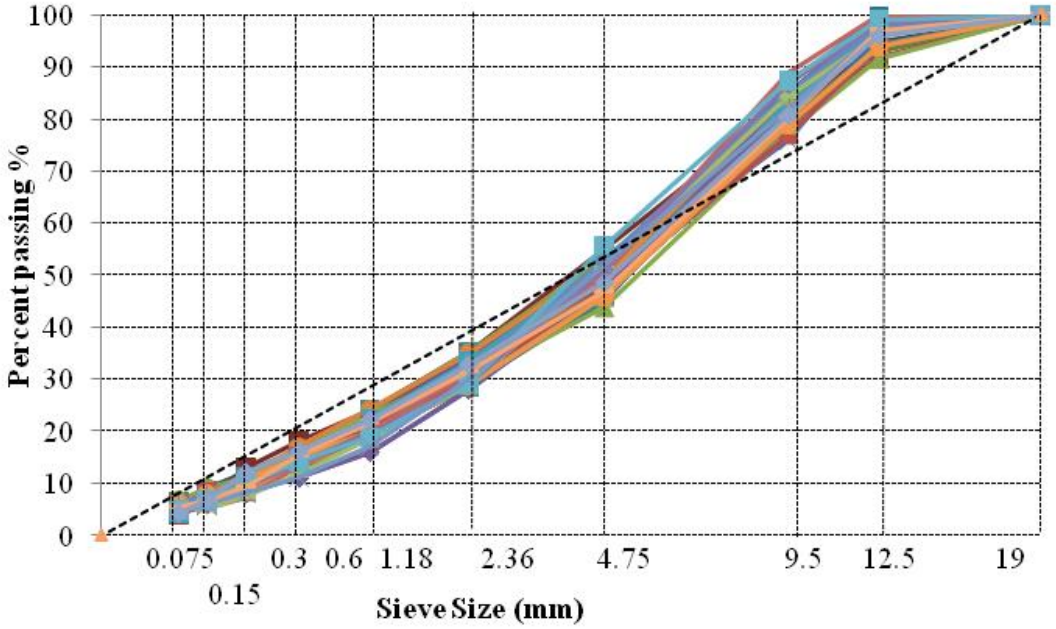

Figure 5-4. Plot of coarse-graded gradations

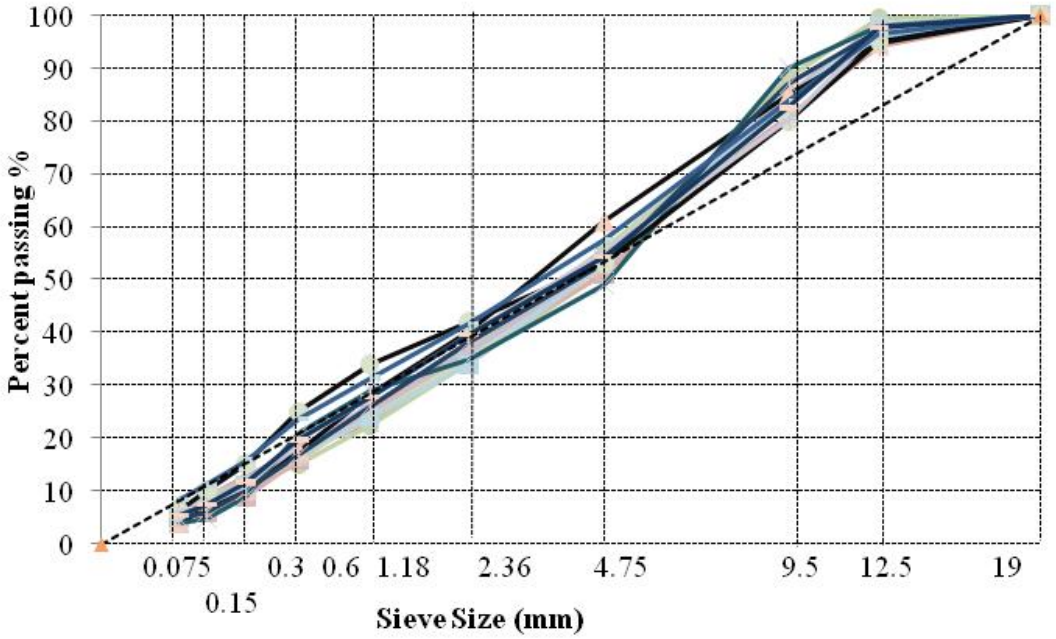

Figure 5-5. Plot of medium-graded gradations

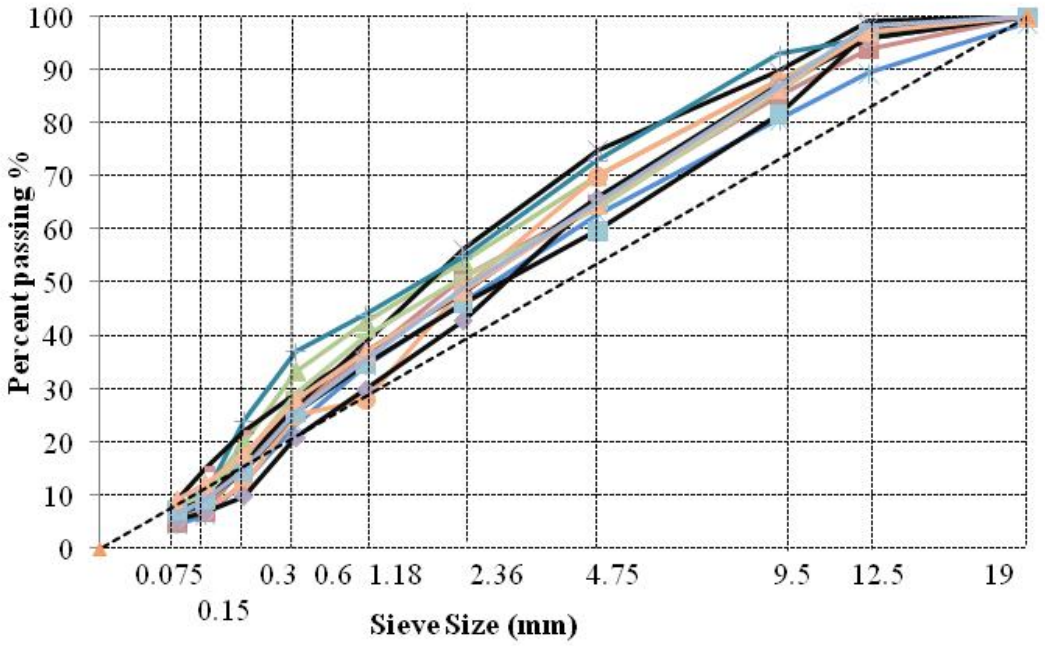

Figure 5-6. Plot of fine-graded gradations

5.2 Relation between Aggregate Gradation and VMA

Because VMA has been considered as a key control parameter in the current Superpave mix design to ensure a successful mixture, the easiness of achieving the target VMA value becomes a critical step in the mix design which is mainly affected by the aggregate properties and gradation. Our study will derive a correlation between aggregate gradations and VMA based on a theoretical analysis of packing theory and DEM simulation. A simple VMA prediction method will be proposed to help designer achieve target VMA at early stage of the mix design, and link aggregate gradation with mix mechanical performance.

A gradation weighing factor, f_v, which is the percent of voids change by volume due to the addition of unit aggregate, is developed to link the gradation information directly to the VMA. The determination of f_v values involves two approaches, either from direct data regression when large numbers of mix designs with the same nominal maximum aggregate size and gradation type are available; or from the discrete element modeling (DEM) simulation. Finally, mix design data from different states are used to verify the applicability of the proposed VMA prediction method to a wide aggregate sources and gradation distributions.

5.2.1 *Parameter Definitions*

State (I): compacted aggregate structure before more aggregate added.

State (II): compacted aggregate structure after adding more aggregate.

V_1: Total volume at state (I)

V_{a1}: Total aggregate volume at state (I)

V_{v1}: Total air void volume at state (I)

p_1: Aggregate porosity or VMA at state (I).

V_2: Total volume at state (II)

V_{a2}: The added aggregate volume at state (II) compared to state (I)

V_{v2}: Total air void volume at state (II)

P_2: Aggregate porosity or VMA at state (II)

5.2.2 *Theoretical Derivation of Volumetric Correlations*

Because different portions of aggregate gradation have different sensitivities to the changes of VMA, their effects on volumetric properties will be analyzed separately. The evaluation of aggregate packing begins with the comparison of two different states of aggregate structures:

(I) Compacted structure with aggregate (1) as shown in Figure 5-7a

(II) Compacted structure with aggregates (1) and (2) as shown in Figure 5-7c.

Figure 5-7b is the intermediate state when aggregate 2 is newly added into the original structure (I) without compaction.

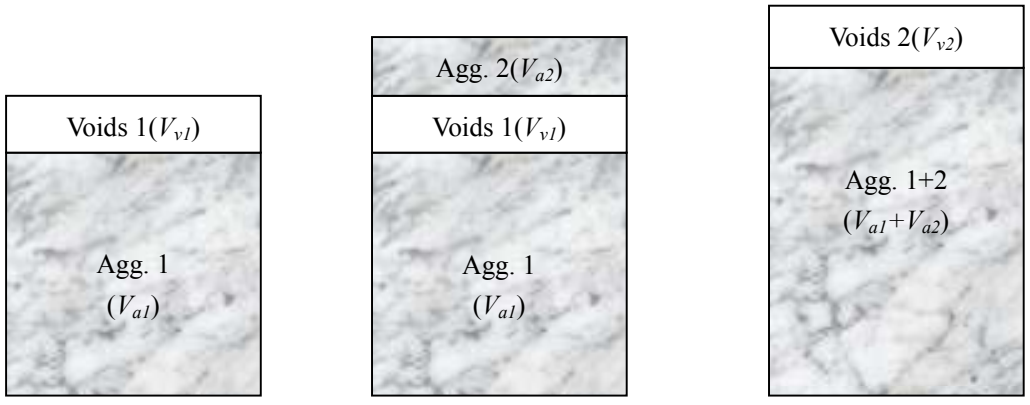

(a)State (I) (b)Add aggregate to state (I) (c)State (II)

Figure 5-7. Aggregate structure phase diagram before and after adding aggregates

In the structure (I) (Figure 5-7a), the following volumetric relation holds:

$$V_1=V_{a1}+V_{v1} \tag{5.5}$$

$$p_1=V_{v1}/V_1=(V_1-V_{a1})/V_1 \tag{5.6}$$

$$V_1=V_{a1}/(1-p_1) \tag{5.7}$$

Define a gradation weighing factor f_v as the percentage of voids change by volume due to the addition of unit aggregate, which is an indication of the resulting volumetric impact when smaller aggregates are added into the structure.

$$f_v=\frac{V_{v2}-V_{v1}}{V_{a2}} \tag{5.8}$$

Where,

$$V_{v1}=V_1 p_1$$

$$V_{v2}=V_2 p_2$$

The newly added aggregates typically have two effects, either enlarge the structures by creating more voids, or fill the voids created by the original aggregates without changing the total volume of the structure. It is possible that part of the added aggregates serves as creating voids while others serve as filling the voids.

As two extreme cases, if all aggregates are contributed to enlarging the structure theoretically based on an analysis of packing theory by Deresiewicz (1958) and the DEM simulation provided later. Therefore, Equation (5.9) yields.

$$f_v = \frac{V_2 - V_1}{V_{a2}} p_1 = \frac{p_1}{1 - p_1}, \tag{5.9}$$

If all aggregate contribute to filling the voids created by the aggregate, the final porosity will be reduced and the f_v will be constant as shown in Equation (5.10).

So,

$$f_v = \frac{V_{v2} - V_{v1}}{V_{a2}} = \frac{-V_{a2}}{V_{a2}} = -1 \tag{5.10}$$

In the gradation and packing analysis, the actual f_v values can be determined for each sieve size when added into the aggregate structure consisting of upper sieve size aggregates. These actual f_v values will be in between these two extreme cases, and can be obtained either by data regression based on existing designs, or from the packing simulation using the DEM modeling. The details of the f_v calculation will be discussed in the later section.

5.2.3 *VMA Prediction Equations*

The development of the f_v parameter provides a straightforward method to estimate the VMA of an aggregate structure. This method is an iteration process starting from an aggregate structure with uniform size (typically NMAS) of aggregates. When smaller size aggregates are added in, the resulting porosity of the new structure can be

determined as:

$$p_2 = \frac{V_{v2}}{V_2} = \frac{f_v V_{a2} + V_{v1}}{V_1 + (1 + f_v) V_{a2}} \tag{5.11}$$

Repeating the same procedure, smaller size aggregates will be added into the mixed aggregate structure, and the corresponding f_v values will be determined. Once all f_v values for each sieve size are determined, the following equation will be used to predict the VMA (or porosity) of the HMA mixtures.

$$p = \frac{\sum_{i=1}^{n} f_{vi} V_{ai}}{\sum_{i=1}^{n} (1 + f_{vi}) V_{ai}} \tag{5.12}$$

Where f_{vi} is the f_v value for *i*th sieve size of the gradation, V_{ai} is the percentage by volume of aggregate retained in the *i*th sieve size, and p is the porosity or VMA of the aggregate structure.

Equation (5.12) provides a linkage between the aggregate gradation properties and the resulting VMA. It can be used to estimate the f_v values or the VMA values when the other information is available.

5.2.4 *Methods for Determining fv Values*

5.2.4.1 *Data regression method*

Because the f_v parameter correlates the VMA property with aggregate gradation, it can be

determined directly from the existing HMA design. In total, 33 coarse-graded Superpave mix designs used for eastern Washington were analyzed. These mix designs represent a wide range of design VMA (12.9% - 19.8%) but all have the same NMAS of 12.5mm.

Table 5-3 f_v values for coarse-graded gradations with NMPS=12.5mm

Sieve size	Data Regression	DEM Simulation Results		
	f_v	f_v for G1	f_v for G2	f_v Avg.
19	0.411	0.426	0.432	0.429
12.5	0.411	0.426	0.432	0.429
9.5	0.411	0.426	0.432	0.429
4.75	0.410	0.426	0.432	0.429
2.36	0.169	0.194	0.198	0.196
1.18	-0.366	-0.396	-0.404	-0.400
0.6	-0.366	-0.396	-0.404	-0.400
0.3	-0.366	-0.419	-0.421	-0.420
0.15	-0.536	-0.600	-0.600	-0.600
0.075	-0.952	-1.000	-1.000	-1.000

It is assumed that the f_v value is not sensitive as long as they have the same NMAS and belongs to the same gradation type (coarse-graded, medium-graded, or fine-graded. This assumption is later verified by the DEM simulation. Based on this assumption, the f_v

values for each aggregate size are back-calculated using Equation (5.12) and by minimizing errors. The fv results for coarse-graded gradation of 12.5mm NMPS are shown in Table 5-3. Due to the limited amount of medium-graded and fine-graded gradation data available, the f_v values for medium-graded and fine-graded gradation are only calculated based on the DEM simulation method described later in this report.

5.2.4.2 *DEM Simulation method*

The DEM simulation provides another method to determine f_v values when a good database of HMA mix design information for the same nominal maximum size is not available. It is particularly important that the developed DEM packing model can be used for the optimization of aggregate gradation design.

Table 5-4. Aggregate gradations for two mix designs used in DEM simulation

ID	Percentage passing sieve size (*mm*, %)									
	19	12.5	9.5	4.75	2.36	1.18	0.6	0.3	0.15	0.075
G1	100	93	80	49	32	23	17	12	8	5.2
G2	100	93	83	55	35	24	18	13	7	5.4

The DEM simulation is based on two existing mix design gradations (G1 and G2)

used by Washington paving projects, as shown in Table 5-4. Both gradations have nominal maximum size of 12.5 mm and primary control sieve size of 2.36 mm.

The determination of f_v values in the DEM simulation follows an iteration process, as shown in Figure 5-8. First, generate a basic model with only large aggregates, and calculate the volume and porosity of this structure. Then, based on the gradation, add appropriate amount of finer aggregates into the structure, mix and compact the structure into equilibrium, and calculate the volume and porosity of the new structure. Third, use Equation (5.12) to get the f_v value for this portion of aggregate. Repeat these steps until all aggregates are added into the structure and the f_v values for each sieve size are determined. It's worth noting although only sphere particles are used in the DEM, the angularity and the surface texture properties are indirectly taken into account by adjusting the particle contact angle in the PFC^{3D} program to achieve different packing conditions.

Using the DEM method, the f_v values for these two gradations are obtained, and the results are provided in Table 5-3. The fv values from two gradations are very similar, indicating the fv values are not sensitive to gradation differences as long as they have the same NMAS. These values are also close to the f_v values obtained from data regression.

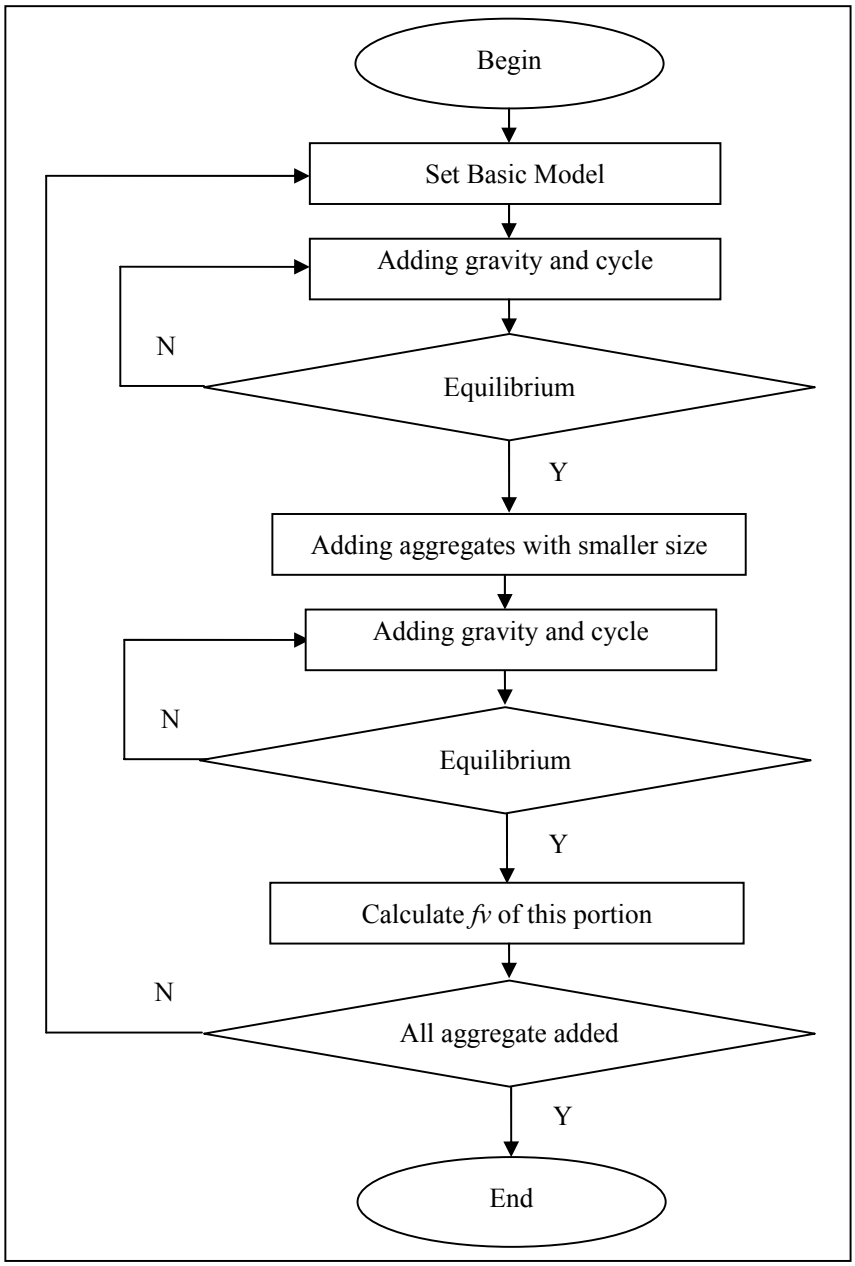

Figure 5-8. The flow chart of DEM simulation to determine the f_v values

5.2.5 *VMA Prediction*

To compare the sensitivity of the f_v values on the VMA prediction, the f_v from both data

regression and DEM simulation are used to calculate the VMA based on Equation (5.12). These results are compared with the design VMA.

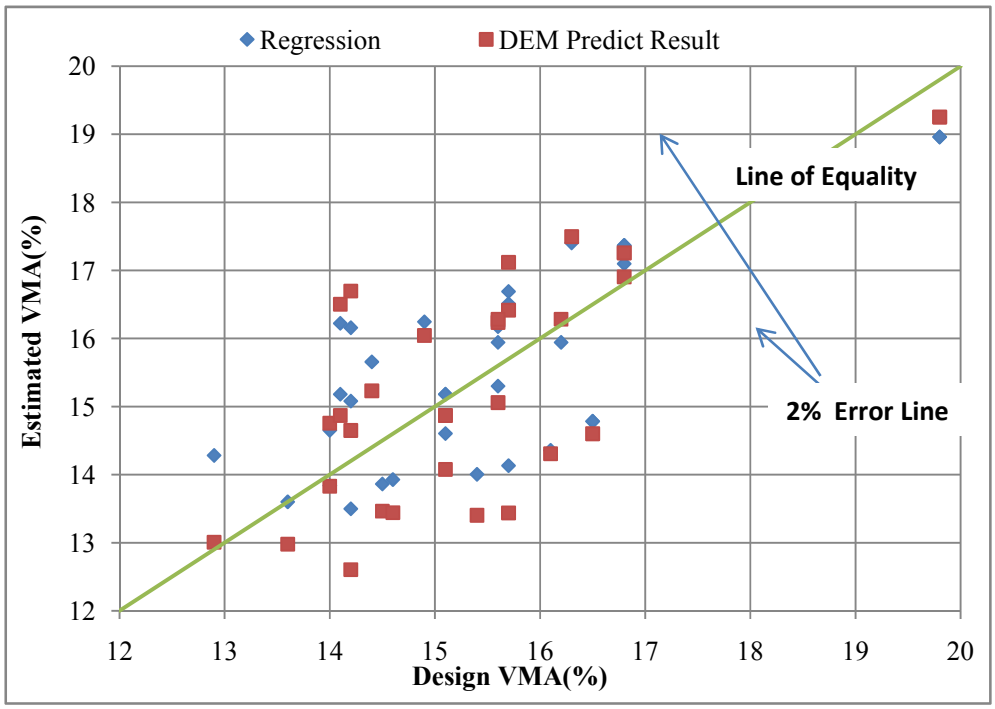

(a)

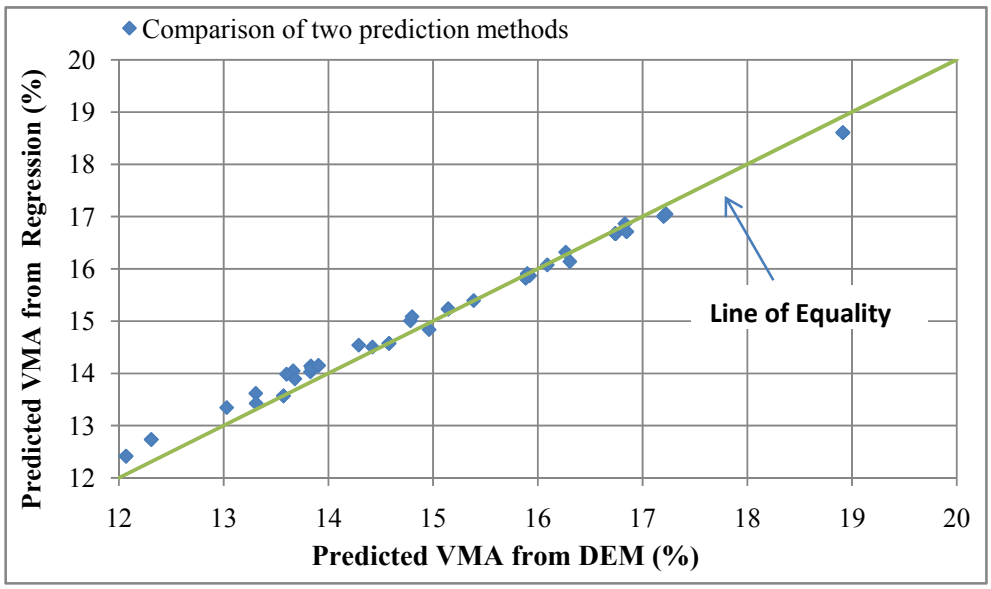

(b)

Figure 5-9. Comparison of Design and Predicted VMA (a) VMA from regression and DEM simulation vs. design VMA, (b) VMA from regression vs. from DEM

Table 5-5. Mix and gradation information for VMA prediction verification

ID	Mix Source	Percentage passing sieve size									
		19	12.5	9.5	4.75	2.36	1.18	0.6	0.3	0.15	0.075
1	WA	100	98	84	53	34	24	17	11	8	5.1
2	WA	100	94	77	47	30	21	15	10	8	5.6
3	WA	100	94	79	46	29	20	15	11	8	6.1
4	WA	100	98	85	53	32	20	14	10	8	6.1
5	WA	100	99	85	46	30	19	14	10	7	5.8
6	MI	100	99	87	51	29	20	14	10	6	4.6
7	MI	100	99	87	56	29	19	14	10	7	4.8
8	AL	100	91	69	35	23	17	14	12	11	10
9	AL	100	97	82	52	30	17	11	8	6	5.1
10	AL	100	94	72	32	23	18	15	13	12	10.8
11	AL	100	92	56	24	18	15	13	12	11	9

As shown in Figure 5-9(a), both data regression and DEM simulation provided reasonable prediction of design VMA. Slightly better results are obtained by using the

data regression method, which has the prediction error within 2%. Figure 5-9(b) further compared the prediction differences between the data regression method and the DEM method. Both methods gave consistent predictions.

5.2.6 *Verification of the VMA Prediction Method*

Table 5-6. VMA prediction and error

ID	Mix Source	Design VMA (%)	VMA from Regression (%)	Error	VMA from DEM (%)	Error
1	WA	15.1	14.2	-0.9	14.5	-0.6
2	WA	15.8	15.9	0.1	16.3	0.5
3	WA	15.8	16.3	0.5	16.7	0.9
4	WA	15.8	15.8	-0.0	16.3	0.5
5	WA	16.3	16.7	0.4	17.2	0.9
6	MI	17.7	17.1	-0.6	17.0	-0.7
7	MI	17.5	17.3	-0.2	17.3	-0.2
8	AL	17.0	17.3	0.3	16.9	-0.1
9	AL	16.9	18.1	1.2	17.7	0.8
10	AL	15.5	16.5	1.0	16.2	0.7
11	AL	19.0	19.0	0.0	18.8	-0.2

The f_v parameters developed in the DEM simulation and the data regression method provides a promising approach to estimate the VMA values without the needs of experimental testing. The determination of the f_v values is based on the data mainly from eastern Washington, which could make it only a locally valid approach. Therefore, this section will validate the applicability of the approach for a wider aggregate source and with a wider gradation variation.

Mix designs from Washington, Michigan, and Alabama's NCAT Test Track are obtained for the data verification, and their gradation details are shown in Table 5-5. Using the approaches discussed before, the predicted VMA for these eleven mixes are obtained and compared with the design VMA, as given in Figure 5-10and Table 5-6.

As can be seen from the results, the predicted VMA matches well with the design VMA for all mix sources, with most errors within 1%. This error appears to be acceptable considering the new suggested VMA variation ranges of 2% (Table 5-6).

By using the method introduced here, the VMA values can be easily estimated based on the gradation properties of the mix without the need for conducting experimental testing. The next step is to determine the relationship between the VMA and the mechanical performance of the mix. Eventually, a direct linkage between aggregate gradation and the mechanical performance of the mix will be obtained for optimizing the

aggregate gradation design.

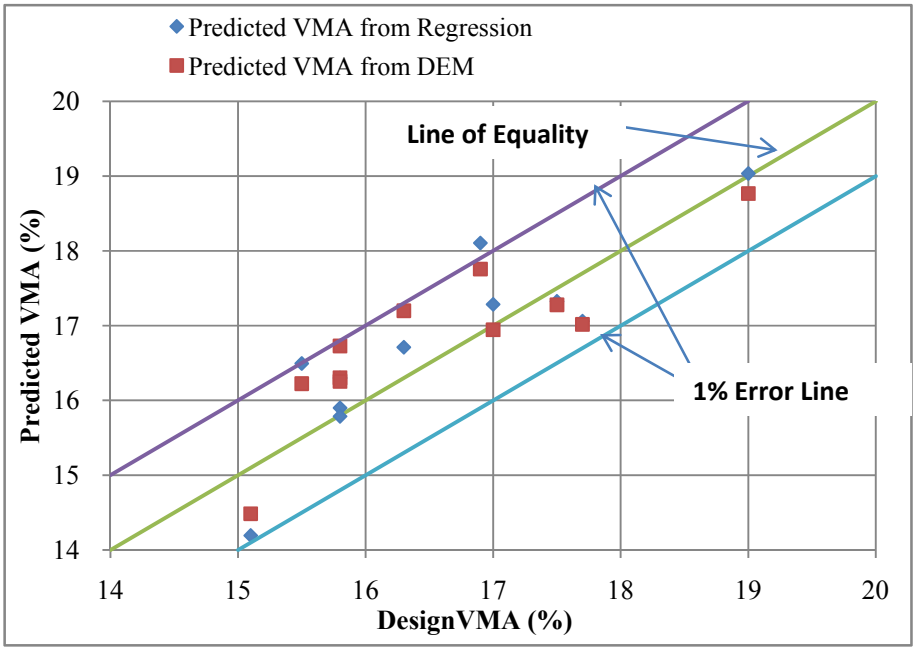

Figure 5-10.Comparisonof design VMA and the predicted VMA

5.3 Investigation of Aggregate Contact and Interlocking Using DEM

5.3.1 *Verification of Aggregate Packing using 3D DEM Model*

The way of aggregate packing and the packing models used in the DEM directly affect the volumetric properties of an aggregate structure. In a classical example of 3-D packing model, two cases of packing are usually considered. Both packings consist of equal-radius balls in contact with no overlap. The first packing is a simple cubic arrangement in which each ball is in contact with six neighbors, as shown in Figure 5-11a. The second packing is a tetrahedral arrangement, which is the densest of all possible

regular three-dimensional packings (Figure 5-11b). For both packings with a fixed ball arrangement, the porosity is independent of the size of the balls, provided that the packing is extended over a very large region so that the effect of boundaries is negligible. A detailed discussion on packing in both two and three dimensions has been provided by Deresiewicz (1958).

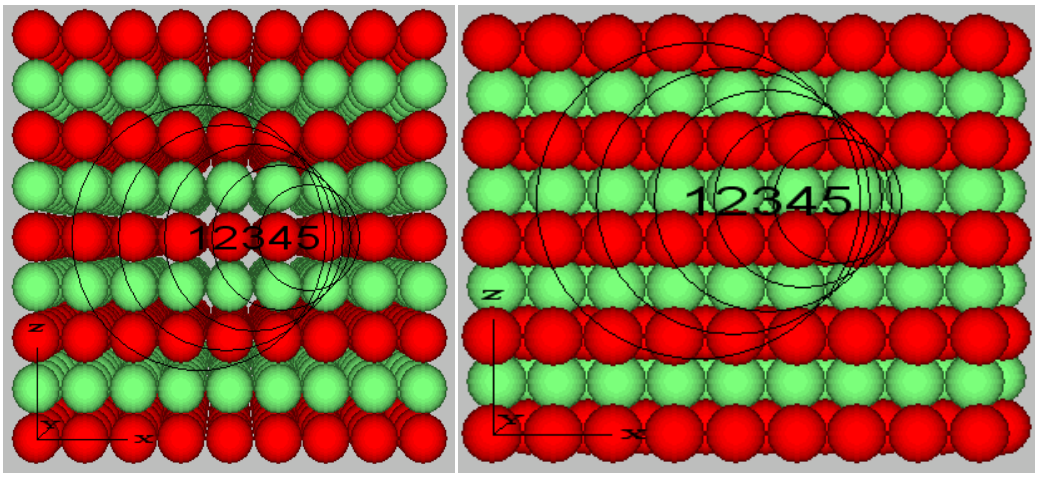

(a) Simple Cubic Packing in a 3-D Model (b) Tetrahedral Packing in a 3-D Model

Figure 5-11. Aggregate packing in 3-D model

The density D of a packing is defined as the ratio of the volume of space occupied by solid matter Vs to the total volume V. If we assume that the total volume is comprised of both solid and void volumes and that there is no overlap, then the density is related to the porosity VMA by the following relation:

$$VMA = 1 - \frac{V_s}{V} \tag{5.13}$$

For the simple cubic packing as shown in Figure 5-11a:

$$VMA = 1 - \frac{\frac{4}{3}\pi R^3}{(2R)^3} = 1 - \frac{\pi}{6} = 0.4764 \tag{5.14}$$

For the tetrahedral packing as shown in Figure 5-11b:

$$VMA = 1 - \frac{\frac{4}{3}\pi R^3}{4\sqrt{2}R^3} = 1 - \frac{\pi}{3\sqrt{2}} = 0.2595 \tag{5.15}$$

Table 5-7.Porositiesunder Different Packing Theories

Packing	Theory	PFC^{3D}	Error
Cubic	0.4764	0.4814	0.010495
Cubic	0.4764	0.4673	-0.0191
Cubic	0.4764	0.4797	0.006927
Cubic	0.4764	0.4653	-0.0233
Cubic	0.4764	0.4834	0.014694
tetrahedral	0.2595	0.2604	0.003468
tetrahedral	0.2595	0.2602	0.002697
tetrahedral	0.2595	0.2591	-0.00154
tetrahedral	0.2595	0.2656	0.023507
tetrahedral	0.2595	0.2431	-0.0632

Table 5-7 compares the results of VMA obtained from PFC3D simulation and the ones calculated directly from the equations. As seen, for a 3-D model, when the aggregates are in unit diameter a, the VMA of the model should be in the range of 0.2595 to 0.4764. Also, the porosity (VMA) calculation in PFC3D is accurate enough.

If all the aggregate particles are assumed to be spheres, the relation between the maximum size of the filling material and the aggregate particles can be found as (Huang et al. 2007):

$$r = \left(\sqrt{\frac{32}{27}} - 1 \right) R = 0.089R \tag{5.16}$$

The result of 0.089R in 3-D model for the diameter of fine aggregate to fill the voids in much smaller than the value of 0.22R as used in the Bailey's method. In practice, due to the friction characteristic of aggregate and angularity, the actual diameter of fine aggregate should be values other than the theoretical value of 0.089R and the average value of 0.22R.

5.3.2 *Model Description*

The DEM method is used in this study to simulate the packing characteristics of aggregate structures with different gradations, and to evaluate the degree of aggregate contact and interlocking. Although aggregate properties such as angularity and surface

roughness can have significant impact on the packing characteristics, they also greatly increase the complexity of the problem. Therefore, this study will start with spherical particles. The effect of aggregate angularity and surface texture will only be considered indirectly by careful model parameter assignment (such as contact friction angle) and data calibration. Once the model for studying the spherical particle packing have been established, other aggregate properties such as surface roughness, angularity, and the effect of binder can be included to develop a more sophisticated packing model.

The process of DEM simulation involves three major steps. Firstly, balls retained on the Nominal Maximum Particle Size (NMPS) are generated in the computer according to the target gradation. These balls are added to a square box ($0.3m$*$0.3m$*$0.5m$) under a unidirectional gravitational force. Secondly, balls are compacted by the assigned gravitational force to its stable position. If the unbalanced force approaches a very small value, this indicates that an equilibrium state has been reached. During the compaction, the velocities and the new positions of each ball were updated at each time step according to Newtonian motion model ($F=m*a$). Based on new particle positions, contact forces are obtained from a relative displacement of pairs of particles. A simplified Hertz-Mindlin law at contacts was used. The iteration stops when the unbalanced force reaches 0.01% of the maximum contact force. Finally, the volumetric properties and the mean contact force are calculated.

The simulation of a complete aggregate gradation requires adding different sizes of balls to the system sequentially (from large to small) following an iteration process. Once the structure of large size particles are established and their volumetrics are determined, finer aggregates will then be added into the structure following the same three steps of ball generating - compaction to equilibrium - data calculation. The corresponding volumetrics and mean contact forces will be determined and compared with the results for larger size particles to check the change in volume and contact force due to the addition of small size particles.

5.3.3 *Model Parameters and Gradation Information*

The study of aggregate packing for an engineering material mainly focuses on two issues: (1) how good different sizes of aggregates will fill up the volume of mixture, and (2) how effective the stress is transmitted from particle to particle through the aggregate skeleton. Packing density, a parameter widely used in the area of soil mechanics, can be used to describe the relative proportion of the solid volume of the aggregate particles to the total volume of HMA, as shown in Equation (5.17).

$$d = \frac{V_s}{V_T} \tag{5.17}$$

Where,

V_s = the volume of aggregate, and

V_T = the total volume of the mix structure.

The porosity (p) of the structure is the ratio of the volume of voids within aggregate particles to the total volume. It can be obtained as follows in Equation (5.18):

$$p = 1 - d = \frac{V_V}{V_T} \tag{5.18}$$

A typical Washington State gradation with nominal maximum aggregate size of 12.5mm is used as an example for the analysis of the aggregate packing characteristics. The gradation is shown in Table 5-8 and plotted in Figure 5-12.

Table 5-8. Aggregate gradation used for simulation

Sieve Size(mm)	19	12.5	9.5	4.75	2.36	1.18	0.6	0.3	0.15	0.075
% Passing	100	93.2	79.5	49.4	32.3	22.5	16.5	12.1	7.7	5.2

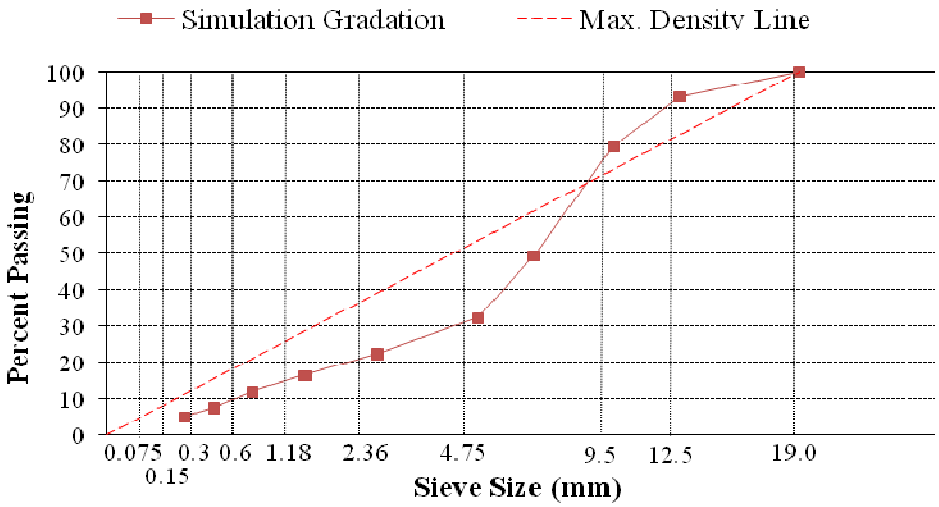

Figure 5-12.Aggregategradation for packing simulation

Previous studies showed that the aggregate elastic modulus value of 30 GPa would predict satisfactory Asphalt Mixture Performance Test (AMPT) parameters (Abbas et al. 2005). Zelelew (2007) used the elastic modulus of 30GPa and assumed that the rigid wall stiffnesses to be 10 times stiffer than the particles stiffness, and reasonable results have been obtained. Also, he used an aggregate-to-aggregate contact friction coefficient μ=0.5, which corresponds to an angle of internal friction of 27^{o}. These successful experiences will be adopted by this study, and the following parameters will be used in the DEM simulation: aggregate elastic modulus of 30GPa, rigid wall stiffness of 300GPa, and aggregate-to-aggregate contact friction coefficient μ=0.5.

5.3.4 *Volumetric Analysis of Aggregate Structure*

Table 5-9. Number and volume of particles at each size for model 1, 2, and 3

	Model 1	
Particle Sieve Size	**Balls No.**	**$V_s(mm^3)$**
12.5-19	68	1160242
9.5-12.5	412	2337546
4.75-9.5	3061	5152839

	Model 2	
Particle Sieve Size	**Balls No.**	**$V_s(mm^3)$**
12.5-19	68	1160242
9.5-12.5	412	2337546
4.75-9.5	3061	5152839
2.36-4.75	13848	2900605

	Model 3	
Particle Sieve Size	**Balls No.**	**$V_s(mm^3)$**
12.5-19	68	1160242
9.5-12.5	412	2337546
4.75-9.5	3061	5152839
2.36-4.75	13848	2900605
1.18-2.36	65450	1689176

	Model 1	Model 2	Model 3
Particle Sieve Size	**$V_s(mm^3)$**	**$V_s(mm^3)$**	**$V_s(mm^3)$**
total volume before compaction	300*300*152.3 =8650628	300*300*190.2 =11551233	300*300*201 =13240409
Percent of volume change before compaction		33.5%	14.6%
total volume after compaction	13707000	17118000	18090000
Percent of volume change after compaction		24.9%	5.68%

Based on the gradation given in Figure 5-12, three DEM simulation models that included different fractions of the gradations were established. Model 1 only includes the aggregate particles larger than 4.75mm. Model 2 includes aggregates larger than 2.36mm. Model 3 consists of all aggregates larger than 1.18mm. Particles smaller than 1.18mm are assumed to behave as fine particles which fills in the voids of the structure and are not included in the packing simulation. The number of balls and volumes for specific size group of each model were then calculated according to the proportions of the given gradation, as shown in Table 5-9. Also included in Table 5-9 are the total volume and

volume changes before and after compaction. Here the percent of volume change for model 2 and 3 are relative to model 1 and 2, respectively.

Table 5-10. Porosity information of three models

Model	Position1	Position2	Position3	Position4	Position5	Average	Porosity change
1	0.3363	0.3419	0.3382	0.3383	0.3323	0.3374	0
2	0.3013	0.2986	0.2939	0.3028	0.2974	0.2988	0.0386
3	0.2466	0.2463	0.2477	0.2492	0.2458	0.2471	0.0517

The porosities of model 1, 2, 3 structures were also calculated in the PFC^{3D}. In order to find a representative value of the porosity, five points were randomly selected. Their porosities as well as the average porosity of the five positions were calculated and presented in Table 5-10 and Figure 5-13. As shown, the results are consistent, indicating a uniformly distributed aggregate structure; the average porosity from the five positions can be treated as the representative porosity of the structure.

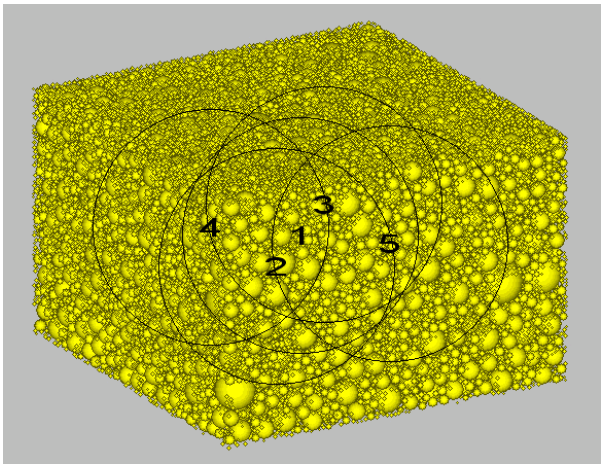

Figure 5-13.Porositymeasure ID and position

By comparing the volume and porosity changes of model 1, 2, and 3, the role of specific particle size is determined. From model 1 to model 2 by adding in 33.5% (by volume) of 2.36-4.75mm particles, the total volume of compacted structure was increased 24.9%. In other words, most of the added particles were contributed to the increase of the total structure volume. Consequently, slight deduction in porosity (3.86% as shown in Table 5-10) was achieved. However, from model 2 to model 3 by adding in 14.6% (by volume) of 1.18-2.36mm particles, the total volume of compacted structure was increased only 5.68%. Most particles have filled in the voids created by the coarse aggregate skeleton without creating additional structure volume. And the decrease of porosity became more significant (5.17% as shown in Table 5-10).

5.3.5 *Roles of Particles in an Aggregate Structure*

To further describe the change of volume due to the addition of finer aggregates, and quantify the roles of aggregate particles in a specific aggregate structure, a new gradation parameter f_s is developed. f_s is defined as the percent of volume increase due to the addition of unit finer aggregates, which can be calculated using Equation (5.19). f_s value greater than 1 will indicate the aggregates more behave like creating the voids. Since gradation weighing factor f_v indicates the resulting air voids change when smaller aggregates are added into the structure and f_s indicates the total volume of structure change due to finer aggregate, so typically a higher f_v value will result in a higher f_s value.

$$f_s = \frac{V_2 - V_1}{V_{a2}} \tag{5.19}$$

Where,

V_1 = the total volume of basic model,

V_2 = the total volume after finer aggregate were added, and

V_{a2} = the volume of finer aggregate added into the basic model.

Table 5-11 and Figure 5-14 show the fs values of each particle size for the given gradation. As shown, f_s values are larger than 1 for aggregates retained on 2.36mm sieve size, indicating the change of the total volume of aggregate structure is larger than the

volume of the added aggregate volume, and some additional voids have been created. For aggregates larger than 9.5mm, it is assumed that they all contribute to forming the skeleton in an aggregate gradation with 12.5mm NMAS. When particles smaller than 2.36mm are included into the structure, f_s becomes smaller than 1. The 2.36mm sieve appears to be a reasonable breaking size between coarse and fine aggregates for aggregates with NMPS equaling to 12.5mm. This finding is consistent with the primary control sieve definition used in the Bailey's method.

Table 5-11. f_s value verse aggregate passing sieve size

Aggregate Passing Sieve Size (mm)	**12.5**	**9.5**	**4.75**	**2.36**
f_s	1.524	1.434	1.176	0.575

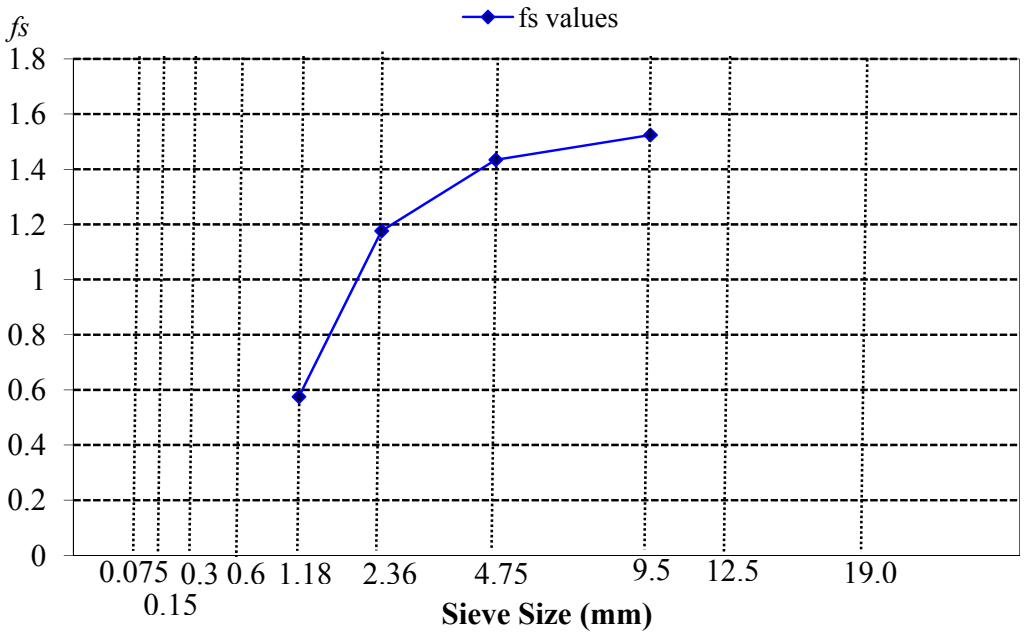

Figure 5-14. f_s information verse aggregate gradation

5.3.6 *Aggregate Contact and Interlocking*

The advantages of DEM computational simulation such as easily adding and deleting balls, and detecting contacts and contact force, make it an excellent tool to study the aggregate contact, which otherwise will be extremely difficult to realize in the laboratory and field. In this study, by applying the PFC^{3D} command and functions a "ball hiding" technique is developed to identify the particle contacts and to quantify the contact force.

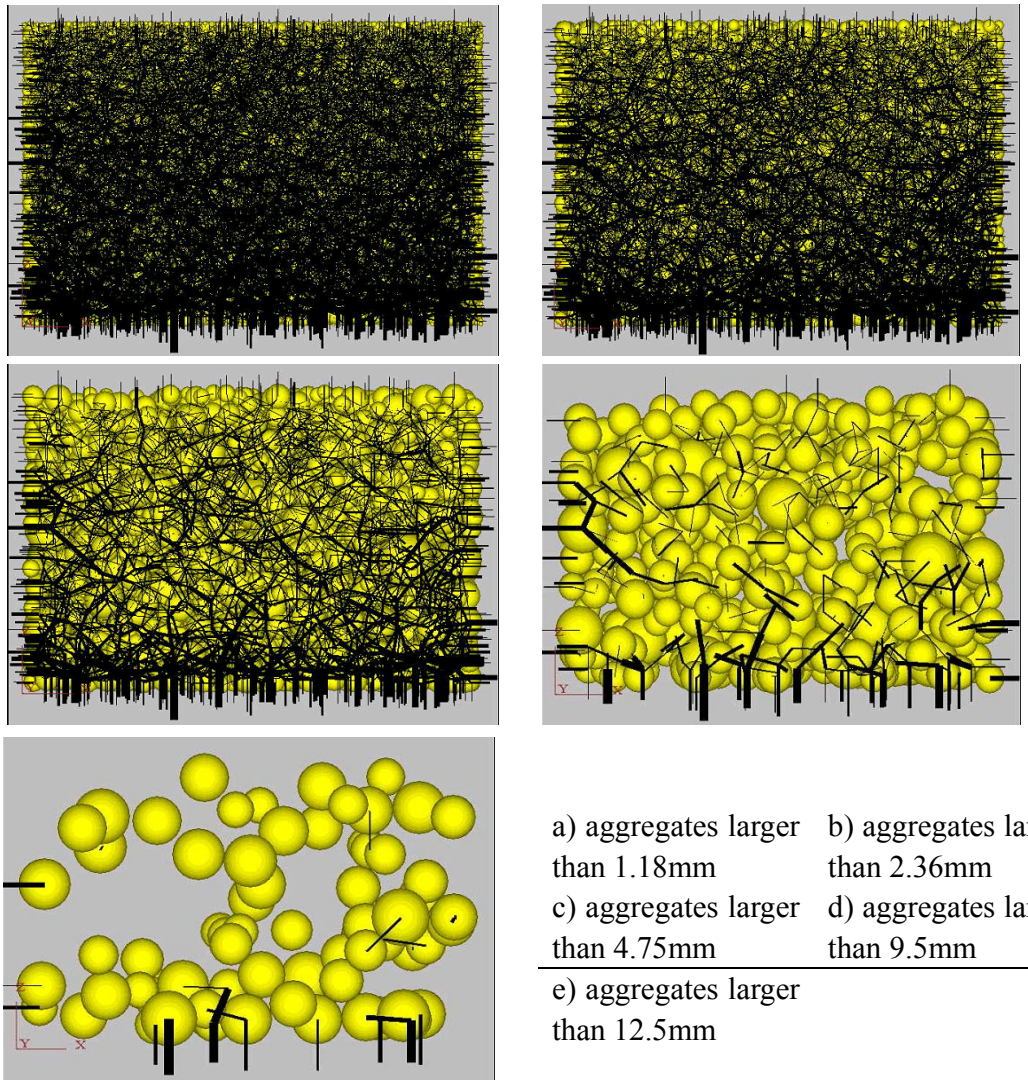

a) aggregates larger than 1.18mm
b) aggregates larger than 2.36mm
c) aggregates larger than 4.75mm
d) aggregates larger than 9.5mm
e) aggregates larger than 12.5mm

Figure 5-15. "Ball hiding" technique for detecting aggregate contact and interlock in DEM simulation

First, all balls larger than 1.18mm as designated in the design gradation were generated in the *PFC*^{3D}, and their contact forces are calculated and plotted as shown in Figure 5-15a. Then the aggregates between 1.18mm and 2.36mm are made invisible in the structure (Figure 5-15b). By only plotting the contacts among those visible balls, we

are able to identify the particle contacts due to aggregates coarser than 2.36mm. Following the same procedure, the contacts among coarse aggregates are able to be identified. Figure 5-15c-e shows the particle contacts for aggregates retained on 4.75mm, 9.5mm, and 12.5mm, respectively.

Also indicated in Figure 5-15 are the magnitudes of contact force (black lines), usually called "force chain". The more the force chain appears, the more contacts are detected. In addition, a wider force chain will indicate a stronger contact force (heavily stressed chains), and thus more stress is transmitted through the aggregate skeleton; the remaining groups of particles are only lightly loaded (Howell et al. 1999). Examining all figures in Figure 5-15, it is clear that very few aggregate contacts exist between particles larger than 12.5mm as well as 9.5mm; and there exists very few stress transmission through the mainly lightly stressed force chains (weak force chains). The force chains start forming a network when 4.75mm and 2.36mm particles are included into the skeleton structure, and more strong force chains are observed. Such observation indicates that the aggregate particles greater than 2.36mm are mainly behaving as forming the structure skeleton to transmit the major portion of the stress and provide major load bearing capacity.

5.3.7 *Aggregate Mean Contact Force*

Because the contact force is strongly dependent on particle arrangement (Antony and Kuhn 2004), it is difficult to relate the individual contact force to the performance of a structure. Mean contact force, which is the total normal contact force divide by total contact numbers, are used in this study to quantify the stability of the aggregate structure. In general, if the same external load is applied to two models, the one with lower mean contact force will have more contact points, less stresses being transmitted through the aggregate skeleton, thus a more stable structure. A mean contact force is considered to be able to relate to the aggregate structure's resistance to permanent deformation.

The mean contact forces for the three models are determined in the PFC^{3D}, and the results are given in Table 5-12 and Figure 5-16. By adding small aggregates into the structures, more aggregate contacts were achieved due to the increased amount of fine aggregate contacts, and thus the mean contact force was decreased. This further confirmed the existing findings that fine aggregates have significant impact on the rutting performance of HMA. Appropriate amount of fine materials increase the particle interconnection, reduce the mean contact force of the overall structure, thereby improve the stability and load distribution capability of the structure as well as the resistance to permanent deformation.

Table 5-12. Mean contact force for three models

Model	1	2	3
Mean Contact Force	0.420	0.237	0.178

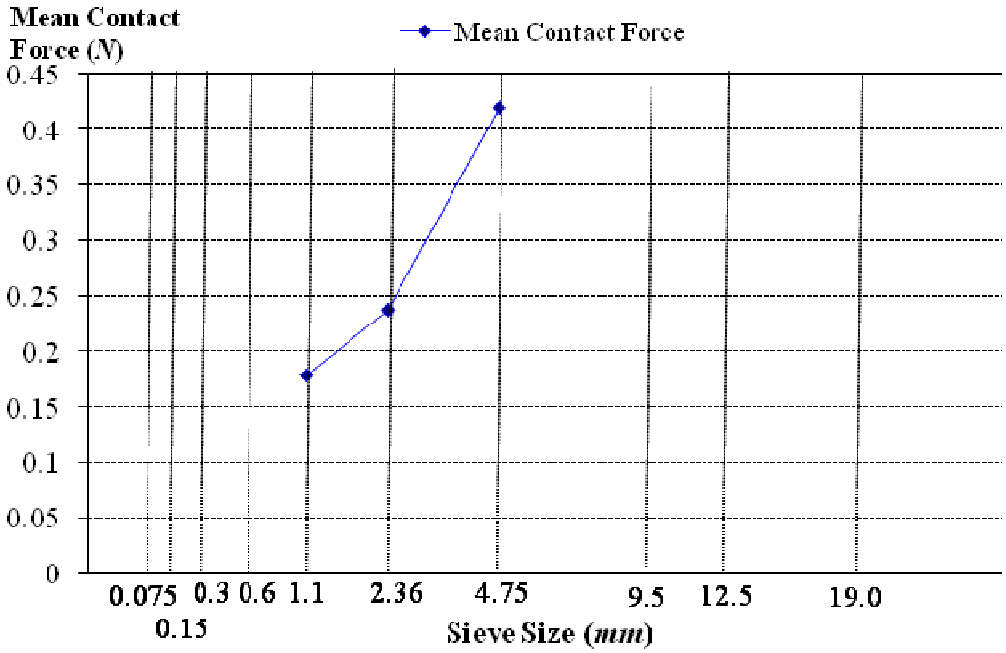

Figure 5-16. Mean contact force verse the sieve size change

5.4 SUMMARY

This chapter presented an analysis of aggregate packing and DEM simulation to link the aggregate gradation property with the VMA of HMA. The roles of aggregates with different sizes in an aggregate structure are evaluated. A promising methodology is presented for a fast VMA estimation which can be used in the HMA mix design to reduce

the design time and effort. When combined with other information such as aggregate absorption rate, this method provides a means to estimate optimum asphalt content, optimize design to produce economical job mix formula, and adjust gradation design to produce high performance mixes. Because VMA has important impact on the HMA mechanical properties and field performance, next chapter will describe the methods of correlating the mechanical performance with the volumetric properties of the mix. The predicted VMA will be utilized as a media to link gradation with mixture performance and as a screening tool at the early stage of the mix design to identify poor performing mixtures.

CHAPTER 6 AGGREGATE GRADATION AND MECHANICAL PROPERTIES OF THE ASPHALT MIXTURES

This chapter conducts the data analysis of experimental testing and establishes correlations between gradation parameters and laboratory mechanical performances of the mixes including dynamic modulus, compactability, and flow number. Existing dynamic modulus prediction models are evaluated, and then a locally calibrated dynamic modulus model is present. Based on the experimental findings and the dynamic modulus prediction models, the effect of aggregate gradation, with respect to individual sieve size and the whole gradation, is evaluated, which will provide insight to the asphalt mixture and gradation design to achieve high performance mixtures.

6.1 Experimental Gradation Design And Materials for Performance Testing

Considering the limited time-frame and the scope of the project, only coarse-graded gradations using the definitions provided in Chapter 3 are studied. Other types of gradations can be evaluated following the similar procedures introduced in this study.

Table 6-1. Gradations Used for Mechanical Experiments

Sieve	3/4"	1/2"	3/8"	#4	#8	#16	#30	#50	#100	#200
	19mm	12.5mm	***9.5mm***	***4.75mm***	***2.36mm***	1.18mm	0.6mm	0.3mm	***0.15mm***	***0.075mm***
C1	100	94	79	46	29	20	15	11	8	6.1
C2L	100	94	***69***	46	29	20	15	11	8	6.1
C2H	100	94	***89***	46	29	20	15	11	8	6.1
C3L	100	94	79	***36***	29	20	15	11	8	6.1
C3H	100	94	79	***56***	29	20	15	11	8	6.1
C4L	100	94	79	46	***20***	20	15	11	8	6.1
C4H	100	94	79	46	***39***	20	15	11	8	6.1
C5L	100	94	79	46	29	20	15	11	***5***	3.1
C5H	100	94	79	46	29	20	15	11	***11***	6.1
C6L	100	94	79	46	29	20	15	11	8	***3.1***
C6H	100	94	79	46	29	20	15	11	8	***8***

One coarse-graded gradation C1 used in the Washington paving project was selected as the base gradation for evaluation. To evaluate the effect of individual sieve size on the mechanical performance, the percentage of aggregates passing five sieve sizes (9.5mm,

4.75mm, 2.36mm, #100 and #200) are varied. For sieve sizes 9.5mm, 4.75mm, and 2.36mm (3/8", #4, and #8), the percentages passing the sieve size were changed plus or minus 10% while for the sieve sizes 0.15mm and 0.075mm (#100 and #200) the percentages passing were changed plus or minus 3% to account for the major gradation variations for Washington mixes. The details of the designed gradations are shown in Table 6-1 and Figure 6-1. With two replicates for each gradation type, in total 11*2=22 samples have be prepared and tested for volumetric properties, compactability, dynamic modulus, and rutting resistance (flow number test).

For the purpose of evaluating aggregate gradation effect, only one type of aggregate (basalt) and one type of asphalt binder (PG58-28) were used in this study.

All experimental specimens are prepared using the same asphalt content, 6.2%, which is the optimal asphalt content for the base gradation mix C1 determined using the current Superpave mix design method. The samples are compacted using Superpave gyratory compactor to target air voids of 7%±1%. It is worth noting that for the dynamic modulus testing, in order to account for the irregular air voids distribution of the gyratory specimen, the six-inch diameter samples are all prepared to a target air void of 8.5% to ensure the cored four-inch dynamic modulus samples have the voids of 7%±1%.

All the experimental testing was conducted at the Washington Center for Asphalt Technology at the Washington State University, an AASHTO accredited laboratory

through AMRL.

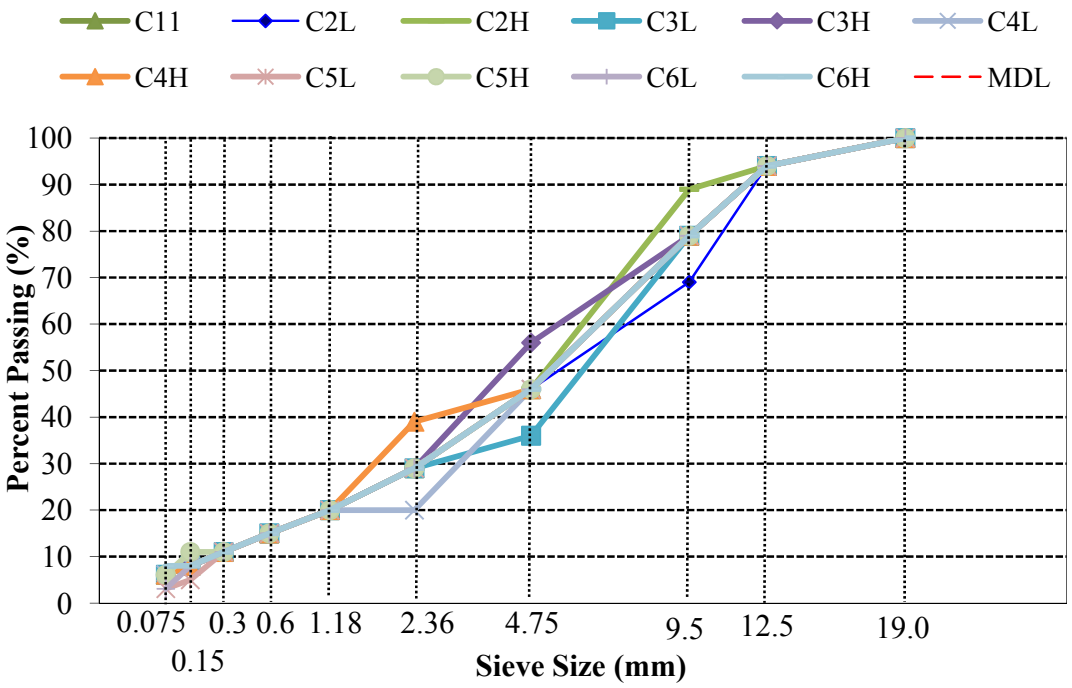

Figure 6-1. Gradation plot for the 11 gradations used for mechanical testing

6.2 Dynamic Modulus

6.2.1 *Dynamic Modulus Testing Procedures*

The dynamic modulus test specimen is 100mm (4.0 in) in diameter and 150 mm (6.0 in) in height, sawed and cored from the 150 mm by 170 mm gyratory compacted specimen. The mixtures were aged in accordance with the short-term oven aging procedure in AASHTO PP2 (2009), and compacted in according with Section 9 of AASHTO T312 (2009). The procedures for dynamic modulus tests are following the

NCHRP report 614 (Bonaquist 2008).

- Attach six targets to the specimen using epoxy. The distance of two targets should satisfy that the measure gauge length is around 100mm and the angle between each set of two targets is 120 degrees. Wait for around 30 minutes to let the epoxy consolidate and then move to next step.
- Place one rubber membrane on each end of the specimen, and place the spherical stainless steel ball at the center and on top of the top platens.
- Put the specimen and the platens inside the environmental chamber on the loading pedestal; make sure that the loading cell is in line with the axis of the end platen and the specimen when put the specimen.
- Place LVDTs on the specimen, and adjusts them to allow the full range of the LVDTs to be available for the measurement of deformation.
- Set the chamber temperature to the specific value, and allow the specimen to be conditioned for a required time. As shown in Table 6-2, each dynamic modulus samples are done under six frequencies (25, 20, 5, 1, 0.5, 0.1Hz) and four temperatures (40, 70, 100, 130^{o}F). A 60-second rest period was used between each frequency to allow some specimen recovery before applying the new loading at the next lower frequency.

The dynamic modulus testing was conducted using the IPC Asphalt Mixture Performance Tester (AMPT), also called Simple Performance Tester (Figure 6-2). The IPC AMPT equipment is a relatively small, computer-controlled testing machine that can perform various tests (dynamic modulus test, flow number test, and flow time test) on HMA over the temperature ranging from 4 to 60°C.

Table 6-2. Frequencies and temperatures used in the dynamic modulus testing

Frequency (Hz)	40(°F)	70(°F)	100(°F)	130(°F)
25	√	√	√	√
10	√	√	√	√
5	√	√	√	√
1	√	√	√	√
0.5	√	√	√	√
0.1	√	√	√	√

6.2.2 *Experimental Results*

Dynamic modulus testing was conducted for mixtures with each gradation type as shown in Table 6-1. Two duplicate samples were tested to verify the repeatability of the testing results. As shown in Figure 6-3, the master curves of the repeating samples match each

other well, indicating good repeatability of the testing results. It should also be noted that the naming system of all the specimens following some specific rules: C11 and C12 refer to the two repeating samples with the same base gradation; CXYZ refers to a sample belonging to gradation group X, either Low or High in percent passing certain sieve size (Y), and representing the first or the second repeating samples (Z). For example, C3H2 means this sample belongs to the C3 gradation group (Table 6-1), the percent passing sieve size 4.75mm is 10% higher than the base gradation, and the sample is the repetition sample 2.

Figure 6-2. Asphalt Mixture Pavement Tester

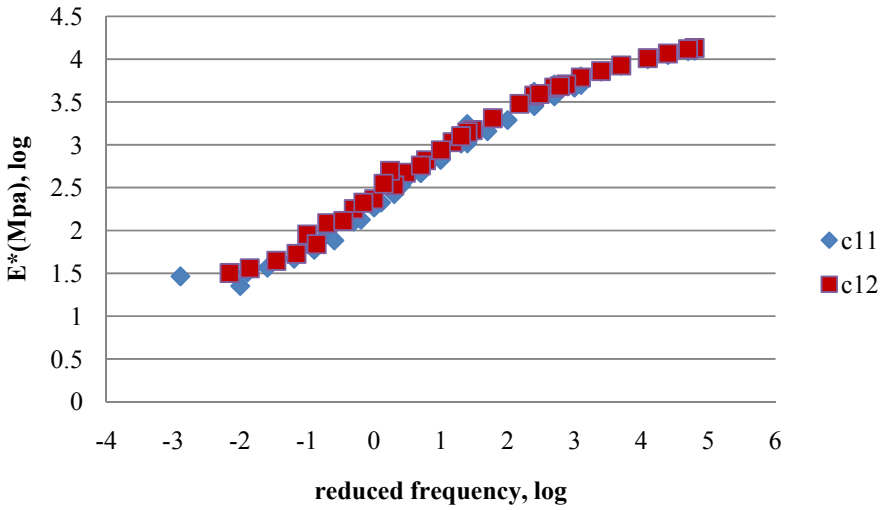

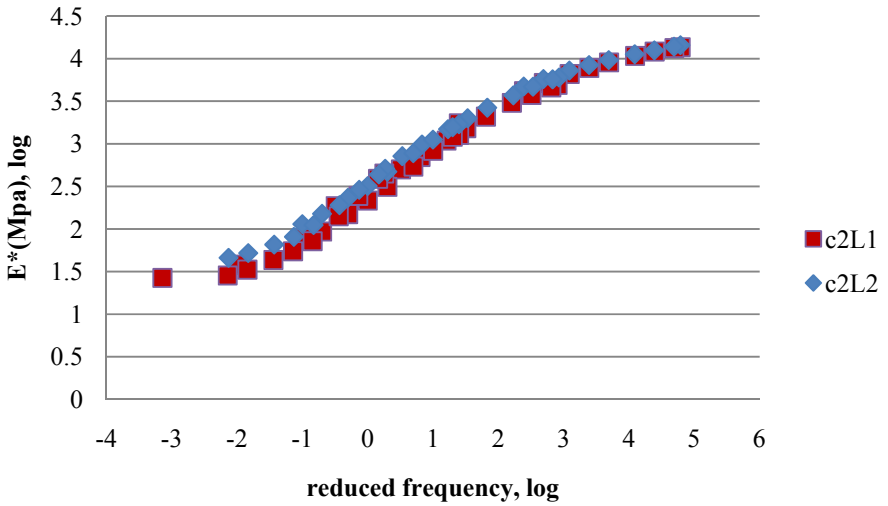

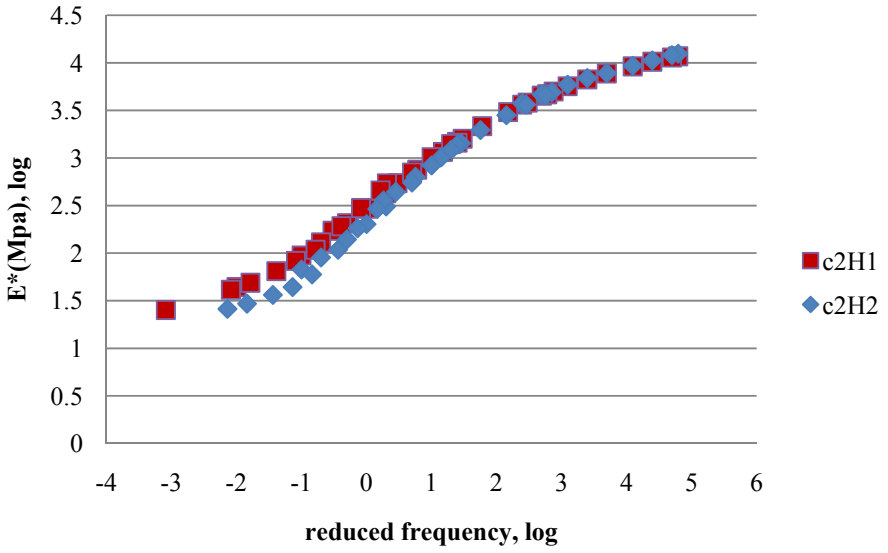

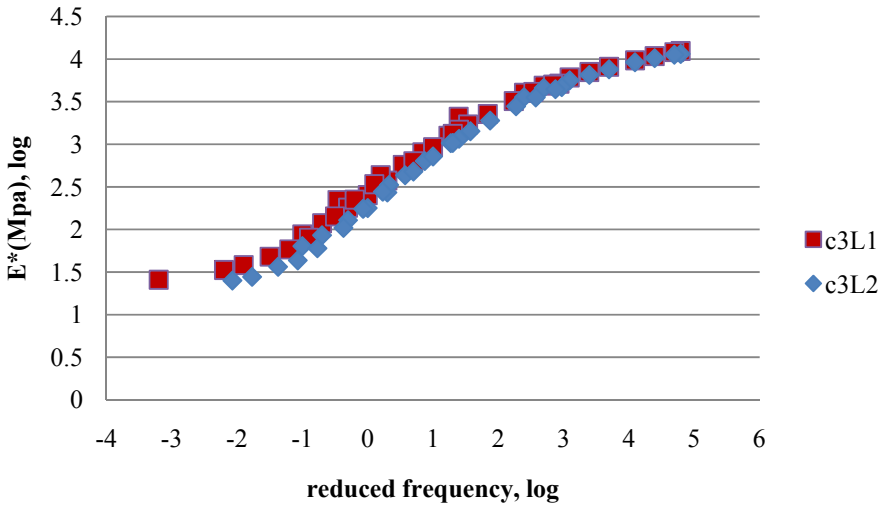

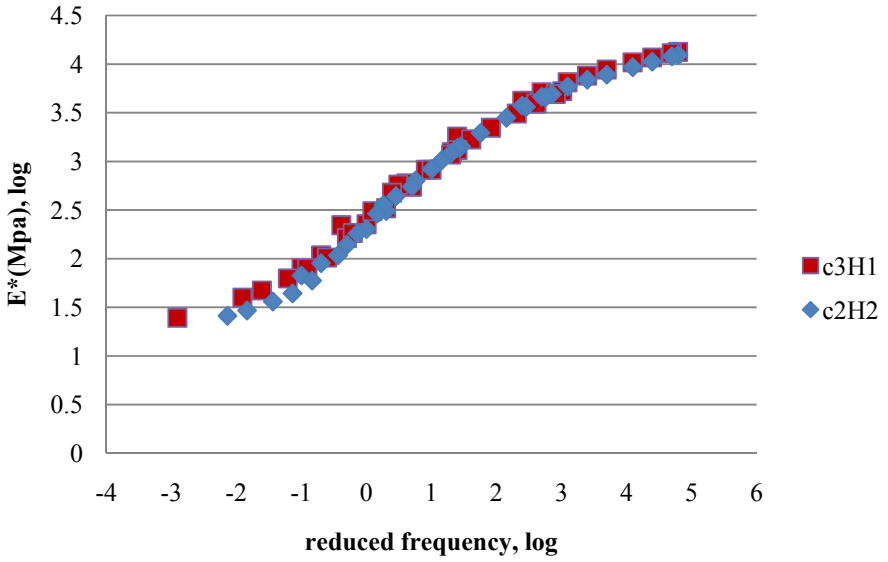

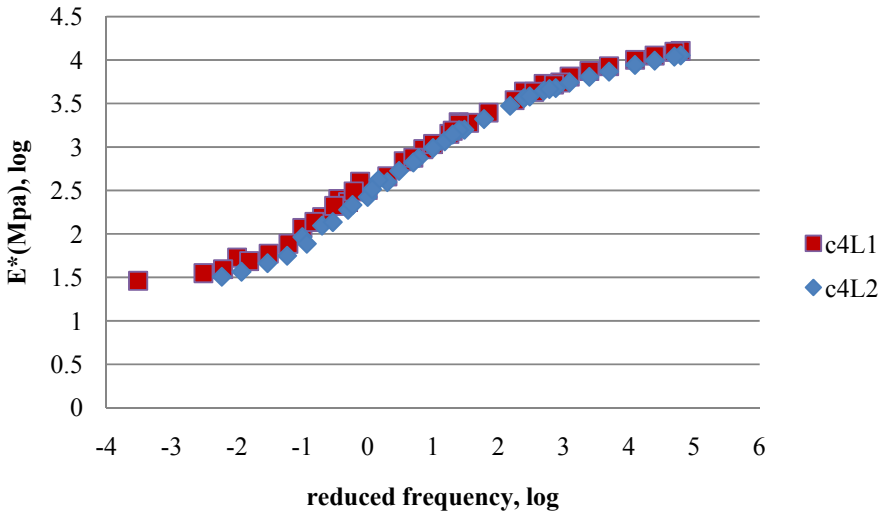

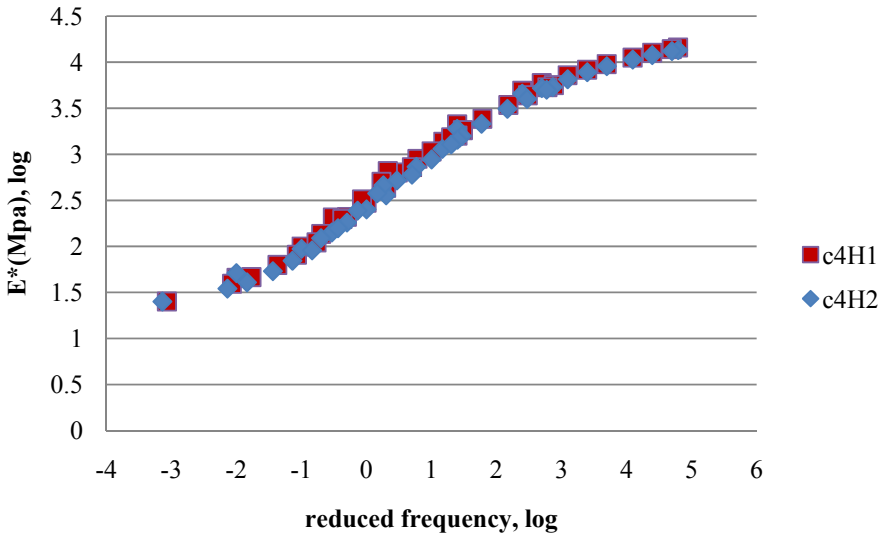

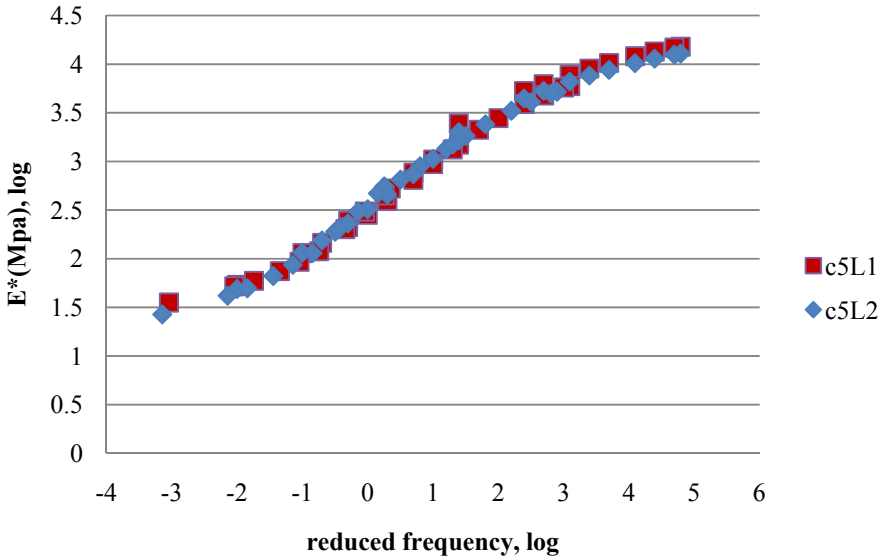

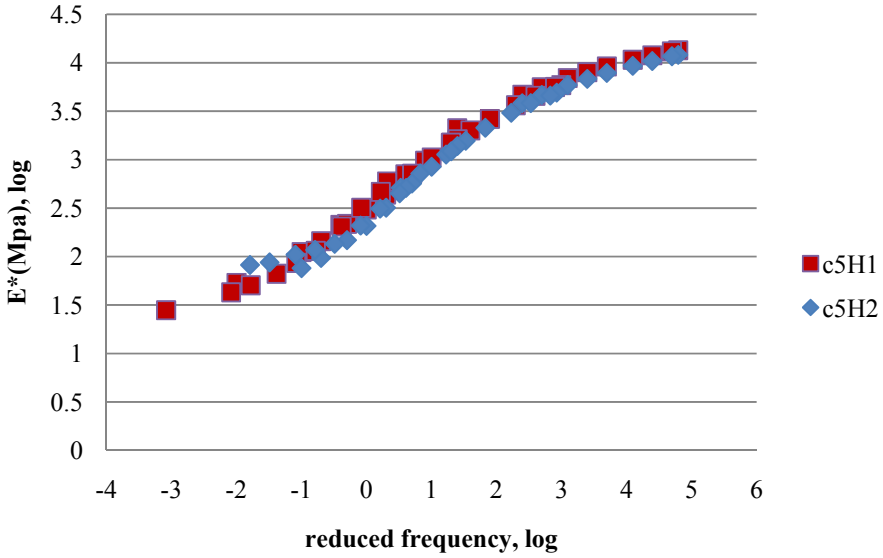

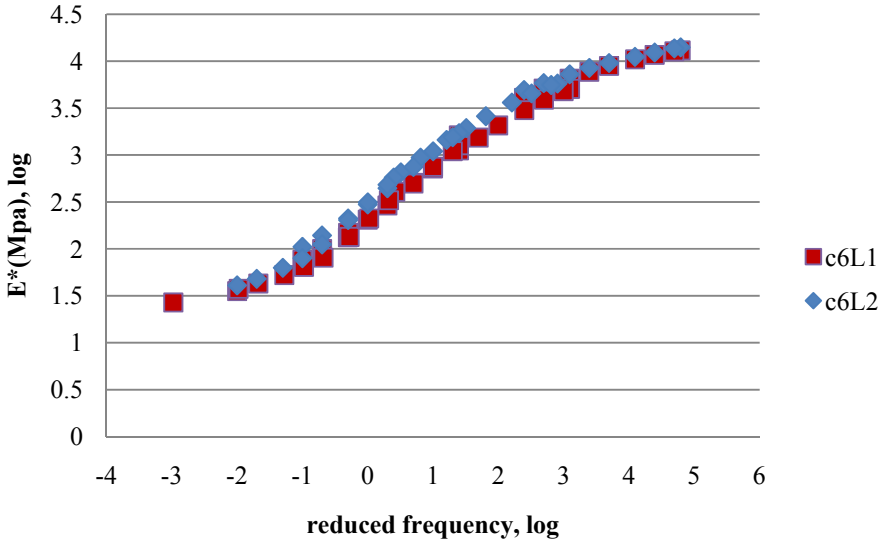

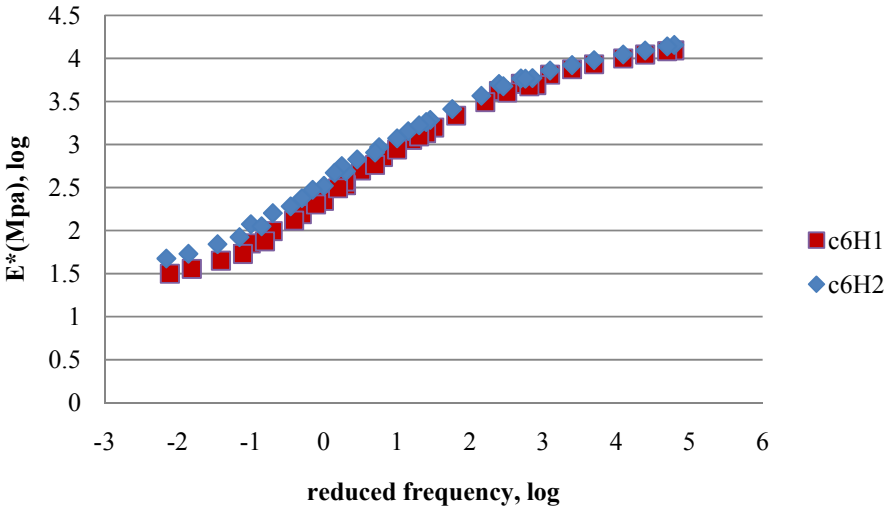

Figure 6-3. Dynamic modulus master curves at 100°F for repeating samples

6.2.3 *Effect of Individual Sieve Size on Dynamic Modulus*

Figure 6-4 showed the dynamic modulus changes corresponding to the variations of the percent particles passing specific sieve sizes, at 4.4°C temperature and 10 rad/second frequency. All samples are with the same type and content of asphalt binder and the same type of aggregate. Also all samples are compacted satisfy the Superpave mix design procedures. As shown, when the percent passing 9.5mm increased from 69 to 89, the dynamic modulus showed a decreasing trend. When the percent passing 4.75mm and 2.36mm are increasing, the trend of dynamic modulus is increasing. For the #100 and #200 sieve sizes, they both showed similar trend of increased dynamic modulus with either increasing or decreasing the percent passing from the base gradation.

Similar trend has been found at other temperatures and frequencies, and the details

are presented in Appendix B.

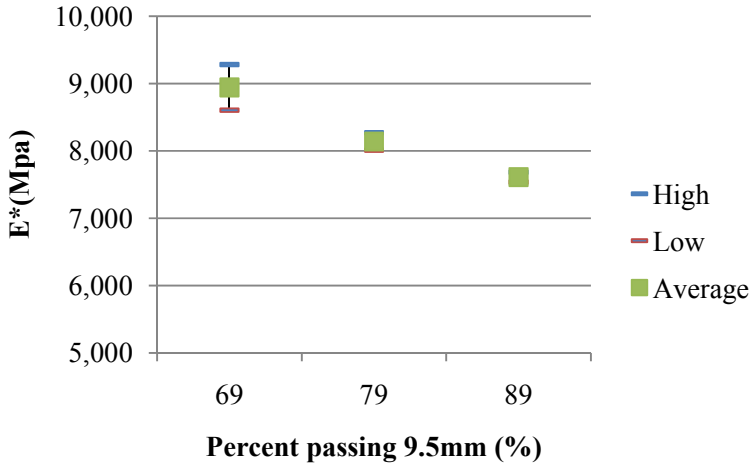

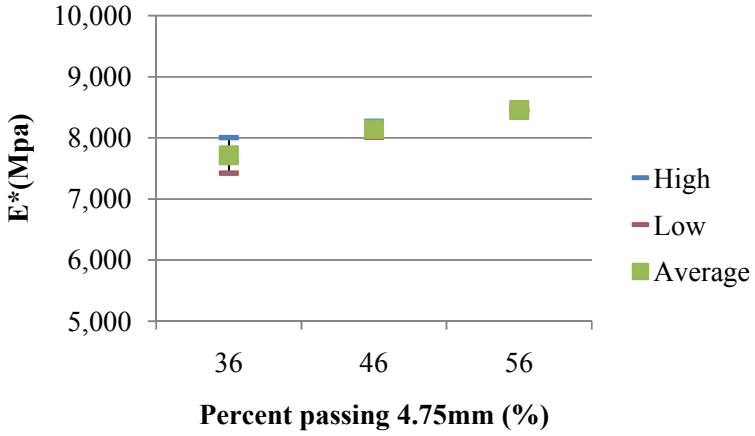

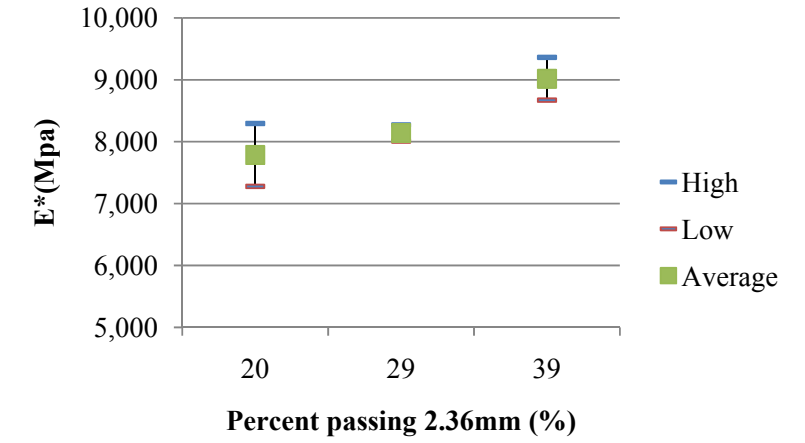

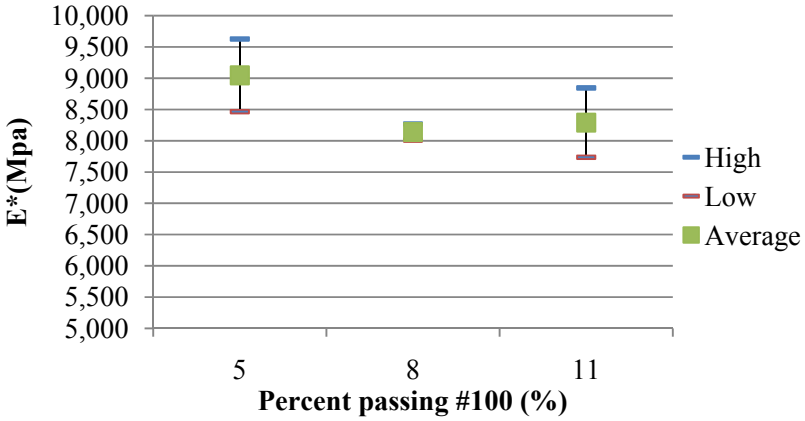

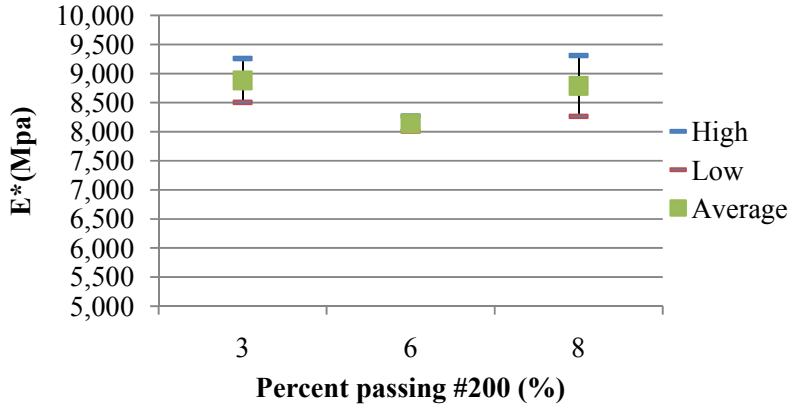

Figure 6-4. E* changes with the change of each sieve size (4.4°C)

6.2.4 *Effect of Aggregate Gradation as a Whole on Volumetric Properties (VMA) and Dynamic modulus*

Because aggregate gradation has direct correlation with the volumetric properties like the VMA, its effect on dynamic modulus can be determined by relating VMA with the dynamic modulus.

Figure 6-5 showed the relation between VMA and dynamic modulus at different temperatures. As can be seen, in general, the increase of the VMA will result in a decrease in the dynamic modulus, for different temperatures. This finding is consistent with previous literature findings (Bonaquist 2008). However, it is also clear that the R-squares of the correlations are not high, indicating the VMA is not the single determinant to the dynamic modulus. It is easy to understand because the dynamic modulus represents the mechanical properties of the mixture it will be influenced by both aggregate properties and the asphalt binder properties.

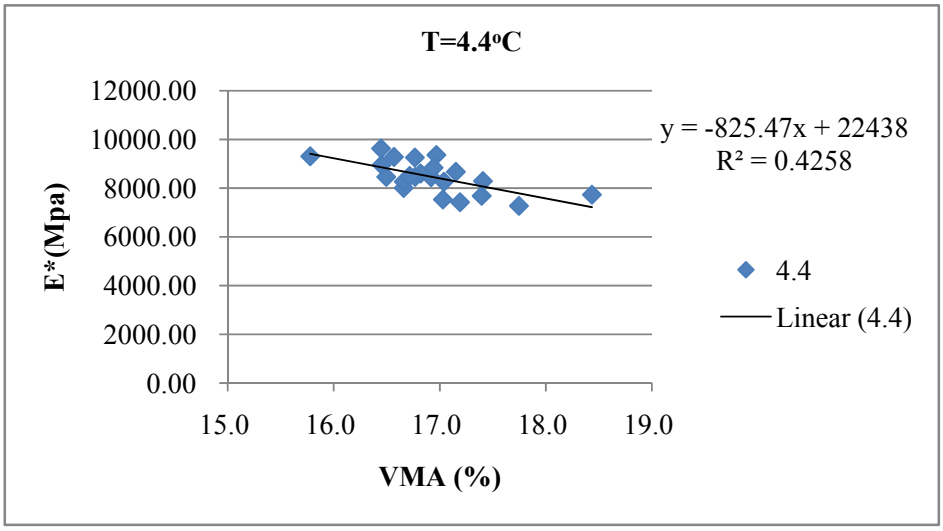

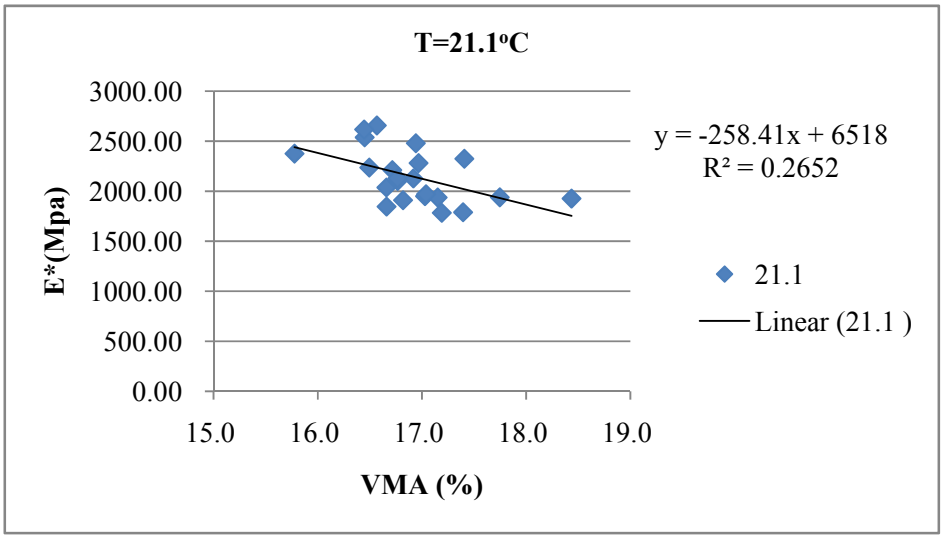

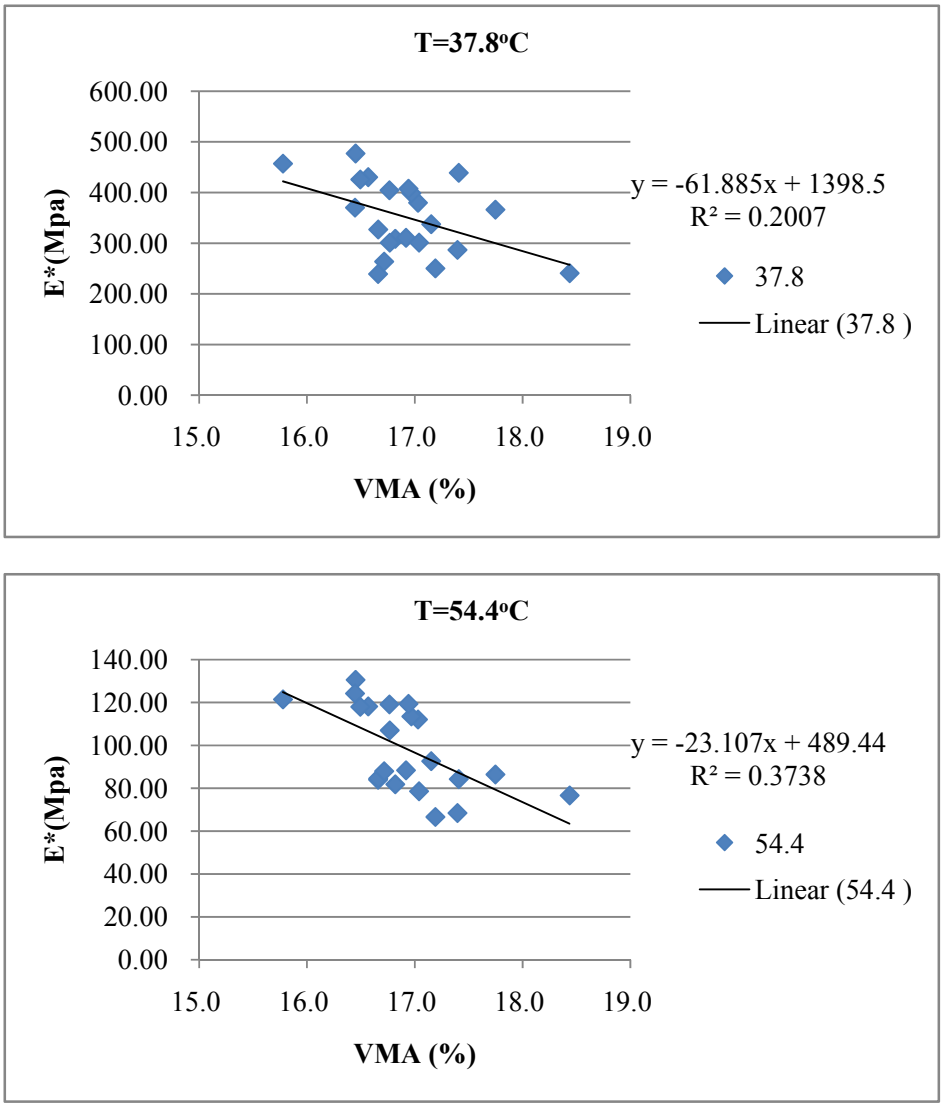

Figure 6-5. VMA vs. E* at different temperatures (10rad/s frequency)

6.2.5 *Predicting Dynamic Modulus Based on Aggregate Gradation and Asphalt Properties*

Given the strong correlations between the gradation and the volumetric properties (VMA) of the asphalt mixtures as established in Chapter 3, it will be desirable if the aggregate gradation properties and/or volumetric properties can be used directly for predicting the dynamic modulus, when combined with asphalt binder properties.

6.2.5.1 *Evaluation of existing prediction models*

As illustrated in Chapter 2 Literature Review, several models have been developed over the past decades to predict the dynamic modulus (E*) of HMA based on multivariate regression analysis of laboratory measurements. Among those models, the most widely used are the Witczak 1999 and 2006 predictive models (Witczak 2002; Bari and Witczak 2002) and the Hirsch model (Christensen et al. 2003). Although all provided reasonable accuracy as globally calibrated models, they were also reported by researchers not being able to capture the dynamic modulus behaviors for some local materials especially in high and low temperature extremes (Leiva-Villacorta 2007; Anderson et al. 2003). In addition, these models were found tend to overemphasize the influence of temperature and understate the influence of other factors or components (Ceylan et al. 2009). Therefore, it is necessary to modify existing prediction models or develop new models to be used in this study for linking dynamic modulus with material properties including the

aggregate gradation properties. Once established, such relationship will allow the material engineers and pavement engineers to estimate the pavement performance at the early stage of the material design, thus to design high quality materials which can lead to more durable pavement with less premature failure.

After reviewing all three models, the Hirsch model was selected in this study for several reasons. It will be further modified based on local materials to achieve a better prediction.

(1) Unlike the Witczak models which are based on regression equations, the Hirsch model is based on the theory of composite materials.

(2) Unlike the Witczak models which consider the effect of aggregates for four individual sieve sizes, the Hirsch model considers the overall effect of aggregate gradations by relating the volumetric properties with the dynamic modulus.

(3) Compared with the Witczak models, the Hirsch model is simpler consisting of less parameter. This is particularly important for the purpose of obtaining a prediction model that can be used for estimating the dynamic modulus of asphalt mixtures at the early stage of the mix design with minimum requirement for the experimental testing.

(4) The initial evaluation of the experimental results for the Washington mixes tested in this study indicated that Hirsch model provided better prediction compared with the Witczak models.

Hirsch model considers the composite material consists of different phases in series and/or in parallel arrangements. The asphalt material behaves as a serial arrangement composite at higher temperatures and as a parallel arrangement composite at lower temperatures. In addition, Hirsch model describes the visco-elastic asphalt material as time and temperature dependent material, and the aggregate contact proportion parameter Pc had a critical influence on the total behavior of the HMA. It was found that the HMA can be simulated with satisfactory accuracy with a simplified Hirsch model for which the general arrangements are in parallel rather than in series. The HMA was treated as a three-phase system which composed of aggregate, asphalt, and air voids. The following Equation (6.1) was proposed for regression process.

$$E_C = Pc \cdot \left(V_a \cdot E_a + V_b \cdot E_b\right) + \left(1 - Pc\right) \cdot \left[\frac{V_a}{E_a} + \frac{\left(V_b + V_v\right)}{V_b \cdot E_b}\right]^{-1} \quad (6.1)$$

Where

Va: true aggregate volume including volume of mineral filler,

V_b: effective binder volume,

E_a: aggregate response (for example modulus),

E_b: binder response (for example modulus),

V_v: air voids volume,

Pc: contact volume that represents the proportion of parallel to total phase volume and could be computed using the following expression:

$$Pc = \frac{\left(P_0 + \frac{VFA \cdot E_b}{VMA}\right)^{P_1}}{P_2 + \left(\frac{VFA \cdot E_b}{VMA}\right)^{P_1}} \quad (6.2)$$

Where

P_0, P_1, P_2: empirically determined constants,

VMA: voids in the mineral aggregate (voids + binder volume + mineral filler volume),

VFA: the percent of the VMA that is filled with the binder.

The Hirsch model for HMA dynamic modulus was developed based on data regression of 206 data points, indicated in Equation (6.3).

$$|E^*|_{mix} = Pc\left[4{,}200{,}000\left(1 - \frac{VMA}{100}\right) + 3|G^*|_b\left(\frac{VFA \times VMA}{10{,}000}\right)\right] + (1 - Pc)\left[\frac{1 - (VMA/100)}{4{,}200{,}000} + \frac{VMA}{3VFA|G^*|_b}\right]^{-1} \quad (6.3)$$

Where;

$$Pc = \frac{\left(20 + \frac{VFA \times 3|G^*|_b}{VMA}\right)^{0.58}}{650 + \left(\frac{VFA \times 3|G^*|_b}{VMA}\right)^{0.58}} \quad (6.4)$$

The measured dynamic modulus for all samples was compared with the predicted dynamic modulus based on the original Hirsch model. In Hirsch model, the aggregate and volumetric properties were determined from experiments following AASHTO specifications. The asphalt binder was short-term aged using the rolling thin film oven method and its dynamic shear modulus (G*) was measured using dynamic shear rheometer (DSR) following AASHTO T-240 (2009). Figure 6-6 presented a comparison between the measured and the predicted E* values. As shown, although the mid-range of the data followed well with the line of equality, the entire curve didn't show a good prediction trend. At low E* values, the original Hirsch model over-predicted the dynamic modulus while at high E* values the original Hirsch model under-predicted the dynamic modulus. In order to use Hirsch model to achieve better prediction, this model needs to be calibrated based on local materials.

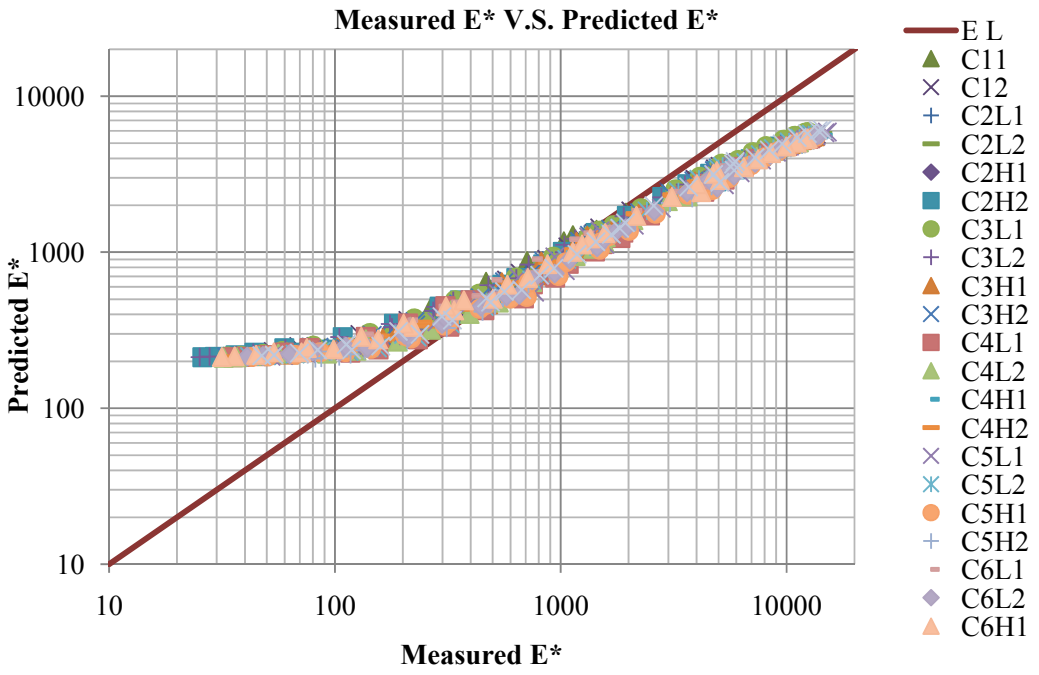

Figure 6-6. Laboratory measured E* and original Hirsch model predicted E*

6.2.5.2 *Modified Hirsch model based on local calibration*

The original Hirsh model was calibrated using the dynamic modulus testing results from 22 samples (11 gradations) by minimizing square errors, and the modified Hirsch model was provided in Equation (6.5). Those equations are obtained from gradation limited to the coarse-graded gradation and the asphalt binder for use is PG58-28.

$$\left|E^*\right| = Pc\left[1.0E10\left(1-\frac{VMA}{100}\right)+0.04\left|G_b^*\right|\left(\frac{VFA\cdot VMA}{10,000}\right)\right] + \left(1-Pc\right)\left[\frac{1-\frac{VMA}{100}}{1E10}+\frac{VMA}{VFA\cdot 0.04\left|G_b^*\right|}\right]^{-1} \quad (6.5)$$

Where,

$$Pc = \frac{\left(0.016+\frac{VFA\cdot 0.04\left|G_b^*\right|}{VMA}\right)^{0.6712}}{120,000+\left(\frac{VFA\cdot 0.04\left|G_b^*\right|}{VMA}\right)^{0.6712}} \quad (6.6)$$

Figure 6-7 compared the measured dynamic modulus with the predicted dynamic modulus based on the modified Hirsch model. It was clear that the prediction quality was significantly improved and most of the data followed the line of equality very well. Although only based on limited data (limited gradation type and binder type), this model showed very promising as it changed the inherent prediction trend of the original Hirsch model (Figure 6-7) and improved the prediction especially at the low and high end of the dynamic modulus curves.

The modified Hirsch model provided a means to estimate the dynamic modulus based on only volumetric properties (VMA, VFA) and asphalt binder dynamic shear modulus. Because the VMA can be estimated based on mainly the aggregate gradation properties as suggested in Chapter 5, and the VFA is a function of VMA, target air voids,

and asphalt absorption rate which is relative constant for given aggregate type, only the binder's G* is the required information for predicting dynamic modulus. This made it possible to estimate the dynamic modulus at the early stage of the mix design. If the predicted dynamic modulus is not appropriate (too low at high temperatures or too high at low temperatures), the modified Hirsch model can also be used as an optimization tool to guide the adjustment of the aggregate gradation to achieve appropriate E* values.

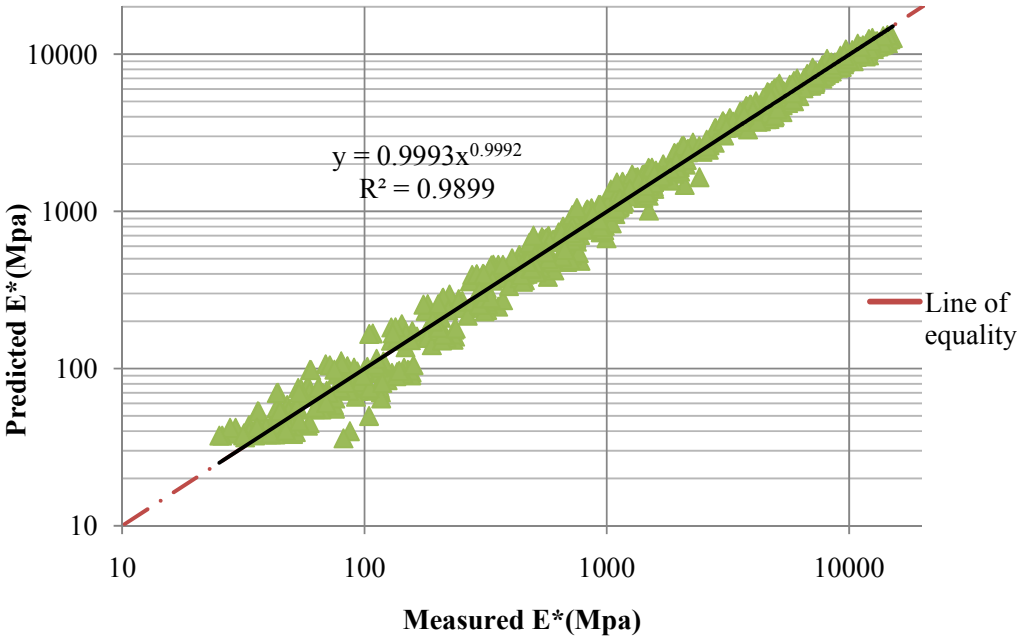

Figure 6-7. Laboratory measured E* and predicted E* based on modified Hirsch model

6.2.5.3 *Sensitivity analysis – effect of VMA on E**

VMA is one of the single most important parameters in the Hirsch model for determining

the dynamic modulus of asphalt mixtures, which also affects the amount of VFA in the mix given the same target air voids. Figure 6-8 showed that the dynamic modulus decreased with the increase of VMA and constant air voids. The VFA is calculated based on Equation (6.7).

$$VFA=100*(1-Va/VMA) \quad (6.7)$$

This finding is consistent with the experimental findings as shown in Figure 6-5. Further, the change rate of dynamic modulus with the change of VMA was plotted in Figure 6-9. At low temperatures (4.4°C, 21.1°C), the change rate of E* due to 5% VMA change is relatively stable, while at higher temperatures (37.8°C, 54.4°C) the change rate of E* decreases when the frequency becomes lower. In other words, the influence of VMA on the E* decreases at higher temperatures and lower frequencies.

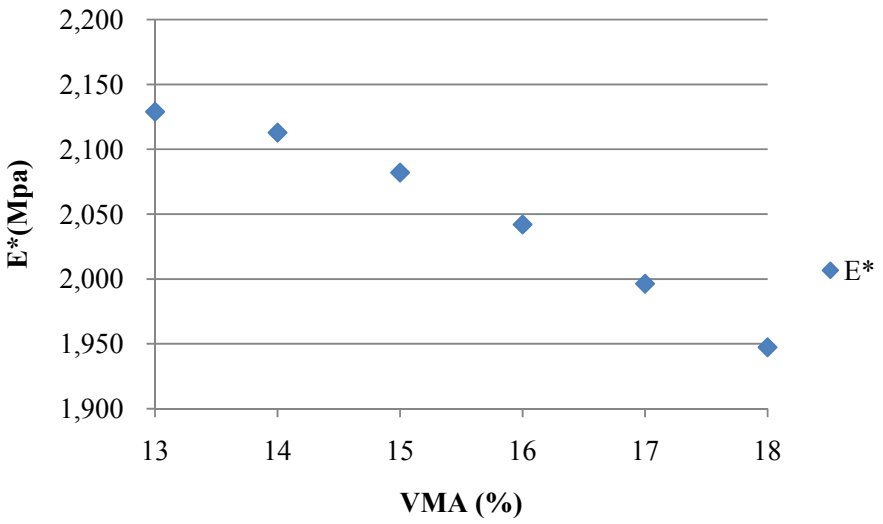

Figure 6-8. The change of E* with the change of VMA

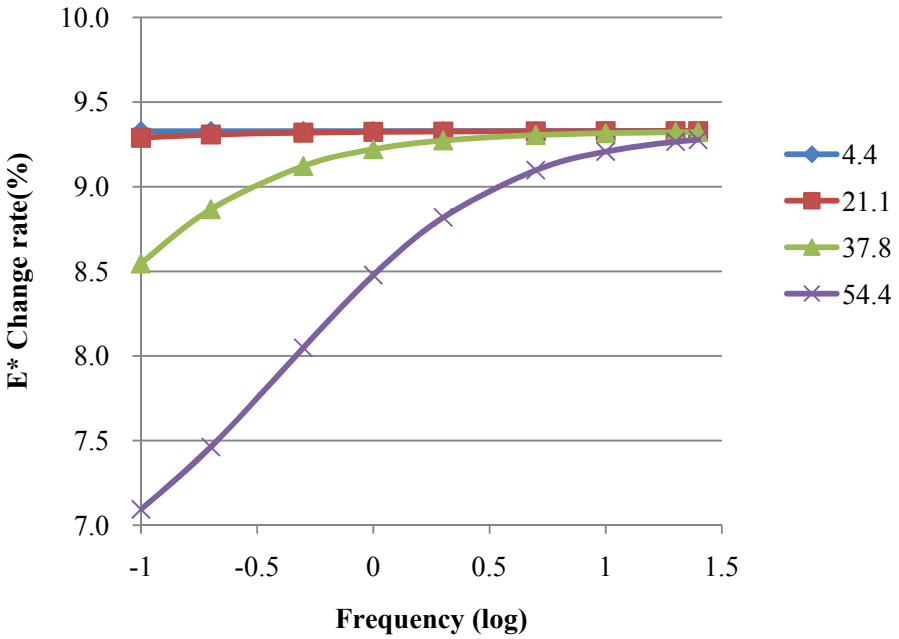

Figure 6-9. E* change rate vs. frequency at individual temperatures when VMA increases from 13% to 18%

6.3 Flow Number Tests

Flow number test was found to be able to correlate with the field rut depths and is recommended by the NCHRP report 465 (Witczak et al. 2002) and 580 (Witczak 2007) as a testing method to evaluate the rutting potential of the mixtures.

6.3.1 *Tests Setup*

In the flow number test, a 600 kPa load is applied to the specimen every second, until the flow point is reached. The flow point represents failure of the specimen, as evidenced by

an increasing rate of total permanent strain during the test. Flow number tests are run at the average 7-day maximum pavement temperature 20 mm from the surface, at 50% reliability as determined using LTPPBind version 3.1 which is corresponding to 49.6^{o}C degree in Eastern Washington.

6.3.2 *Effect of Individual Sieve Size on Flow Number*

The relation between the percent of particles passing different sieve sizes and flow number are shown in Figure 6-10. As indicated from the experimental results, the flow number decreases with the increase of the percent of particles passing 9.5mm sieve, while increases with the increase of the percent of particles passing 4.75mm sieve. This trend is similar as the effect of sieve size on dynamic modulus. However, a different trend of the effect of particles passing sieve size 2.36mm, 0.15mm (#100), and 0.075mm (#200) on flow number was found. As the percent passing 2.36mm increases from 20-39, the flow number shows an increase trend and then decrease. And with the increasing of percent passing #100, the flow number is decreasing. For percent passing #200, when the percent pass increasing from 3% to 6%, it shows a trend of increase, and when the percent passing #200 keep on increasing from 6% to 8%, the flow number show a slight decrease.

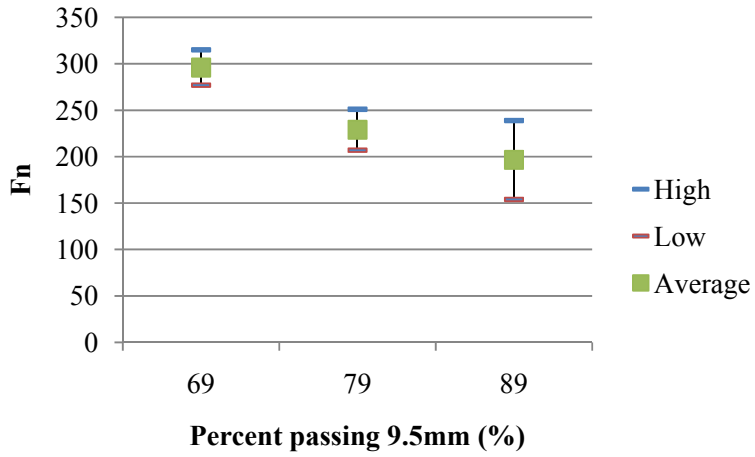

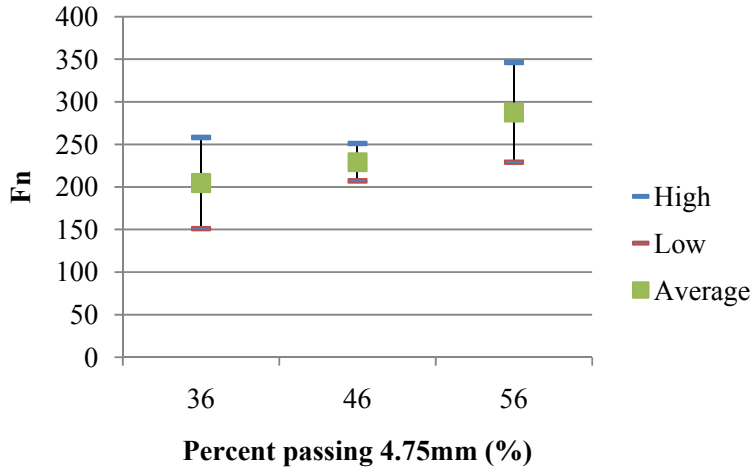

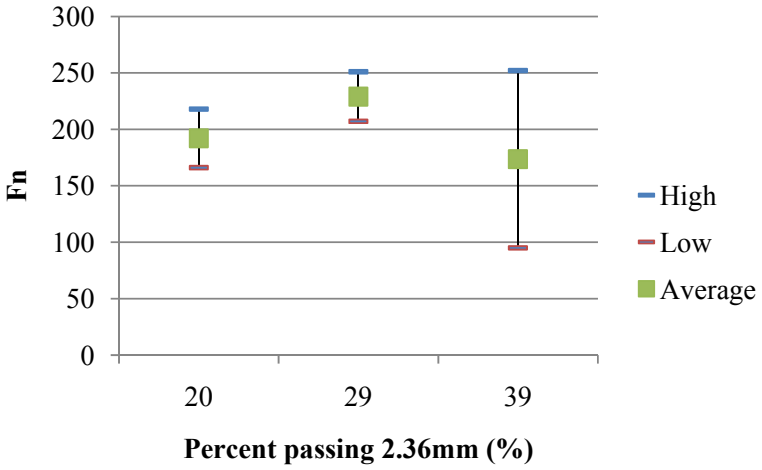

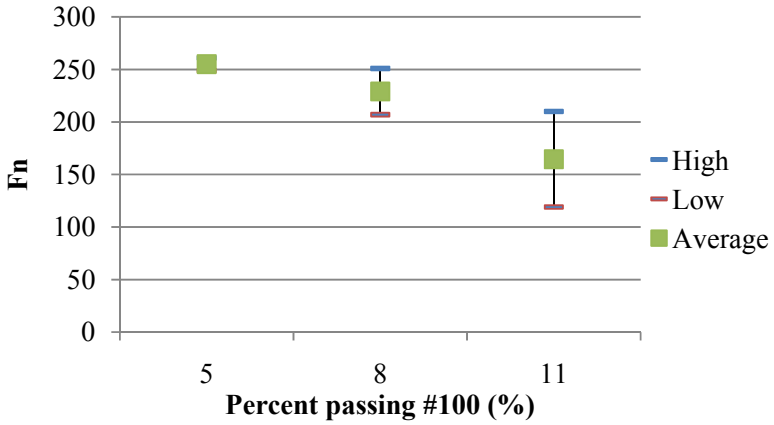

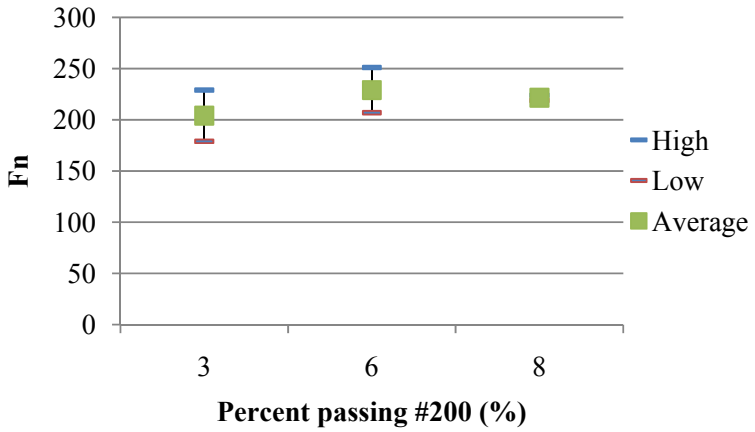

Figure 6-10. Flow number vs. the change of % passing individual sieve size

6.3.3 *Relation between VMA and Flow Number*

The relation between VMA and flow number is shown in Figure 6-11, which indirectly indicates the overall effect of gradation on flow number. With the increase of VMA, the flow number showed a decreasing trend, which is similar as the trend between VMA and dynamic modulus.

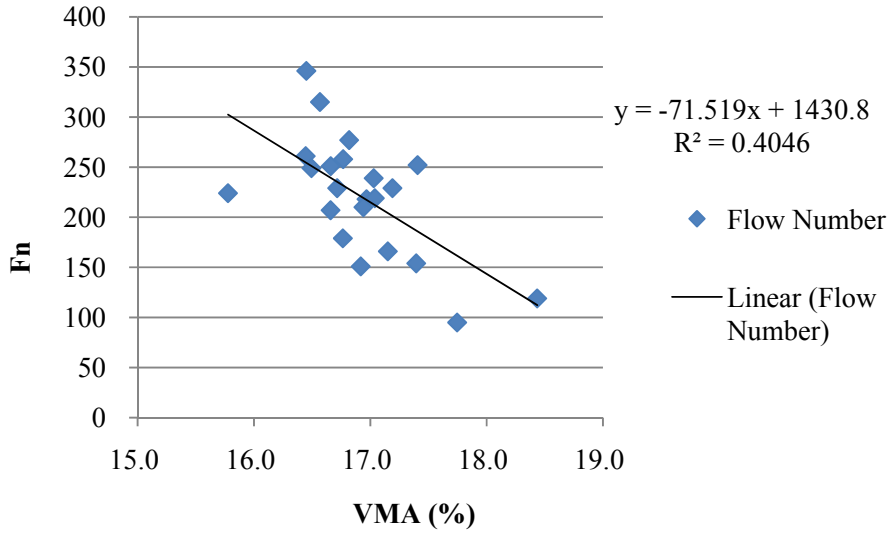

Figure 6-11. VMA vs. Flow number

6.4 COMPACTABILITY EVALUATION

As stated in the Strategic Highway Research Program (SHRP) Report A-407 (Cominsky et al. 1994), it is the aggregate characteristics rather than the asphalt binder characteristics dominate the rate of compaction in the Superpave gyratory compactor and the field compaction process. In this study, the compaction slopes for each gyratory compacted sample were calculated to evaluate how different aggregate gradation properties can affect the compaction characteristics of different mixtures.

6.4.1 *Effect of Aggregate Gradation on Compactability of Mixtures*

Figure 6-12 showed the compaction slope change corresponding to the change of each

sieve size. As show in the figure, increasing the percent passing 9.5mm sieve particles (from 69% to 79%) in general increase the compaction slope and improve the compactability of the mix because the mix will consist of less large size particles. However, this effect is leveled when the amount of large size particles are below a certain limit (in this case 20%). The effect of particles passing 4.75mm and 2.36mm showed similar trend on compactability, both having reduced compaction slope with the increase of percent passing that sieve size. It is suggested that increasing the amount particles passing the intermediate size particles (separators), in other words decreasing the total amount of coarse aggregates, will generally reduce the compactability of the mix. This result supports the previous findings by NCHRP report 478 (Anderson et al. 2003). It is also reasonable that for both sieve size #100 and #200 there exists an optimal percent passing rate at which the compactability will reach maximum. Both too few and too many fine particles will inversely affect the compactability of the mix.

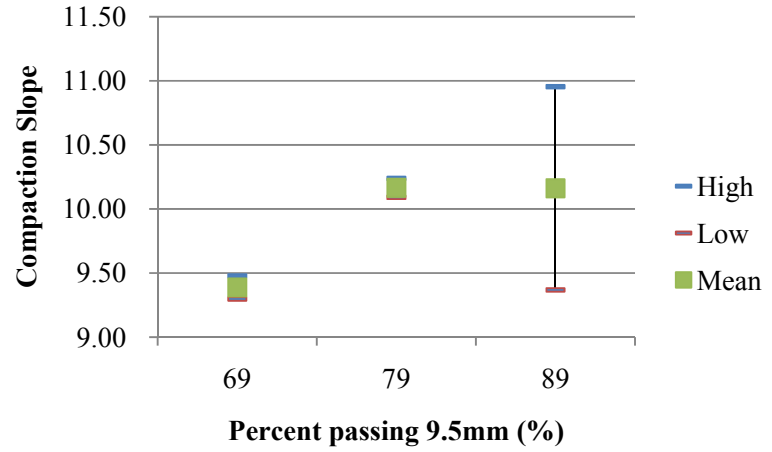

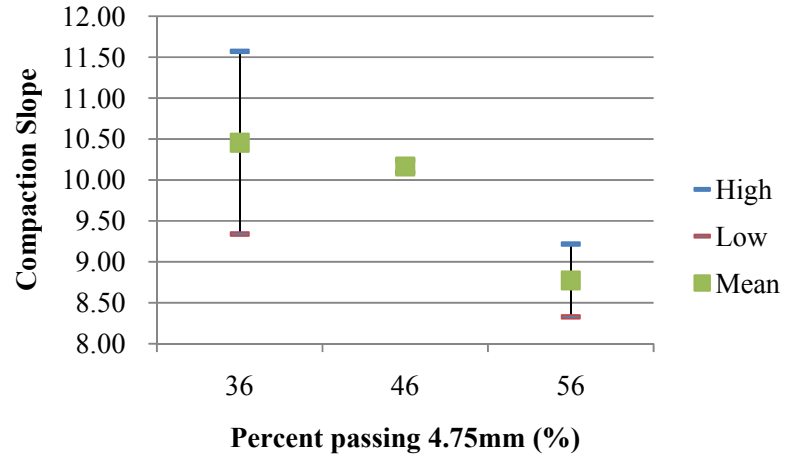

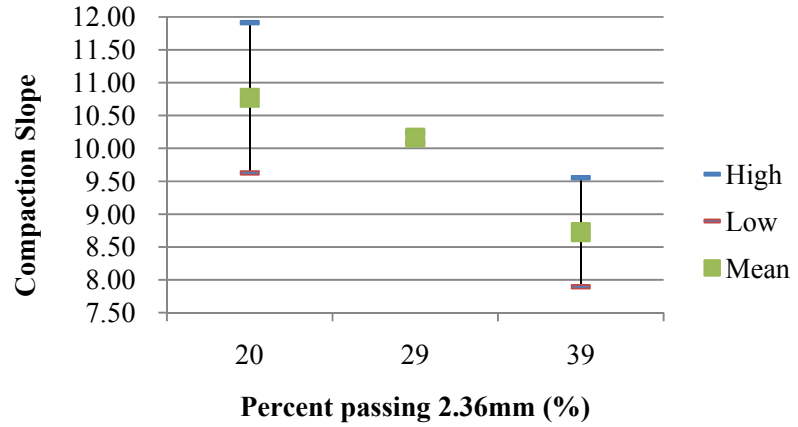

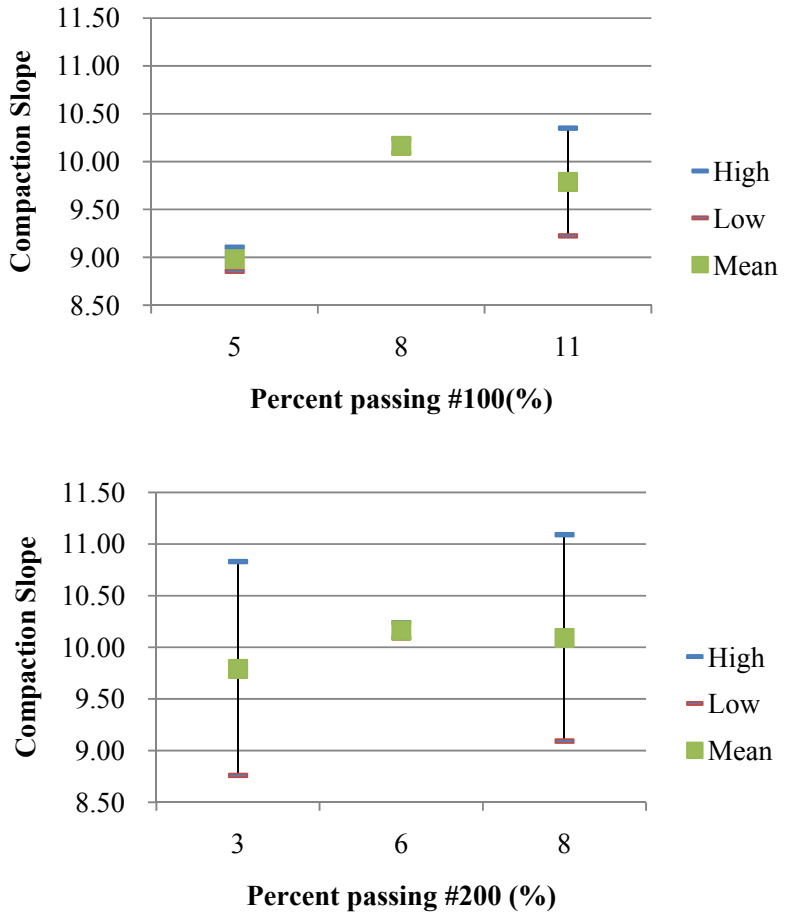

Figure 6-12. Compaction slope vs. the change of percent passing individual sieve size

6.4.2 *Relation between VMA and Compaction slope*

The relation between VMA and compaction slope is presented in Figure 6-13 which showed no strong correlation between the VMA and the compaction slope. This finding

suggested that the compactability of the mix is more related to the size distribution and the packing characteristics of the aggregate structure. The mixes with the same VMA but different size distributions (gradations) may have different compactability. Therefore, the analysis of aggregate packing as introduced in Chapter 5 plays a significant role in evaluating the aggregate gradations.

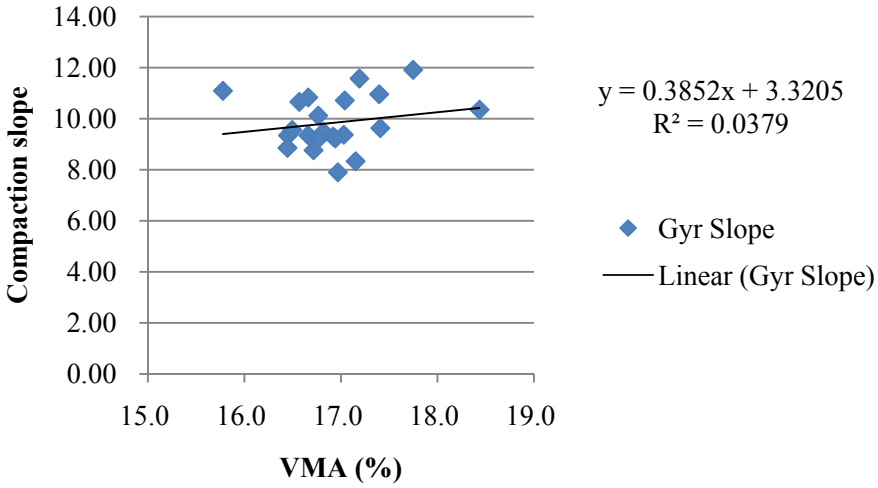

Figure 6-13. VMA vs. Compaction Slope

6.5 SUMMARY

In summary, aggregate gradation and the resulting volumetric properties of the mix was found to have strong influence on the mechanical performance of the asphalt mixture. By presenting how changing the individual size of aggregate gradation can affect the dynamic modulus, compactability, and flow number of the mixtures, this chapter

provided valuable information on the adjustment of aggregate gradations when specific performance is in question. In addition, because the aggregate gradation can be directly related to the VMA of the mixture, the impact of VMA on the mechanical performances, as demonstrated in this chapter, can be regarded as the overall impact of aggregate gradation on performance.

A modified Hirsch model was provided which can be used as both a designing tool and a screening tool to estimate the mixture's dynamic modulus at the early stage of the mix design. Relying on only very limited experimental testing, this modified Hirsch model will help designer exclude poor performing mixtures, provide guidance on adjusting aggregate gradations to achieve better long-term field performance.

CHAPTER 7 DYNAMIC MODULUS AND FLOW NUMBER OF ASPHALT MIXTURE

Dynamic Modulus (|E*|) is one of the key elements of a mechanistic-empirical based flexible pavement design procedure. It is used to characterize the material properties of asphalt mixtures and determine the stress strain responses of a pavement at different loading conditions, and is a direct input parameter in several pavement performance models to estimate the field fatigue cracking and rutting performance. As part of the asphalt mixture performance tests, the flow number has been found to be able to correlate well with the field rutting depth by a number of projects.

Over the time, there have been great efforts to establish prediction models of mechanical properties of asphalt mixture. Several models have been developed over the past decades to predict the dynamic modulus (E*) of HMA based on multivariate regression analysis of laboratory measurements. Among those models, the most widely used are the Witczak 1996 and 2006 predictive models and the Hirsch model. Besides, some researchers have proposed different prediction models of flow numbers to characterize the rutting potential of asphalt mixture. This chapter evaluated the accuracy of those models for predicting the dynamic modulus of asphalt mixtures. Based on the evaluation results, a revised Hirsch model for dynamic modulus prediction is established

which significantly improved the predication quality. In addition, a locally calibrated flow number prediction model is provided.

7.1 INTRODUCTION

Pavement design is currently in the trend of moving toward more mechanistic based design methodologies for the purpose of producing more durable and higher performance pavements in a cost-effective manner. The recent Mechanistic-Empirical pavement design guide (MEPDG) is a product under such direction and is making progresses in improving current design methods. Dynamic Modulus (|E*|) is proposed by the MEPDG as an important asphalt material characterization property and a key input parameter which correlates material properties to field fatigue cracking and rutting performance.

The AASHTO M-E design guide have three hierarchical levels which either requires the direct laboratory testing for dynamic modulus or using the Witczak model to predict dynamic modulus values which was based on conventional multivariate regression analysis. The NCHRP Projects 9-19 (Witczak 2007), Superpave Support and Performance Models Management, and project 9-29 (Bonaquist 2008), Simple Performance Tester (SPT) for Superpave Mix Design, have stated the detailed experimental procedures to conduct simple performance tests (recently renamed as asphalt mixture performance tests, AMPT) and documented the possibility of using the

simple performance tests for evaluating the resistance of asphalt mixtures to permanent deformation and fatigue cracking. In the case of using Witczak model to estimate |E*| values, many researchers evaluated the predictive capability of the Witczak model through the comparison of predicted and measured dynamic modulus using various mixtures across the United States (Ceylan2009). The Witczak model was also refined and revised to give better prediction results (Bari and Witczak 2006). A good understanding of the dynamic modulus properties of the local mixtures will provide mechanistic based knowledge for improving pavement serviceability and its expected long-term field performance.

As part of the AMPT tests, the flow number test was found to be able to correlate with field rut depth as verified by field projects at MNRoad, Westrack, and the FHWA Pavement Testing Facility in the NCHRP project 9-19 (Witczak 2007). It has been recommended by the NCHRP project 9-33 (Advanced Asphalt Technologies, LLC., 2011) for evaluating the rutting potential of the mix. Testing the flow number properties of the local mix as part of the local material characterization plan will be very beneficial for evaluating the mix, developing material-performance relationship, and improving the overall quality of the pavement system.

The primary objective of this section is to evaluate the dynamic modulus and flow number properties of asphalt mixtures. In total, seven plant produced mixtures from

different regions which represented the typical asphalt binder, gradation, and mix designs of the state were sampled and tested. The measured dynamic modulus data were compared with the prediction results using the traditional Witczak E* model, the new Witczak E* model, and the Hirsch model. A modified Hirsch model was proposed which was found to be more suitable for predicting the dynamic modulus of the asphalt mixtures.

7.2 PROJECTS DESCRIPTION

7.2.1 *General Information*

The dynamic modulus and flow number testing was conducted based on plant mixed lab compacted gyratory samples. Loose asphalt mixtures were sampled directly from the plant. The plant mixed asphalt mixture is more representative of the materials used in the field, when compared to the lab mixed asphalt mixtures. In order to build a catalog of dynamic modulus to conduct subsequent model verification and calibration, the material procurements have covered a range of typical materials and mix designs for the state, in terms of asphalt binder, aggregate type, gradation, and usage of RAP.

Based on the selection criteria, seven paving projects were identified with the assistance of the WSDOT material's lab. Table 7-1 listed a summary of the seven projects, and Figure 7-1 indicated the geographic location of each project.

Table 7-1. Asphalt mixture general information

	Contract No.	Project Section	Region
#1	C8046	I-90, Ritzville to Tokio - Paving of Outside Lanes Only	Eastern
#2	C8017	US 395, Lee Rd to Vic I-90 Paving	Eastern
#3	C8013	SR 26, Grant County Line to SR 17 - Paving	Northcentral
#4	C8033	US 12, SR 124 Intersection Build Interchange	Southcentral
#5	C8016	I-5, Joe Leary Slough to Nulle Rd. Vicinity - Paving	Northwest
#6	C7879	SR 510, Yelm Loop - Phase 1	Olympic
#7	C7465	I-5, Grand Mound to Maytown Stage One - Add Lanes	Olympic

Figure 7-1. Geographic locations for all projects

7.2.2 *Summary of Materials*

Loose mixtures were collected from the dump trucks at the asphalt plants and transported to the Washington State University for testing. Once acquired, mixtures were only allowed to be reheated once for specimen compaction to minimize the effect of reheating on the mix.

A copy of the job mix formula (JMF) for each project is obtained. The basic properties of the mixtures are shown in Table 7-2. For project #4 (C8033), both the HMA

and WMA (foaming technology) were evaluated. The gradations of the mixtures are shown in Table 5 and plotted in Figure 7-2. As shown, all mixtures have a nominal maximum aggregate size (NMAS) of 12.5 mm. Four asphalt binder types (PG76-28, PG70-28, PG64-28, and PG64-22) are included, which are the typical asphalt binders based on local climatic and traffic conditions. The design asphalt content varies from 5.2% to 5.7%. Most mixtures included approximately 20% recycled asphalt pavement (RAP) material.

Table 7-2. Basic properties of asphalt mixture

	Contract No.	Asphalt	HMA/WMA	RAP	Design AC (%)
#1	C8046	PG 76-28	HMA	20%	5.4
#2	C8017	PG 70-28	HMA	20%	5.7
#3	C8013	PG 64-28	HMA	20%	5.2
#4	C8033	PG 64-28	HMA/WMA	20%	5.2
#5	C8016	PG 64-22	HMA	20%	5.3
#6	C7879	PG 64-22	HMA	0	5.4
#7	C7465	PG 64-22	HMA	18%	5.6

Table 7-3. Mixture Gradations

Sieve	3/4"	1/2"	3/8"	#4	#8	#16	#30	#50	#100	#200
	19mm	12.5mm	9.5mm	4.75mm	2.36mm	1.18mm	0.6mm	0.3mm	0.15mm	0.075mm
C8046	100	96	81	53	31	20	14	11	8	6.3
C8017	100	94	82	55	36	24	18	15	9	6.3
C8013	100	95	83	53	33	23	18	14	8	5.7
C8033	100	93	85	53	35	24	16	11	8	5.5
C8016	100	94	83	60	46	33	22	12	7	5.1
C7879	100	95	78	54	36	24	17	12	8	6
C7564	100	95	82	55	35	23	16	10	7	4.9

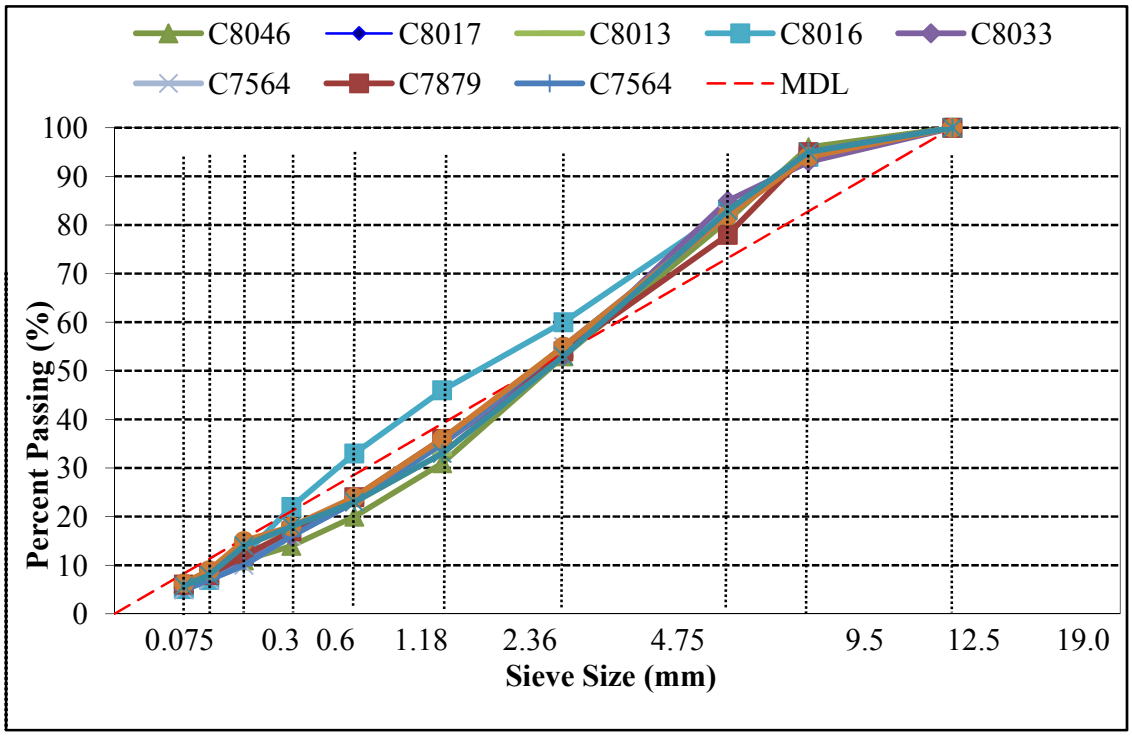

Figure 7-2. Asphalt mixture gradations

7.2.3 *Sample Preparation*

The dynamic modulus test was conducted in accordance with AASHTO TP 62-03. The specimens were compacted with a Superpave gyratory compactor into 150 mm in diameter and approximately170 mm in height. To ensure the quality of each specimen prepared for testing, great care was given to maintain a consistent compaction process. The stored asphalt mixtures were subjected to short term aging in oven at compaction temperature for 2 hours before compaction. Then specimens were cored from the center into 100 mm in diameter, and approximately 10 mm were sawed from each end of the

test specimen. Sawing operations were performed carefully to ensure the ends maintained as parallelism as possible. The bulk specific gravities and air void contents for each test specimen were measured voids in accordance with AASHTO T-269, Percent Air Voids in Compacted Dense and Open Bituminous Paving Mixtures. Three target air void levels,4%±0.5%, 7%±0.5%, and 9%±0.5%, are used, to evaluate the effect of air voids on dynamic modulus and flow numbers. If any specimen was outside the required air void range, the specimen was discarded and a new sample will be made. Once the specimens were prepared, they were stored at room temperature at dry condition until testing.

7.3 Experimental Results

7.3.1 *Dynamic Modulus Results*

Dynamic modulus testing was conducted for each asphalt mixture at three target air void levels: 4%, 7%, and 9%. Two replicate samples at each air void level were tested to verify the repeatability of the testing results. The master curves of the replicate samples are shown in Figure 7-3 to Figure 7-10. It should also be noted that the naming system of all the specimens following some specific rules. X-Y-Z refers to a sample belonging to project # X, air void level Y, and sample number Z. The relation between project number and contract number can refer to Table 7-1. In other words, a sample number of 3-4-2 means that this sample belongs to project number 3 (contract C8013 according to Table

7-1), at 4% target air voids, and is the second replicate samples.

As shown from Figure 7-3 to Figure 7-10, the master curves of the replicate samples match each other well, indicating good repeatability of the testing results. Figure 7-14 shows the master curves of all samples with the same air voids levels..

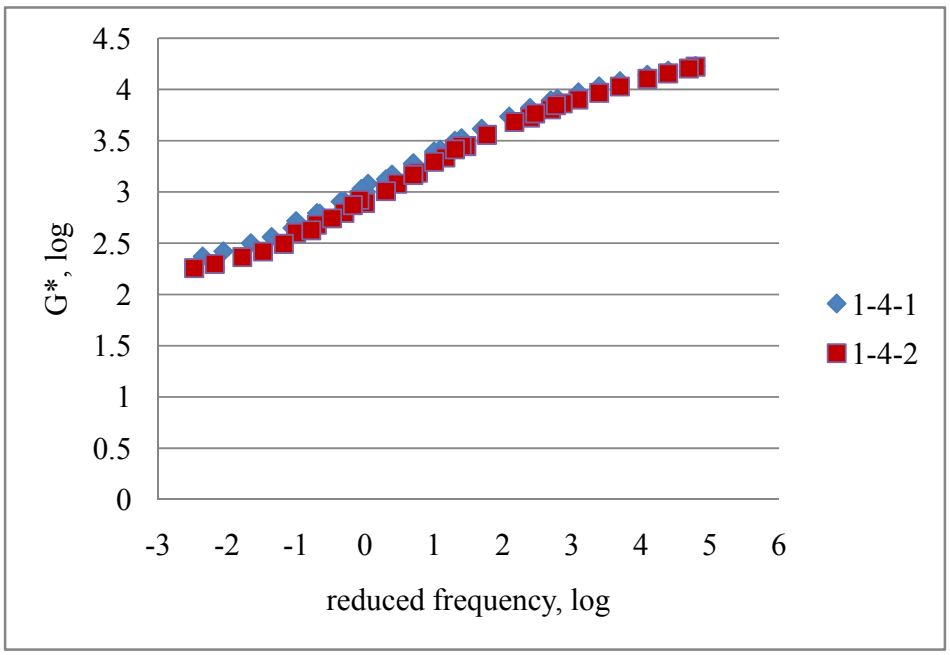

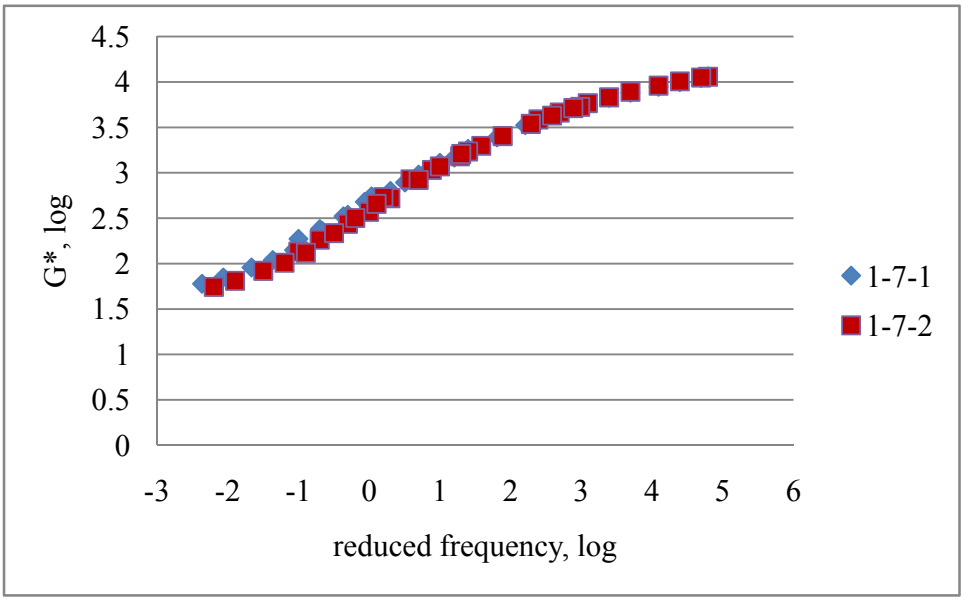

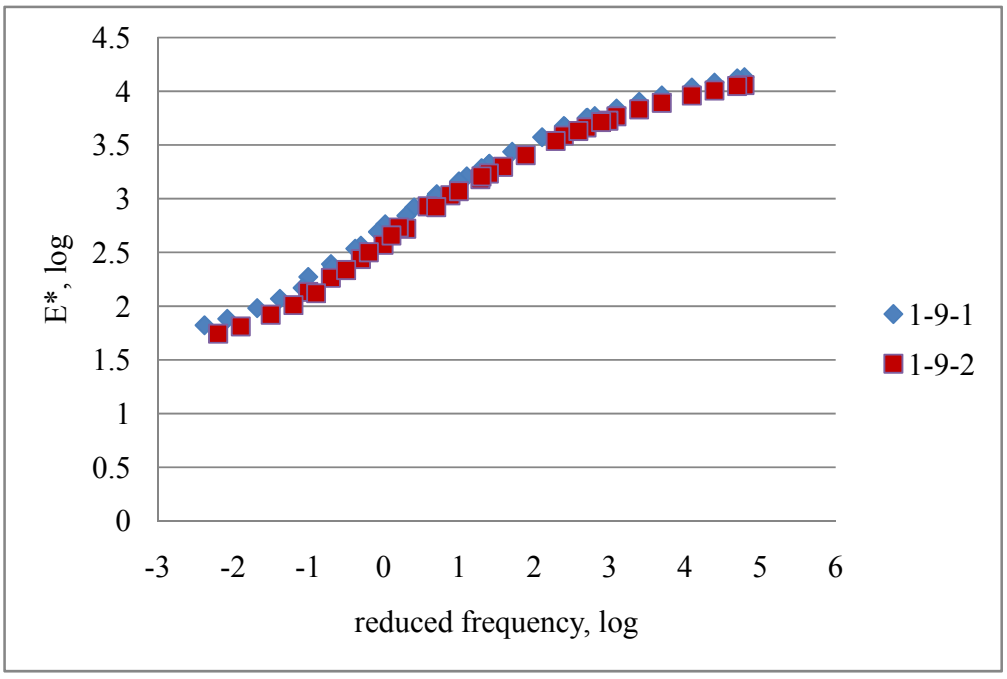

Figure 7-3. |E*| master curves of project C8046 at 100°F for repeating samples

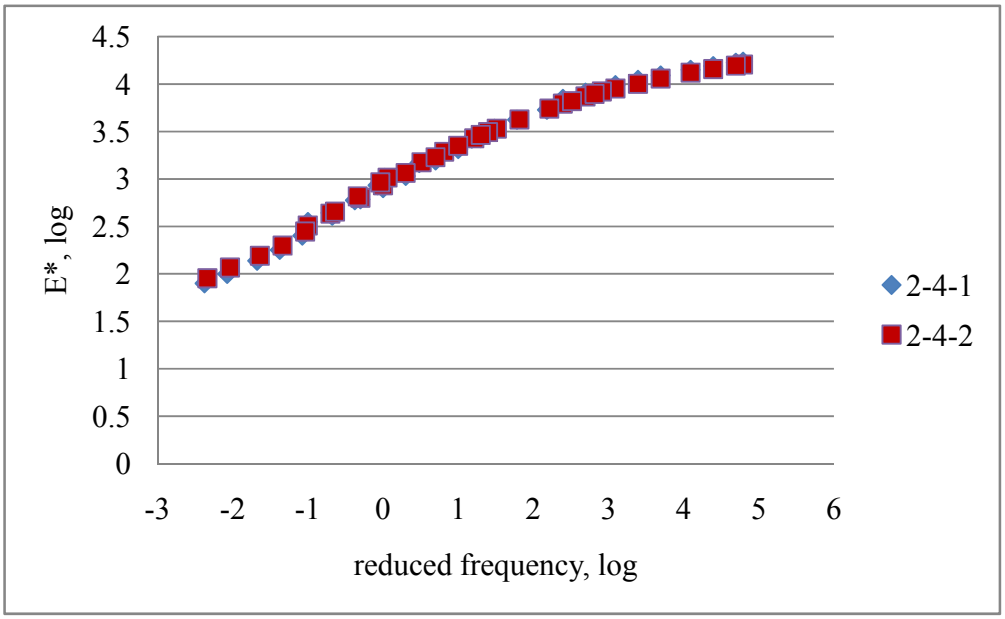

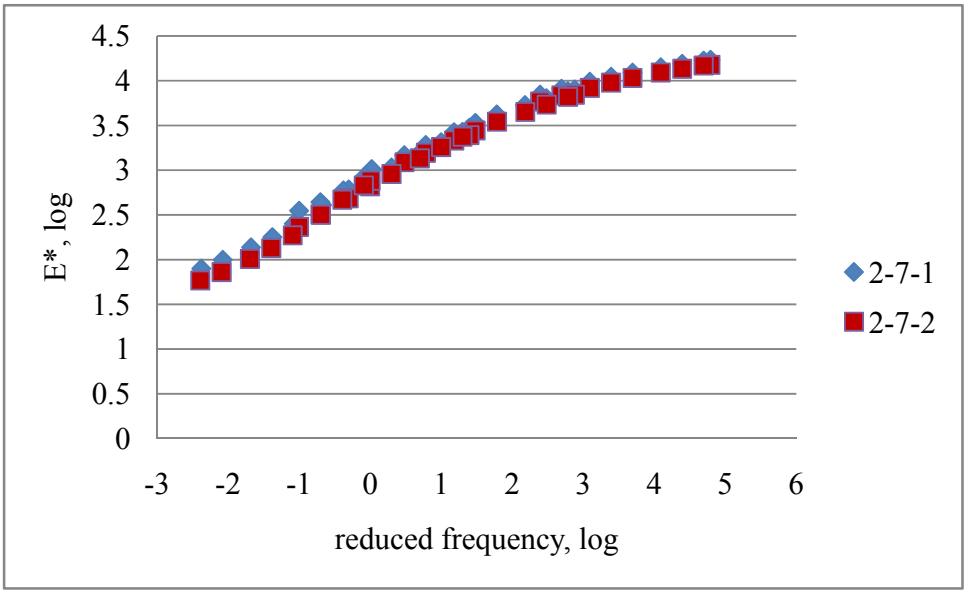

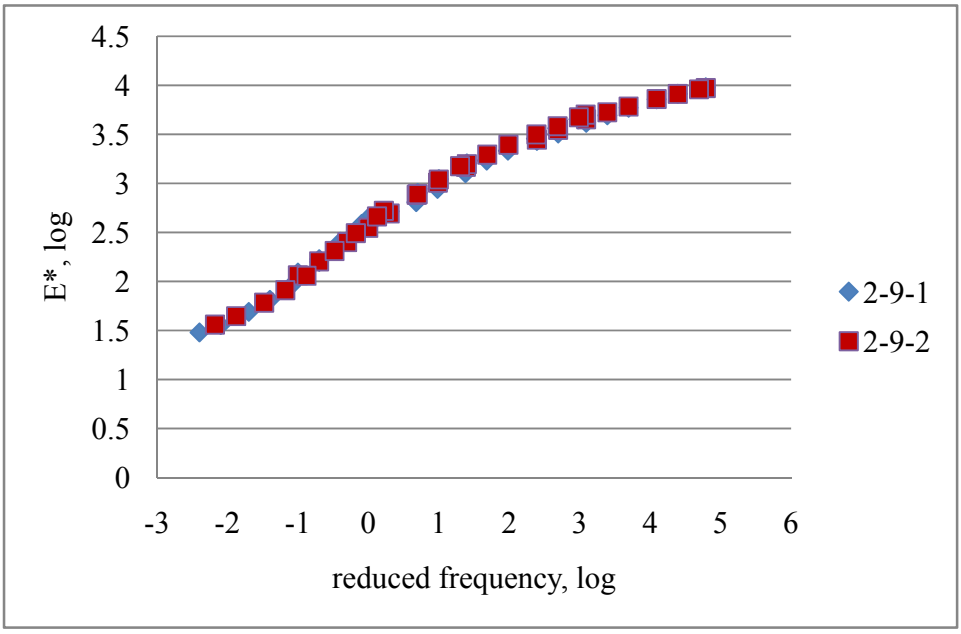

Figure 7-4. |E*| master curves of project C8017 at 100°F for repeating samples

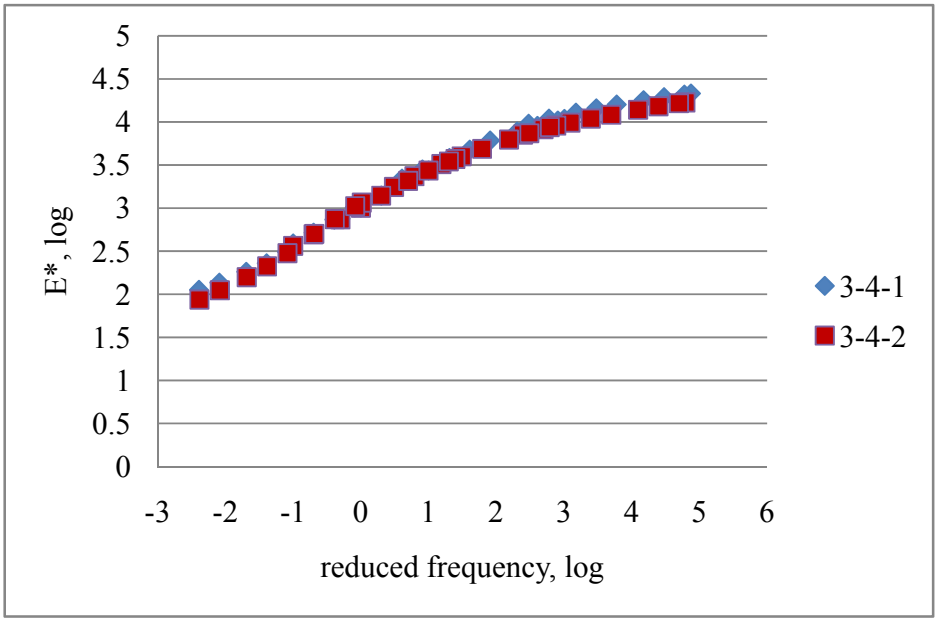

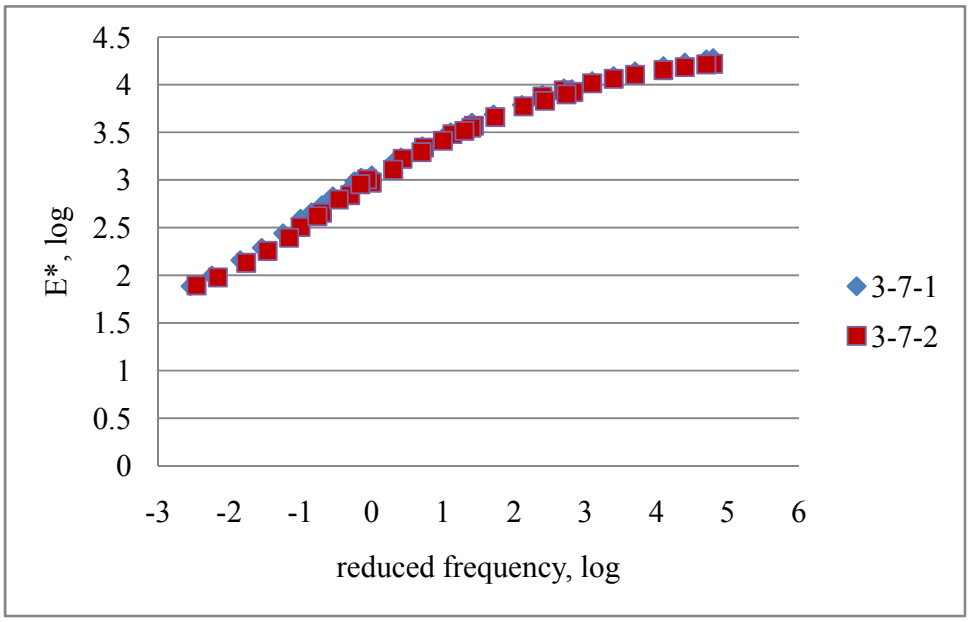

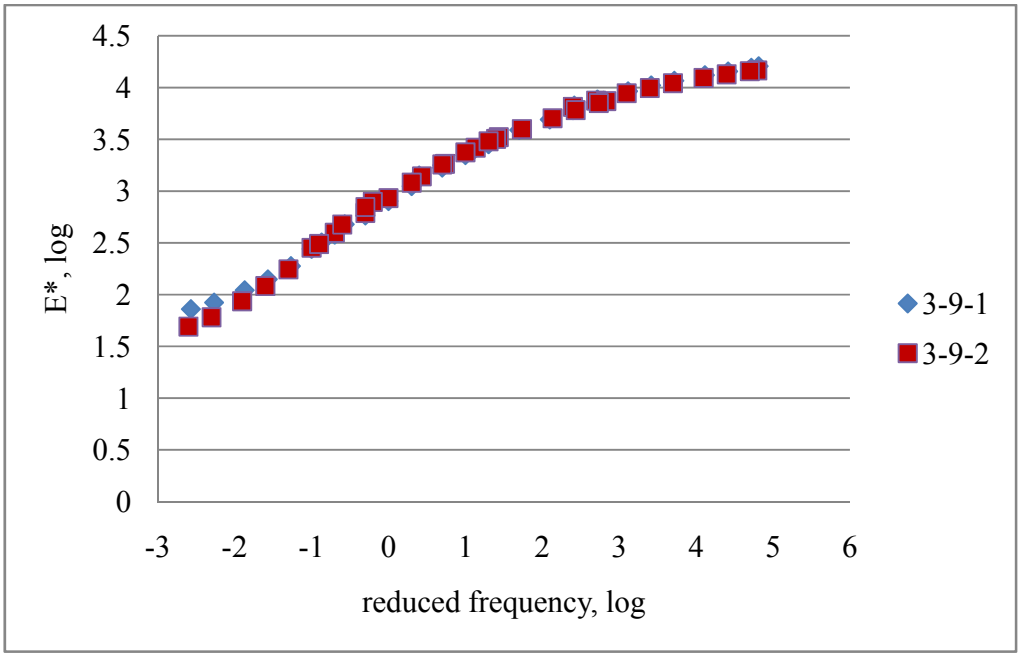

Figure 7-5. |E*| master curves of project C8013 at 100°F for repeating samples

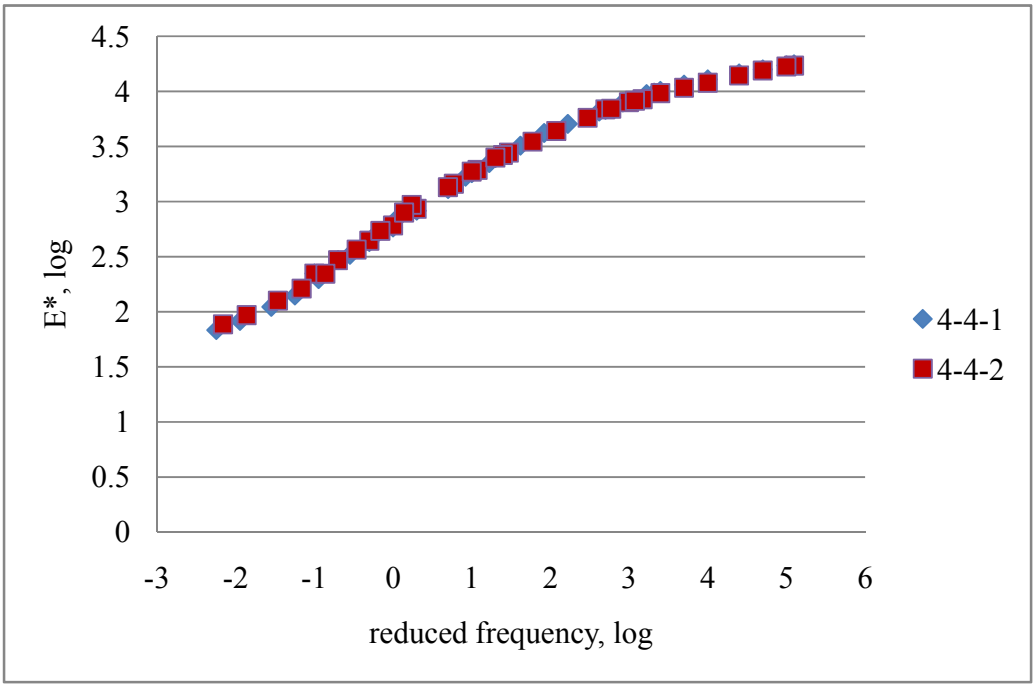

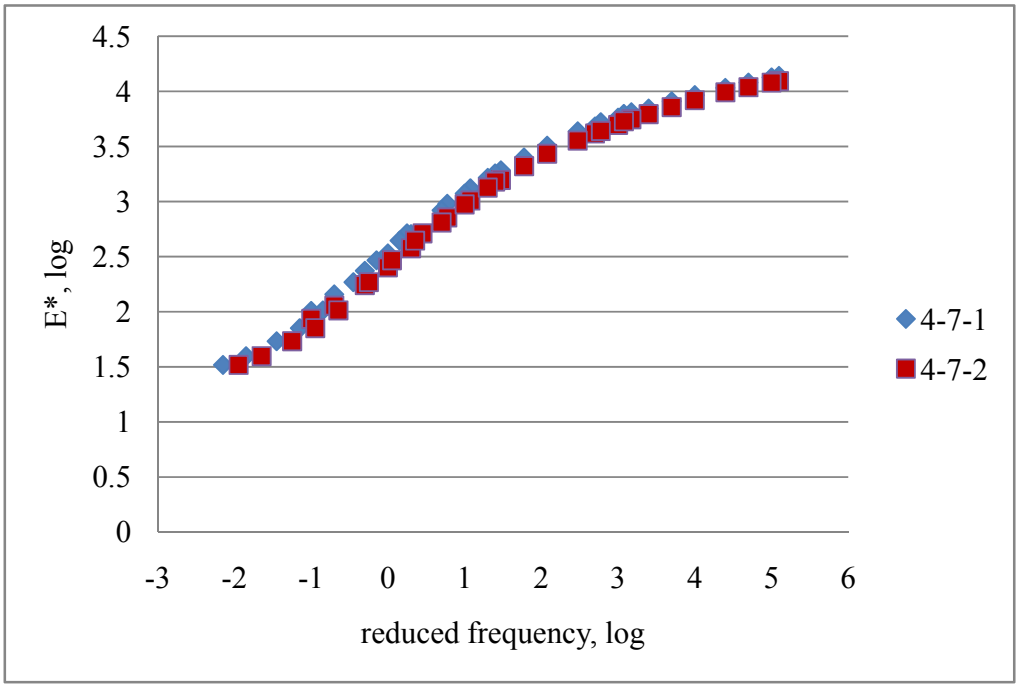

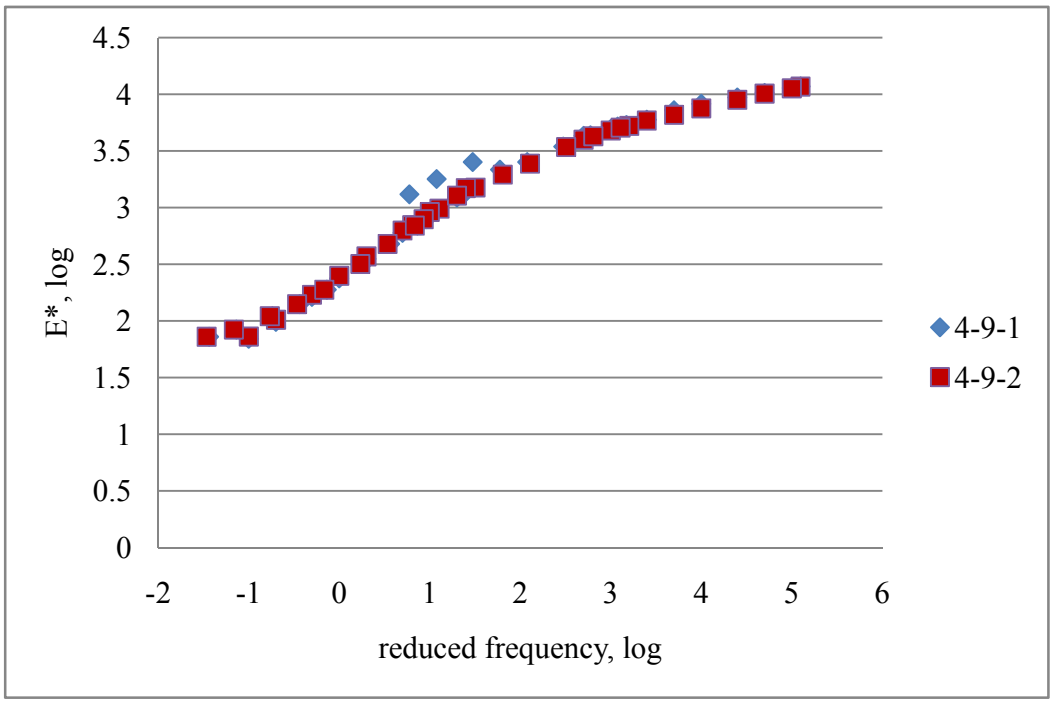

Figure 7-6. |E*| master curves of project C8033 at 100°F for repeating samples

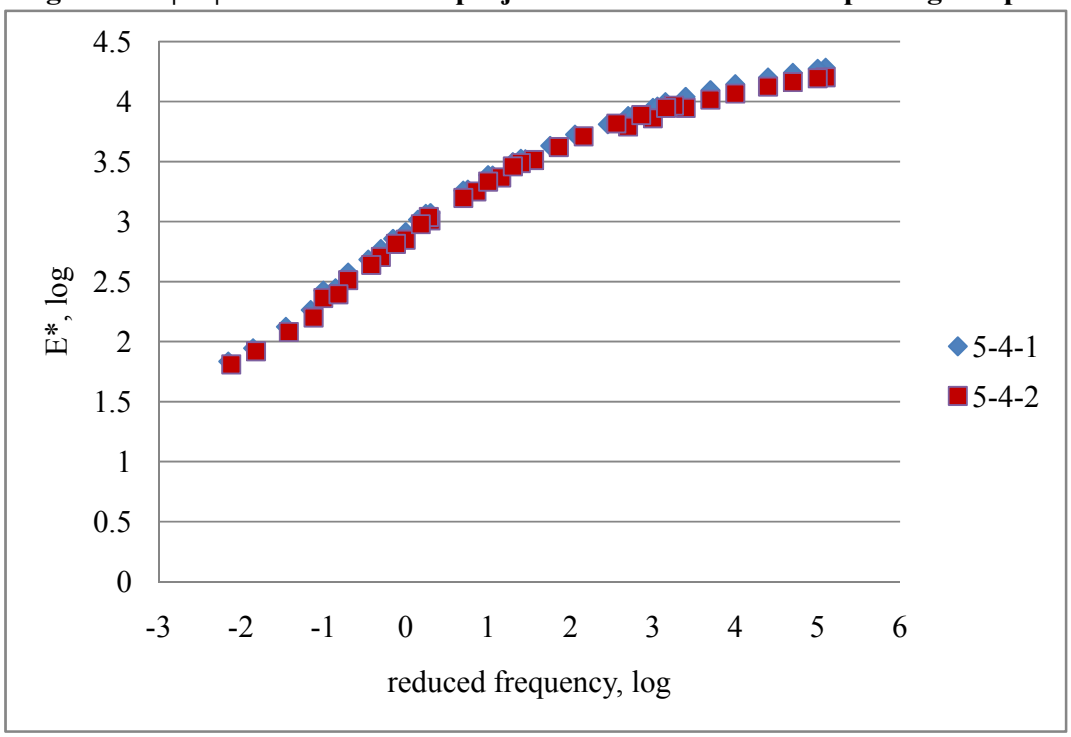

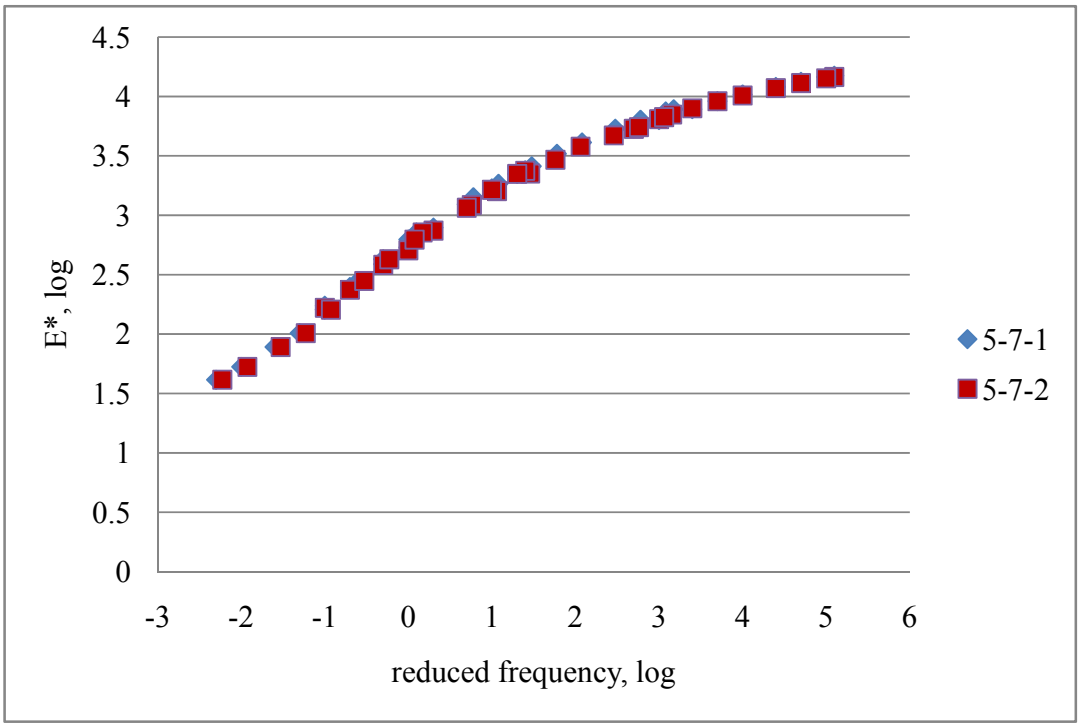

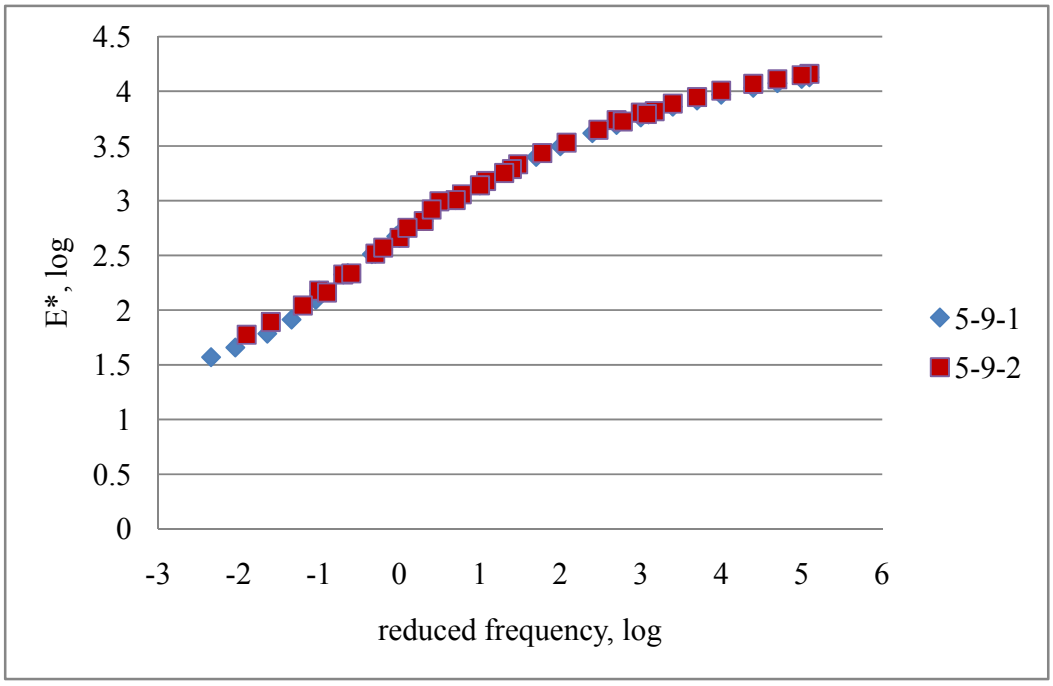

Figure 7-7. |E*| master curves of project C8016 at 100°F for repeating samples

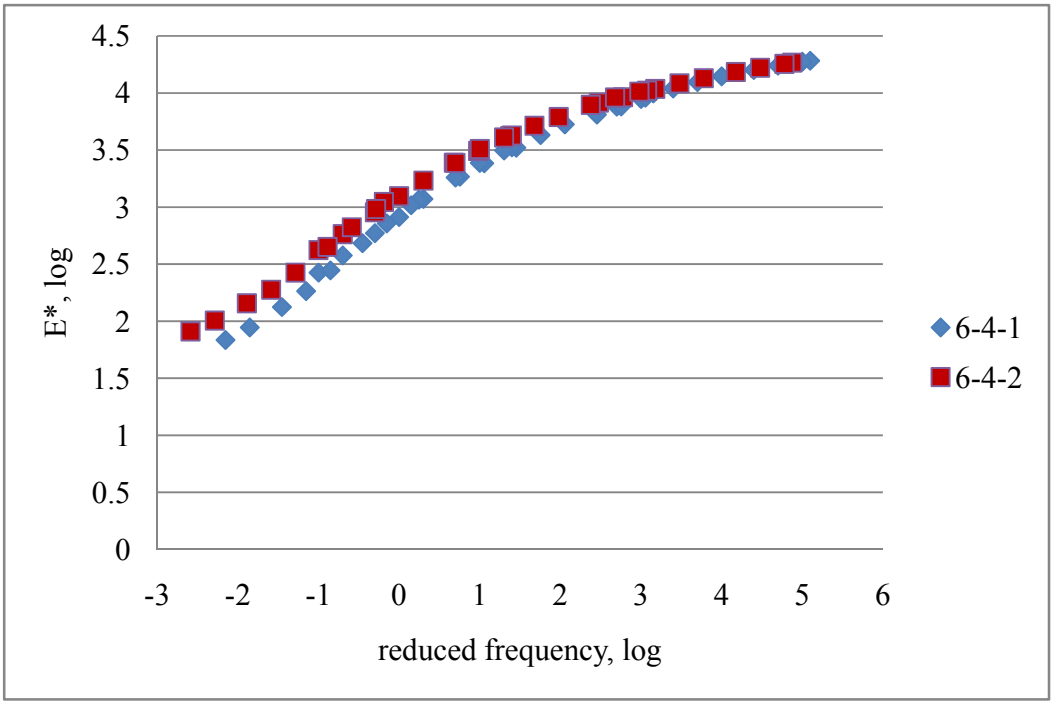

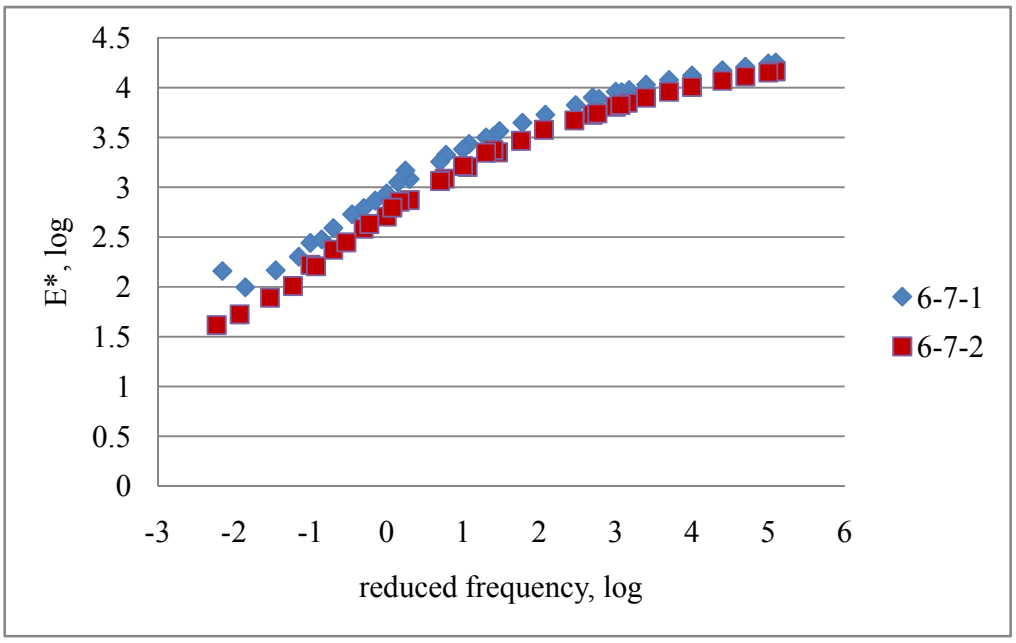

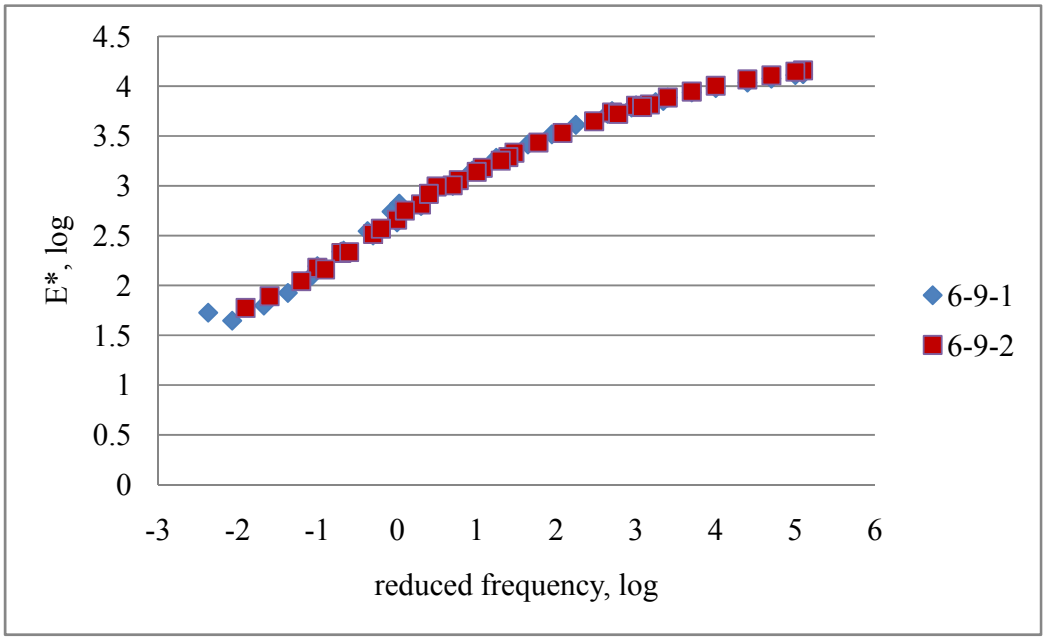

Figure 7-8. |E*| master curves of project C7879 at 100°F for repeating samples

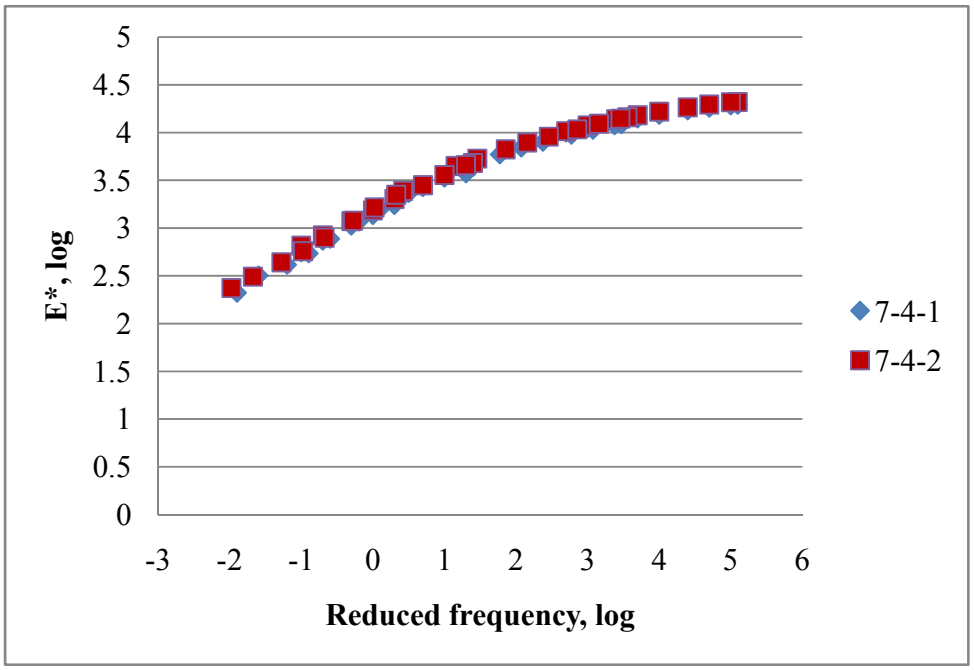

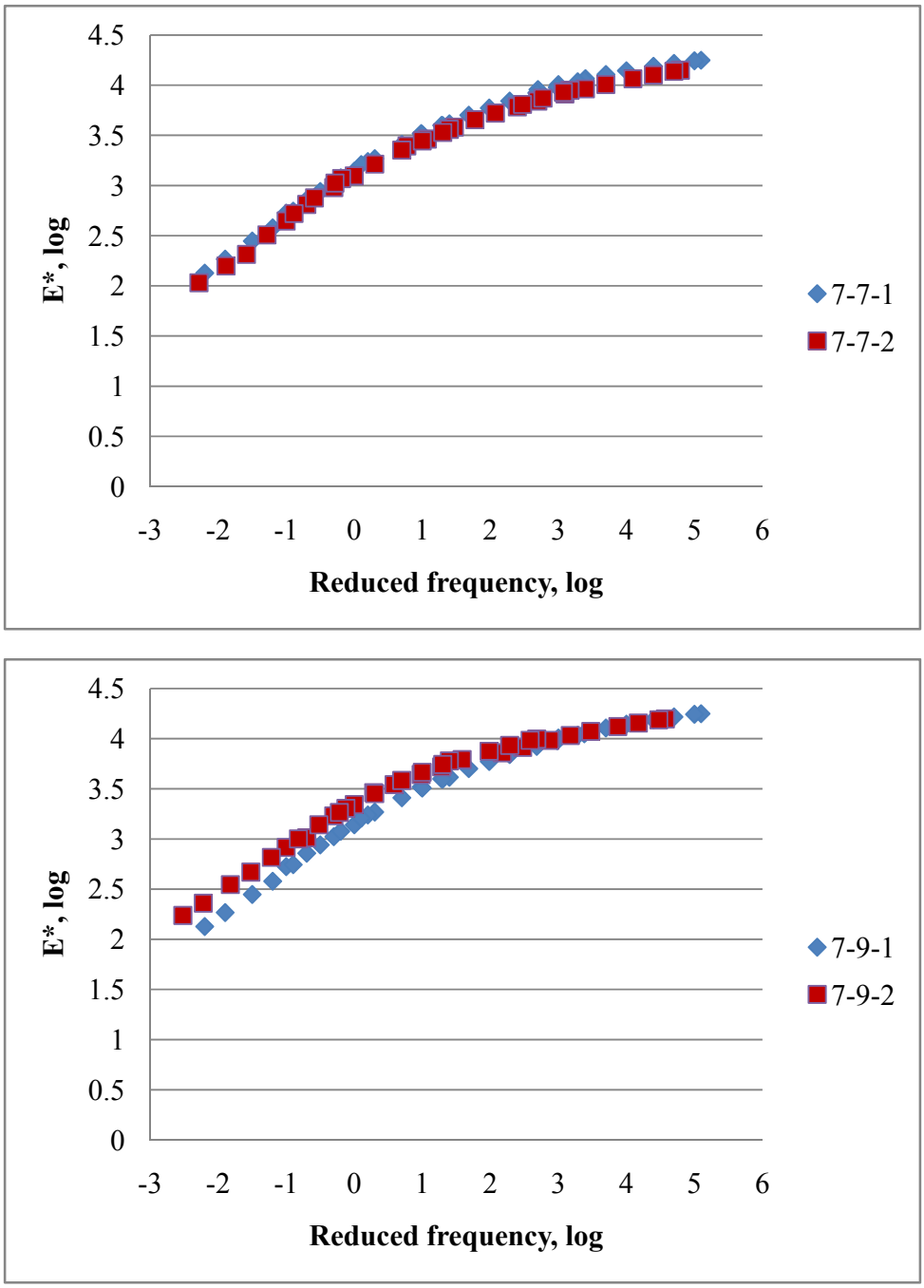

Figure 7-9. |E*| master curves of project C7465 at 100°F for repeating samples

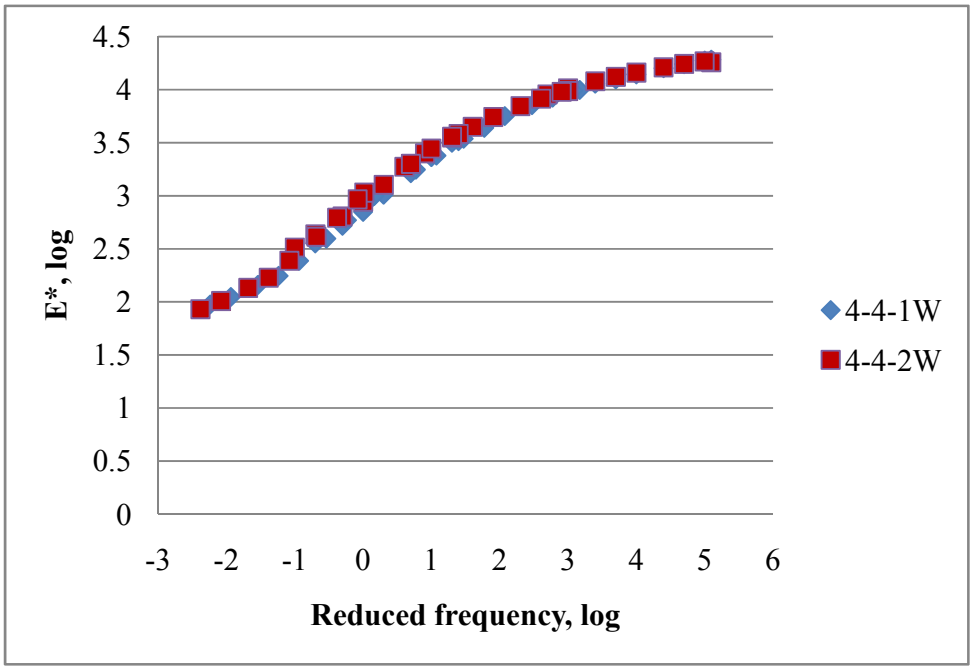

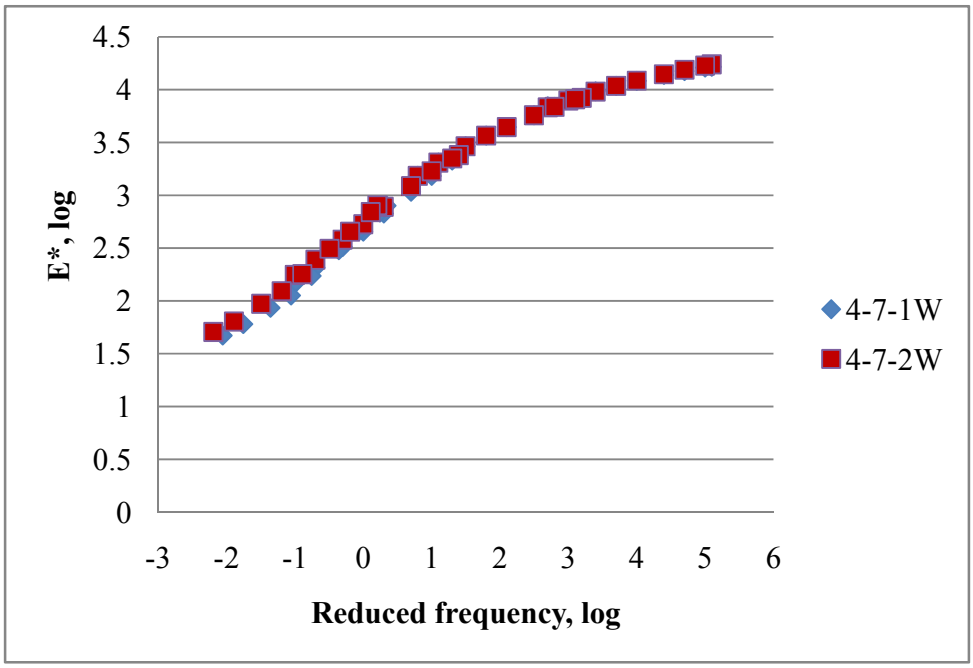

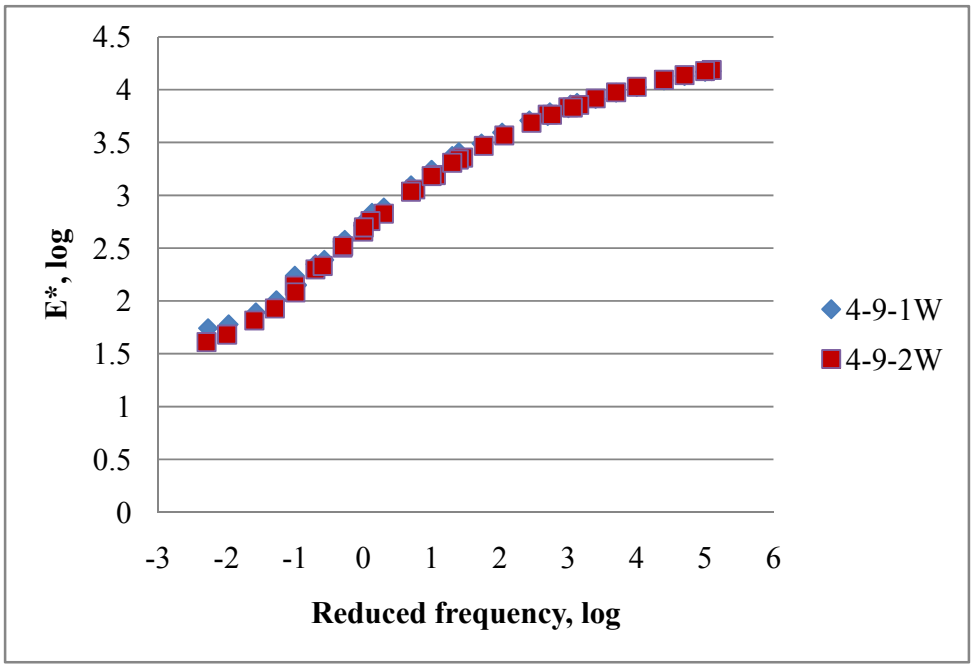

Figure 7-10. |E*| master curves of project C8033 warm mix at 100°F for repeating samples

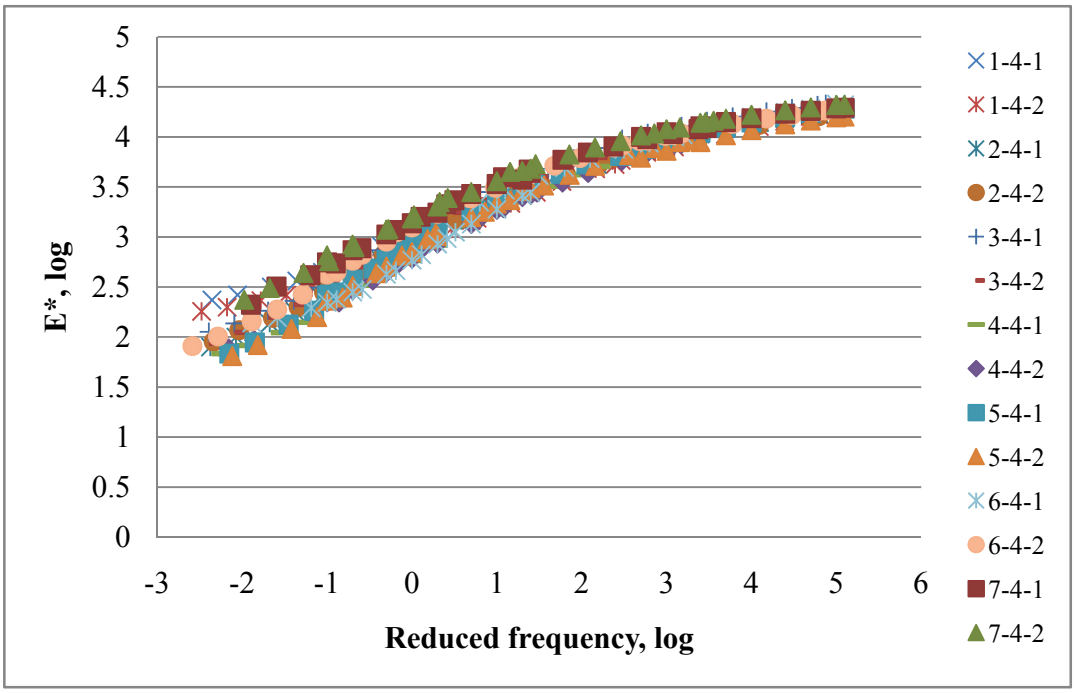

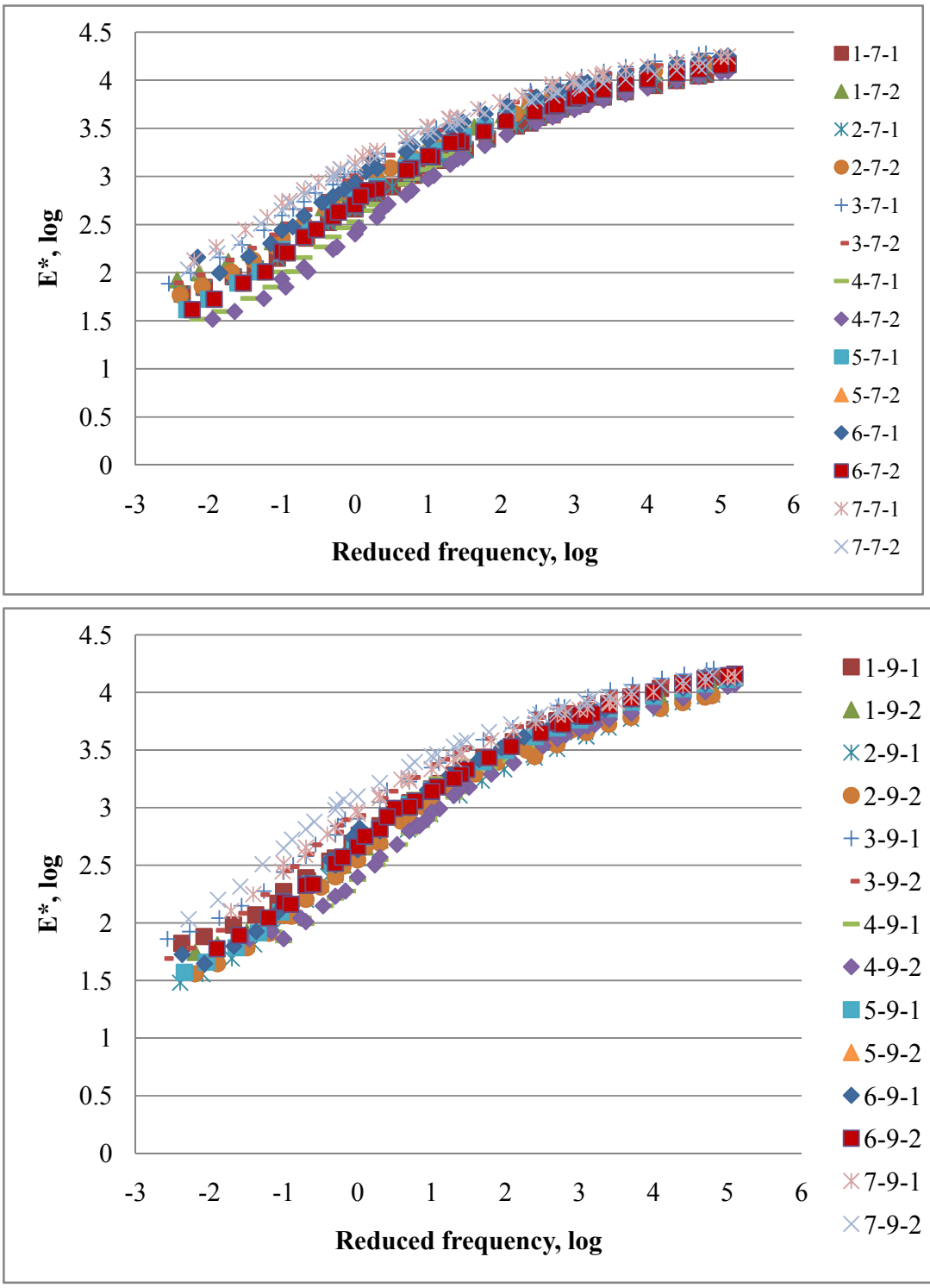

Figure 7-11. |E*| master curves with the same air voids levels

7.3.2 *Effect of Air Voids on Dynamic Modulus*

The air void property is a very important QA/QC control parameter for asphalt pavement. This study evaluated the effect of air voids on the dynamic modulus of asphalt mixture. Dynamic modulus at two levels is evaluated: (a) high E* level with temperature of 40°F and loading frequency of 10Hz; and (b) low E* level with temperature of 130oF and loading frequency of 0.1Hz. The results are shown in Figure 7-12 and Figure 7-13. As shown, in general, samples with higher air voids will have lower dynamic modulus. At low E* levels (high temperature and low frequency), more testing variation is observed.

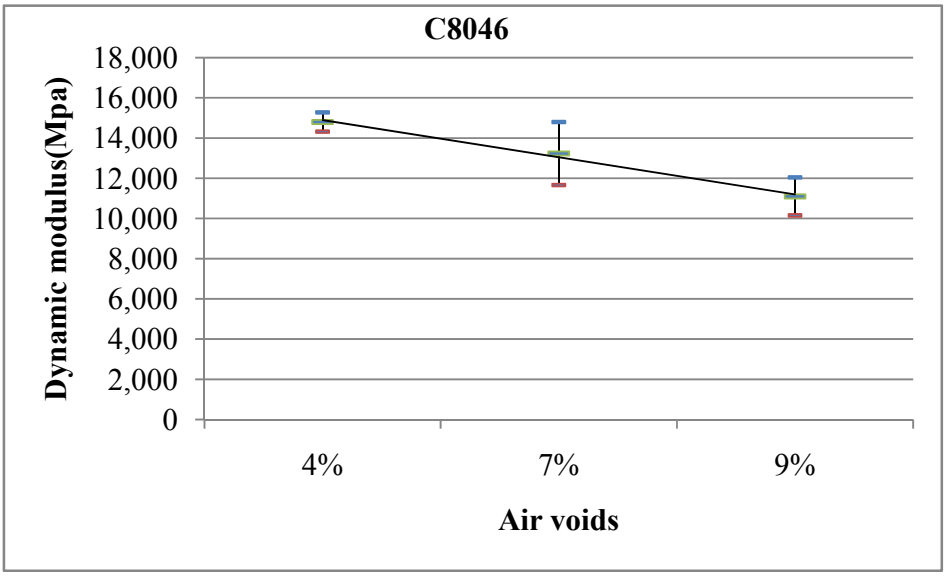

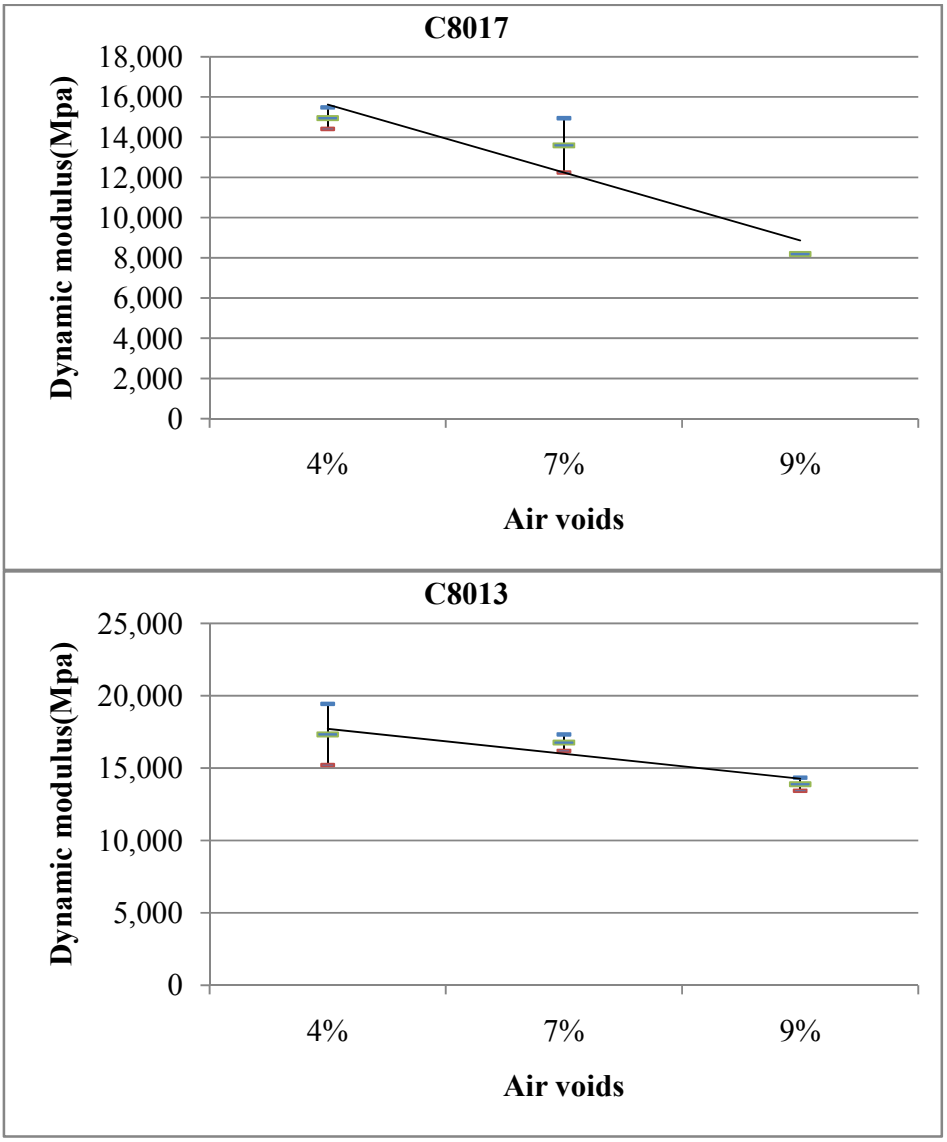

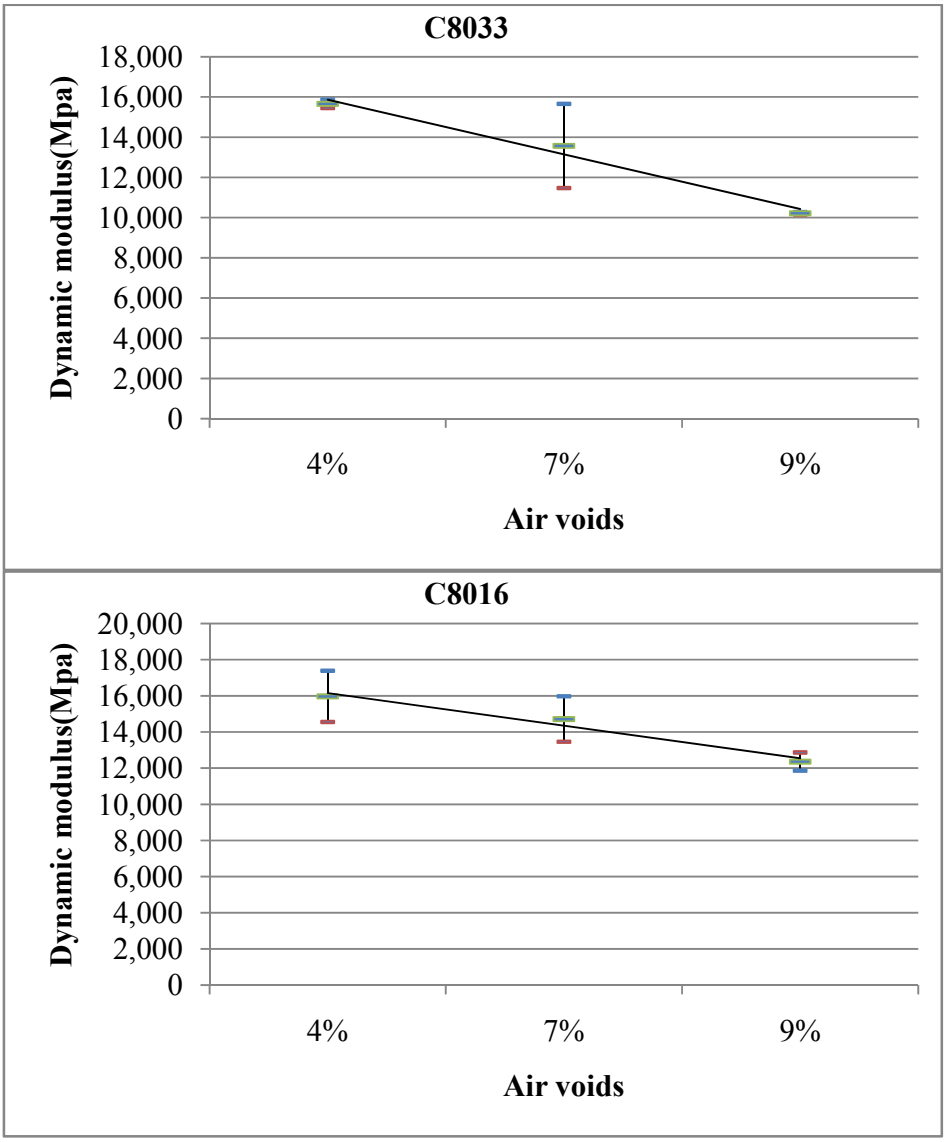

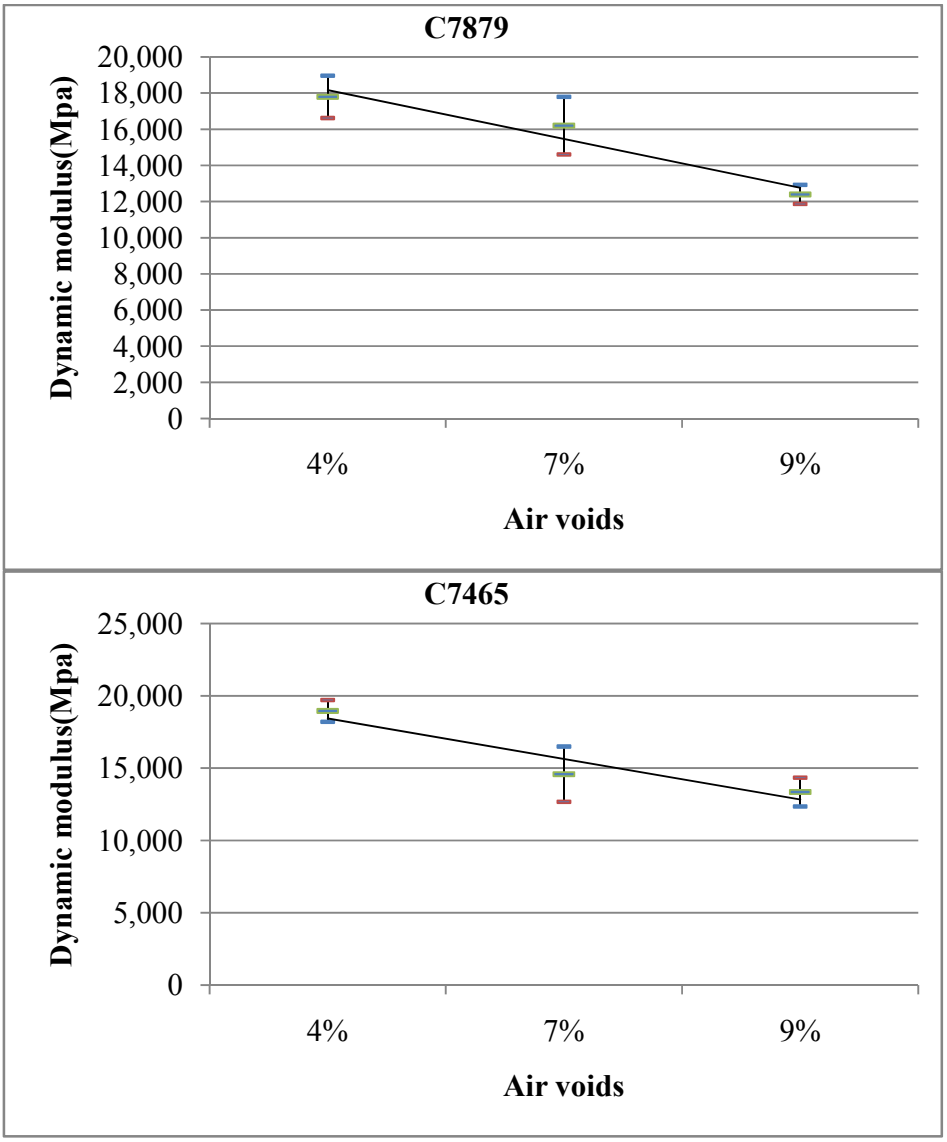

Figure 7-12. |E*| at temperature of 40°F and frequency of 10Hz

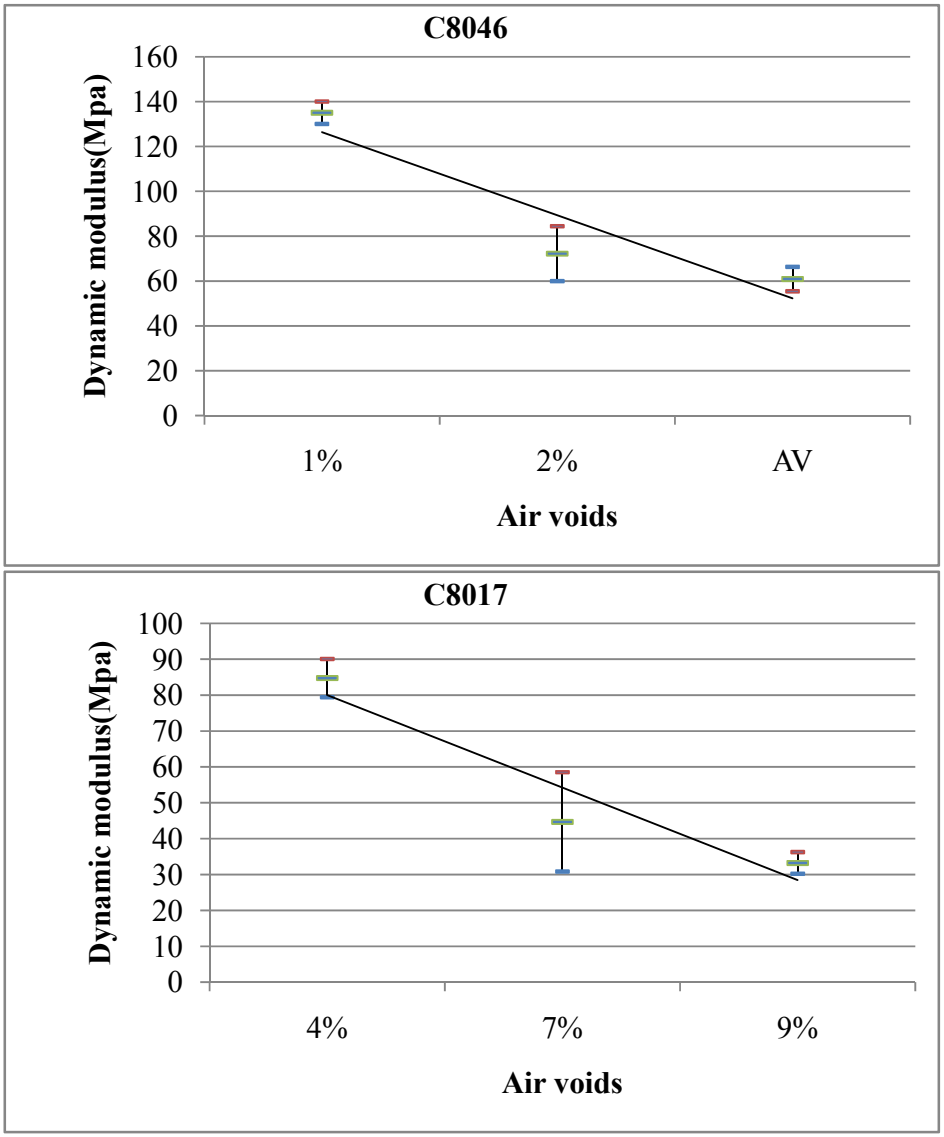

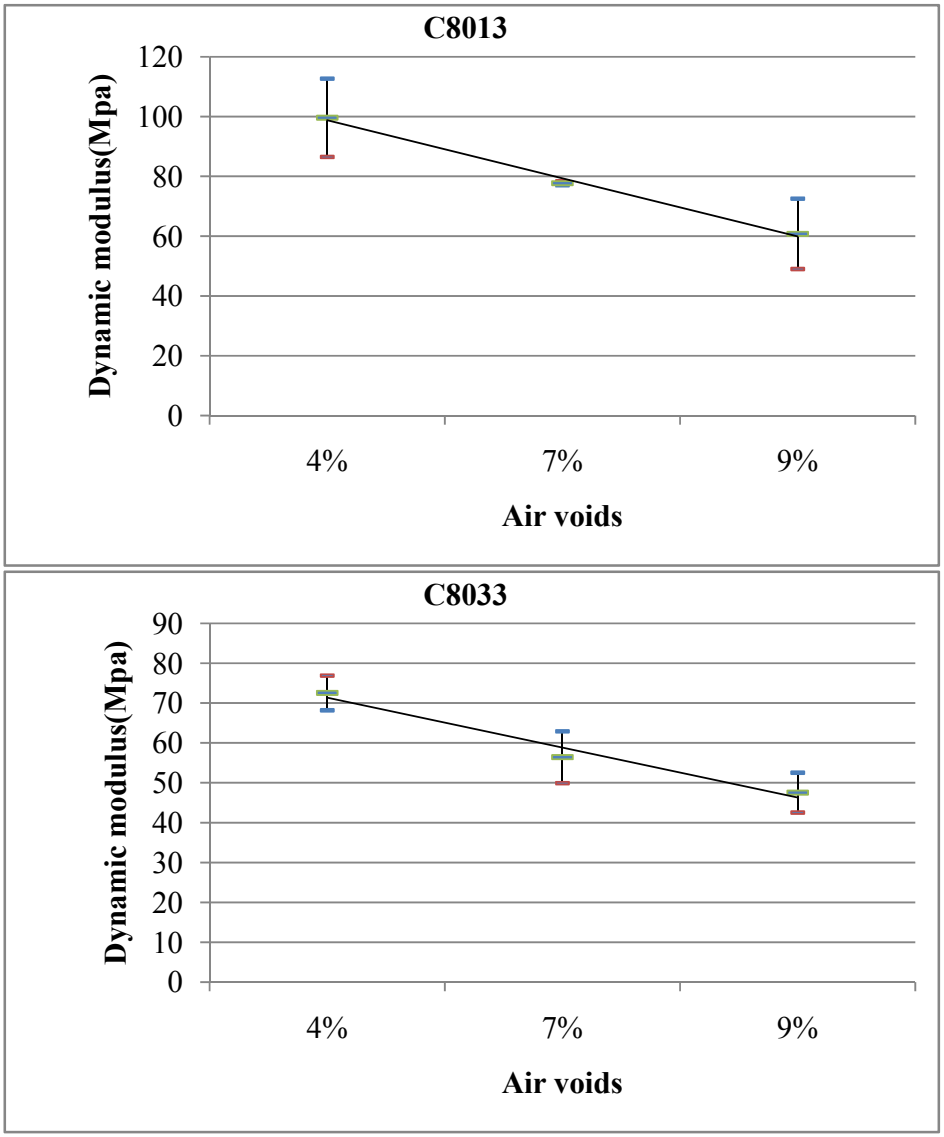

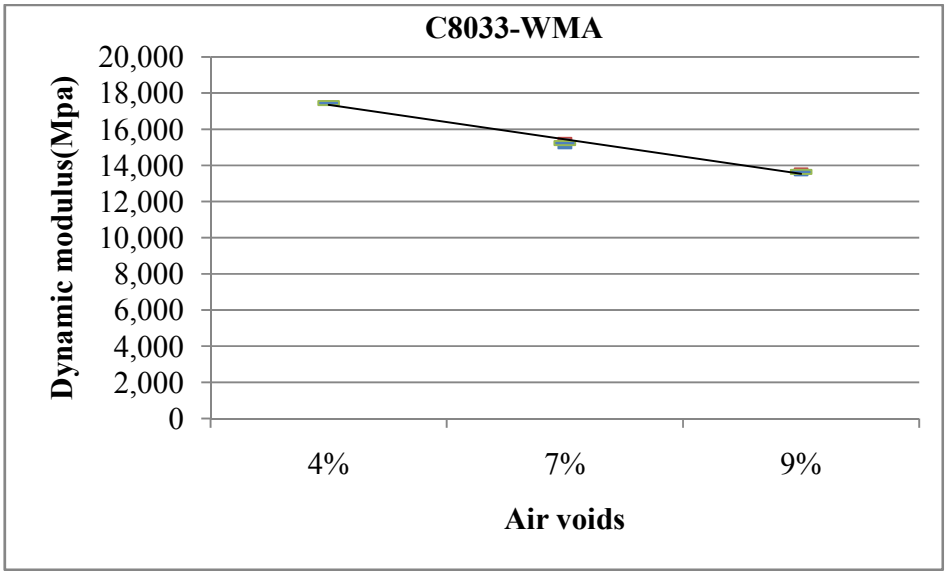

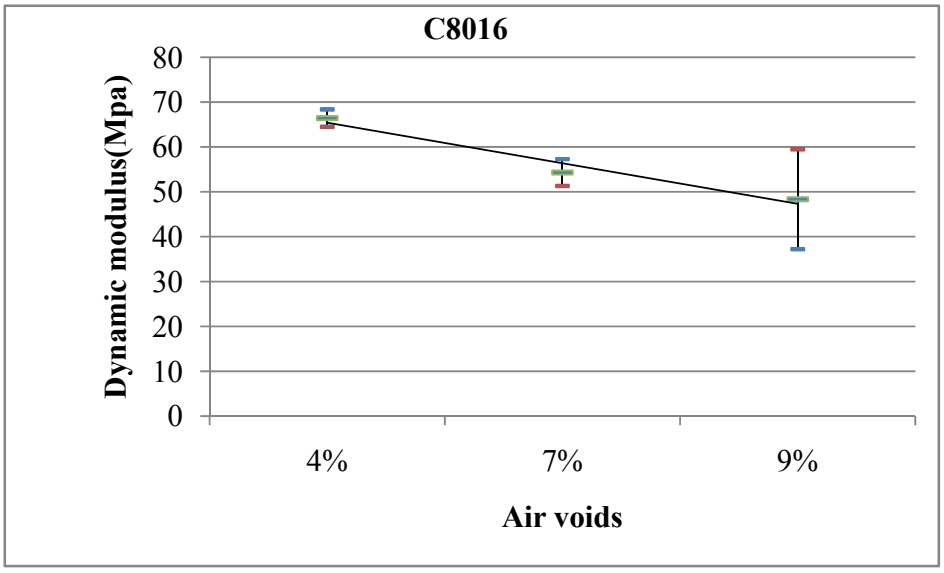

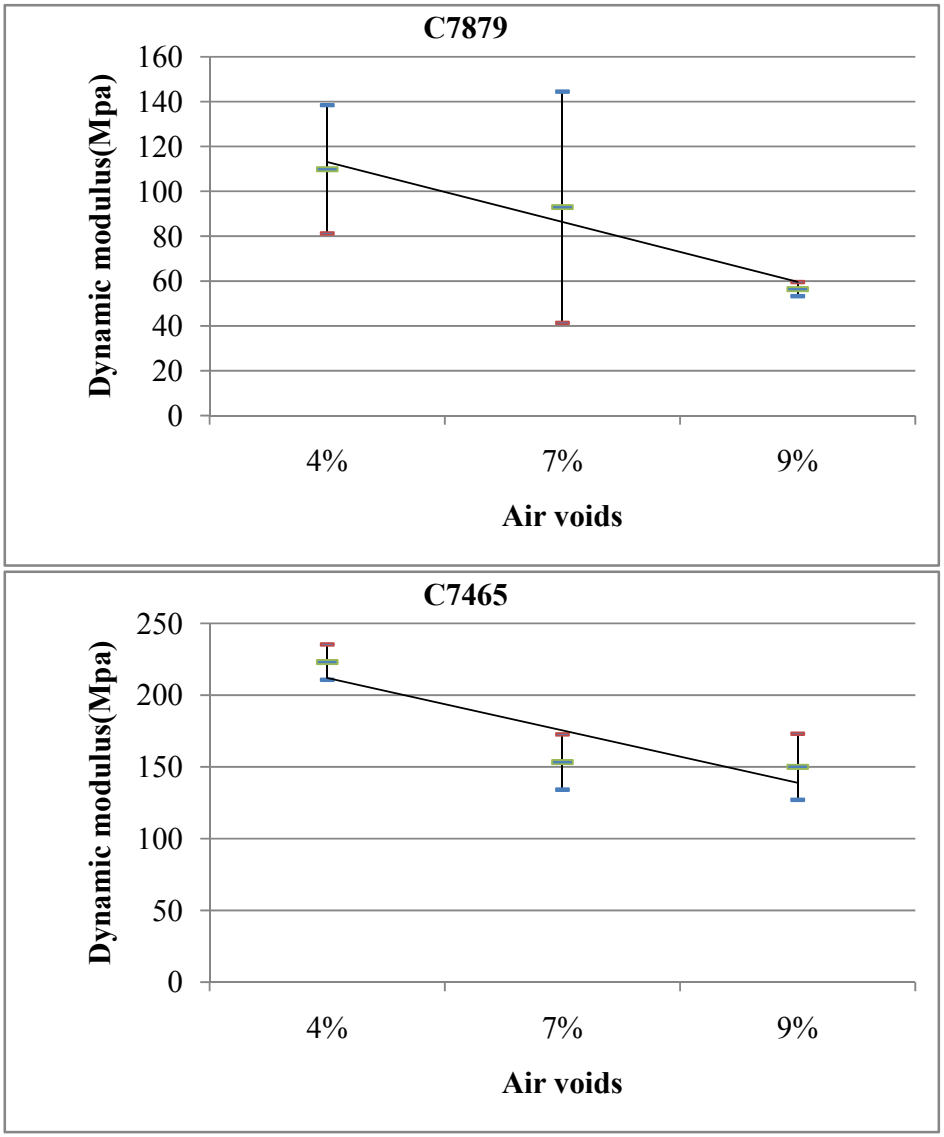

Figure 7-13. |E*| at temperature of130°F and frequency of 0.1Hz

7.3.3 *Effect of Asphalt Binder on Dynamic Modulus*

The asphalt binder is an essential component of asphaltic mixtures. The performance

of an asphaltic mixture is directly related to mechanical characteristics of the binder. Therefore, there is a need to evaluate the relationship between the properties of binders and asphaltic mixtures such that a proper understanding and selection of an asphalt binder can be made to improve the performance of an asphaltic mixture. In this study, the effects of asphalt binder properties on asphaltic mixtures at high temperatures low frequencies and low temperature high frequencies were evaluated based on experimental data.

Figure 7-14 shows the comparison of four types of binders at low E* level (high temperature and low frequency 130^{o}F/0.1Hz), which is associated with the rutting resistance of the asphalt mixture. The results show that the PG grade, especially the high PG grade, has a significant influence on the dynamic modulus at high temperature low frequency.

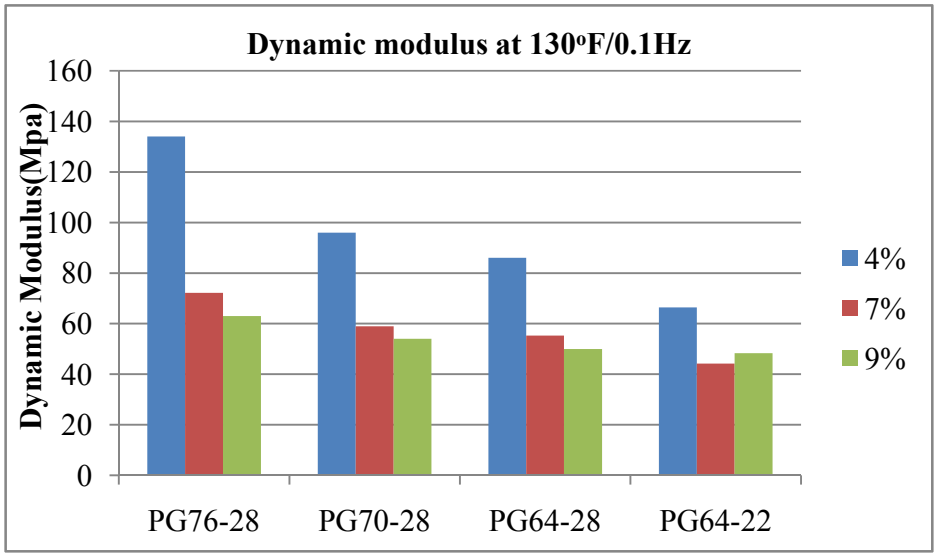

Figure 7-14. Effect of asphalt binder on dynamic modulus

Figure 7-15 shows the comparison of four types of binders at high E* level (low temperature and high frequency 40°F/10Hz), which relates to the crack resistance of the asphalt mixtures. The results show that the binder type do not has a significant influence on the dynamic modulus at high E* level (low temperature and high frequency), partially due to the similar low PG grade all the mixes have.

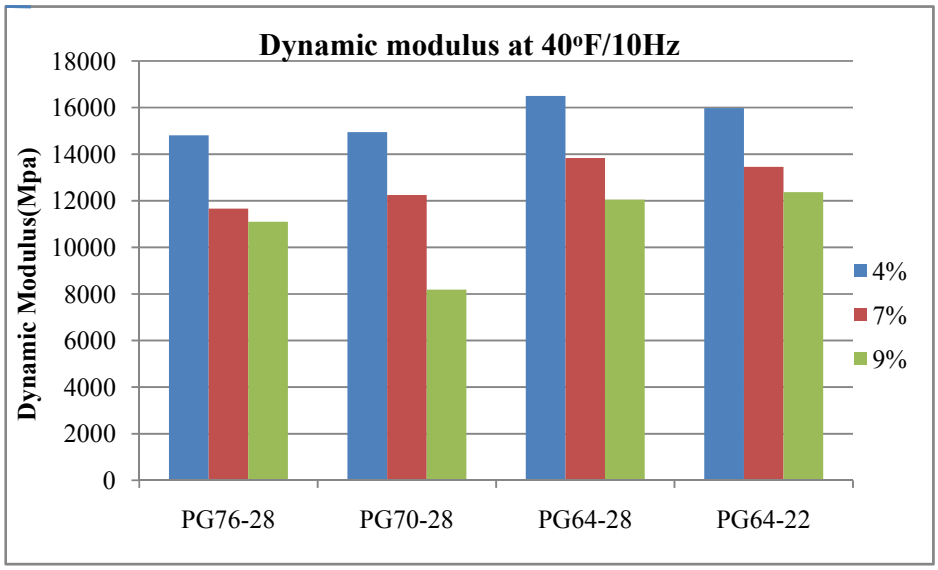

Figure 7-15. Effect of asphalt binder on dynamic modulus

7.3.4 *Effect of Aggregate Gradations on Dynamic Modulus*

The majority of dense-graded asphalt mixture is made up of aggregate. As one of the key mix design components, the proper design of aggregate gradation has an influence on the resulting asphalt mixture performance. In this study, the effects of aggregate gradation on the dynamic modulus at both high and low E* levels are evaluated.

Figure 7-16 (a) shows the comparison of dynamic modulus at low E* level (high temperatures low frequencies) for four different asphalt mixtures types, and Figure 7-16 (b) shows the comparison of dynamic modulus at high E* level (low temperatures higher frequencies) for four different asphalt mixtures types. Contracts C 8013 and C8033 share the same asphalt binder, and contracts C8016 and C7879 share the same asphalt binder. The result shows that aggregate properties have an effect on dynamic modulus but the

trend is not clear.

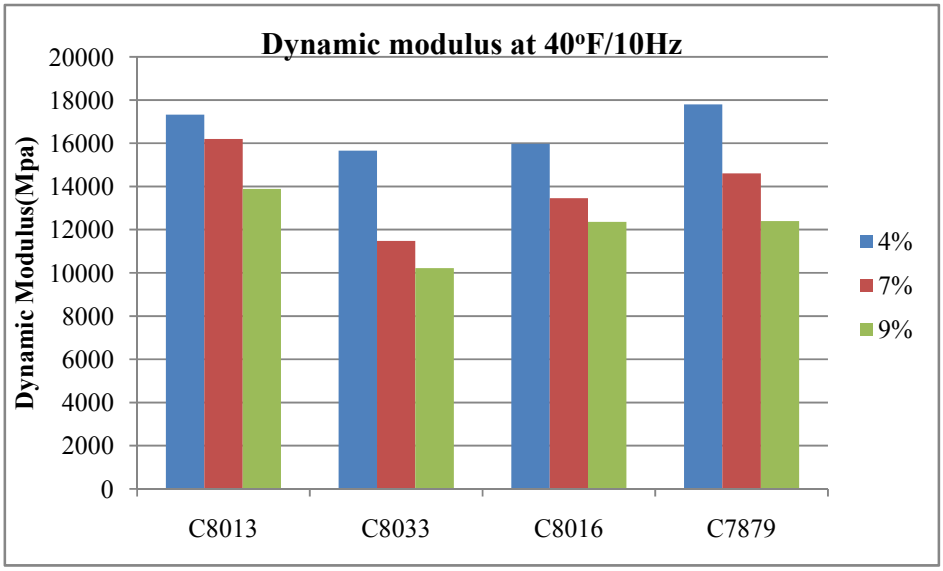

(a)

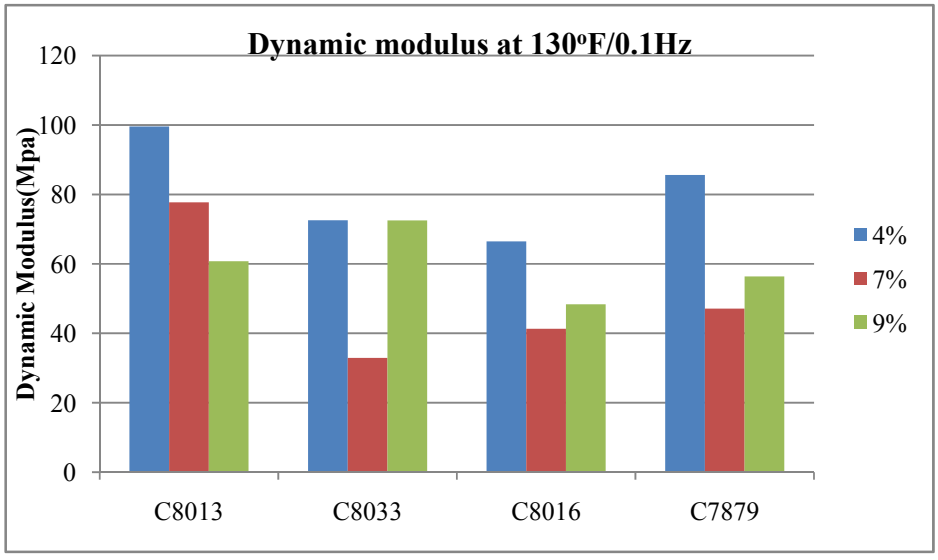

(b)

Figure 7-16. Effect of aggregate gradation on dynamic modulus

7.3.5 *Flow Number Test Results*

Flow number tests are run at the average 7-day maximum pavement temperature 20 mm from the surface, at 50 %reliability as determined using LTPPBind version 3.1. The complete testing temperatures for those projects are shown in Table 7-4.Complete summary results of the average flow numbers for each mix at each air void levels are shown in Table 7-5.

Table 7-4. Flow number testing temperatures

	Contract No.	Testing Temp. .(degC)
#1	C8046	53.5
#2	C8017	55.1
#3	C8013	55.5
#4	C8033	45.4
#5	C8016	56.9
#6	C7879	48.5
#7	C7465	45.4

Table 7-5. Flow number testing results

Sample ID	Flow number (cycles)	Sample ID	Flow number (cycles)
1-4-1	2463	5-4-1	440
1-4-2	3435	5-4-2	119
1-7-1	2966	5-7-1	74
1-7-2	2445	5-7-2	60
1-9-1	681	5-9-1	48
1-9-2	620	5-9-2	32
2-4-1	363	6-4-1	578
2-4-2	918	6-4-2	487
2-7-1	369	6-7-1	263
2-7-2	213	6-7-2	263
2-9-1	206	6-9-1	241
2-9-2	117	6-9-2	201
3-4-1	431	7-4-1	871
3-4-2	428	7-4-2	987
3-7-1	279	7-7-1	651
3-7-2	234	7-7-2	362
3-9-1	362	7-9-1	331
3-9-2	179	7-9-2	478
4-4-1	320	4-4-1W	1971

4-4-2	439	4-4-2W	1441
4-7-1	104	4-7-1W	751
4-7-2	374	4-7-2W	631
4-9-1	46	4-9-1W	391
4-9-2	282	4-9-2W	430

7.3.6 *Effect of Air Voids on Flow Number*

The relation between the air voids and flow number are shown in Figure 7-17. As indicated from the experimental results, the flow number decreases with the increase of air voids.

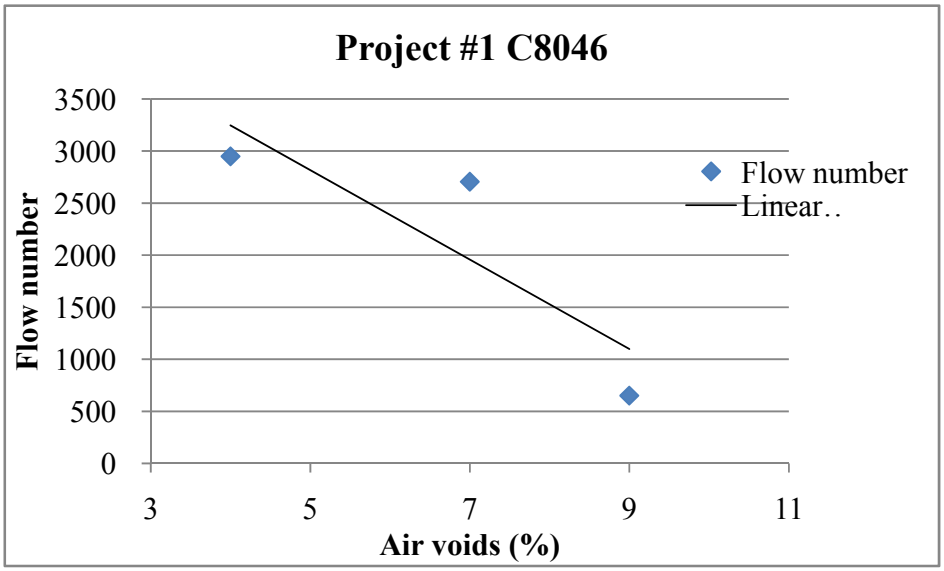

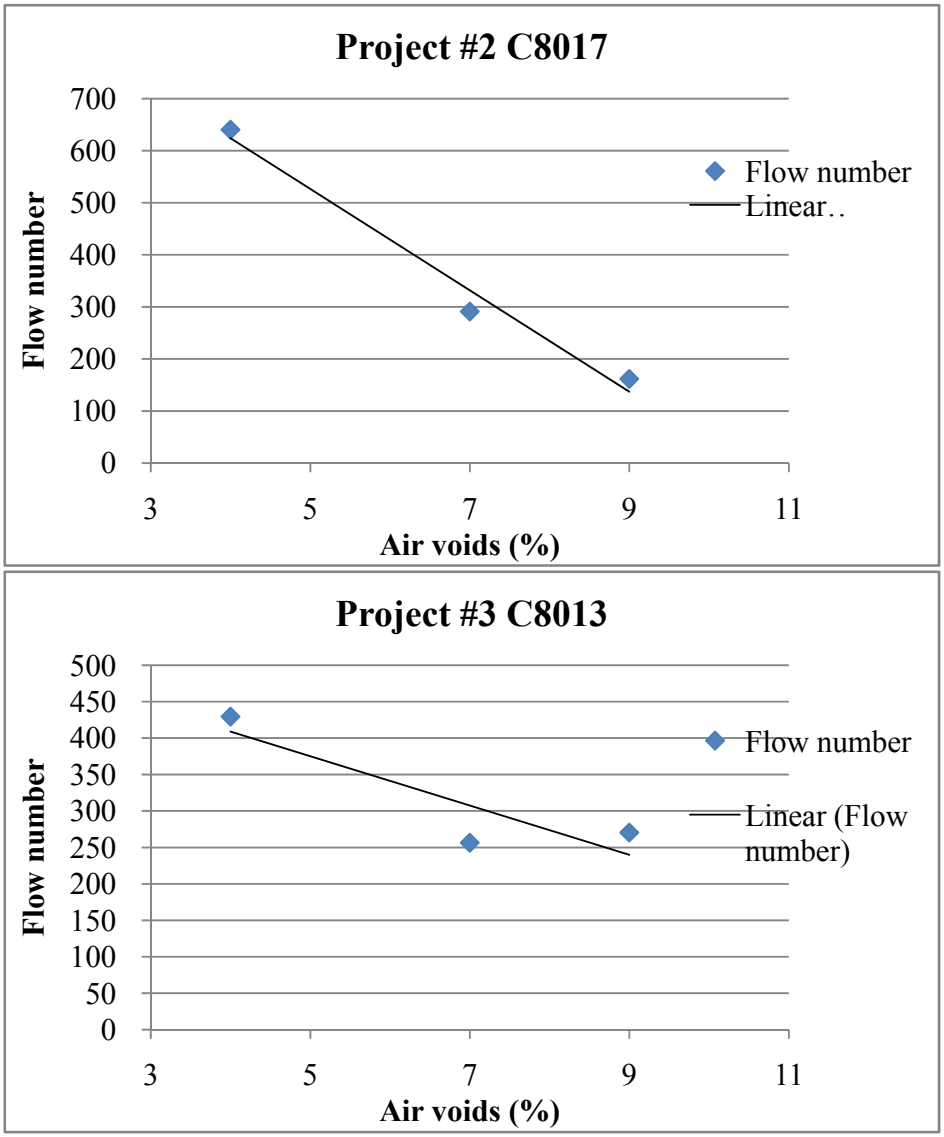

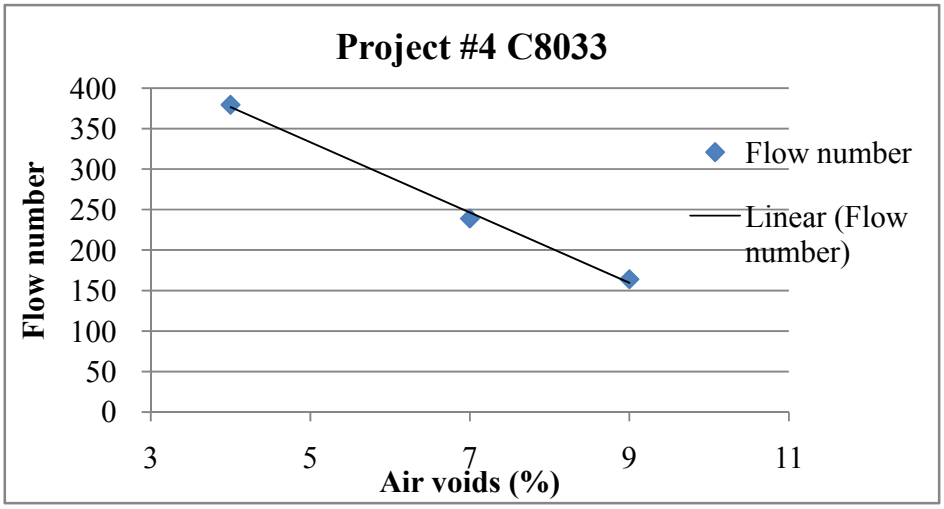

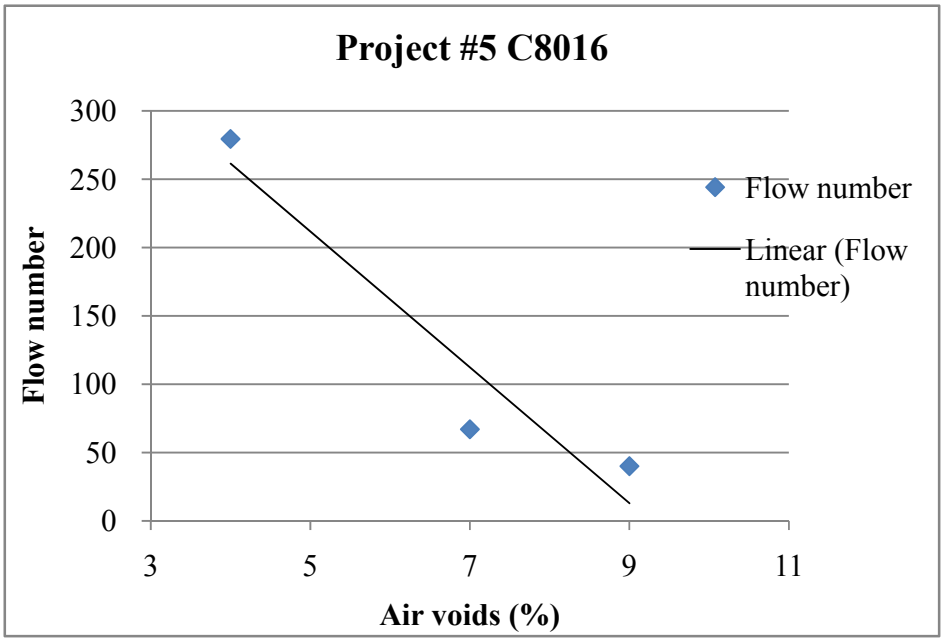

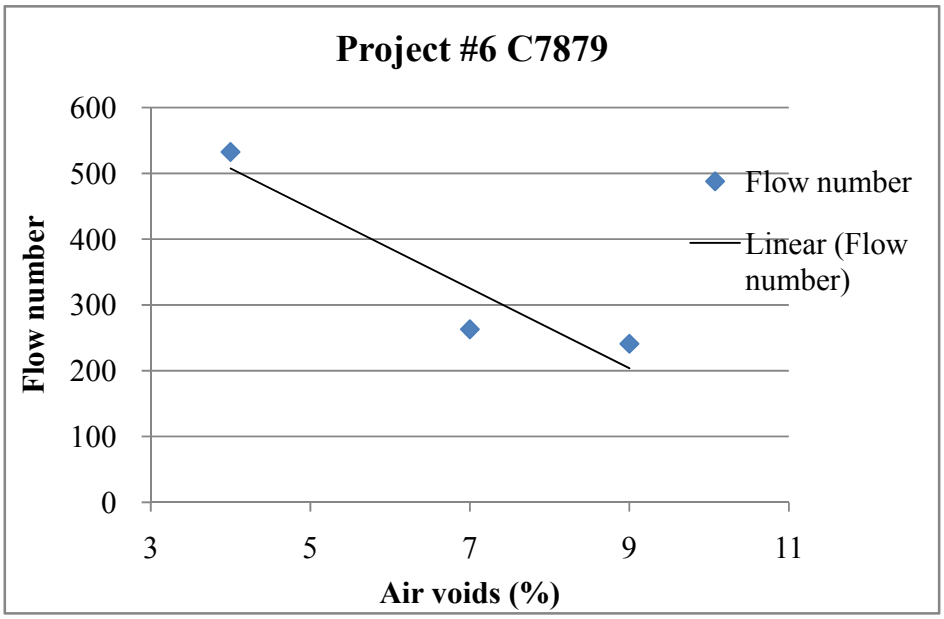

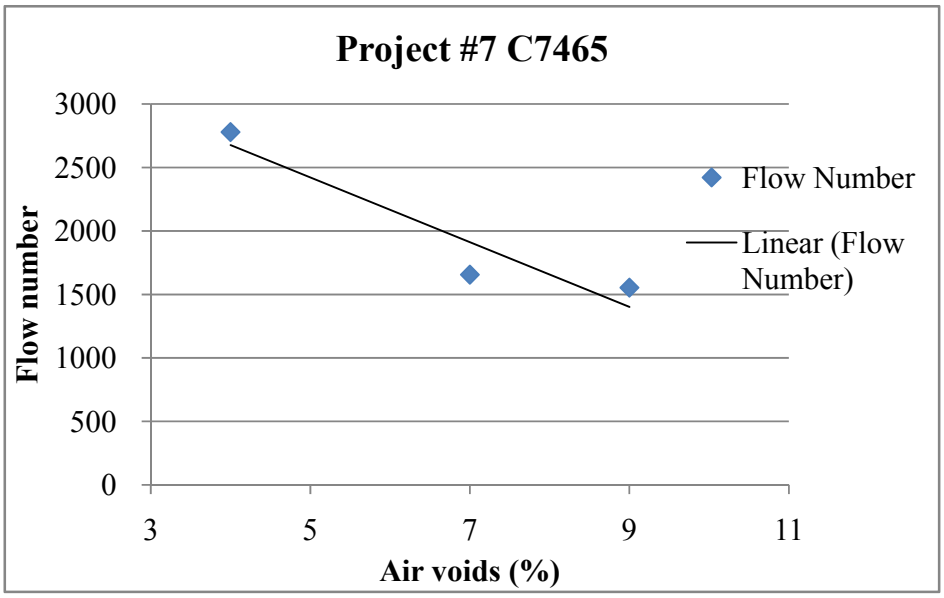

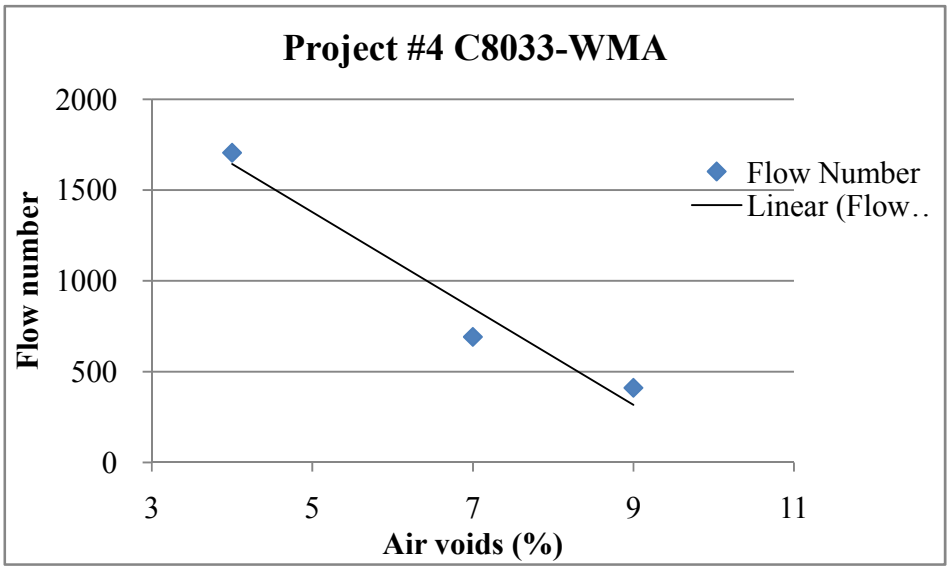

Figure 7-17. Flow number vs. air voids

7.3.7 *Effect of Asphalt Binder on Flow Numbers*

The effects of asphalt binder properties on the flow numbers are also evaluated in this study. Figure 7-18 shows the comparison of flow numbers of four types of binders, results shows that the PG binder has a direct influence on the flow numbers, the flow number values increases with the increase of PG grade at high temperature, this result confirmed with the dynamic modulus test that PG grade at high temperature have a directly influence on the rutting potential of asphalt mixture.

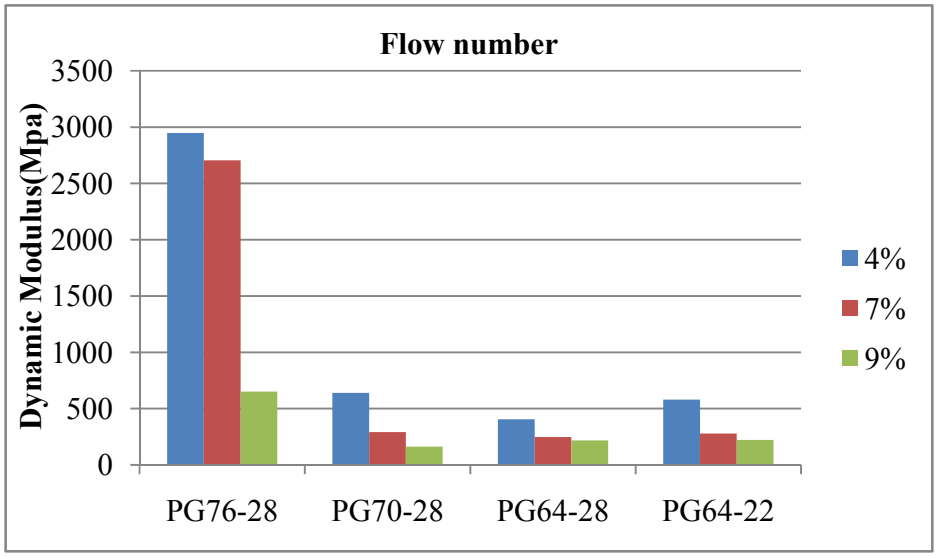

Figure 7-18. Effect of asphalt binder on flow number

7.3.8 *Effect of Aggregate Gradations on Dynamic Modulus*

The effect of aggregate properties on flow numbers are evaluated, Figure 7-19 shows the comparison of flow number for four different asphalt mixture types, Contracts C 8013 and C8033 share the same asphalt binder, and contracts C8016 and C7879 share the same asphalt binder, it is observed that even though C8016 and C7879 shares the same binder, the flow number varied a lot, which means the aggregate properties have a large effect on the flow number. This can be explained because the effect of asphalt binder becomes less at high temperature, the asphalt binder becomes softer and the aggregate form a skeleton to support the traffic loads.

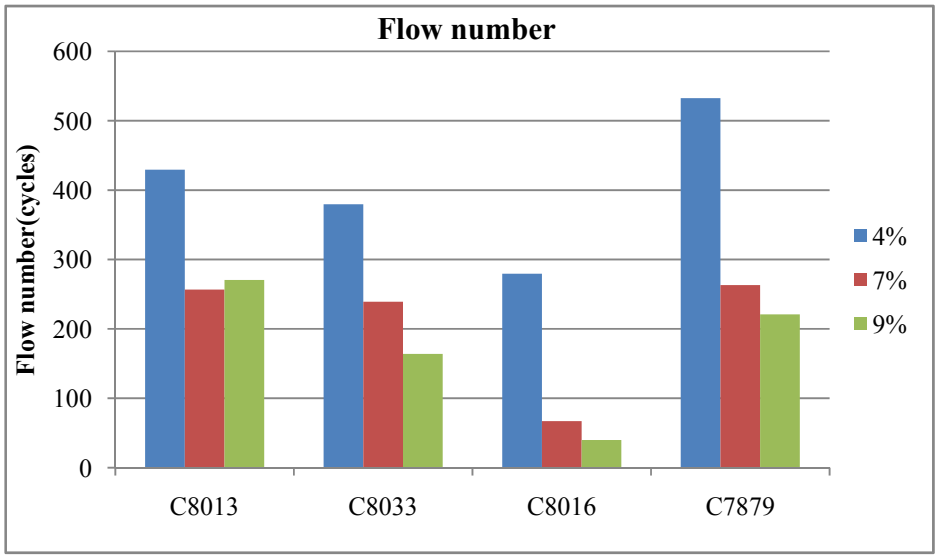

Figure 7-19. Effect of aggregate gradation on flow number

7.4 Dynamic Modulus Prediction Models

7.4.1 *Evaluation of Existing Prediction Models*

As illustrated in literature review, the most widely used dynamic modulus prediction models are the Witczak 1996 and 2006 predictive models and the Hirsch model. Although all provided reasonable accuracy as globally calibrated models, they were also reported by researchers not being able to capture the dynamic modulus behaviors for some local materials especially in high and low temperature extremes (Witczak 2002). In addition, these models were found to tend to overemphasize the influence of temperature and understate the influence of other factors or components (Ceylan et al. 2009). Therefore, it is necessary to modify existing prediction models or develop new models

based on local field mixtures.

7.4.1.1 *Prediction of dynamic modulus based on 1996 Witczak Model*

The input variables for the Witczak 1996 E*predictive model include aggregate gradation, mixture volumetric properties, viscosity of the asphalt binder, and loading frequency *f*. The aggregate gradation variables are the percent passing the #200 sieve, percent retained on the #4, percent retained on the 9.5 mm sieve, and percent retained on the 19 mm sieve. The mixture volumetric properties are the air void percentage (Va) and effective binder percentage by volume (Vbeff).The aggregate and volumetric properties were determined from experiments following AASHTO specifications. The asphalt binder was short-term aged using the rolling thin film oven method and its dynamic shear modulus (G*) was measured using dynamic shear rheometer (DSR) following AASHTO T-240. For the use of G* information, all test results are shown in Appendix D.

Figure 7-20 presented a comparison between the measured and the predicted E* values. As shown, the Witczak model under predicts the dynamic modulus at lower temperature and over predicts the dynamic modulus at higher temperature. The total prediction results did not followed well with the line of equality indicating that those results cannot reasonably represent the dynamic modulus properties of tested asphalt mixtures.

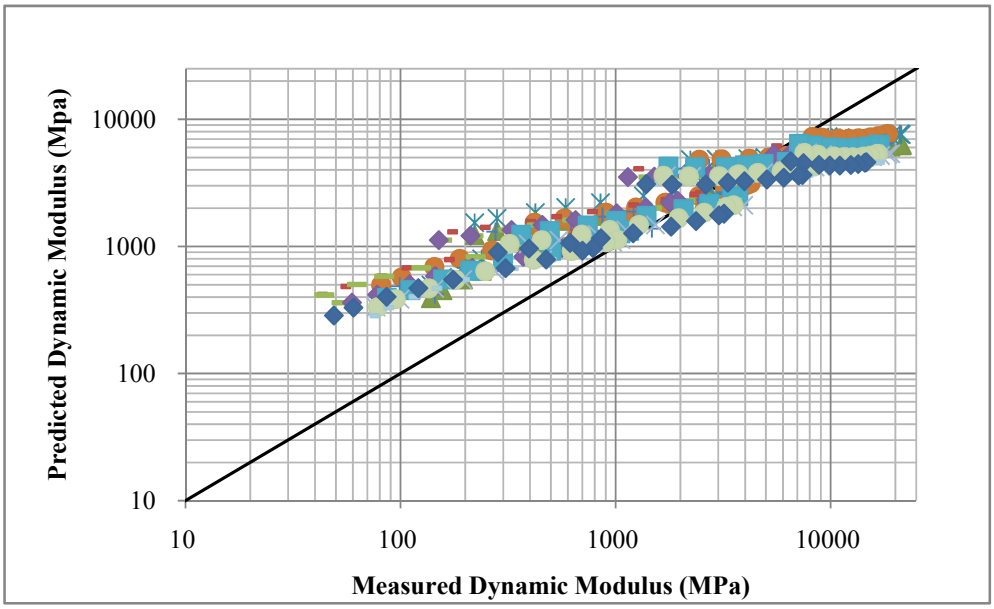

Figure 7-20. Dynamic modulus results based on 1996 Witczak model

7.4.1.2 *Prediction of dynamic modulus based on New Witczak Model*

This new Witczak Model was developed using a database (Bari 2005) of 7,400 measured E* values obtained from346 different HMA mixes. This expanded database also included the data used to develop the earlier1996 version of the model. In addition to the expanded database, the Witczak 2006 model replaced the binder's viscosity (η) and loading frequency (f) with dynamic shear modulus (G^*) and phase angle (δ).

Figure 7-21 presented a comparison between the measured and the predicted E* values. As shown, the New Witczak model has a better prediction of dynamic modulus at higher (54.4^{o}C) and lower temperature (4.4^{o}C) compared to the 1996 Witczak model.

However, it under predicts the dynamic modulus at medium temperatures (21.1°C and 37.8°C). Overall, the prediction results did not followed well with the line of equality, which means the New Witczak model is not a good prediction model for tested asphalt mixtures.

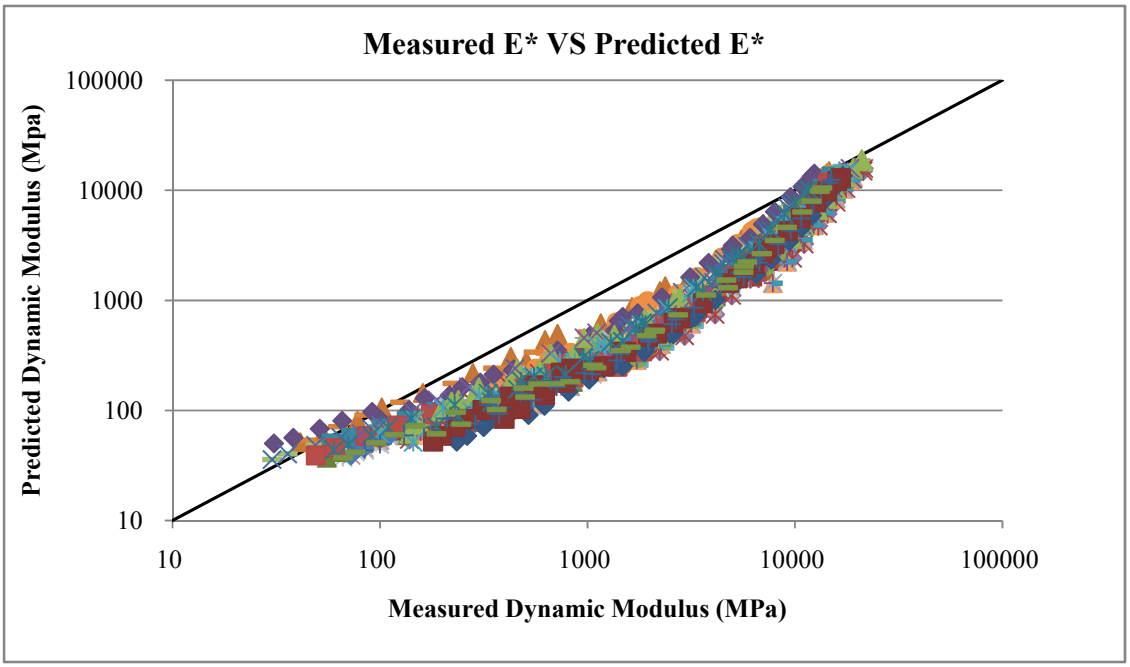

Figure 7-21. Laboratory measured E* and New Witczak model predicted E*

7.4.1.3 *Prediction of dynamic modulus based on Hirsch Model*

The Hirsch model for HMA dynamic modulus was developed based on data regression of 206 data points, indicated in Equation (7.1).

$$|E^*|_{mix} = Pc\left[4{,}200{,}000\left(1-\frac{VMA}{100}\right)+3|G^*|_b\left(\frac{VFA\times VMA}{10{,}000}\right)\right]+ (1-Pc)\left[\frac{1-(VMA/100)}{4{,}200{,}000}+\frac{VMA}{3VFA|G^*|_b}\right]^{-1} \quad (7.1)$$

Where;

|E*| = dynamic modulus, psi

$|G^*|_{binder}$ = binder dynamic modulus, psi

VMA= voids in the mineral aggregate, %

VFA = voids filled with asphalt, %

Pc = aggregate contact factor, where

$$Pc = \frac{\left(20+\frac{VFA\times 3|G^*|_b}{VMA}\right)^{0.58}}{650+\left(\frac{VFA\times 3|G^*|_b}{VMA}\right)^{0.58}} \quad (7.2)$$

The measured dynamic modulus for all samples was compared with the predicted dynamic modulus based on the original Hirsch model. In Hirsch model, the aggregate and volumetric properties were determined from experiments following AASHTO specifications. The asphalt binder was short-term aged using the rolling thin film oven method and its dynamic shear modulus (G*) was measured using dynamic shear rheometer (DSR) following AASHTO T-240. Figure 7-22 shows a comparison between

the measured and the predicted E* values. As shown, the prediction of Hirsch model is better than the prediction of Witczak model. The total prediction of Hirsch model at mid-range and low temperature follows the line of equality well. However, the prediction at higher temperature and low frequency is not good, which may affect the capability of capturing the rutting resistance of the mix. A modified Hirsch model calibrated by local materials is thus needed.

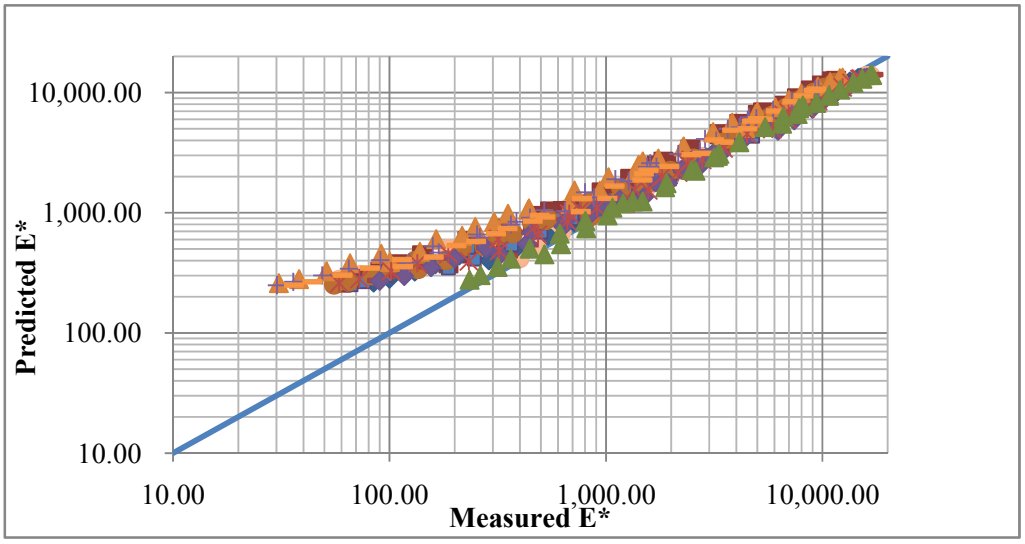

Figure 7-22. Laboratory measured E* and original Hirsch model predicted E*

7.4.1.4 *Summary of previous prediction models*

After reviewing all available models, the Hirsch model was selected in this study for several reasons listed below. It will be further modified based on local materials to achieve a better prediction.

(1) Unlike the Witczak models which are based on regression equations, the Hirsch model is based on the theory of composite materials.

(2) Unlike the Witczak models which consider the effect of aggregates for four individual sieve sizes, the Hirsch model considers the overall effect of aggregate gradations by relating the volumetric properties with the dynamic modulus.

(3) Compared with the Witczak models, the Hirsch model is simpler consisting of less parameter. This is particularly important for the purpose of obtaining a prediction model that can be used for estimating the dynamic modulus of asphalt mixtures at the early stage of the mix design with minimum requirement for the experimental testing.

(4) The initial evaluation of the experimental results for the Washington mixes tested in this study indicated that Hirsch model provided better prediction compared with the Witczak models.

7.4.2 *Modification of Hirsch Model*

7.4.2.1 *Theoretical background of Hirsch model*

Hirsch model (Christensen et al. 2003) considers that the composite material consists of different phases in series and/or in parallel arrangements. The asphalt material behaves as a serial arrangement composite at higher temperatures and as a parallel arrangement

composite at lower temperatures. In addition, Hirsch model describes the visco-elastic asphalt material as time and temperature dependent material, and the aggregate contact proportion parameter Pc had a critical influence on the total behavior of the HMA. The dynamic modulus of the asphalt concrete (|E*|) in the Hirsch model can be estimated from binder modulus (G*), voids in the mineral aggregate (VMA), and voids filled with asphalt (VFA) directly. This is practically important for estimating the dynamic modulus at the early design stage when only limited mix information and material properties are available, and some preliminary data analysis indicated the Hirsch model a promising model to be modified and used for local mixtures.

It was found that the HMA can be simulated with satisfactory accuracy with a simplified Hirsch model for which the general arrangements are in parallel rather than in series. The HMA was treated as a three-phase system which composed of aggregate, asphalt, and air voids. Based on such considerations, Equation (7.3) was proposed by Christensen et al. (2003) for regression process.

$$E_C = Pc \cdot (V_a \cdot E_a + V_b \cdot E_b) + (1 - Pc) \cdot \left[\frac{V_a}{E_a} + \frac{(V_b + V_v)}{V_b \cdot E_b} \right]^{-1} \quad (7.3)$$

Where

Va: true aggregate volume including volume of mineral filler,

V_b: effective binder volume,

E_a: aggregate response (for example modulus),

E_b: binder response (for example modulus),

V_v: air voids volume,

Pc: contact volume that represents the proportion of parallel to total phase volume and could be computed using the following expression:

$$Pc = \frac{\left(P_0 + \frac{VFA \cdot E_b}{VMA}\right)^{P_1}}{P_2 + \left(\frac{VFA \cdot E_b}{VMA}\right)^{P_1}} \quad (7.4)$$

Where

P_0, P_1, P_2: empirically determined constants,

VMA: voids in the mineral aggregate (voids + binder volume + mineral filler volume),

VFA: the percent of the VMA that is filled with the binder.

7.4.2.2 *Modified Hirsch model based on local calibration for virgin binder*

The original Hirsh model was calibrated in this study using the dynamic modulus testing results from 42 samples 7 asphalt mixtures at three different air voids) by minimizing square errors, and the modified Hirsch model was provided in Equation (7.5). Those equations are obtained from four different asphalt binder types.

$$|E^*| = Pc\left[4800000\left(1-\frac{VMA}{100}\right)+3|G_b^*|\left(\frac{VFA\cdot VMA}{10,000}\right)\right] + (1-Pc)\left[\frac{1-\frac{VMA}{100}}{4800000}+\frac{VMA}{VFA\cdot 3|G_b^*|}\right]^{-1} \quad (7.5)$$

Where,

|E*| = dynamic modulus, psi

$|G^*|_{binder}$ = binder dynamic modulus, psi

VMA= voids in the mineral aggregate, %

VFA = voids filled with asphalt, %

Pc = aggregate contact factor, where

$$Pc = \frac{\left(0.2+\frac{VFA\cdot 3|G_b^*|}{VMA}\right)^{0.56}}{600+\left(\frac{VFA\cdot 3|G_b^*|}{VMA}\right)^{0.56}} \quad (7.6)$$

All other parameters are the same as Equation (7.1).

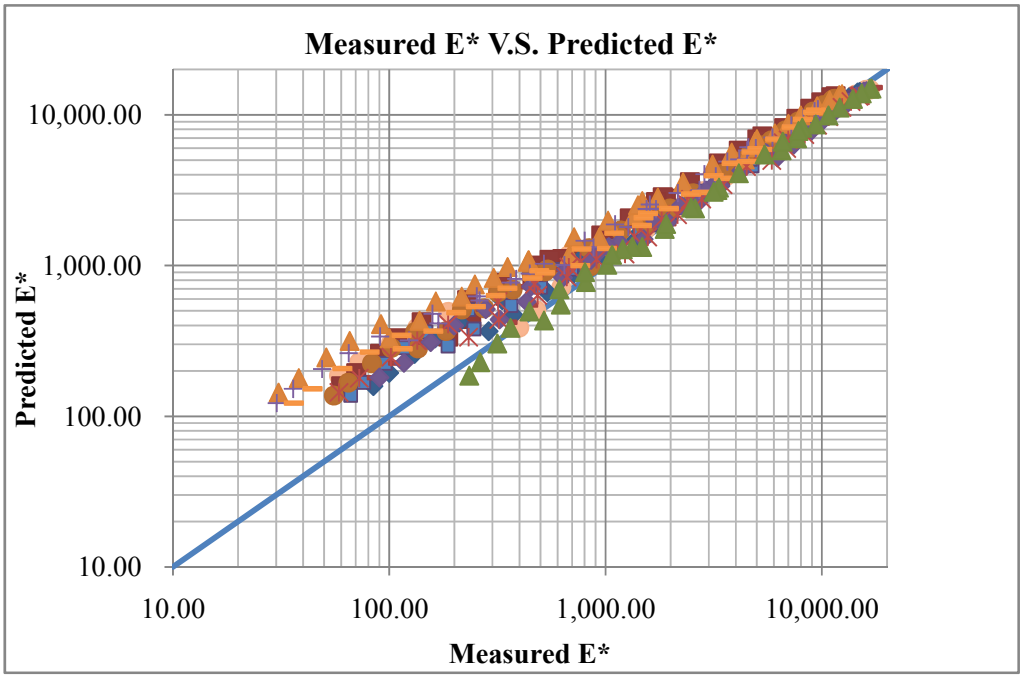

Figure 7-23. Measured E* and predicted E* based on modified Hirsch model

Figure 7-23 compares the measured dynamic modulus with the predicted dynamic modulus based on the modified Hirsch model. It is clear that the prediction quality is improved and the prediction trend for high temperature is better than the original Hirsch model. However, results still shows that the revised Hirsch model over predicts the dynamic modulus at higher temperatures.

7.4.2.3 *Modified Hirsch model based on local calibration for asphalt mastic*

The addition of mineral fillers to asphalt binder as very fine materials improves the stiffness of the binder; this combination produces the asphalt mastic. Asphalt mastics play an important role in the compaction and performance of bituminous mixtures, and

its influence should be taken into account as a combined material component rather than being treated separately as current predictive models did. Therefore, this study proposes to use the shear complex modulus of mastics to replace the binder's shear modulus term in the Hirsch model. The properties of mastics is influenced by the Dust/Asphalt ratio, and the Dust/Asphalt ratio is calculated by the ratio of aggregate content passing the 0.075 mm (75 μm) sieve over the effective asphalt binder content (Pbe, percent by mass of aggregate).The modified Hirsch model based on asphalt mastic is shown in Equation (7.7),

$$\left|E^*\right| = Pc\left[1.0E7\left(1-\frac{VMA}{100}\right)+3\left|G_m^*\right|\left(\frac{VFA\cdot VMA}{10{,}000}\right)\right] + \left(1-Pc\right)\left[\frac{1-\frac{VMA}{100}}{1E7}+\frac{VMA}{VFA\cdot 3\left|G_b^*\right|}\right]^{-1} \quad (7.7)$$

where,

|E*| = dynamic modulus, psi

|G*|m = mastic dynamic modulus, psi

VMA= voids in the mineral aggregate, %

VFA = voids filled with asphalt, %

Pc = aggregate contact factor, where

$$Pc = \frac{\left(20 + \frac{VFA \cdot 3\left|G_m^*\right|}{VMA}\right)^{0.67}}{10{,}000 + \left(\frac{VFA \cdot 3\left|G_m^*\right|}{VMA}\right)^{0.67}} \tag{7.8}$$

Figure 7-24 compares the measured dynamic modulus with the predicted dynamic modulus based on the modified Hirsch model with asphalt mastic. It is clear that the prediction quality is significantly improved and most of the data followed the line of equality very well. The prediction trend is good for a wide range of temperatures and frequencies. Although only based on limited data (limited gradation type and binder type for Washington mixes), this model is very promising as it changed the inherent prediction trend of the original Hirsch model (Figure 7-22) and improved the prediction especially at the high temperature of the dynamic modulus curves.

The modified Hirsch model provides a means to estimate the dynamic modulus based on only volumetric properties (VMA, VFA) and asphalt mastic dynamic shear modulus. It can be used for a quick check of the material properties at the early stage of the mix design. If MEPDG is implemented as a pavement design procedure, this model can also serve It as the level 2 and level 3 material property prediction equation for obtaining material properties.

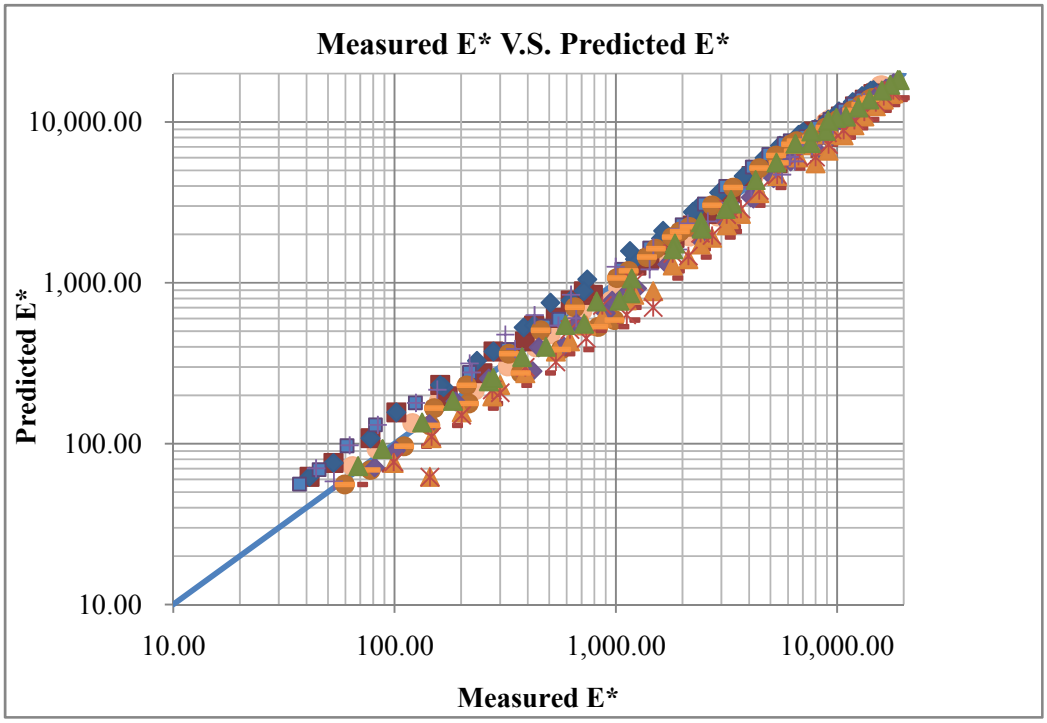

Figure 7-24. Measured E* and predicted E* based on modified Hirsch model of mastic

7.5 Flow Number Prediction Models

7.5.1 *Local calibration of flow number prediction model*

The previous effects on the prediction of mechanical properties of asphalt mixture have been put on the dynamic modulus, and there is no widely applied flow number prediction model available at this moment. A model capable of predicting or providing general guidance on the Flow Number characteristics can be of great value. In this study, an effort was undertaken to develop a calibrated Flow Number predictive model for

Washington State. The flow number prediction model was calibrated according to Kaloush (2001) flow number prediction model which was developed based on mixtures volumetric properties, binder type, and test temperature. The final calibrated model had fair statistical measures of accuracy and it covers the whole testing temperatures and frequencies. As more testing data become available, the model could be refined and re-calibrated for better accuracy.

The original Kaloush (2001) model used 135 unconfined laboratory FN tests and was presented as follows:

$$FN = (432367000)T^{-2.215}Visc^{0.312}V_{beff}{}^{-2.6604}V_a{}^{-0.1525} \qquad (7.9)$$

where, FN = Flow Number

T = Test Temperature, °F

Visc = Binder Viscosity at 70°F, 106 poise

Vbeff = Effective Asphalt Content, % volume

Va = Air Voids, %

The local calibrated model is shown in Equation (7.10),

$$FN = 2.865E10 \cdot T^{-2.83354}G^{0.462887}V_{beff}{}^{-4.98023}V_a{}^{-1.25751} \qquad (7.10)$$

And the comparison of prediction and measured results are shown in Figure 7-25.

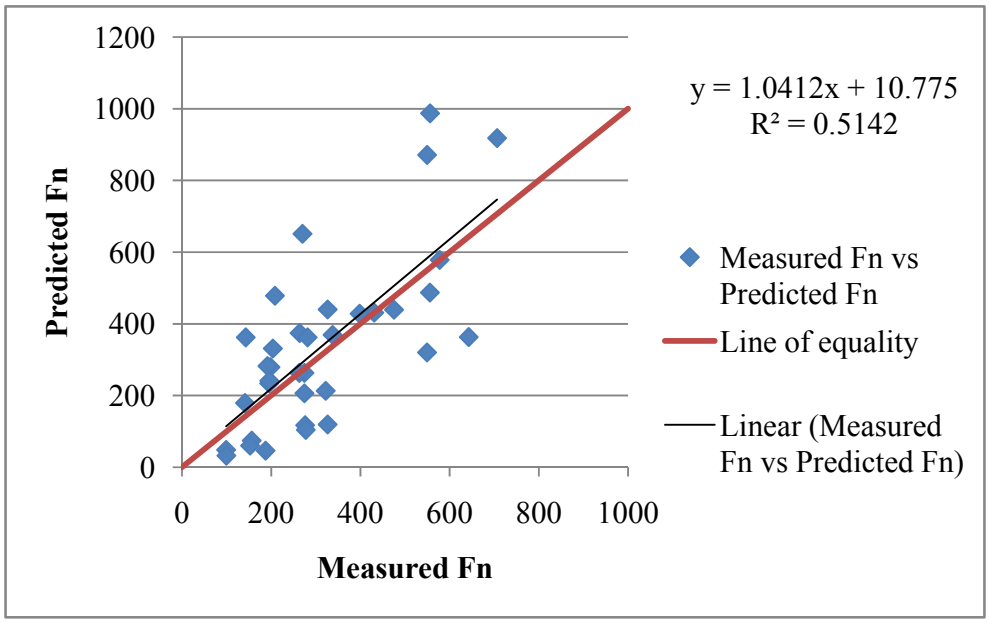

Figure 7-25. Measured E* and predicted E* based on modified Hirsch model of mastic

The data used for regression includes projects #2 to #7, and the contract numbers are including C8017, C8013, C8033, C8016, C7879, C7465, the asphalt binders are PG 70-28, PG 64-28 and PG 64-22. It is found that due to the high polymer modification of asphalt binder (PG76-26), the flow number results of project #1 (C8046) are significantly higher that the prediction results. It is therefore suggested that the presented flow number prediction model only be used for mixtures with conventional binder.

7.5.2 *Sensitivity analysis of flow number prediction model*

Air voids is one of the most important control parameters for asphalt mixture design and field construction, which is also one of the parameters in the prediction model for determining the flow number of asphalt mixtures, this section studied the sensitivity of air voids on the flow numbers. Air voids levels from 3% to 7% are evaluated as shown in Figure 7-26. It can be seem that with the increase of air voids level, the flow number is decreasing which in consistent with the experimental results.

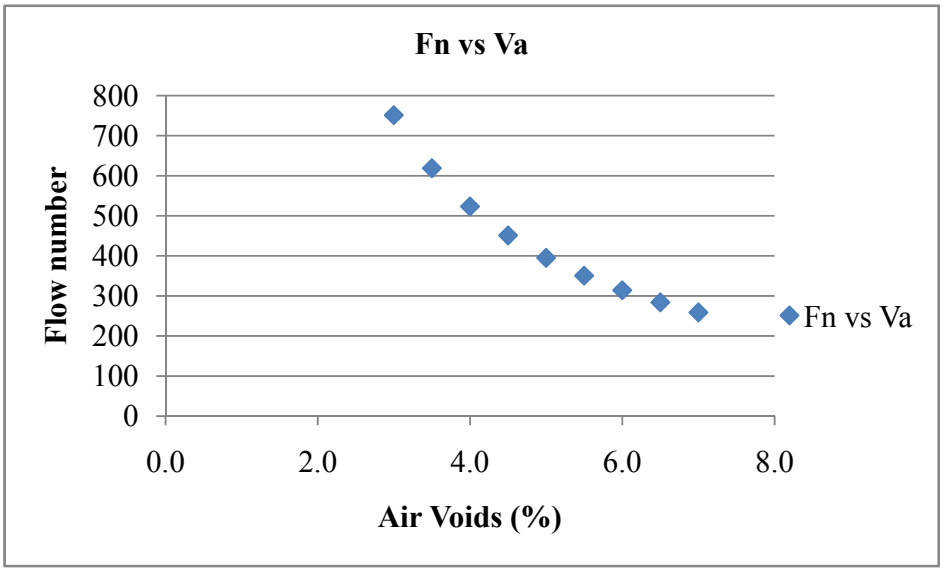

Figure 7-26. Measured Fn and predicted Fn based on modified Hirsch model of mastic

7.6 SUMMARY

Firstly, this section evaluated the influence of material properties on the mechanical

properties of asphalt mixture, summarized the experimental results of dynamic modulus tests and flow number tests for seven field projects. The influence of air voids, binder type, and aggregate gradation on dynamic modulus and flow number is shown. It is found that air voids have an important effect on E* and flow number. In general, higher air voids will result in lower E* and flow numbers. High PG grade has clear influence on E* and flow number; higher PG grade leads to higher E* and flow number. Aggregate gradation has some impact on E* and flow number but the trend of impact is not clear.

And then, this chapter compared the Hirsch model, 1996 Witczak model and New Witczak model using the dynamic modulus testing results conducted in this study. Based on the comparison results, the Hirsch model was selected as the basic model for further modification. A modified Hirsch model, based on the properties of asphalt mastic, was presented. It can reasonably predict the dynamic modulus properties of tested asphalt mixture, considering a wide range of temperature, binder type, aggregate gradations, etc. The revised Hirsch can be used as both a designing tool and a screening tool to estimate the mixture's dynamic modulus at the early stage of the mix design.

A flow number prediction model was also developed based on experimental data on local mixes. The prediction model took into account the effects of volumetric properties, binder type, and test temperatures. The prediction results were reasonable for mixtures

with conventional PG binder (PG 70-28, PG 64-28 and PG 64-22). It was however not recommended for highly polymer modified PG binder (i.e., PG76-28).

CHAPTER 8 ASPHALT MIXTURE DESIGN GUIDELINE

The development of the new aggregate gradation design and mix design method is based on the strong correlations among aggregate gradation, volumetric properties and mechanical performance. VMA, as the most important volumetric property which is mainly affected by the aggregate properties and gradation, is used as a media to connect the aggregate gradation with performance. The concept of the performance based asphalt mixture design method consists of three major steps, which is also schematically shown in Figure 8-1.

Firstly, the VMA of asphalt mixtures based on the aggregate gradation is predicted based on packing theory. The VMA prediction method introduced in this paper will help the designer to adjust aggregate gradation to reach VMA requirement.

Secondly, the VFA can be calculated based on the design air voids of 4% as specified in the Superpave specifications and the estimated VMA. Consequently, the effective asphalt content can be calculated and the target optimum asphalt content can be estimated. A few gyratory specimens can be made to verify the volumetrics at the estimated asphalt content.

Thirdly, a mechanical model, such as the modified Hirsch model suggested in this paper, will be applied to predict the dynamic modulus of the mix, an important mechanical property to be related to the field performance.

It should be noted that aggregate is considered in this paper as the major factor controlling the VMA properties of the mix. Although other properties such as binder type, binder content, and compaction level (number of design gyrations) may influence the asphalt lubricant effect and the packing, their effect on VMA is less noticeable than aggregate effect (Shen and Yu 2011).

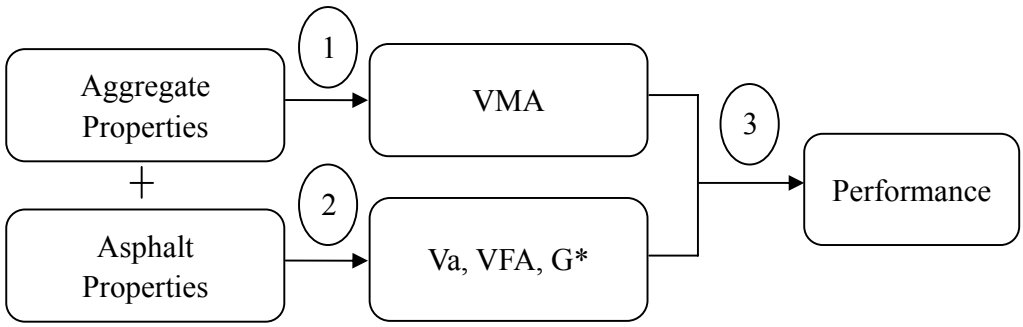

Figure 8-1. Methodology of the performance modeling and design guideline

8.1 Selecting Gradation Based on VMA

VMA is a critical parameter that links the mixture composition with the engineering performance. The easiness of achieving the target VMA value is a critical step in the mix design which is mainly affected by the aggregate properties and gradation. This section derives a correlation between aggregate gradations and VMA based on a theoretical

analysis of packing theory and DEM simulation. A simple VMA prediction method is proposed to help designer achieve target VMA at early stage of the mix design, and link aggregate gradation with mix mechanical performance.

8.2 Gradation Type Definition

As a first step for a systematic gradation design, more scientific definitions of gradation types and shapes are needed since different gradations can behave quite differently in terms of particle packing, volumetric properties, and field performance. Conceptually, coarse and fine graded mixtures are usually categorized depending on whether the gradation curve is passing below or above the maximum density line. A new method was developed by Shen and Yu (2011) which categorize the different gradation types based on their packing characteristics and was proved to be able to be related to the aggregate contact performance.

The CMD plot as proposed in the NCHRP 9-33 report (Advanced Asphalt Technologies, LLC. 2011) can be developed for the gradation of interest according to their deviations from the maximum density line. $P_d(d)$, the percent of aggregates (size d) deviating from the maximum density line, can be obtained from Equation (8.1).

$$P_d(d)=P(d)- P_{Dens.} \quad (8.1)$$

Where

$P(d)$.: Percent of aggregates passing sieve size d for a specific gradation (%);

$P_{Dens.}$: Percent of aggregates passing the maximum density line (%), which can be calculated from Equation (8.2);

$$P_{Dens.} = \left(\frac{d}{D_{\max}}\right)^{0.45} \times 100\% \tag{8.2}$$

Where

d: sieve size (mm);

D_{max}: maximum sieve size for that gradation (mm).

Table 8-1. P_{dc} criteria for different gradation types (Shen and Yu 2011)

P_{dc}	Gradation type
$P_{dc} \leq 0$	coarse-graded
$0 < P_{dc} \leq 20$	medium-graded
$P_{dc} > 20$	fine-graded

A critical deviation value, P_{dc}, is proposed in this study to classify different gradation types. The P_{dc} is the sum of the deviations of four medium sieve sizes, the sieves that play important roles in determining a gradation curve shape. For a gradation with a nominal maximum particle size (NMPS) of 12.5mm, the P_{dc} can be calculated using Equation (8.3).

$$P_{dc} = P_d(9.5) + P_d(4.75) + P_d(2.36) + P_d(1.18) \quad (8.3)$$

Table 8-1 listed the recommended ranges for P_{dc} to categorize three different gradation types, coarse-graded, medium-graded, and fine-graded gradations. The selections of the breaking points are to be consistent with the existing gradation type definitions and have been verified based on an analysis of packing (Shen and Yu 2011).

8.3 VMA PREDICTION

A gradation weighing factor, f_v, defined as the percent of voids change by volume due to the addition of unit aggregate, is developed to link the gradation information directly to the VMA (Shen and Yu 2011). The prediction of VMA is an iteration process starting from an aggregate structure with the largest uniform size aggregates (i.e. NMPS). When the aggregates with one size smaller were added into the structure based on the target gradation, the percent of voids change of the aggregate structure due to the newly added aggregates can be determined by Equation (8.4)

$$f_v = \frac{V_{v2} - V_{v1}}{V_{a2}} \quad (8.4)$$

Where,

V_{v1}: Total air void volume of the initial aggregate structure

V_{v2}: Total air void volume of the new aggregate structure after adding smaller size aggregates

V_{a2}: The added aggregate volume determined according to aggregate gradation.

The newly added aggregates typically have two effects, either enlarge the structures by creating more voids, or fill the voids created by the original aggregates without changing the total volume of the structure. If all added aggregates are contributed to enlarging the structure, theoretically the porosity of structure after the aggregate being added and compacted should be the same as the previous structure when packed in the same manner, based on an analysis of packing theory by Deresiewicz (1958) and the DEM simulation by Shen and Yu (2011). Therefore, Equation (8.5) can get,

$$f_v = \frac{p_1}{1-p_1} \tag{8.5}$$

Where, p_1 is the aggregate porosity or VMA of the initial aggregate structure.

If all added aggregates contribute to filling the voids created by the aggregate, the final porosity will be reduced and the f_v will be constant -1. In real gradations, it is typical that part of the added aggregates serves as creating voids while others serve as filling the voids. The actual f_v values will thus be in between these two extreme cases, i.e., between $p_1/(1-p_1)$ and -1.

Following the same procedure, smaller aggregates can be further added into the structure of upper sieve size aggregates according to the target gradation, and the corresponding *fv* values for each added sieve sizes can be determined. Shen and Yu (2011)

suggested two ways to determine the *fv* values, either by data regression based on existing designs, or from the packing simulation using the DEM modeling. The recommended f_v results for coarse-graded, medium-graded and fine-graded gradations of 12.5mm NMPS are shown in Table 8-2.

Table 8-2. f_v values for gradations with NMPS=12.5mm

	Coarse-grade		Medium-graded	Fine-graded
Sieve size (*mm*)	Data Regression	DEM Simulation	DEM Simulation	DEM Simulation
19	0.411	0.429	0.436	0.455
12.5	0.411	0.429	0.436	0.455
9.5	0.411	0.429	0.436	0.455
4.75	0.410	0.429	0.436	0.455
2.36	0.169	0.196	0.178	0.174
1.18	-0.366	-0.400	-0.405	0.107
0.6	-0.366	-0.400	-0.405	-0.035
0.3	-0.366	-0.420	-0.430	-0.397
0.15	-0.536	-0.600	-0.589	-0.568
0.075	-0.952	-1.000	-0.899	-0.755

Due to the limited amount of medium-graded and fine-graded gradation data available, only f_v values calculated based on the DEM simulation method were presented for these two gradation types. It should also be noted that f_v value is found to be not sensitive as long as they have the same NMAS and belongs to the same gradation type (coarse-graded, medium-graded, or fine-graded).

Once all f_v values for each sieve size are determined, Equation (8.6) will be used to predict the VMA (or porosity) of the asphalt mixtures.

$$p = \frac{\sum_{i=1}^{n} f_{vi} V_{ai}}{\sum_{i=1}^{n} (1 + f_{vi}) V_{ai}} \tag{8.6}$$

Where f_{vi} is the f_v value for ith sieve size of the gradation, V_{ai} is the percentage by volume of aggregate retained in the ith sieve size, and p is the porosity or VMA of the aggregate structure.

Shen and Yu (2011) verified that the predicted VMA based on this approach matches well with the design VMA, with most errors within 1%.

8.4 Gradation Selection

The method of predicting VMA can be used for selecting design gradations. Given any trial gradations, their target VMA can be determined in the excel spread sheet using

the procedure described above. Initial adjustment on gradation could have been made based on the VMA criteria. It is possible the gradations need to be adjusted again to satisfy performance requirement and volumetric requirement, which will be described in later section of this paper.

8.5 Estimating Design Asphalt Content

Based on the selected aggregate gradation and the predicted VMA, the design asphalt content corresponding to 4% air voids can be estimated. This is realized by first determining the void filled with asphalt (VFA) using Equation (8.7).

$$VFA=100*(1-Va/VMA) \tag{8.7}$$

Consequently, the effective asphalt content (P_{be}) is calculated using Equation (8.8).

$$P_{be}=(VMA-V_a)*\ G_b/G_{sb} \tag{8.8}$$

For a given type of aggregate and asphalt binder, the absorption rate of asphalt binder should be relative consistent and can be determined from experiments. Therefore, the design asphalt content (P_b) required producing a mix with known VMA and a design air void of 4% can be estimated based on Equation (8.9).

$$P_b = P_{be} + \frac{P_{ba}}{100} \times P_s \tag{8.9}$$

Where,

P_{ba} is the asphalt absorption rate by weight of total aggregates, and

Ps is the amount of aggregates by weight.

This proposed method can also be used to optimize asphalt content by adjusting the gradations. As indicated above, the optimum asphalt content is mainly determined by the VMA for a given type of aggregate and asphalt binder. By adjusting the proportions of aggregates and the way of aggregate packing, a designer will be able to minimize the asphalt binder content for cost and other consideration while still maintain the necessary volumetric properties. To verify the design asphalt content, it is recommended to prepare 2-3 gyratory specimens using the selected aggregate gradation and the design asphalt content and determine the volumetric properties of the specimens.

8.6 Evaluating The Mechanical Performance Of The Mixture

For a performance based mix design procedure, it is desirable that the properties of aggregate and asphalt component can be directly related to the mechanical properties or the engineering performance of the mixture. In this paper, the volumetric property, the VMA, has been found to be a good media to link these two aspects so that the aggregate and binder properties can be related to the dynamic modulus of the mixture, one of the most important properties in the current DARWin ME mechanistic-empirical pavement design guide (MEPDG) for pavement performance evaluation and prediction.

8.7 Dynamic Modulus Prediction Models

For the purpose of practical and routine usage, a dynamic modulus model is recommended to be included into the new mix design procedure which can provide a quick estimate of the mechanical property of the mix without the need to perform time-consuming and costly experiments. Therefore, a modified Hirsch model is calibrated as shown in Equations (8.10)-(8.11).

$$\left|E^*\right| = Pc\left[1.0E7\left(1-\frac{VMA}{100}\right)+3\left|G_b^*\right|\left(\frac{VFA\cdot VMA}{10,000}\right)\right] + \left(1-Pc\right)\left[\frac{1-\frac{VMA}{100}}{1E7}+\frac{VMA}{VFA\cdot 3\left|G_b^*\right|}\right]^{-1} \quad (8.10)$$

where,

|E*| = dynamic modulus, psi

$|G^*|_{binder}$ = binder dynamic modulus, psi

VMA= voids in the mineral aggregate, %

VFA = voids filled with asphalt, %

Pc = aggregate contact factor, where

$$Pc = \frac{\left(20 + \frac{VFA \cdot 3\left|G_b^*\right|}{VMA}\right)^{0.67}}{10,000 + \left(\frac{VFA \cdot 3\left|G_b^*\right|}{VMA}\right)^{0.67}} \tag{8.11}$$

In the modified Hirsch model, the aggregate and volumetric properties were determined using the predictive method introduced earlier in this paper. The asphalt binder was short-term aged using the rolling thin film oven method and its dynamic shear modulus (G*) was measured using dynamic shear rheometer (DSR) following AASHTO T-240 (1999).

The modified Hirsch model provided a method to estimate the dynamic modulus based on only volumetric properties (VMA, VFA) and asphalt binder dynamic shear modulus. Because the VMA can be estimated based on mainly the aggregate gradation properties, and the VFA is a function of VMA, target air voids, and asphalt absorption rate which is relative constant for a given aggregate type, only the complex shear modulus (G*) of the binder is required from the experimental testing. This made it possible to estimate the dynamic modulus at the early stage of the mix design. If the predicted dynamic modulus is not appropriate (too low at high temperatures or too high at low temperatures), the modified Hirsch model can also be used as an optimization tool to guide the adjustment of the aggregate gradation to achieve appropriate E* values.

8.8 SUMMARY

This chapter describes in detail a comprehensive aggregate gradation and asphalt mixture design method that estimates the engineering performance of the mix at early stage. In order to better understanding the concept of this mixture design method, a design example is provided at Appendix C to describe the new design method step by step.

CHAPTER 9 DEM SIMULATION OF ASPHLAT MIXTURE

9.1 INTRODUCTION

The accurate information of volume, angularity, shape and texture are needed in order to reconstruct 3-D model of an aggregate particle in the computer. The University of Illinois Aggregate Image Analyzer (UIAIA) developed by Tutumluer et al. (2005) can provide accurate and automated measurement of individual particles. This research considers the effect of shape and angularity by combining tens of balls together in PFC^{3D} to match the 3-D image of the individual particles obtained from the UIAIA. The effect of surface roughness is taken into account through model parameter assignment such as contact friction angle. The simulation results are calibrated based on experimental results to establish a reasonable DEM model for further evaluation. The details about generating particles and conducting DEM simulations are discussed below.

9.2 PARTICLE GENERATION

9.2.1 *Introduction of UIAIA (Pan et al. 2005)*

The University of Illinois Aggregate Image Analyzer (UIAIA) is a image analysis device which was developed and evaluated by the NCHRP 4-30A project, the UIAIA

provides a fast, objective, and automated means to describe particle shape and size distribution characteristics for quantifying the influence of particle shape, angularity, and surface texture on asphalt mixture performance. As far as the validation results from Illinois DOT, the UIAIA system showed high accuracy and can precisely and reliably quantified for shape, angularity, texture, and gradation properties for coarse aggregate by the means of video imaging. Compared to previous image analysis systems, the UIAIA have following advantages, it can characterize the 3D properties of aggregate, it can also calculate the volume and quantity the shape and angularity effects. For the advantages described above, the UIAIA have the potential to replace four of the standard coarse aggregate shape test procedures, i.e., ASTM D 4791, ASTMD5821, ASTM D3398, AASHTO TP56. Figure 9-1 shows a schematic of the UIAIA illustrating the operating principle and the various components of the UIAIA.

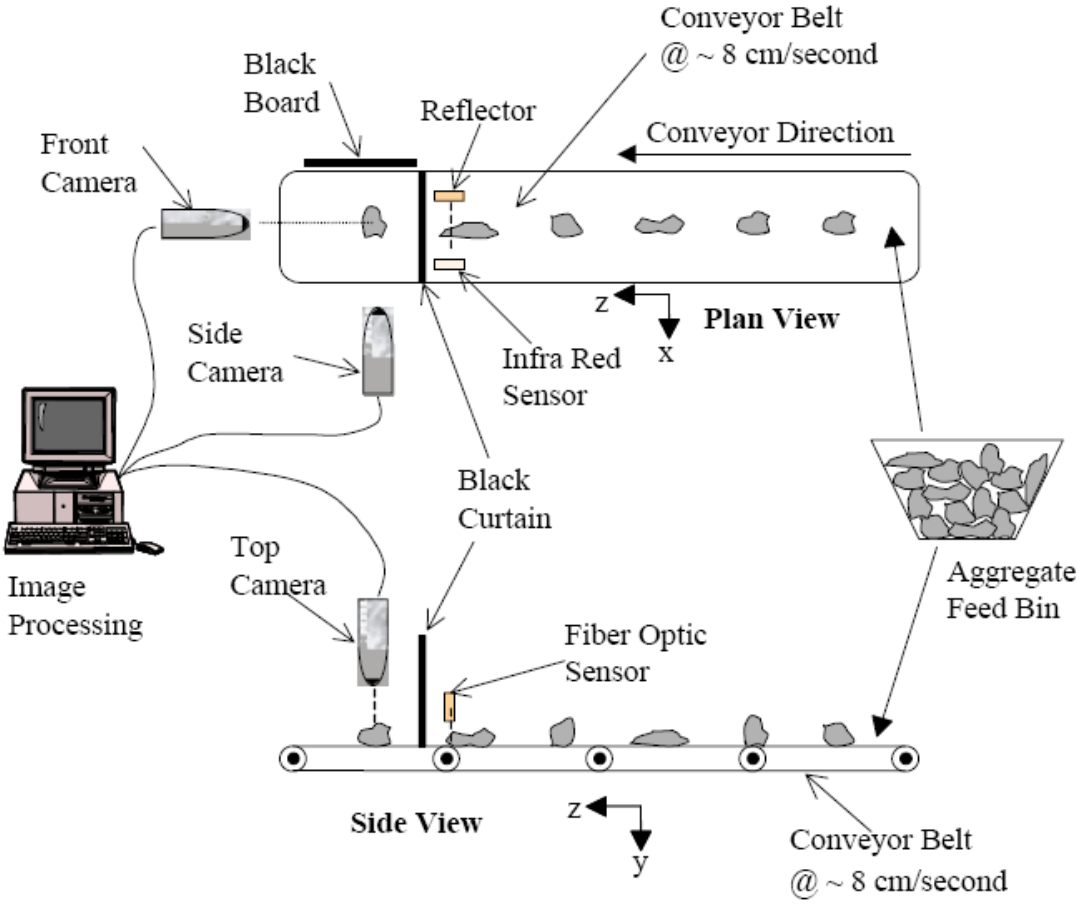

Figure 9-1. Schematic of the University of Illinois Aggregate Image Analyzer (Pan et al. 2005)

9.2.2 *Particle scanning*

Around eighty aggregate particles from four sieve size groups (2.36-4.75mm, 4.75-9.5mm, 9.5-12.5mm, and 12.5-19mm) (twenty particles per group) were randomly selected from the design gradation. These particles were scanned using UIAIA and the

aggregate angularity index (AI) and flat and elongated ratio was determined. For each group, the particle scanning results are shown in Figure 9-2.

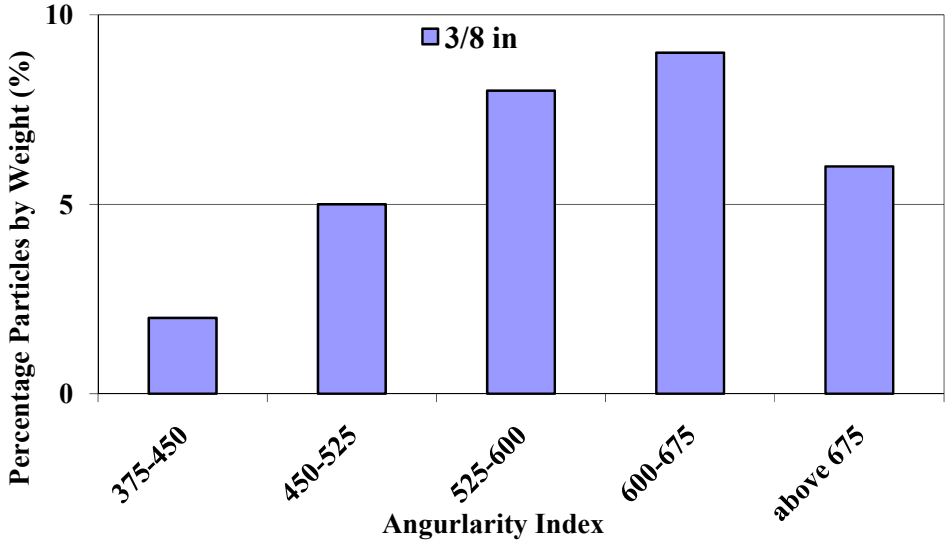

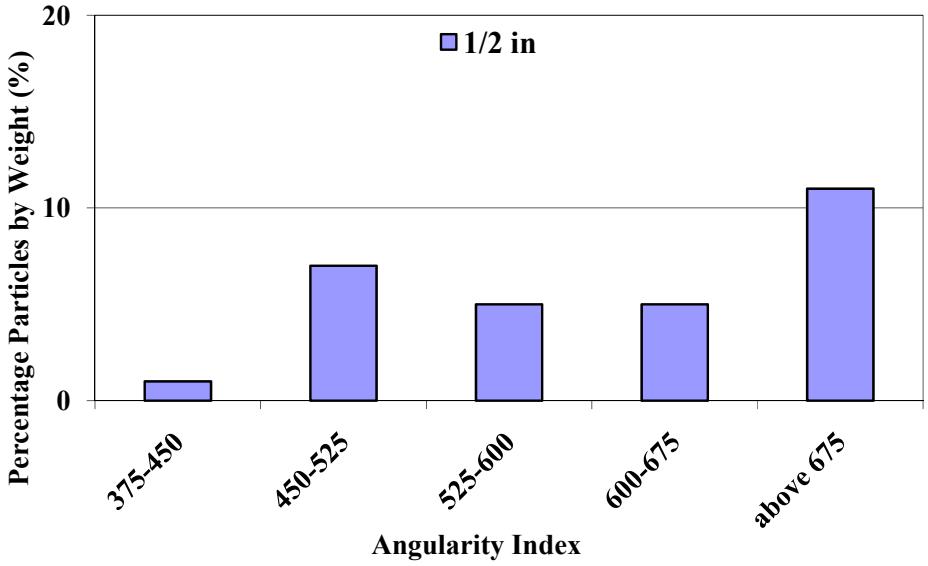

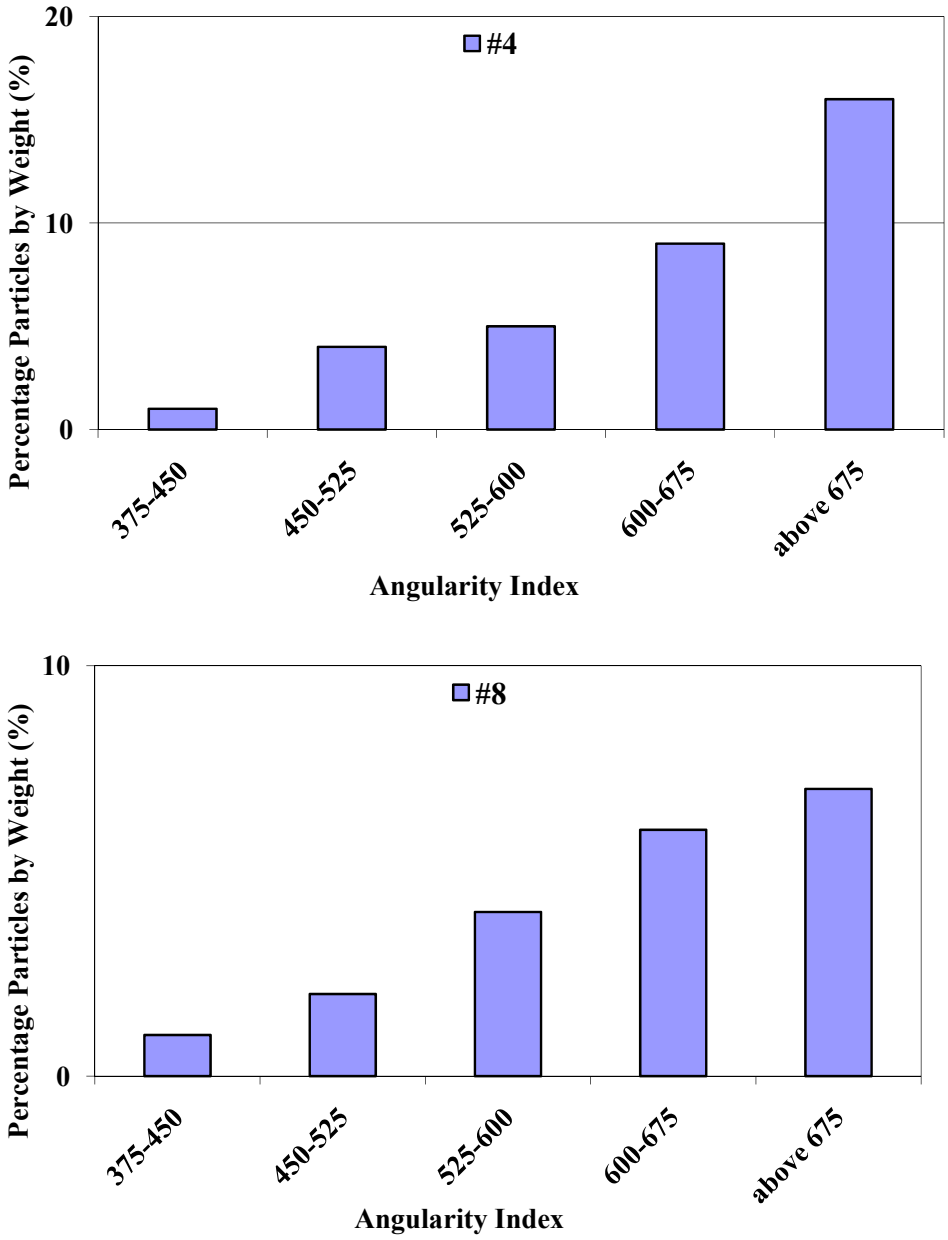

Figure 9-2. Angularity index of aggregate

For each particle, three orthogonal views taken by the UIAIA were utilized to compute the volume and angularity information. As shown in Figure 9-3 and Figure 9-4, the three images in the x-y, y-z, and z-x planes corresponded to front view, side view and top view individually. Figure 9-5 showed the 3-view pictures of representative aggregates of five different AI types. The three images from top to bottom in each column represented the front view, side view and top view of one particle individually. From top to down in Figure 9-5, the angularities of the particles were increasing with the most angular particles on the bottom.

Figure 9-6 showed the histogram of the AI distributions for the twenty randomly selected aggregate particles from each sieve size. This distribution is considered as a representative AI distribution of the overall aggregate blend, and is used later for determining the proportions of aggregate particles in the DEM model.

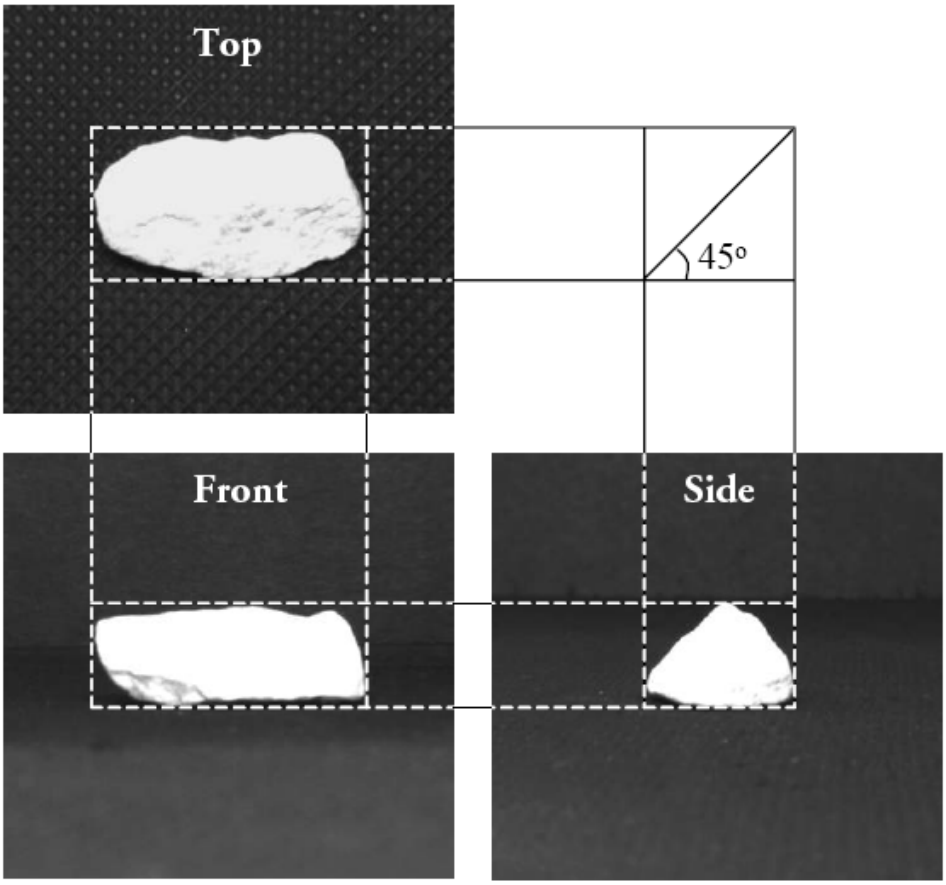

Figure 9-3. Three Orthogonal Views of a Particle Captured by the UIAIA

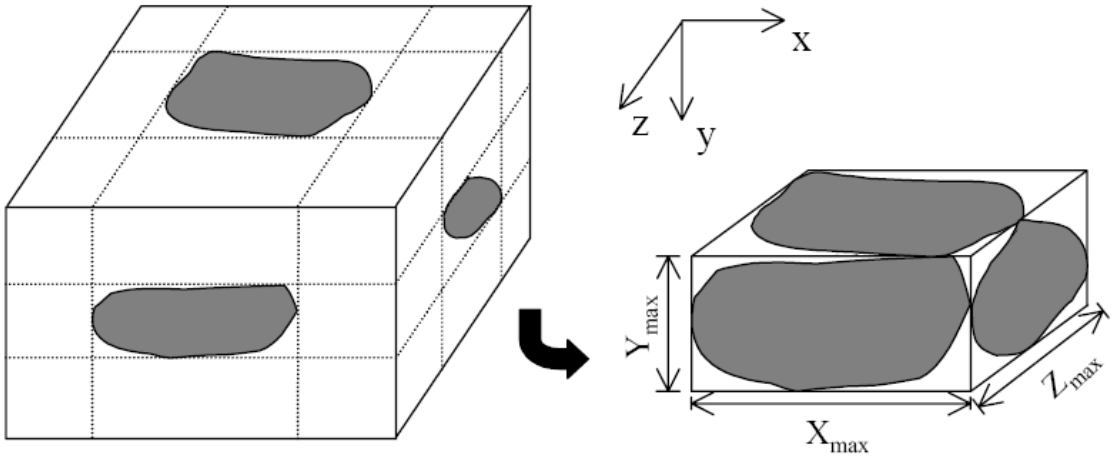

Figure 9-4. Acquiring array subsets for images

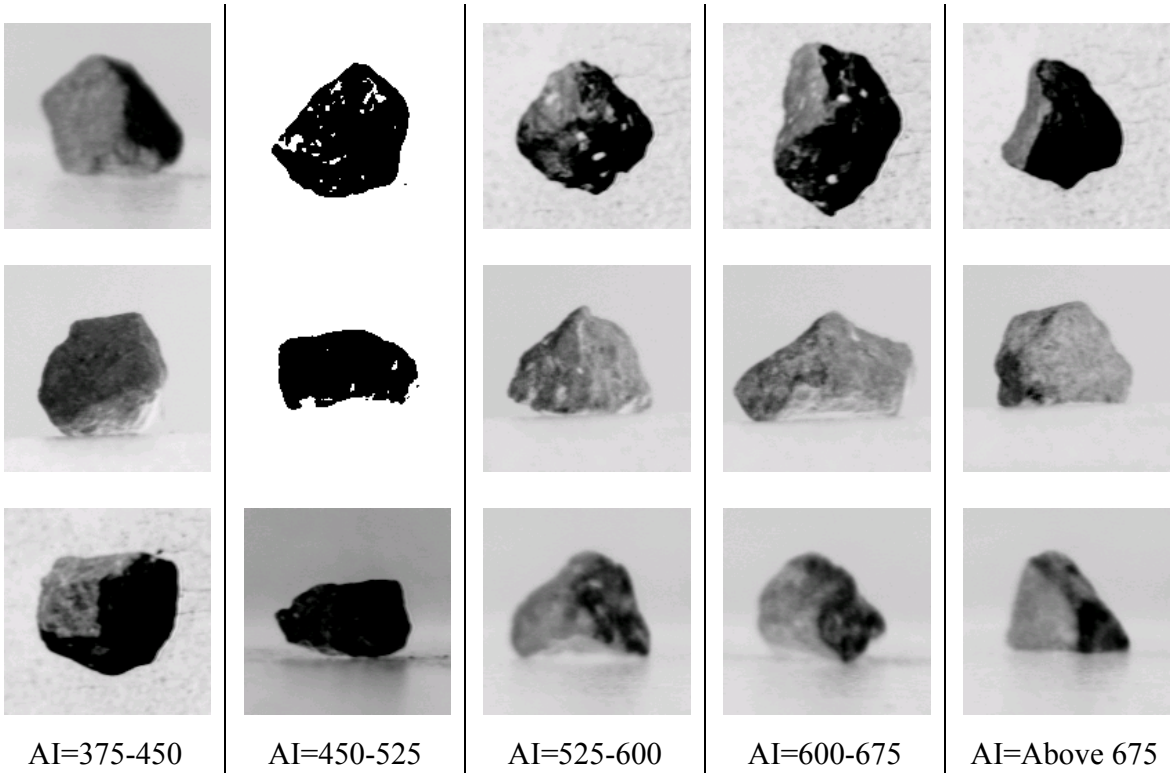

Figure 9-5. Three-view pictures of five AI types

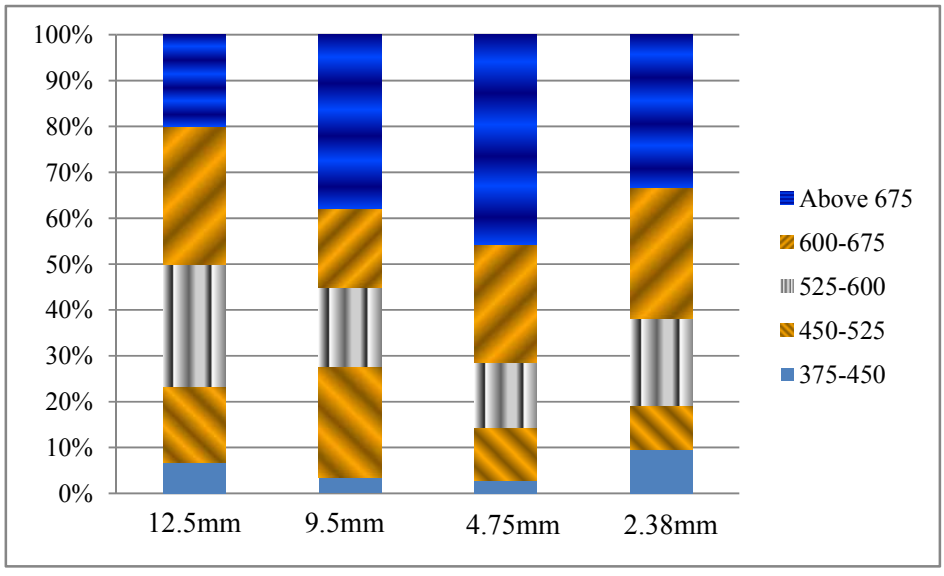

Figure 9-6. Histogram of the AI distributions for selected aggregates

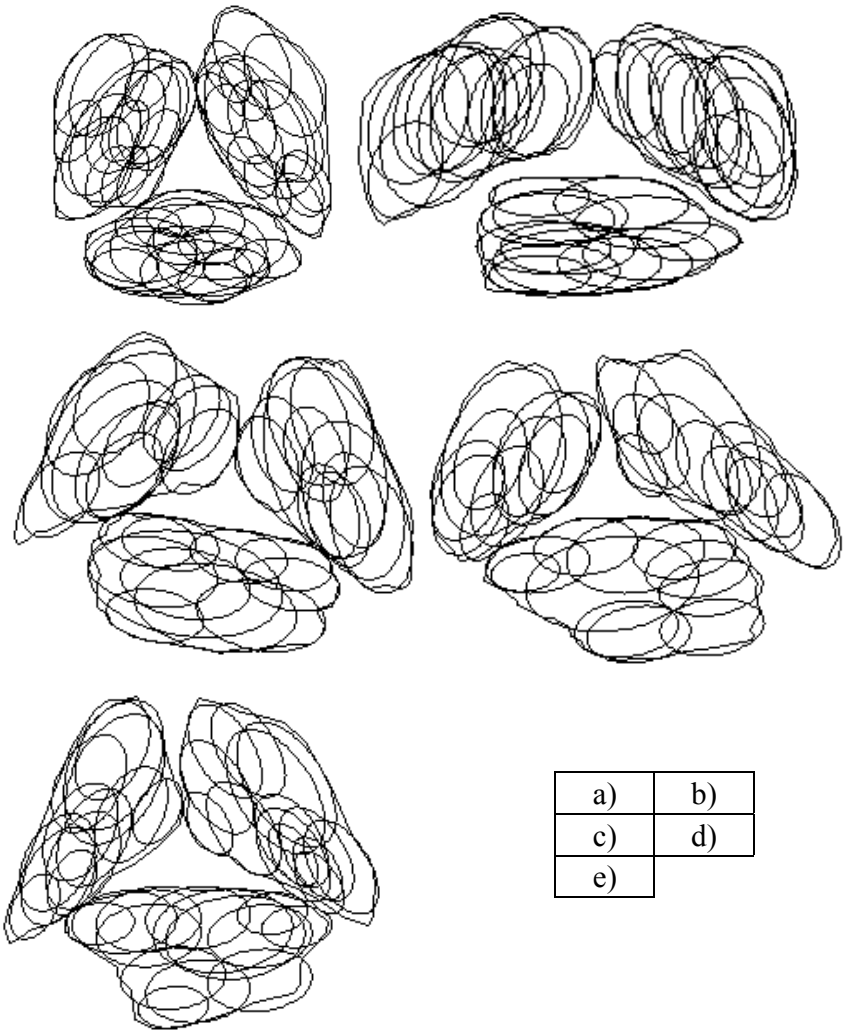

Figure 9-7. Representative 3D particle models for each angularity index (AI)group **a)**. AI group: 375-450; **b)**. AI group: 450-525; **c)**. AI group:525-600; **d)**. AI group: 600-675;**e)**. AI group: above 675

One particle with an average AI of each AI group was used for the 3D PFC particle generation in PFC^{3D}. As shown in Figure 9-7, 11 to 16 different sizes of balls were clumped together to match the 3D angularity and shape of each representative aggregate

particle shown in Figure 9-5, and their 3D views were presented in Figure 9-7 a)-e). These generated 3D PFC particles were further used in the DEM modeling to represent aggregates of a specific AI group.

The generation of the aggregate particles in the DEM model takes into account two distributions, (a) particle size distribution controlled by the aggregate gradation; and (b) aggregate shape and angularity distribution controlled by the angularity index (AI). The aggregate AI properties describe the angularity of an aggregate particle. The higher the AI value is, the more angular an aggregate is. In this study, a DEM particle library with particles representing different AIs was first established as shown in Figure 9-8. It is worth noting that aggregates finer than 2.36mm were not generated directly in the PFC3D for saving computational time. They were mixed into asphalt binder and treated together with binder as asphalt mastic.

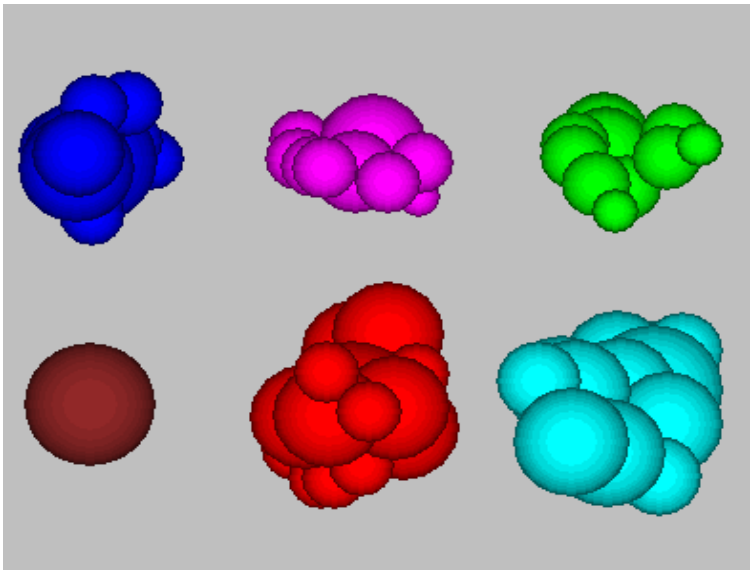

Figure 9-8. DEM particle library with aggregates representing each AI group

9.3 Model Calibration

The Burger's contact model uses eight parameters to describe the contact relations between two microscopic particles, as indicated in Figure 9-9 and listed in Table 9-1. Being related to the micromechanical properties of the material, the calibration of these model parameters is not straightforward and their values cannot be obtained directly from the experimental results. Therefore, a macroscale Burger's model, as shown in Figure 9-9, will first be established to be correlated to the experimental dynamic modulus and the phase angle. The parameters of the macroscopic Burger's model can then be converted into the microscopic model parameters.

Table 9-1. Burger's model parameters denotations.

	Normal Stiffness	Normal Viscosity	Shear Stiffness	Shear Viscosity
Kelvin	K_{kn}	C_{kn}	K_{ks}	C_{ks}
Maxwell	K_{mn}	C_{mn}	K_{ms}	C_{ms}

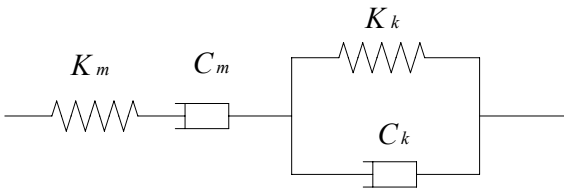

Figure 9-9. Macroscale mechanical entities of the Burger's model

When asphalt mixtures are subjected to dynamic stress $\sigma(t) = \sigma_0 e^{i\omega t}$, the resulting dynamic strain is described as $\varepsilon(t) = \varepsilon^* e^{i\omega t}$. Consequently, the complex compliance can be expressed using Equation (9.1)

$$D^*(\omega) = \frac{\varepsilon^*}{\sigma_0} = \frac{1}{K_m} + \frac{1}{i\omega C_m} + \frac{1}{K_k + i\omega C_k} \tag{9.1}$$

where, σand ε* are the stress and strain at time equals zero, ω is the radial frequency, and *t* is the elapsed time.

The complex compliance consists of real portion and imaginary portion, and is normally written as:

$$D^*(\omega) = D'(\omega) + iD''(\omega) \tag{9.2}$$

$$D'(\omega) = \frac{1}{K_m} + \frac{K_k}{K_k^2 + \omega^2 C_k^2} \tag{9.3}$$

$$D''(\omega) = \frac{1}{\omega C_m} + \frac{\omega C_k}{K_k^2 + \omega^2 C_k^2} \tag{9.4}$$

The dynamic compliance is determined as $\left|D^*\right| = \sqrt{\left(D'\right)^2 + \left(D''\right)^2}$. And the dynamic modulus $\left|E^*\right|$ is the reciprocals of the complex compliance, that is,

$$\left|E^*\right| = \frac{1}{\left|D^*\right|} = \frac{1}{\sqrt{\left(D'\right)^2 + \left(D''\right)^2}} = \frac{1}{\sqrt{\left(\frac{1}{K_m} + \frac{K_k}{K_k^2 + \omega^2 C_k^2}\right)^2 + \left(\frac{1}{\omega C_m} + \frac{\omega C_k}{K_k^2 + \omega^2 C_k^2}\right)^2}} \tag{9.5}$$

The phase angle δ can be expressed as:

$$\delta = \tan^{-1}\left(\frac{D''}{D'}\right) = \tan^{-1}\left(\frac{K_m}{\omega C_m}\frac{K_k^2 + \omega^2 C_k^2 + \omega^2 C_k C_m}{K_k^2 + \omega^2 C_k^2 + K_k K_m}\right) \tag{9.6}$$

Equations (9.1)-(9.6) describe the equations for determining the macroscale parameters of asphalt mixtures. Once the macroscale parameters are obtained, the microscale parameters can be obtained from the following equations:

$$K_{mn} = K_m L \qquad K_{ms} = K_m L/(1+\nu) \tag{9.7a}$$

$$C_{mn} = C_m L \qquad C_{ms} = C_m L/(1+\nu) \tag{9.7b}$$

$$K_{kn} = K_k L \qquad K_{ks} = K_k L/(1+\nu) \tag{9.7c}$$

$$C_{kn} = C_k L \qquad C_{ks} = C_k L/(1+\nu) \tag{9.7d}$$

where $L=R(A)+R(B)$, which is the sum of radius of two contact balls A and B. ν is the Poisson's ratio, which is set to 0.5 for asphalt mastic (Christensen et al. 1992).

The parameters of the macroscale Burger's model can be calibrated based on the following procedures. Theoretically, the stiffness and viscosity of the Maxwell model can be express as:

$$K_m = \lim_{\omega\to\infty}\left|E^*\right| \; C_m = \lim_{\omega\to 0}\left|\frac{E^*}{\omega}\right| \tag{9.8}$$

The actual range of frequency used in the experiments of this study is between 25Hz to 0.1Hz. Hence the stiffness and viscosity of the Maxwell model can be approximated using Equation (9.9).

$$K_m = \left|E^*\right|_{\omega=25} \; C_m = \left|\frac{E^*}{\omega}\right|_{\omega=0.1} \tag{9.9}$$

Substituting Equation (9.9) into Equations (9.5-9.6), the stiffness and viscosity for Kelvin model can be obtained. Finally, Equations (9.7a-d) can be used to determine the parameters for the microscopic Burger's contact model.

9.4 Experiment for Calibration

Complex modulus testing was conducted for one asphalt mixture with PG58-28 binder and basalt aggregate following the design gradation shown in Table 9-2. The test was performed using an asphalt mixture performance tester (AMPT). Two replication samples were compacted into 150mm in diameter and approximately 170mm in height using a Superpave gyratory compactor. The samples were cored and saw-cut into 100mm by 150mm specimens to achieve more uniform air voids distribution. The bulk specific gravities and air void contents for each test specimen were measured before and after the specimen were cored and cut, prior to dynamic modulus testing. The final air voids of the two testing samples were 6.7% and 7.0%, respectively, satisfying the specification requirement of 7.0±0.5%.

The complex modulus test was conducted according to AASHTO TP 79 (2011) at four temperatures (40, 70,100,130°F) and six frequencies (25, 10, 5, 1, 0.5, and 0.1 Hz.). The average experimental results of the two replicate samples are shown in Table 9-3.

Table 9-2. Experimental and simulation gradation information

Sieve Size (mm)	19.0	12.5	9.5	4.75	2.36	1.18	0.6	0.3	0.15	0.075
Percent Passing (%)	100	94	79	46	29	20	15	11	8	6.1

Table 9-3. Average complex modulus from experimental testing

Test Temp. (°C)	Frequency	Dynamic modulus (MPa)	Phase angle (Degrees)	Test Temp. (°C)	Frequency	Dynamic modulus (MPa)	Phase angle (Degrees)
40	25	13053	12.9	100	25	1269	39.6
40	10	11423	15.1	100	10	788	39.3
40	5	10135	17.0	100	5	521	39.5
40	1	7215	21.6	100	1	209	37.5
40	0.5	6201	23.9	100	0.5	155	35.4
40	0.1	3955	28.9	100	0.1	80	29.9
70	25	5036	28.9	130	25	458	33.5
70	10	3812	31.2	130	10	211	37.3
70	5	2920	33.1	130	5	131	38.0
70	1	1465	36.3	130	1	56	33.0
70	0.5	1056	36.6	130	0.5	45	30.1
70	0.1	472	36.0	130	0.1	32	23.8

9.5 DEM Simulation of Complex Modulus

Compressive sinusoidal dynamic loading was applied on the top and bottom walls from the opposite direction, while other directions of the top and bottom walls were fixed. Prior to the actual simulation, a small contact load was applied to ensure the loading plate had seated on the sample. For each simulation test at a specific temperature and frequency, totally 20 cycles were applied. The first 10 cycles were treated as conditioning loading and only the last 10 cycles were used for calculating the dynamic modulus and the phase angle.

Figure 9-10 presented the applied axial stress loading wave and the corresponding strain curve at 40^{o}F temperature and 1Hz frequency used in the DEM simulation. The corresponding stress-strain hysteresis loop for one loading cycle was plotted in Figure 9-11, and was compared with the experimental results. As shown, the simulation results reasonably described the viscoelastic behavior of the asphalt mixture and the hysteresis loop from the simulation matched fairly well with the experimental testing. Based on the simulation data, the dynamic modulus and the phase angle can be calculated using Equation (9.10).

$$\left|E^*\right| = \frac{\sigma_{\max} - \sigma_{\min}}{\varepsilon_{\max} - \varepsilon_{\min}} \quad \delta = \frac{\Delta t}{T} \cdot 360 \tag{9.10}$$

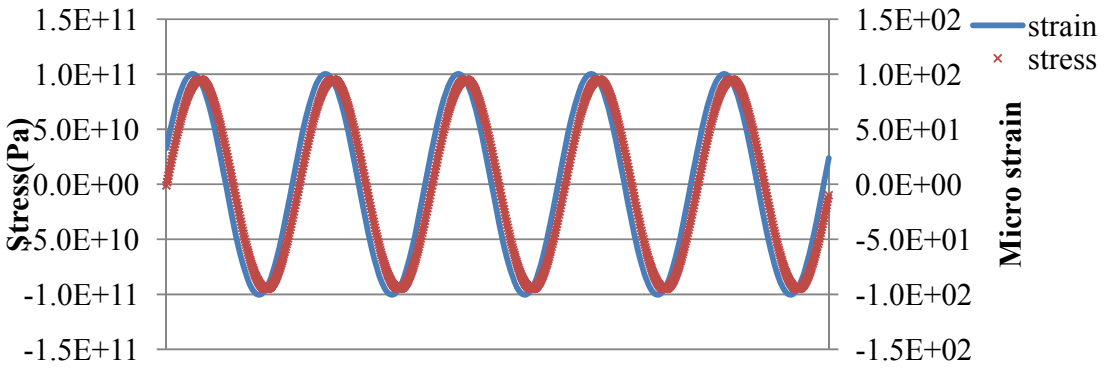

Figure 9-10. Applied stress and corresponding strain in DEM simulation

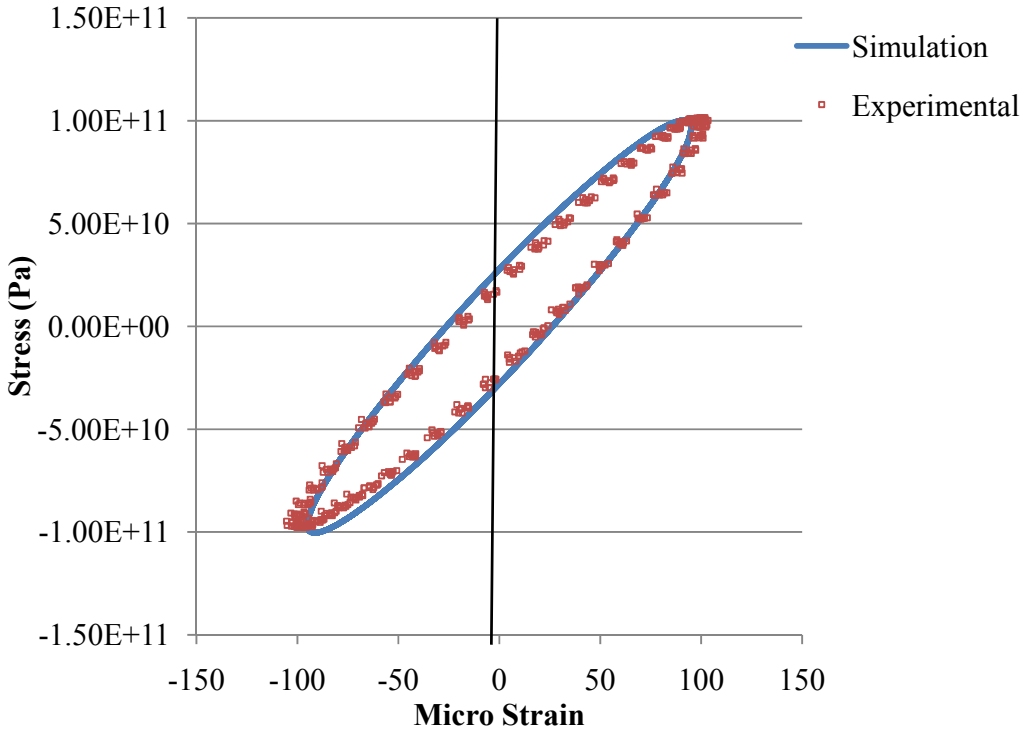

Figure 9-11. Comparison of stress-strain hysteresis loop between simulation results and experimental measurements.

where σ_{max}, σ_{min}, ε_{max} and ε_{min} are maximum and minimum values of the applied stress and responding strain. Δt equals to the time difference between two adjacent stress and strain, and T is loading time of one cycle.

Table 9-4. Calibrated Burger's model parameters (1Hz)

Temp. (^{o}F)	C_{nk}	C_{nm}	C_{sk}	C_{sm}	K_{nk}	K_{nm}	K_{sk}	K_{sm}
40	540140.1	540140.1	360093.4	360093.4	43351.9	43351.9	28901.3	28901.3
70	110613.4	110613.4	73742.3	73742.3	17772.7	17772.7	11848.5	11848.5
100	36024.8	36024.8	24016.5	24016.5	2290.9	2290.9	1527.3	1527.3
130	24347.7	24347.7	16231.8	16231.8	584.8	584.8	389.8	389.8

Four DEM simulation tests were conducted at one frequency of 1Hz and four temperatures (40, 70, 100, and 130^{o}F). Experimental testing results at the same temperature and frequency were used to calibrate the DEM models, and Equations (9.5)-(9.9) were used to determine the model parameters. The calibrated model parameters for the specific mixture were summarized in Table 9-4. The same set of model parameters at each temperature and 1Hz frequency was further used to determine the dynamic modulus at the same temperatures but other frequencies (25, 10, 5, 0.5, and 0.1Hz) for generating master curves. The prediction results were compared with the

measured dynamic modulus and phase angle from experimental testing to verify the effective of the model in predicting viscoelastic properties.

Figure 9-12(a) compared the dynamic modulus from the DEM simulation with the results obtained from the experiments for four temperatures and six frequencies. As shown, all data were located along the line-of-equality well, indicating good prediction of dynamic modulus had been achieved over a wide range of temperatures and frequencies. The comparison of the phase angles between the predicted and the measured values were presented in Figure 9-12(b). Taking into consideration of larger data variation of the experimental phase angle measurements, the prediction results of the phase angle for all four temperatures and six frequencies matched well with the experimental results. Although based on limited data verification, the viscoelastic DEM model used in this study showed good potential in predicting the complex modulus properties of the asphalt mixtures.

The master curves of the dynamic modulus and the phase angle for both the experimental results and the predicted results were also plotted in Figure 9-13. As shown, the master curve of the phase angle is nonlinear with a peak value at approximately 40 degree for both the experiments and the predictions. This finding is consistent with the literature (Rowe 2009). Instead of considering such nonlinear behavior of the phase angle master curve as due to the experimental error, we hypothesize it could be related to the

effect of aggregate contact and interlocking. At high temperatures and/or low frequencies, the asphalt binder is soft and flowable resulting in increased viscous behavior and hence increased phase angle. If the temperature continues increasing, the binder is softer and behaving more like a lubricant; the aggregate contact and interlocking could then become dominant in determining the viscoelastic properties of the mixture and result in reduced viscoelasticity of the mix. As an extreme case, at very high temperature when the asphalt is more like a low viscosity liquid, the granular aggregate structure will take the lead in supporting compressive dynamic load and thus the bulk property of the mixture will be more like an elastic granular material. In this case, the phase angle of the mixture should be more close to zero (pure elastic) rather than 90 degree (pure viscous).

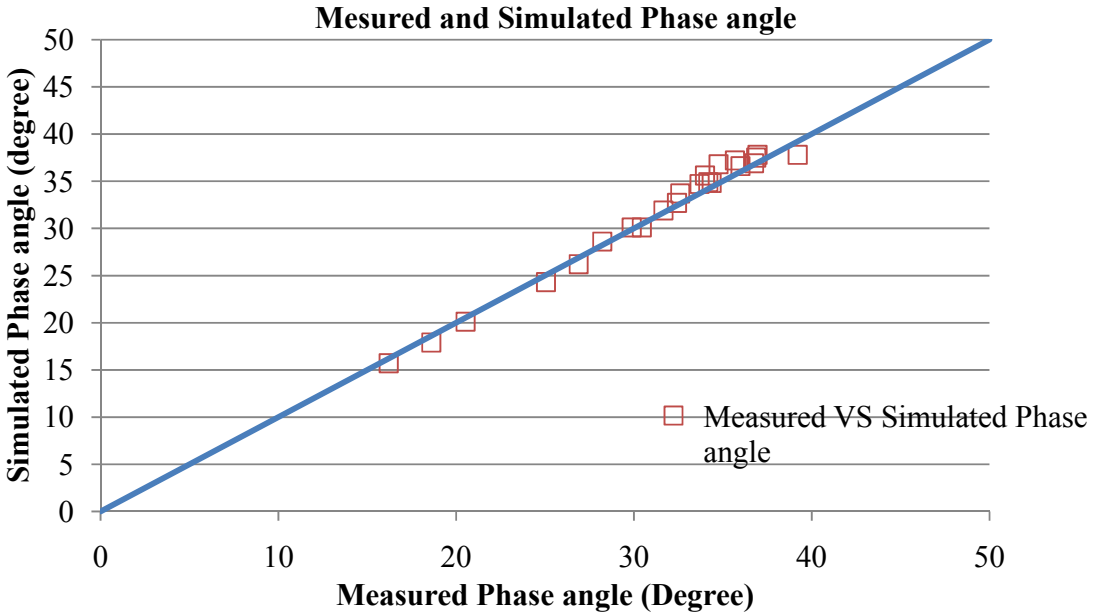

(a)

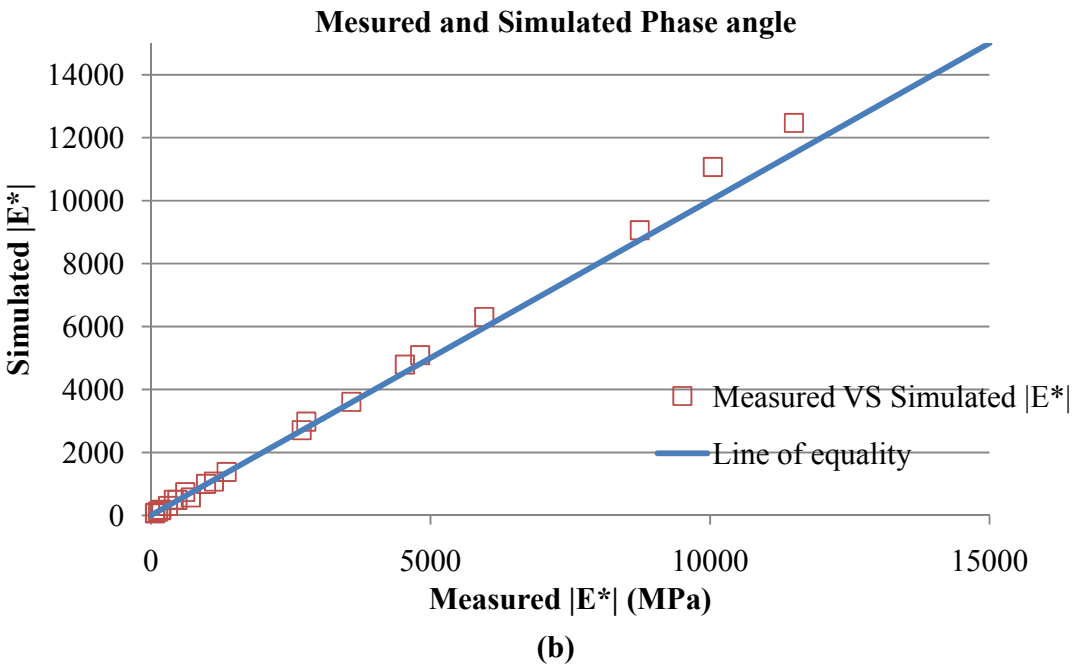

Figure 9-12. Line of equality plot to compare experimental results and DEM simulation results for (a) dynamic modulus; and (b) phase angle

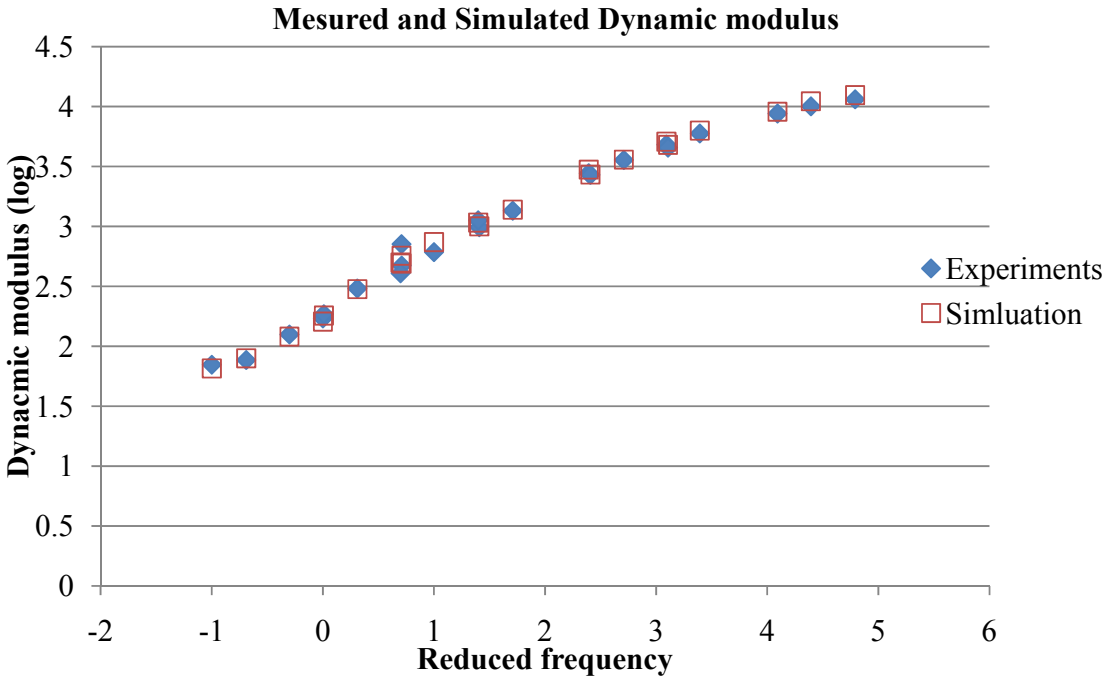

(a)

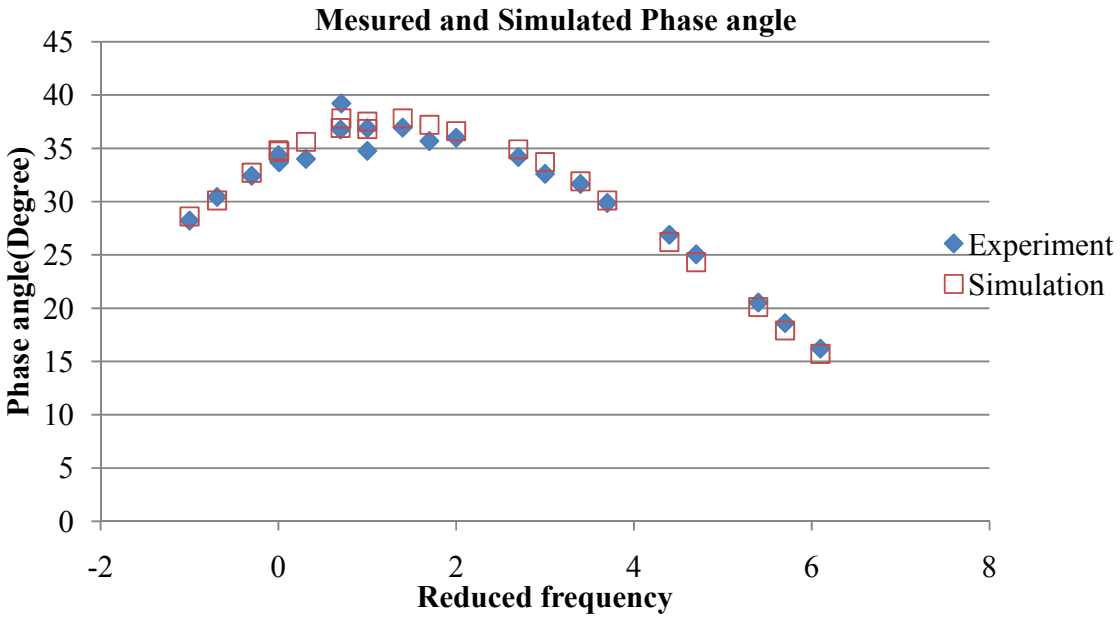

(b)

Figure 9-13. Master curves of experimental and DEM simulation results for (a)

dynamic modulus; and (b) phase angle

9.6 Sensitivity Analysis

9.6.1 *Sensitivity Analysis of Burger's Model parameters*

The microscale Burger's contact model used in the DEM simulation consists of eight parameters. Each parameter describes the specific mechanical properties of the material at contact and may have different contributions to the dynamic modulus and the phase angle. A sensitivity analysis is thus conducted to evaluate how the change of individual parameter while maintaining other parameters the same could affect the dynamic modulus and the phase angle, respectively. In addition, knowing the effect of each parameter on the complex modulus could facilitate the model calibration process so that appropriate values could be quickly assigned to specific model parameters. Because the normal stiffness and viscosity have direct relationship with the shear stiffness and the shear viscosity as shown in Equation (9.7), only the sensitivity of model parameters in normal direction (Cnk, Cnm, Knk, and Knm) is studied.

The base model used for the sensitivity analysis kept the values of all the parameters provided in Table 9-4 except the one that was to be changed. Figure 9-14 showed how the change of individual parameter over the specified range could influence both the dynamic modulus and the phase angle. As shown, compared to the Cnk, the Cnm had a

larger influence on the phase angle and the dynamic modulus, and the Knm was more sensitive to both the phase angle and the dynamic modulus than the Knk. It is interesting to note that there is a peak point in the relationship between the Cnk and the phase angle and between the Knk and the phase angle, indicating the effect of the Kelvin's model parameters (Cnk and Knk) on the phase angle is not linear. Recall the master curve of the phase angle is not linear as shown in Figure 9-13, this finding confirmed the hypothesis that the nonlinear behavior of the phase angle master curve is not simply due to the experimental error. The micromechanical contact behavior of the material, determined by the Kelvin's contact parameters, played a significant role in the nonlinear behavior of the phase angle especially at high temperatures and/or low frequencies.

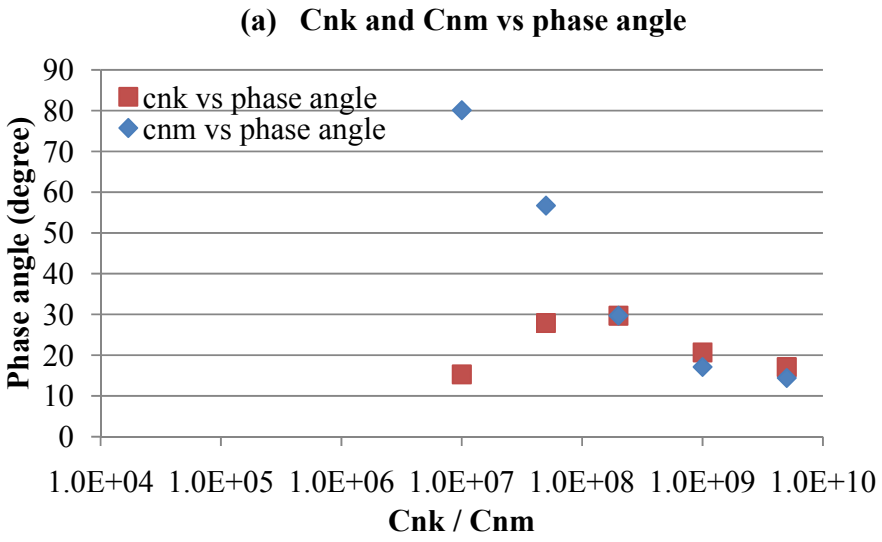

(b) Cnk and Cnm vs log(E)

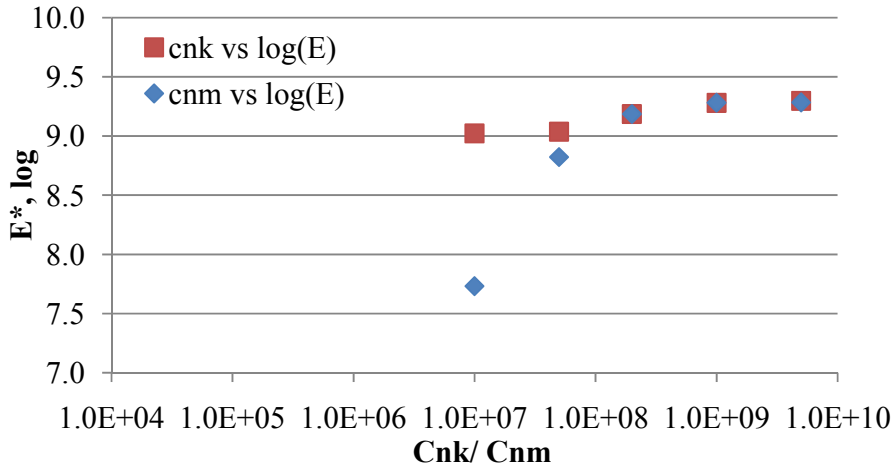

(c) Knk and Knm vs phase angle

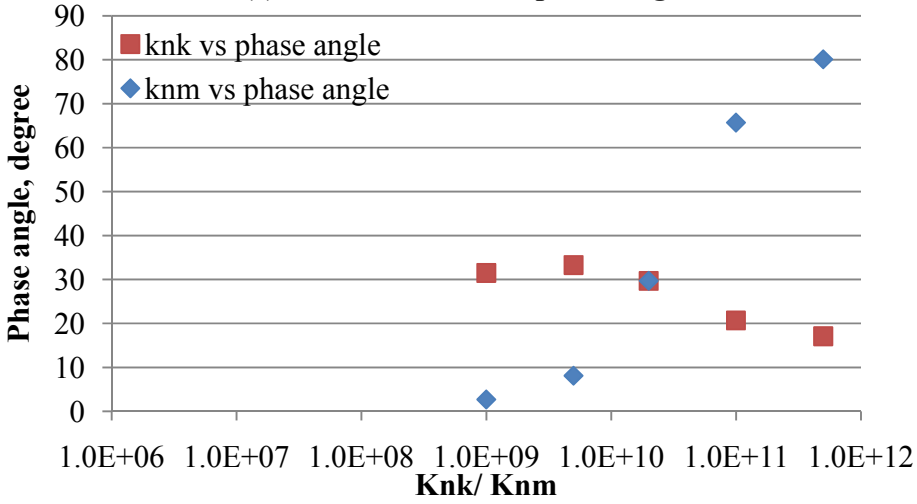

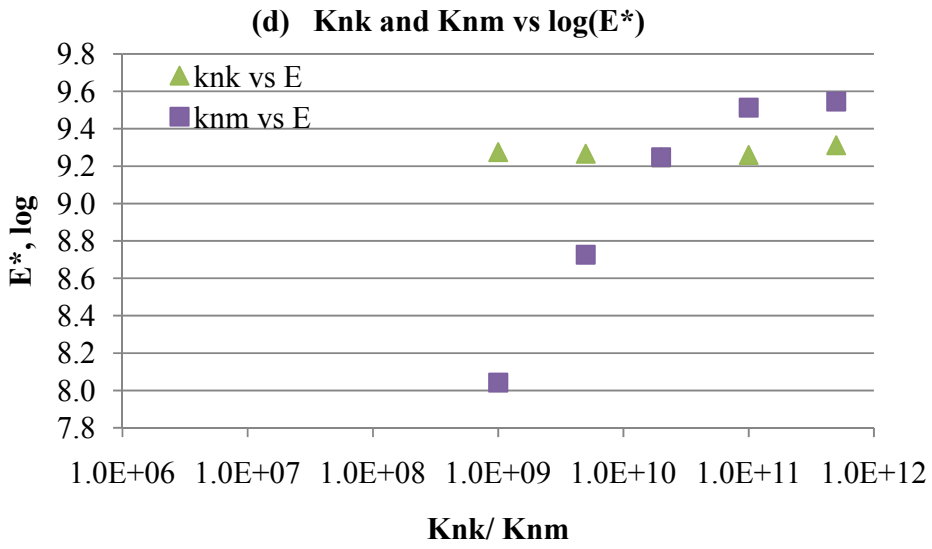

Figure 9-14. Sensitivity of Burger's model parameters on complex modulus

9.6.2 *Effects of friction coefficient on porosity of DEM model*

Studies (Shu and Huang 2008) show that the porosity of DEM model will influence the simulation results; hence it is necessary to select an appropriate friction coefficient to get the desired porosity of DEM model. In order to study the effects of friction coefficient on the porosity of DEM model, six models with different friction coefficient (0, 0.2, 0.4, 0.6, 0.8, 1) were generated separately, Figure 9-15 shows the relation between friction and porosity, as shown in the figure, a well linear relation shows the relation between friction and porosity in this model, and a higher friction will reduce a higher porosity.

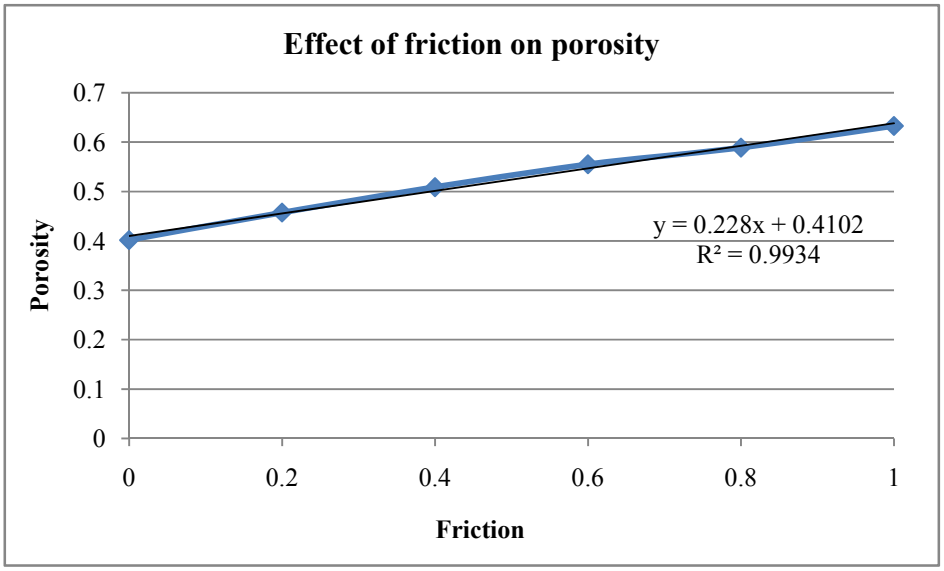

Figure 9-15. The relation between friction coefficient and porosity

9.6.3 *Impact of particles with different sizes and proportions on dynamic modulus*

The effect of different particle sizes and proportions on dynamic modulus is further evaluated in this study. As shown in Figure 9-16 for the C-4 mixture, by increasing 10% of the percent of aggregates passing 2.36mm sieve from the basic C-1 gradation, we reached the largest dynamic modulus increase. Similarly, the C-3 mixture with 10% increase of the percent of aggregates passing 4.75mm sieve is the second highest in dynamic modulus, followed by the C-2 mixture with 10% decrease of the percent passing in 9.5mm sieve. Of all the four mixes, the C-1 base gradation gives the lowest dynamic modulus results.

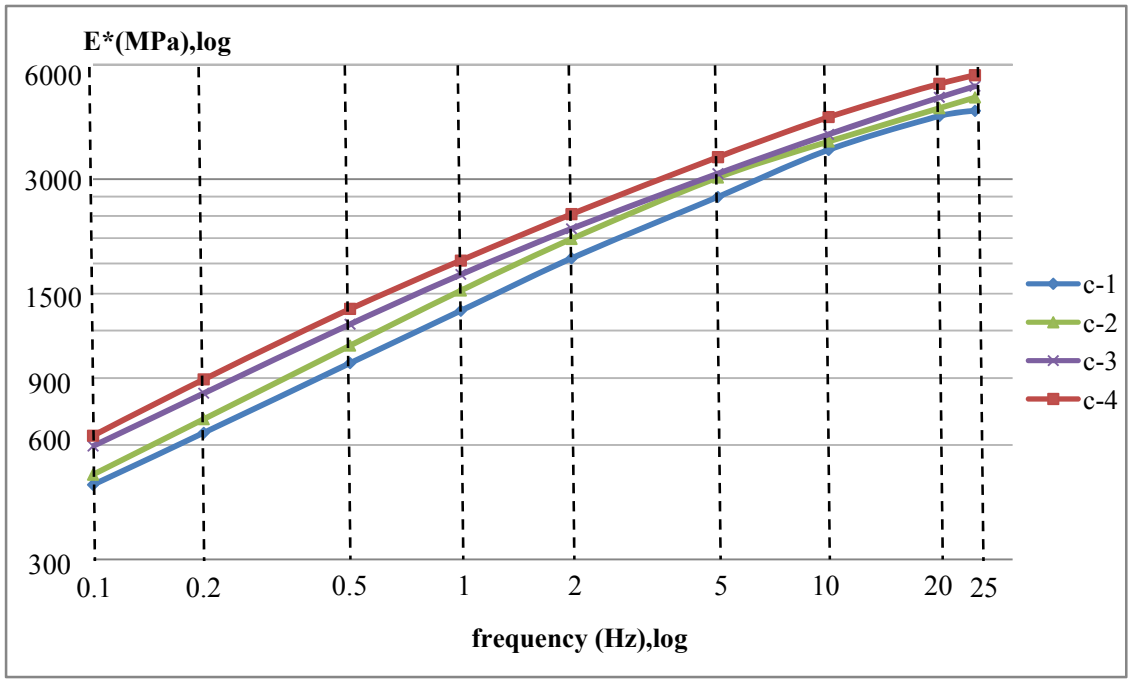

Figure 9-16. Dynamic modulus of four gradations

9.6.4 *Impact of angularity on dynamic modulus*

Based on the successfully developed 3D DEM model, we are able to study the influence of aggregate angularity on dynamic modulus. Using the same C-1 mixture gradation but replacing all particles with different AI properties, different dynamic modulus values at 70^{o}F temperature and 1Hz frequency are obtained, and the results are plotted in Figure 9-17. The first column shows the experimental dynamic modulus of mixture, while other columns show the simulation result.

The dynamic modulus is a combination effect of many factors. When only aggregate

morphology is studied, the result clearly shows that with the increase of angularity, the dynamic modulus also presents an increasing trend. This simulation result is comparable with experimental experiment by Pan (2006), which observed that coarse aggregates with more irregular morphologies will improve the resilient modulus of the asphalt mixture. These findings indicate the importance of particle angularity on forming a stable structure, which can be beneficial to reach a strong skeleton with higher dynamic modulus.

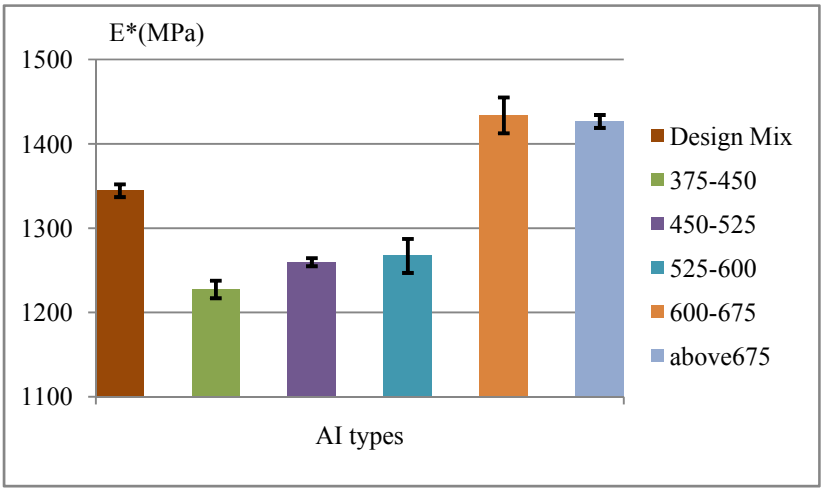

Figure 9-17. Dynamic modulus VS. AI type

9.7DEM SIMULATION OF STRENGTH TESTS

9.7.1 *Experimental Program for Strength Tests*

In order to develop a valid constitutive or simulation model, the selection of a

standardized and reasonable testing procedure is also very critical for the calibration of model parameters (Sousa and Weissman 1995; Masad and Little 2003). Lytton (2000) and Cela(2002) have shown that the strength test is one of the most suitable testing method for its relative simplicity and accuracy compared to other tests. In addition, the damage in a strength test is induced by a state of shear action which is believed to be the main state of stress that causes rutting in asphalt pavements (1997).

Uniaxial compression tests were conducted in this study to determine the failure strength of the mix at different loading conditions, so that constitutive properties of asphalt mixtures can be deducted from the experimental results for the calibration and verification of the DEM model. Standard Washington mix was used with PG58-28 asphalt binder and basalt aggregate following the design gradation shown in Table 9-5. Tests were performed using a servo-hydraulic material testing system (MTS) testing machine under controlled temperatures of 100^{o}F and 130^{o}F, respectively. A monotonic constant compressive loading rate of 50mm/min was applied until the load reduced to 50% of the peak load. By the end of the test, the samples were completely damaged.

Samples were compacted into 150mm in diameter and approximately 170mm in height using a Superpave gyratory compactor. The samples were cored and saw-cut into 100mm by 150mm specimens to achieve more uniform air voids distribution. The bulk specific gravities and air void contents for each test specimen were measured before and

after the specimen were cored and cut, prior to dynamic modulus testing. The target air void of the specimens is 7% and the compacted air voids of two samples are 6.8% and 6.7% respectively.

Table 9-5. Experimental and simulation gradation information

Sieve Size (mm)	19.0	12.5	9.5	4.75	2.36	1.18	0.6	0.3	0.15	0.075
Percent Passing (%)	100	94	79	46	29	20	15	11	8	6.1

9.7.2 *Displacement Softening Model*

The constitutive behavior of a material is simulated in DEM by associating a contact model with each contact. There are several models available in PFC3D DEM software. Previous study showed that a linear contact model with parallel bonding can simulate the dynamic modulus well, but is insufficient to simulate the phase angle which requires considering the viscous behavior of asphalt mixture (Yu and Shen 2012). A viscoelastic Burger's model was successfully used to characterize the dynamic modulus and phase angle properties within linear viscoelastic range. It is found in our study to be unable to catch the nonlinear viscoelastic-plastic behavior especially when damage is involved. A displacement softening model, which has the capability of capturing strength deterioration as a resultant effect of damage accumulation, is thus used.

The displacement-softening model provides bonded behavior in which the strength is reduced as a function of applied displacement. If the contact is under tension, the contact strength F_{max} is calculated from the two strength parameters (i.e., F_{nc} and F_{sc}) as a function of the current orientation of the contact force. It is assumed that contact strength varies as a linear function of the angle α.

$$F_{\max} = (1 - \frac{2\alpha}{\pi}) \cdot F_c^n + \frac{2\alpha}{\pi} \cdot F_c^s \tag{9.10}$$

where α is the angle between the directions of the contact force and the line segment connecting the centers of the balls.

The yielding of the bond in tension is determined by comparing the resultant contact force with the contact strength. The contact yields if the contact force is larger than the contact strength. In the case of yielding of contact bonds, the increment of contact displacements, Uk (k = n, s), can be decomposed into elastic and plastic contact displacement increments:

$$\Delta U^k = \Delta U_e^k + \Delta U_p^k \tag{9.11}$$

The force increment, F_k, is a function of the increment of the elastic displacement only

$$\Delta F^k = K^k \Delta U_e^k \tag{9.12}$$

Where,

$$\Delta U_e^k = \Delta U^k - \Delta U_p^k \tag{9.13}$$

The increment of the plastic displacements obeys the flow rule. It is assumed that, if the normal force is tensile, the plastic displacement increment is always in the direction of the resultant contact force:

$$\Delta U_p^k = \Delta\lambda \frac{F^k}{F} \tag{9.14}$$

Where $\Delta\lambda$ is the plastic multiplier.

If the normal contact force is compressive, the maximum contact shear force is defined by the slip condition:

$$F_{\max}^s = \mu |F^n| + F_c^s \tag{9.15}$$

If slip takes place, the plastic shear displacement is assumed to be in the direction of the shear force, and the contact strengths are functions of the accumulated plastic displacements.

$$F_c^k(U_p/U_{p\max}) = F_c^k \left(1 - \frac{U_p}{U_{p\max}}\right) \tag{9.16}$$

9.7.3 *Comparison of simulation and experimental results*

The basic stress-strain relationships obtained from the strength tests are compared with the simulation results as shown in Figure 9-18. It is observed that the simulated stress-strain curves are corresponding well with the experimental data until the sample experience exclusive dilation. The small tail for the simulation results as seen in Figure

9-18 could be attributed to the effect of lateral confinement. In the laboratory experiment, no confinement was applied to the sample while in the simulation a very small confinement was used in order to set the boundary and prevent particles flying out.

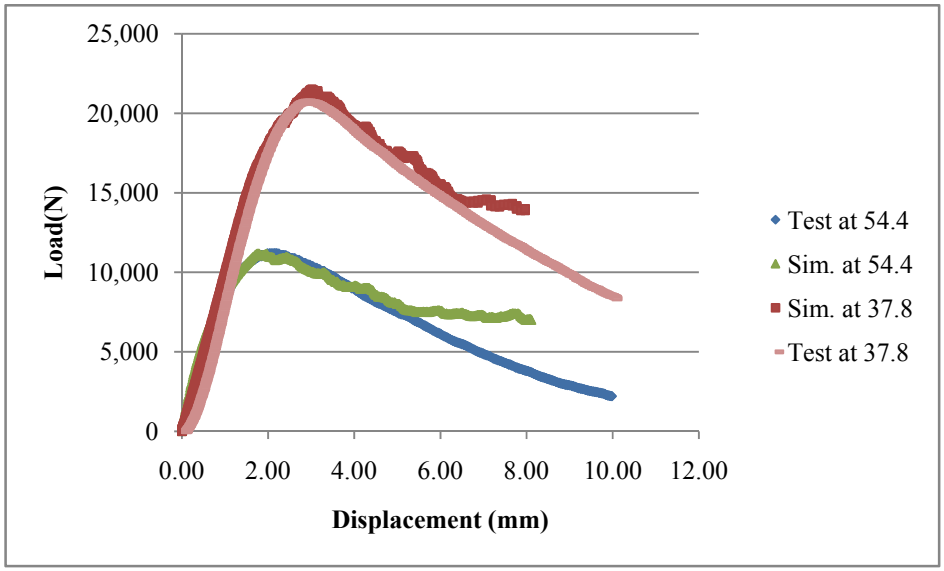

Figure 9-18. Comparison of simulation and experimental results

9.7.4 *Impact of angularity on strength test of asphalt mixture*

Based on the successfully developed 3D DEM model, we are able to study the influence of aggregate angularity on the strength test. Using the same mixture gradation but replacing all particles with different AI properties, different strength responding at 100°F and 130°F temperature is obtained, and the results are plotted in Figure 9-19. The compressive strength of asphalt mixture is a combination effect of many factors. When

only aggregate morphology is studied, the result clearly shows that with the increase of angularity, the higher the compressive strength will behave. Also, the impact of angularity on dynamic modulus also show similar trend (Yu and Shen 2012), and which is comparable with experimental experiment by Pan (2006), which observed that coarse aggregates with more irregular morphologies will improve the resilient modulus of the asphalt mixture. These findings in Figure 9-19 dictate the importance of particle angularity on forming a stable structure, which can be beneficial to reach a strong skeleton with higher dynamic modulus.

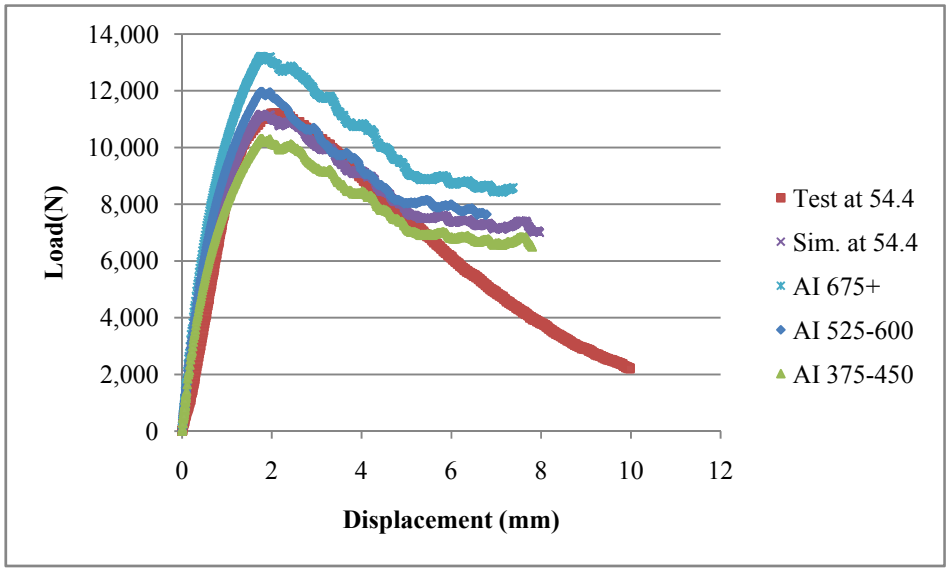

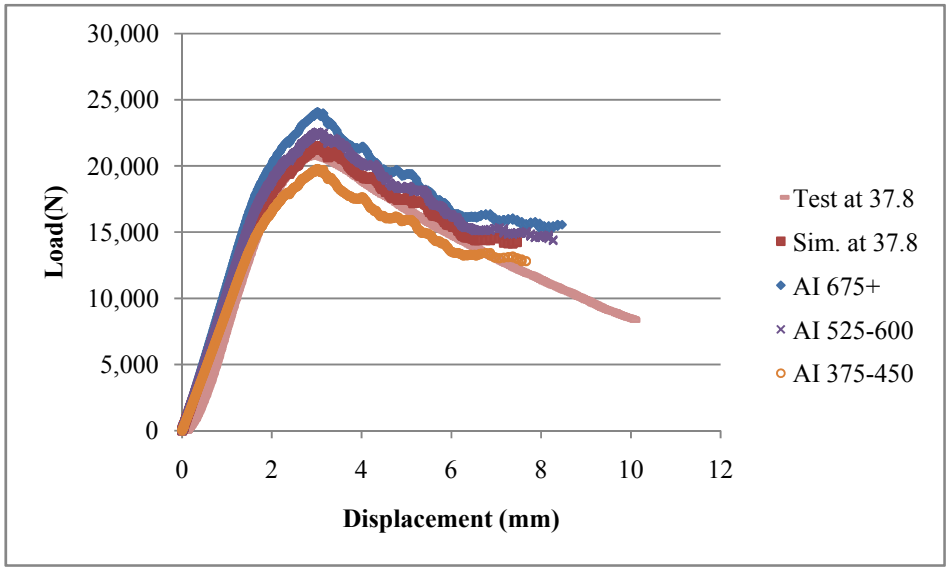

Figure 9-19. The effects of angularity index on strength tests

9.7.5 *Impact of loading rate on strength of asphalt mixture*

Since the rate of loading affects the deformation behavior and performance of asphalt concrete which can then be characterized by strength test, this study conducted a set of experiments to study the effects of loading on the strength of asphalt mixture. Three different loading rates were conducted at a strain controlled strength tests. The three levels of loading rate are 10mm/min, 50mm/min and 100mm/min separately. As shown in Table 9-6. Following results are be drawn from the simulation results,

1. The loading rate have an influence on the strength of asphalt mixture, with the increase of loading rate, the strength is increasing.

2. The influence of loading rate on the strength of asphalt mixture is different, the influence of loading rate are higher at high temperature compared to low temperature. The strength increased by 32.5% from 10mm/min to 100mm/min at 54.4°C, and increased by 12.9% from 10mm/min to 100mm/min at 37.8°C.

Table 9-6. The influence of loading rate on maximum strength

	Testing Temp. 54.4			Testing Temp. 37.8		
Loading Rate(mm/min)	10	50	100	10	50	100
Maximum Strength(N)	9276	11176	12294	19995	21500	22575

9.8 SUMMARY

This section described a micromechanical discrete element modeling method to simulate the mechanical of asphalt mixtures, and the complex modulus and strength properties of asphalt mixtures are simulated. An aggregate library for DEM with six representative particles covering a wide range of aggregate shape and angularity index was established. These particles were generated by clumping small number of spherical balls to represent the 3D images of real aggregate particles scanned by the University of Illinois Aggregate Image Analyzer (UIAIA). This method significantly reduced the number of balls needed while still maintaining adequate accuracy for considering the particle angularity impact.

The model was found to be successful in predicting both the dynamic modulus and the phase angle over a wide range of temperatures and frequencies. The effect of the key model parameters on the dynamic modulus and the phase angle were evaluated. It was found that the effect of the Kelvin's model parameters (Cnk and Knk) on the phase angle was not linear. This finding further confirmed that the micromechanical contact behavior of the material, determined by the Kelvin's contact parameters, played a significant role in the nonlinear behavior of the phase angle especially at high temperatures and/or low frequencies. The overall findings from the sensitivity analysis of the model parameters provided meaningful guidance for the fundamental understanding of the material mechanical properties and the selection of model parameters for other mixtures.

This section also presented a modeling to characterize the asphalt mixture's resistance to heavy traffic load. Displacement softening model was successfully implemented to describe the visco-elastic-plastic behavior of asphalt mixtures and thus capture the damage properties under heavy load. It was found the developed 3D DEM model can predict the compressive strength of asphalt mixtures under different loading conditions well. Based on simulation results, particle angularity has important impact on the compressive strength of asphalt mixture. Highly crushed angular aggregates can provide better resistance to heavy loads especially at high temperatures. Loading rates also have an influence on the strength of asphalt mixture, the influence of loading rate are

higher at high temperature compared to lower temperature. Based on both the experimental results and the predictions from the modeling, it was found that the master curve of the phase angle is not linear, with a peak value of 40degree for the specific mixture studied. It is hypothesized that such nonlinearity of the phase angle master curve is related to the aggregate contact and interlocking. At very high temperatures, the binder behaves more like a lubricant; the aggregate contact and interlocking are responsible for supporting the compressive dynamic loading used in a dynamic modulus test hence reducing the viscoelasticity of the mix.

CHAPTER 10 NONLINEAR ELASTO-VISCO-PLASTIC MODEL FOR RUTTING OF ASPHALT MIXTURES

10.1 INTRODUCTION

Asphalt mixture is a composite particulate material that consists of aggregates, asphalt binder, and voids. The complex interactions among these constituents results in a wide spectrum of distresses of this material including pavement rutting, thermal cracking, and fatigue cracking. When the pavement is under rutting, the pavement undergoes longitudinal depressions as well as upheavals toward the edges, resulting in loss of load carrying capacity. Consequently, pavement will be susceptible to moisture damage and fatigue cracking. Studies have shown that in well-compacted pavements, the most primary rutting mechanism is shear deformation because the densification under the wheel is insignificant (Eisenmann and Hilmer, 1987). In order to provide a fundamental analysis to the mechanics of the rutting of asphalt pavement, the constitutive characterization and modeling of the asphalt material is needed.

The properties of asphalt mixture highly depend on the spatial distribution of the granular particles, the associated air voids, and the cracks induced during deformation (e.g. Oda and Nakayama, 1989; Kuo and Frost, 1995; Li and Dafalias, 2002; Wang et al., 2003).

Granular materials exhibit anisotropic microstructure distribution (e.g. Tobita, 1989; Oda and Nakayama, 1989). This anisotropic distribution is one of the fundamental features that need to be incorporated in the constitutive modeling of such particulate materials (Gutierrez et al., 1991). In addition, as the material deforms, microcracks nucleate and grow causing degradation in its strength. The knowledge of the spatial distribution of these discontinuities is crucial to predict the macroscopic behavior of the material (Maire et al., 2001).

Advances in constitutive modeling of asphalt mixture have been reported by a number of researchers. Eisenmann and Hilmer(1987) proposed a model for rutting in asphalt mixture, however, this model assumed that rutting is caused by a reduction of air voids and with little consideration of the lateral movement of material. Sousa et al (1993) developed a nonlinear elastic-viscous model with damage parameters incorporated to predict rutting. Subsequently, Sousa and Weissman (1994) revised the elastic-viscous formulas by adding a plastic component. Lytton et al. (1993) developed a permanent deformation model for HMA using the associated plasticity model of Vermeer (1984).

Defects in the form of air voids and cracks exist initially in most geomaterials including asphalt mixture. The growth and coalescence of these defects within the microstructure decrease the load-carrying capacity of asphalt mixture leading ultimately to failure. Sousa et al. (1993) have noted that adding a damage component to a

permanent deformation model significantly improves its ability to predict the experimental measurements. Other researchers (Tashman et al. 2004, Masad et al. 2004) have also shown that use of a damage parameter is essential that significantly improved the prediction results of constitutive model. These studies have used a scalar measure that represents the area fraction of air voids and cracks to represent damage evolution. However, the damage is directional in nature and as such it is necessary to include tensor measures to properly account for its evolution (Wang et al., 2003). We propose direction dependent damage parameters in the proposed constitutive model.

The time dependent deformation of asphalt mixture is often modeled by decomposing the total strain into elastic, plastic, and visco-plastic components. Most past models have used linear elastic model in the calculation of elastic component. However, studies have shown that elastic component is highly nonlinear (Bahuguna et al. 2006). These authors have proposed a hyper elastic model to capture nonlinearity. We propose similar but physically more robust model here.

The plastic component of the strain decomposition requires the choice of yield surface that separates plastic and elastic domain. Researchers have used either the Mohr-coulomb or the Drucker-Prager yield criterion for this purpose (e.g. Tashman et al. 2005). The Drucker-Prager criterion assumes equal values in extension and compression yield which is not the case for geomaterials (Bishop, 1971). In this sense, Mohr-coulomb model is a

better choice but it is wrought with problems of corner discontinuities. We propose to the model proposed by Matsuoka-Nakai which is based on the concept of spatially mobilized planes and envelops the Mohr-coulomb surface with a smooth curve.

Following conventional practice we use the Perzyna's theory to model the visco-plastic component with the Matusoka-Nakai function as the choice of the yield function. All of the basic elements of the model are enhanced with the use of the vector magnitude first proposed by Curray (1956) to represent the directional distribution of angular particles.

10.2 NONLINEAR ELASTIC MODEL

Equation (10.1) describes the nonlinear stress-strain relation of a hyperelastic or Green elastic material, where Ω is the elastic strain energy density function. Equation (10.2) is the general expression of Ω for an elastic material (Chen and Han, 1988):

$$\varepsilon_{ij} = \frac{\partial \Omega}{\partial \sigma_{ij}} \tag{10.1}$$

$$d\Omega = \frac{I_1 dI_1}{9B} + \frac{dJ_2}{2G} \tag{10.2}$$

where I_1 is the first invariant of the stress tensor,

$$I_1 = \sigma_1 + \sigma_2 + \sigma_3 \tag{10.3}$$

J_2 is the second invariant of the deviatoric stress tensor,

$$J_2 = \frac{1}{2}\left(s_x^2 + s_y^2 + s_z^2 + 2s_{yz}^2 + 2s_{xz}^2 + 2s_{xy}^2\right) \tag{10.4}$$

B is the bulk modulus,

$$B = \frac{E}{3(1-2v)} \tag{10.5}$$

G is the shear modulus,

$$G = \frac{E}{2(1+v)} \tag{10.6}$$

The deviatoric stresses in Eq. (10.4) are given by:

$$s_x = \sigma_x - (1/3)I_1 = 1/3\left[(\sigma_x - \sigma_y) + (\sigma_x - \sigma_z)\right] \tag{10.7a}$$

$$s_y = \sigma_y - (1/3)I_1 = 1/3\left[(\sigma_y - \sigma_x) + (\sigma_y - \sigma_z)\right] \tag{10.7b}$$

$$s_z = \sigma_z - (1/3)I_1 = 1/3\left[(\sigma_z - \sigma_y) + (\sigma_z - \sigma_x)\right] \tag{10.7c}$$

and,

$$s_{yz} = \tau_{yz}\,, s_{zx} = \tau_{zx}\,, s_{xy} = \tau_{xy} \tag{10.7d,e,f}$$

And v is the Poisson's ratio, E is the Young's modulus,

From Equation (10.2), following equations can be obtained,

$$\frac{\partial \Omega}{\partial I_1} = \frac{I_1}{9B} \tag{10.8}$$

$$\frac{\partial \Omega}{\partial \sqrt{J_2}} = \frac{\sqrt{J_2}}{G} \tag{10.9}$$

In addition:

$$\frac{\partial^2 \Omega}{\partial I_1 \partial \sqrt{J_2}} = \frac{\partial^2 \Omega}{\partial \sqrt{J_2} \partial I_1} \tag{10.10}$$

Substituting Equations (10.8) and (10.9) into (10.10), results in:

$$\frac{I_1}{9B} \frac{\partial \Omega}{\partial \sqrt{J_2}} = \frac{\sqrt{J_2}}{G} \frac{\partial \Omega}{\partial I_1} \tag{10.11}$$

Substituting Equations (10.5) and (10.6) into (10.11), leads to:

$$\frac{I_1}{9B} \frac{1}{\sqrt{J_2}} \frac{\partial E}{\partial \sqrt{J_2}} = \frac{9B}{I_1 G} \frac{\partial E}{\partial I_1} \tag{10.12}$$

It is noted that Equation (10.12) satisfies the principle of energy conservation. Energy is neither generated nor dissipated in a closed-loop stress or strain paths. Lade and Nelson (1987) developed a nonlinear isotropic model which satisfied Equation (10.12) as:

$$E = M p_a \left[\left(\frac{I_1}{p_a} \right)^2 + R \frac{J_2}{p_a^2} \right]^{\lambda} \tag{10.13}$$

Where,

$$R = \frac{9B}{G} = \frac{6(1+v)}{1-2v} \tag{10.14}$$

p_a is the atmospheric pressure. The magnitude of E is actually determined by dimensionless constants M and λ. Material parameters M and λ can be determined by applying the least square error method for the predicted and experimental results. Both triaxial compression tests and three-dimensional cubical triaxial tests with various stress paths can be used to determine the model parameters (Lade and Nelson, 1987).

10.3 VISCOPLASTIC MODEL INCORPORATING ANISOTROPY AND DAMAGE

10.3.1 *Viscoplastic Model*

The loading surface (yield surface), the hardening rule, and the flow rule are the three key components that need to carefully chosen in the modeling of plastic as well as viscoplastic material. The loading surface is defined the boundary of the elastic range of an elastic-plastic material. The hardening rule describes the rule for the evolution of the subsequent yield surfaces or loading surfaces in the course of plastic flow. The flow rule describes the rule for the evolution of the subsequent loading surface or yield surface which connects the plastic strain increment with the stress and the stress increment.

In this model, the loading surface equation is similar to the extended Matsuoka–Nakai (E-M-N) criterion (Matsuoka and Nakai, 1974; Griffith, 2009) shown below.

$$\frac{I_1' I_2'}{I_3'} = K_{mn} \tag{10.15}$$

Or

$$f = \frac{I_1' I_2'}{I_3'} - K_{mn} \tag{10.16}$$

where,

$$K_{mn} = \frac{9 - \sin^2 \phi}{1 - \sin^2 \phi} \tag{10.17}$$

And $I_1^{'}, I_2^{'}$ and $I_3^{'}$ are the invariants of the modified stress tensors shifted as shown below:

$$\sigma^{'} = \sigma + \sigma_0 \tag{10.18}$$

where,

$$\sigma_0 = \text{-}c \cot \phi \tag{10.19}$$

where ϕ is the friction angle.

It is noted that the E-M-N criterion reduces to the von-Mises criterion when $\sigma_0 \to \infty$ or when $\phi = 0$ and $c \neq 0$. As shown in Figure 10-1, E-M-N envelops Mohr-Coulomb (M-C) and coincides at all apexes corresponding to triaxial extension and compression.

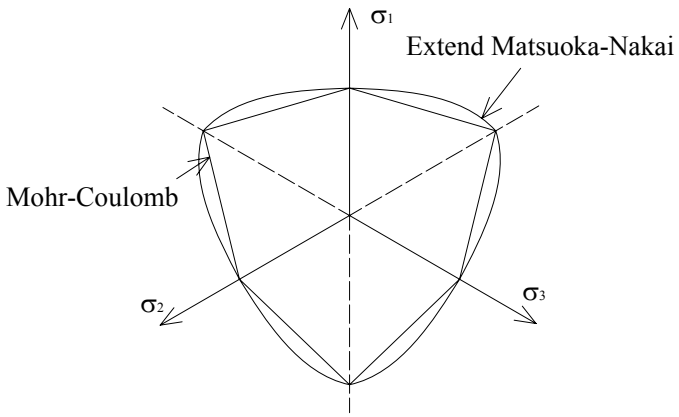

Figure 10-1.Comparison of M-C and E-M-N criteria.

Using Perzyna's viscoplasticity flow rule formulation, the viscoplastic strain rate is defined as:

$$\dot{\varepsilon}^{vp} = \left(\frac{\langle f \rangle}{\eta} \right)^m \frac{1}{\left(x + k^l \right)} v \tag{10.20}$$

Where f is the loading surface, η the temperature dependent viscosity parameter, k is the hardening variable and x, l, and m are parameters, v is the normal to the viscoplastic potential which is expressed as

$$v = \frac{\partial \Psi}{\partial \sigma} \tag{10.22}$$

The Macauley bracket operator $\langle f \rangle$ is defined as

$$\langle f \rangle = \begin{cases} 0, & f \le 0 \\ f, & f > 0 \end{cases} \tag{10.21}$$

If Ψ is the same as loading surface equation, the resulting viscoplastic strain will be normal to f and follow the associated flow rule (AFR). However, AFR has the disadvantage of predicting excessive plastic dilation (Vermeer 1984) which is not common in asphalt mixtures. In order to avoid the material experiences excessive dilation, a non-associated flow rule is used in this study. The non-associated flow rule defines the strain increments occur normal to a potential surface g, where $g \neq f$. For the visco-plastic potential, the Drucker-Prager form is chosen:

$$\Psi = \alpha I_1 + \sqrt{J_2} \tag{10.23}$$

Where, α is a material parameter.

$$\text{So}, \nu = \frac{\partial \Psi}{\partial \sigma_{ij}} = \alpha \delta ij + \frac{s_{ij}}{2\sqrt{J_2}} \tag{10.24}$$

Where, α is a material parameter.

10.3.2 *Damage Model*

Damage parameters are needed to characterize the progressive deterioration of mixtures under loading. In order to describe the damage accumulation in an isotropic material, Kachanov(1986) introduced a scalar function $\omega(\sigma_{ij}, \varepsilon_{ij}, \dot{\varepsilon}_{ij}, T)$. $\omega = 0$ for undamaged material and it increases with accumulation of damage. Panoskaltsis and Panneerselvam (2005) adopted this damage scalar ω into their model of asphalt mixture, in which, the damage scalar ω is defined as,

$$\omega = \frac{A_d}{A}; \quad 0 \le \omega \le 1, \tag{10.25}$$

where A_d is the damaged area and A is the original undamaged area.

Accordingly, the effective stress is given by:

$$\sigma_a = \frac{\sigma}{1-\omega}, \tag{10.26}$$

where σ is the nominal stress.

The asphalt mixtures are anisotropic and with increase in plastic deformation, the need to account for multiaxiality of damage and its evolution becomes more important. To address these concerns, researchers (Murakami, 1988; Kachanov, 1992; Karihaloo

and Fu, 1990) have introduced a second-order or fourth order tensor damage parameters. The second-order symmetrical damage tensor defined by Murakami (1988) is a generalization of the classical Kachanov's damage theory for direction dependence as shown:

$$\omega_i = \left(\frac{A_d}{A} \right)_{n_i} \tag{10.27}$$

where n_i is the principal direction.

Using the above formulation, the damage at any other plane inclined to the principal direction can be defined as:

$$\omega_n = \omega_{ij} n_i n_j \tag{10.28}$$

The damage tensor ω_{ij} has three real principal values ω_i and the corresponding principal directions n_i. For asphalt mixtures, the principal stress with damage tensor incorporated can be modified as:

$$\sigma_1^e = \frac{\sigma_1}{1-\omega_1} \tag{10.29a}$$

$$\sigma_2^e = \frac{\sigma_2}{1-\omega_2} \tag{10.29b}$$

$$\sigma_3^e = \frac{\sigma_3}{1-\omega_3} \tag{10.29c}$$

For cylindrical axisymmetric asphalt specimens, we have $\omega_2 = \omega_3$. Incorporating the direction dependent damage the modified extended Matsuoka–Nakai (E-M-N) criterion

becomes:

$$f^e = \frac{I_1^e I_2^e}{I_3^e} - K_{mn} \tag{10.30}$$

Following the work of Panoskaltsis and Panneerselvam(2005), the damage variable ω is assumed to be a function of the total viscoplastic strain:

$$\omega_1 = d_{11} + d_{12}\left(\varepsilon^{vp}\right)^{d_{13}} \tag{10.31a}$$

$$\omega_2 = d_{21} + d_{22}\left(\varepsilon^{vp}\right)^{d_{23}} \tag{10.31b}$$

whered_{11}, d_{12} ,d_{13}, d_{21} ,d_{22}, and d_{23} are parameters.

10.3.3 *Directional Distribution of Aggregates (Anisotropy) Model*

A fabric tensor F_{ij} for three-dimensional assemblies of aggregates is widely used as an index showing the anisotropy due to the preferred orientation of constituent particles. In general, the components of the microstructure tensor can be determined using three-dimensional measurements of particle distribution (Pietruszczak and Krucinski 1989; Muhunthan et al. 1996). Unfortunately, this is a laborious process and researchers have resorted to using two-dimensional measurements as followed in material science and extending it to obtain the components of F_{ij}. In this regard, the contribution by Oda and Nakayama (1989) in extending the work on vector magnitude by Curray (1956) is particularly valuable.

Curray defined the vector magnitude Δ as an index measure to show the intensity of

preferred orientation in a 2-D arrangement of particles (Figure 10-2) as:

$$\Delta = \frac{1}{M}\left[\sum_{k=1}^{M}\left(\cos 2\theta^{(k)}\right)^2 + \sum_{k=1}^{M}\left(\sin 2\theta^{(k)}\right)^2\right]^{1/2} \tag{10.32}$$

As shown in Figure 10-2, $\theta^{(k)}$ is the inclination angle of a unit vector $m^{(k)}$ (corresponding to k^{th} particle) to the horizontal axis and ranges from $-\frac{\pi}{2}$ to $\frac{\pi}{2}$, M is the total number of particles.

Assuming that the material exhibits axial symmetry with the axis of symmetry being parallel to the applied load (transverse anisotropy), and that that the major and minor axes of the aggregate distribution correspond to the directions perpendicular and parallel to the applied load, respectively Oda and Nakayama (1989)express the 3-D microstructure tensor F_{ij} as:

$$F = \begin{pmatrix} (1-\Delta)(3+\Delta) & 0 & 0 \\ 0 & (1+\Delta)(3+\Delta) & 0 \\ 0 & 0 & (1+\Delta)(3+\Delta) \end{pmatrix} \tag{10.33}$$

As shown in Figure 10-2, $\theta^{(k)}$ is the inclination angle of a unit vector $m^{(k)}$ (corresponding to k^{th} particle) to the horizontal axis and ranges from $-\frac{\pi}{2}$to $\frac{\pi}{2}$, M is the total number of particles.

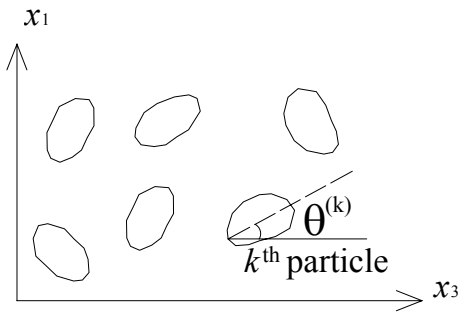

Figure 10-2. 2-D particle orientation of granular aggregates

The viscoplastic model developed above is now completed with the incorporation of the fabric tensor F_{ij}. Accordingly, the extended Matsuoka–Nakai (E-M-N) criterion is further modified as:

$$\overline{f^e} = \frac{\overline{I_1^e}\,\overline{I_2^e}}{\overline{I_3^e}} - K_{mn} \tag{10.34}$$

Where

$$\overline{I_1^e} = a_1\sigma_{ii}^e + a_2 F_{ij}\sigma_{ij}^e \tag{10.35a}$$

$$\overline{I_2^e} = 2b_6\sigma_{ik}^e\sigma_{jk}^e + 4b_7 F_{ik}\sigma_{kj}^e\sigma_{ij}^e \tag{10.35b}$$

$$\overline{I_3^e} = c_1\sigma_{lj}^e\sigma_{nl}^e\sigma_{jn}^e + c_2 F_{il}\sigma_{ij}^e\sigma_{nl}^e\sigma_{jn}^e \tag{10.35c}$$

where,

$$a_1 = 1 - \xi\left(2D_2\right)^{1/2} \tag{10.36a}$$

$$a_2 = 3\xi\left(2D_2\right)^{1/2} \tag{10.36b}$$

$$b_6 = \frac{1}{4} - \frac{\mu}{2}\left(2D_2\right)^{1/2} \tag{10.36c}$$

$$b_7 = \frac{3}{4}\mu\left(2D_2\right)^{1/2} \tag{10.36d}$$

$$c_1 = \zeta\left(2D_2\right)^{1/2} \tag{10.36e}$$

$$c_2 = 1 - 3\zeta\left(2D_2\right)^{1/2} \tag{10.36f}$$

where ξ, μ and ς are anisotropy material constants. D_2 is the second invariant of the deviatoric fabric tensor and is given by

$$D_2 = \frac{4\Delta^2}{3\left(3+\Delta\right)^2} \tag{10.37}$$

It should be noted that $\overline{I_1^e}, \overline{I_2^e}, \overline{I_3^e}$ in Equations (10.35a-c) are simplified for only the first term of F_{ij} are considered.

10.4 Evolution of Work Hardening Parameter

The hardening parameter reflects the combined effect of the cohesion of asphalt binders, the adhesion properties between binder and aggregate and frictional properties of aggregate structure (Tashman et al. 2005). Following the work by Panoskaltsis and Panneerselvam(2005), Perzyna's viscoplasticity flow rule is also applied as hardening law in this study. Thus, the hardening parameter evolution rate is given by:

$$\dot{k} = \frac{\dot{\varepsilon}^{vp}}{\nu} \tag{10.38}$$

Where $\dot{\varepsilon}^{vp}$ is the viscoplastic strain rate representing the change rate of magnitude of the viscoplastic deformation. By substituting Equations (10.20) and (10.24) into Equation (10.38), one gets:

$$\dot{k} = \left(\frac{\left\langle f^e \right\rangle}{\eta} \right)^m \frac{1}{\left(x + k^l \right)} \tag{10.39}$$

10.5 NUMERICAL IMPLEMENTATION

Under small strain condition, the incremental strain consists of elastic and viscoplastic components,

$$\dot{\varepsilon}_{ij} = \dot{\varepsilon}_{ij}^e + \dot{\varepsilon}_{ij}^{vp} \tag{10.40}$$

$\dot{\varepsilon}_{ij}^e$ is the elastic portion and $\dot{\varepsilon}_{ij}^{vp}$ is the viscoplastic portion, respectively.

From Equation (10.40), the elastic strain rate can be obtained,

$$\dot{\varepsilon}_{ij}^e = \dot{\varepsilon}_{ij} - \dot{\varepsilon}_{ij}^{vp} \tag{10.41}$$

By following the effective stress principle, the elastic stress rate is defined as,

$$\dot{\sigma}_{ij} = C_{ijkl} \left(\dot{\varepsilon}_{kl} - \dot{\varepsilon}_{kl}^{vp} \right) \tag{10.42}$$

where $\dot{\sigma}_{ij}$ is the Cauchy effective stress rate tensor, and C_{ijkl} is the non-linear stiffness tensor introduced by Lade and Nelson (1987). Having the time period (t_n-t_{n+1}), where, $\Delta t = t_{n+1} - t_n$, hence, at the iteration $n+1$, Equation (10.42) reduces to

$$\dot{\sigma}_{ij(n+1)} = C_{ijkl(n+1)} \left(\dot{\varepsilon}_{kl(n+1)} - \dot{\varepsilon}_{kl(n+1)}^{vp} \right) \tag{10.43}$$

Firstly, it is assumed that the damage parameters at $t_{n+1}$are calculated from total plastic strain at t_n, i.e.:

$$\omega_{1(n+1)} = d_{11} + d_{12}\left(\varepsilon_n^{vp}\right)^{d_{13}} \tag{10.44a}$$

$$\omega_{2(n+1)} = \omega_{3(n+1)} = d_{21} + d_{22}\left(\varepsilon_n^{vp}\right)^{d_{23}} \tag{10.44b}$$

Subsequently, the stresses are modified by effective stress to account for damage based on Equations (10.29a-c), resulting in,

$$\sigma_{1(n+1)}^{e} = \frac{\sigma_{1(n)}}{1-\omega_{1(n+1)}} \tag{10.45a}$$

$$\sigma_{2(n+1)}^{e} = \frac{\sigma_{2(n)}}{1-\omega_{2(n+1)}} \tag{10.45b}$$

$$\sigma_{3(n+1)}^{e} = \frac{\sigma_{3(n)}}{1-\omega_{3(n+1)}} \tag{10.45c}$$

Next, formulations are modified to account for fabric using the fabric tensor leading to:

$$\overline{I_{1(n+1)}^{e}} = a_1\sigma_{ii(n+1)}^{e} + a_2F_{ij}\sigma_{ij(n+1)}^{e} \tag{10.46a}$$

$$\overline{I_{2(n+1)}^{e}} = 2b_6\sigma_{ik(n+1)}^{e}\sigma_{jk(n+1)}^{e} + 4b_7F_{ik}\sigma_{kj(n+1)}^{e}\sigma_{ij(n+1)}^{e} \tag{10.46b}$$

$$\overline{I_{3(n+1)}^{e}} = c_1\sigma_{lj(n+1)}^{e}\sigma_{nl(n+1)}^{e}\sigma_{jn(n+1)}^{e} + c_2F_{il}\sigma_{ij(n+1)}^{e}\sigma_{nl(n+1)}^{e}\sigma_{jn(n+1)}^{e} \tag{10.46c}$$

The loading surface using Equation (10.34) is then used to determine whether the visco plastic strain has occurred or not, i.e:

$$\left\langle \overline{f_{n+1}^{e}} \right\rangle = \begin{cases} 0, & \overline{f_{n+1}^{e}} \le 0 \ \text{ no viscoplastic strain} \\ \overline{f_{n+1}^{e}}, & \overline{f_{n+1}^{e}} > 0 \ \text{ occurs viscoplastic strain} \end{cases} \tag{10.47}$$

The next step is to update the hardening parameter according to Equation (10.39) to get Equation (10.48) and then calculate visco plastic strain use Equation (10.49):

$$k_{n+1} = k_n + \left(\frac{\left\langle f^e_{n+1} \right\rangle}{\eta} \right)^m \frac{1}{\left(x + k^l_{n+1} \right)} \Delta t \tag{10.48}$$

$$\varepsilon^{vp}_{n+1} = \varepsilon^{vp}_n + \left(\frac{\left\langle f^e_{n+1} \right\rangle}{\eta} \right)^m \frac{\nu_{n+1}}{\left(x + k^l_{n+1} \right)} \Delta t \tag{10.49}$$

Finally, the damage parameters at $t_{n+1}$are updated with total viscoplastic strain at time t_{n+1}, i.e.:

$$\omega_{1(n+1)} = d_{11} + d_{12} \left(\varepsilon^{vp}_{n+1} \right)^{d_{13}} \tag{10.50a}$$

$$\omega_{2(n+1)} = \omega_{3(n+1)} = d_{21} + d_{22} \left(\varepsilon^{vp}_{n+1} \right)^{d_{23}} \tag{10.50b}$$

The residual strain is calculated by the test strain minus the predict elastic and viscoplastic strain:

$$\varepsilon^R_{n+1} = \varepsilon^t_{n+1} - \varepsilon^e_{n+1} - \varepsilon^{vp}_{n+1} \tag{10.51}$$

The above recursive-iterative algorithm is continued until the residual strain is reduced to a specified tolerance.

10.6 Laboratory Tests and Analysis

10.6.1 *Laboratory Tests*

Indirect tension tests are conducted to measure the constitutive properties of asphalt mixtures for the calibration and verification of the proposed nonlinear elasto-visco-plastic model. Stress-strain relations are calculated from equations derived by Wen and Kim (2002). Total strain and Poisson's ratio (v) are calculated based on Equations (10.52) and (10.53):

$$v = -\frac{\alpha_1 U(t) + V(t)}{\alpha_2 U(t) + \alpha_3 V(t)} \tag{10.52}$$

$$\varepsilon_{x=0} = U(t)\frac{\gamma_1 + \gamma_2 v}{\gamma_3 + \gamma_4 v} \tag{10.53}$$

Where,

$U(t)$ = horizontal displacement (m),

$V(t)$ = vertical displacement(m),

Parameters α_1, α_2, α_3, γ_1, γ_2, γ_3, γ_4 are constants, and the parameter values varied with sample diameters and gauge length. For samples with 100mm diameter and gauge length of 50.8mm, their values are:

α_1=4.580, α_2=1.316, α_3=3.341, γ_1=12.4, γ_2=37.7, γ_3=0.471, γ_4=1.57.

Two types of asphalt mixtures typically used in the State of Washington are used. These mixtures are designed following the Superpave mix design specification, with key mix design information as shown in Table 10-1. Cylindrical specimens are compacted

using Superpave Gyratory Compactor (SGC) to a target air void of 4%, and then specimens are cored and cut into100mm in diameter and 38.4mm in height.

Table 10-1. Asphalt mixture gradation and binder information

Sieve Size	3/4”	1/2”	3/8”	#4	#8	#16	#30	#50	#100	#200
G-1	100	98	84	53	34	24	17	11	8	5.5
G-2	100	97	85	56	36	22	16	11	9	6.5

	Binder Type	Binder Content
G-1	PG 70-28	5.0%
G-2	PG 64-28	5.7%

All tests are performed using a servo-hydraulic material testing system (MTS) testing machine under room temperature of 25^{o}C. A monotonic test with constant compressive loading rate of 50mm/min is applied until the load reduced to 25% of the peak load.

10.6.2 *Analysis*

In this section, the basic stress-strain relationships obtained from the indirect tension tests of two mixtures are utilized to determine the model parameters by curve fitting. The parameters of the nonlinear elastic component of the model are obtained by only fitting

the curve to the low stress level segment of the curve. The viscoplastic parameters are determined using the later part of the stress-strain curve when the specimen has experienced damage. The fitted model parameters for each component of the model are summarized in Table 10-2. The atmospheric pressure is fixed as a constant value of 101.325 Kpa. The predicted results using the model parameters with the experimental results are shown in Figure 10-3. It is evident that the model predicted values match the experimental data well for the entire loading range.

Figure 10-4 shows the comparison of the prediction of the nonlinear elastic model and the experiments. The non-linear elastic model predicts the experimental results quite well at low stress levels. The damage occurs after the threshold points, and then the viscoplastic strain begins to accumulate. Figure 10-5 shows the damage evolution for mixture type G-1 and type G-2. ω_1 and ω_2 represented the damage parameters for principal stress direction and confining pressure stress direction, respectively. From the results of those two mixtures, it is found that ω_1 is much larger than ω_2 since ω_1 is the loading direction. By comparison of those two mixtures, it is clear that the fast increment of ω_1 parameter for G1 mixture, an indication of fast damage accumulation, resulted in the quicker stress drop in G1 mixture after reaching peak stress values. In other words, G1 mixture behaved more brittle than G2 mixture.

Combining both Figure 10-4 and Figure 10-5, it is clear that the development of

damage varies from different types of asphalt mixture. Though G-1 has a higher loading capacity compared with G-2, the damage occurs at a relatively earlier period and lower strain level.

Table 10-2. Model Parameters for the Non-linear Elastic Component

Mixture Type	Poisson's Ratio ν	Modulus Number M	Material Constant λ	Anisotropy Δ	Cohesion c	Friction Angle φ
G-1	0.40	2.2E+5	-0.154	0.5	1000	0.500
G-2	0.38	1.0E+4	-0.170	0.5	1000	0.500

Model Parameters for the Viscoplastic Component

Mixture Type	η	m	x	l	α	ξ	μ	ζ
G-1	4E-6	0.60	1E+07	1.0	2.8E+06	20	18.0	17
G-2	8E-9	0.10	2E+07	1.0	2.9E+10	20	20.4	15

Model Parameters for the Damage Component

Mixture Type	d11	d12	d13	d21	d22	d23
G-1	0	1.15	0.3	0	0.1	0.3
G-2	0	3.00	0.8	0	0.2	0.7

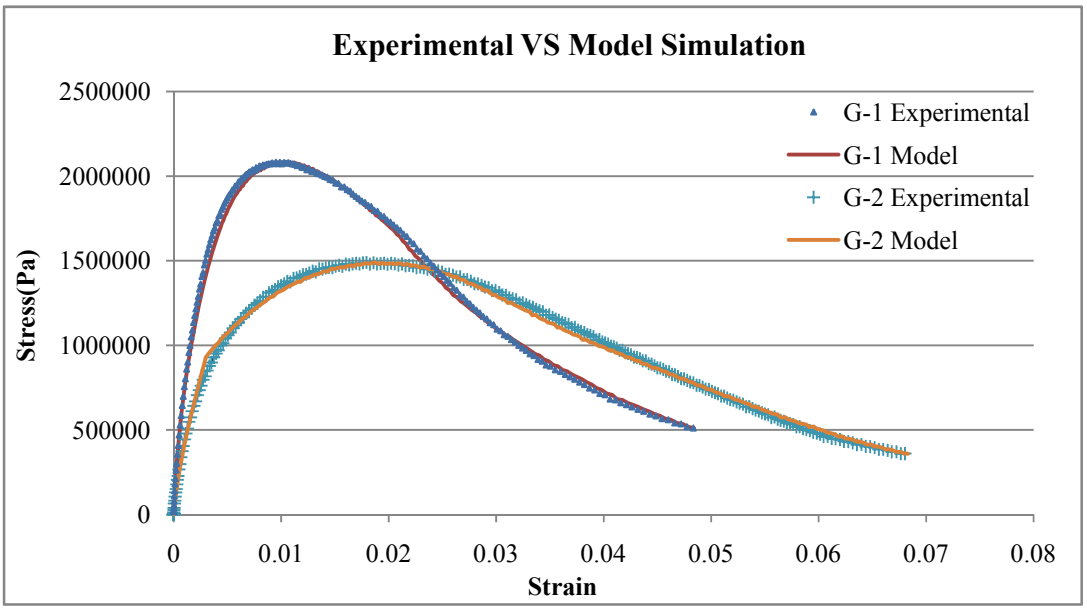

Figure 10-3. Comparison of experimental data and model simulation

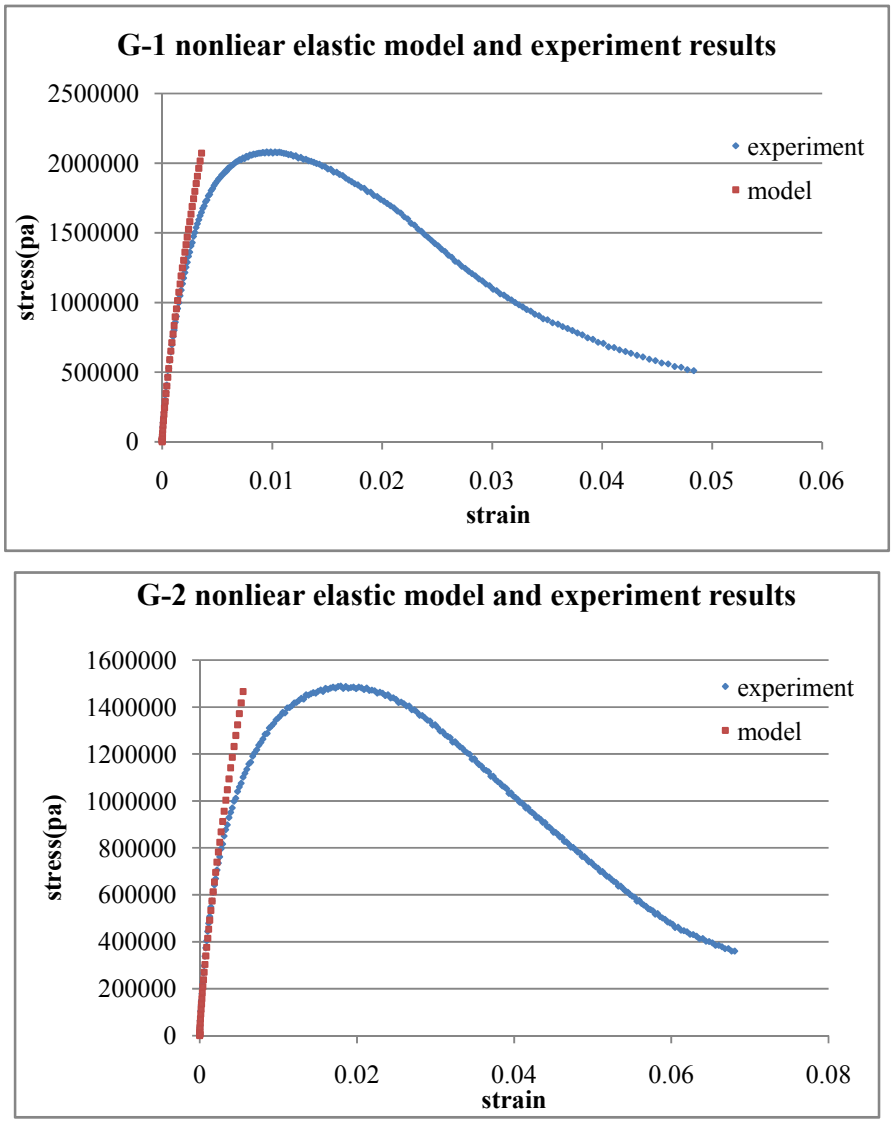

Figure 10-4. Nonlinear elastic model

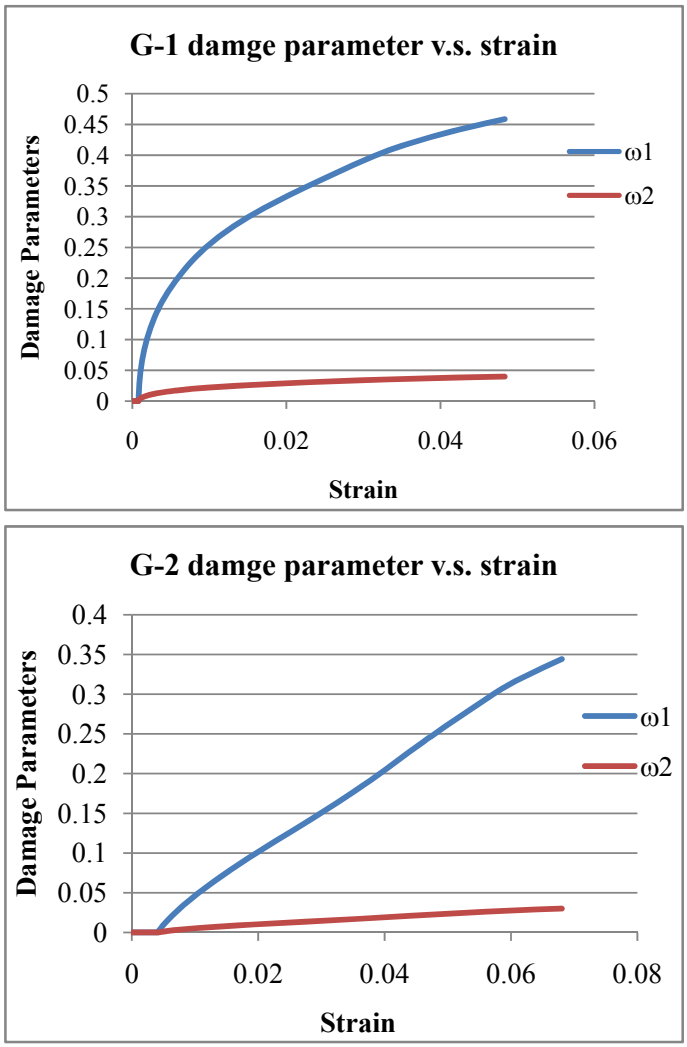

Figure 10-5. Damage parameters evolution with total strain.

10.7 SUMMARY

A nonlinear elasto-visco-plastic model is developed to describe the behavior of asphalt mixtures under traffic loads. The reversible deformation portion is modeled by a nonlinear elastic model, and the irreversible deformation which is normally resulting to rutting is modeled by a viscoplastic model. The microstructure parameter which

describes the anisotropic property of aggregate orientation as well as damage tensors are also incorporated into the model to account for the effect of damage on the performance of asphalt mixture. The viscoplastic loading surface of the extended Matsuoka–Nakai (E-M-N) is used in this study, and the Perzyna's viscoplasticity non associated flow rule is applied.

In order to determine the model parameters, indirect tension tests on two different asphalt mixtures were conducted. The model simulation results fit well with the experimental results, indicating the model is capable of capturing the development of permanent deformation under loads. It is found that damage occurs after a threshold, but the threshold value varies with different type of asphalt mixture. Once reached the threshold, the damage propagates with the increase of strain. It is of interest to note that damage in the axial direction grows much faster with deformation than the one in the lateral direction.

CHAPTER 11 CONCLUSIONS AND RECOMMENDATIONS

11.1 CONCLUSIONS

This research aimed to study the design and characterization of the asphalt mixtures based on particle packing theories, discrete element method and macromechanical modeling. A commercial software PFC3D was used in the DEM simulation process.

The overall contributions of this study include: 1) a new aggregate gradation design and mix design based on DEM and packing theory is developed which can guide design to achieve appropriate volumetric and mechanical properties; 2) a micromechanical based three dimensional DEM model is developed and calibrated with experimental results, which can capture the complex modulus and strength properties of asphalt mixtures; 3) a macromechanical constitutive model is developed which can capturing the permanent deformation performance of asphalt mixtures.

In details, the specific findings of this study include:

1) This thesis conducted an analysis of aggregate packing based on DEM simulation to characterize the roles of aggregates with different sizes in the structure, and evaluate

the aggregate contact with respect to different aggregate packing skeleton. Using DEM simulation, a gradation weighing factor f_v is developed which can link the aggregate structures with volumetric properties. An f_v calculation equation was derived based on an analysis of aggregate packing and the resulting volumetric properties of an aggregate structure. This equation can be used for determining f_v values and back-calculating VMA, based on either data regression or DEM simulation. The f_v values are found to be not sensitive to different aggregate gradations as long as the gradations have the same NMAS and belong to the same gradation type. The results confirmed that the DEM is a good approach to simulate the packing of aggregate structure and to provide correlations between aggregate gradation and the volumetric properties of an aggregate structure.

2) Based on packing theory, a simple method was developed for fast VMA estimation. This method can be used in the asphalt mixture design to reduce the needs of trial-and-error and provide direct guidance to the adjustment of aggregate gradation for adequate VMA and other volumetric properties. Verified by mix designs from different states and aggregate sources, the method provided in this study appears to be a good method to predict the VMA without the need of experimental testing. Most prediction errors are within 1%.

3) This research evaluated the influence of material properties on the mechanical properties of asphalt mixtures. The influence of air voids, binder type on dynamic modulus and flow number was studied. It was found that air voids have an important effect on E* and flow number. In general, higher air voids will result in lower E* and flow numbers. High PG grade has clear influence on E* and flow number; higher PG grade leads to higher E* and flow number.

4) A modified Hirsch model based on asphalt mastic is proposed which can successfully predict the dynamic modulus of the WSDOT mixtures. Although only validated with limited data, this model is very promising for practical usage as it requires limited inputs (volumetric properties and asphalt binder properties) and is relatively simpler than other popular dynamic modulus prediction models. Most importantly, it provides direct linkage between volumetric properties and mechanical performance. The revised Hirsch can be used as both a designing tool and a screening tool to estimate the mixture's dynamic modulus at the early stage of the mix design. A flow number prediction model was also developed based on experimental data on local mixes. The prediction model took into account the effects of volumetric properties, binder type, and test temperatures. The prediction results were reasonable for mixtures with conventional PG binder. However, it was not recommended for highly polymer modified PG binder (i.e., PG76-28).

5) By using VMA as a linkage between asphalt components (aggregates and asphalt) and the overall mixture properties, this study proposed a new mix design method for fast and convenient determination of optimum asphalt content. This method can also be used for optimizing mix designs by adjusting aggregate structure and asphalt content. A step by step guideline on how to use the design method to design a gradation with more knowledge of mixture volumetric properties and expected performance was explained in details. This guideline introduced the parameters that reasonably describe a gradation and recommended control ranges of these parameters. This proposed gradation design guideline will also help the optimization of mix designs to achieve the most economical design with good field performance. In order to have a better understanding of the design guideline, a design example was provided at Appendix C which should help designer at different levels to quickly understand and apply this new method to practice.

6) This research explored micromechanical discrete element models to simulate the complex modulus and strength properties of the asphalt mixture. An image-aided 3D ball-clumping approach using *PFC*^{3D} DEM program was introduced which was promising to study the effect of aggregate packing on HMA properties. This method significantly reduced the number of balls needed while still maintaining adequate accuracy for considering the particle angularity impact. The Burger's contact model

was found to be successful in predicting both the dynamic modulus and the phase angle over a wide range of temperatures and frequencies. The peak point of phase angle by simulation is consistent with the experimental data and previous research. The effect of the key model parameters on the dynamic modulus and the phase angle was evaluated. It was found that the effect of the Kelvin's model parameters (Cnk and Knk) on the phase angle was not linear. This finding further confirmed that the micromechanical contact behavior of the material, determined by the Kelvin's contact parameters, played a significant role in the nonlinear behavior of the phase angle especially at high temperatures and/or low frequencies. The overall findings from the sensitivity analysis of the model parameters provided meaningful guidance for the fundamental understanding of the material mechanical properties and the selection of model parameters for other mixtures. It can be used to thoroughly evaluate the aggregate effect on HMA performance, and help to improve the mix design by linking aggregate packing with HMA performance.

7) A displacement softening model was successfully implemented to describe the visco-elastic-plastic behavior of asphalt mixtures and thus capture the damage properties under heavy load. It was found the developed 3D DEM model can describe the compressive strength of asphalt mixtures under different loading conditions well. Based on simulation results, particle angularity has important

impact on the compressive strength of asphalt mixture. Highly crushed angular aggregates can provide better resistance to heavy loads especially at high temperatures. Loading rates also have an influence on the strength of asphalt mixture, the influence of loading rate are higher at high temperature compared to lower temperature.

8) A nonlinear elasto-visco-plastic model was developed to describe the behavior of asphalt mixtures under traffic loads. The reversible deformation portion was modeled by a nonlinear elastic model, and the irreversible deformation which normally resulting to rutting was modeled by a viscoplastic model. The aggregate directional distribution and damage propagation during the accumulation of permanent deformation was accounted by incorporating a fabric tensor for aggregates and a direction dependent damage parameter into the yield and potential functions and by the use of Perzyna's viscoplastic formulation. The comparison of indirect tensile test results with the predictions from the model show that the model was adequate in capturing the permanent deformation performance of asphalt mixtures.

11.2 RECOMMENDATIONS

Based on this study, we recommended the following research directions as future work:

1) fv provided in this study are based on two methods: data regression and DEM simulation. It is suggested a larger data base including more states and a wider range of material properties be investigated in order to apply the volumetric prediction methods nationally. And for the DEM method, mix design data from different states are suggested to verify the applicability of the proposed fv values for local areas.

2) The dynamic modulus and flow number prediction models were calibrated based on materials from Washington State. The concept of dynamic modulus prediction based on mastic rather than asphalt could be evaluated by other states to provide better prediction of dynamic modulus.

3) This study mainly focused on the 12.5mm NMAS as it is the most popular asphalt mixture type used in the United States. It is recommended to verify the proposed design methods for mixtures with other NMAS. Most importantly, the corresponding fv values for each NMAS should be studied and determined.

4) For the technique of DEM simulation, a higher resolution of the angular particles will result in a more accurate simulation results. The resolution of the simulation models is closely related to the computational power of the computers. With the development of computer technology, it is anticipated that a more realistic

simulation with accurate angularity properties and more fine particles will result in better results.

5) The proposed design methodology should be validated by field performance data so that to ultimately realize a performance based mix design method.

REFERENCE

AASHTO (2009). AASHTO PP2 – Standard Practice for Mixture Conditioning of Hot-Mix Asphalt (HMA). *American Association of State Highway and Transportation Officials*, Washington D.C.

AASHTO (2009). AASHTO PP3 – Standard Practice for Preparing Hot-Mix Asphalt (HMA) Specimens by Means of the Rolling Wheel Compactor. *American Association of State Highway and Transportation Officials*, Washington D.C.

AASHTO (2009). AASHTO T240: Effect of heat and Air on a Moving Film of Asphalt Binder (Rolling Thin-Film Oven Test). *American Association of State Highway and Transportation Officials*, Washington D.C.

AASHTO (2009). AASHTO T312-09: Preparing and determining the density of Hot mix asphalt (HMA) specimens by Means of the Superpave Gyratory. *American Association of State Highway and Transportation Officials*, Washington D.C.

AASHTO (2009). AASHTO TP-62: Determining Dynamic Modulus of Hot-Mix Asphalt Concrete Mixtures. *American Association of State Highway and Transportation Officials*, Washington D.C.

AASHTO (2009). AASHTO TP 79: Determining the Dynamic Modulus and Flow

Number for Hot Mix Asphalt (HMA) Using the Asphalt Mixture Performance Tester (AMPT), *American Association of State Highway and Transportation Officials*, Washington D.C.

AASHTO (2009). AASHTO TP8 – Standard Test Method for Determining the Fatigue Life of Compacted Hot-Mix Asphalt (HMA) Subjected to Repeated Flexural Bending. *American Association of State Highway and Transportation Officials*, Washington D.C.

AASHTO Guide for Design of Pavement Structures, (1993), *American Association of State Highway and Transportation Officials*, Washington D.C.

Abbas, A., Papagiannakis, A.T., Masad, E., and Shenoy A. (2005). "Modelling Asphalt Mastic Stiffness using Discrete Element Analysis and Micromechanics based Models" *The International Journal of Pavement Engineering*, Vol.6(2): 137-146.

Abdo, A. Abu., F. Bayomy, R. Nielsen, T. Weaver, S.J. Jung, M.J. Santi (2009). "Prediction of the dynamic modulus of Superpave mixes." *proceedings of Bearing Capacity of Roads, Railways and Airfields*, Taylor & Francis Group, London, ISBN 978-0-415-87199-0.

Advanced Asphalt Technologies, LLC., (2011) "NCHRP Report 673: A Manual for Design of Hot Mix Asphalt with Commentary." *Transportation Research Board*,

National Research Council, Washington, DC.

Anderson, R.M., and Bahia, H.U. (1997). "Evaluation and Selection of Aggregate Gradations for Asphalt Mixtures Using Superpave." *Transportation Research Record*, No. 1583, Washington D.C. 91–97.

Anderson, R. M., Cominsky, R. J. and Killingsworth B. M.(1998) "Sensitivity of Superpave Mixture Tests to Changes in Mixture Components," *Asphalt Paving Technology*, Vol. 67, Association of Asphalt Paving Technologists.

Anderson, R. M., Turner, P. A. and Peterson, R.L. (2003) "NCHRP report 478: Relationship of Superpave Gyratory Compaction Properties to HMA Rutting Behavior." *Asphalt Institute*, Lexington, KY.

Andreasen, A.H.M., and Anderson, J. (1929). "The Relation of Grading to Interstitial Voids in Loosely Granular Products (With Some Experiments)," *Kolloid-Z.*, 49, 217-228.

Anthony, D. S., Bahia, H.U. (2003) "The Effect of Fine Aggregate Angularity, Asphalt Content and Performance Graded Asphalts on Hot Mix Asphalt Performance." *WisDOT Highway,* Research Study 0092-45-98.

Antony,S. J., Kuhn, M. R. (2004) "Influence of particle shape on granular contact signatures and shear strength: new insights from simulations" *International Journal of Solids and Structures*, 41, pp. 5863-5870

Asphalt Institute. (1994). “Mix Design Methods for Asphalt Concrete and Other Hot Mix Types. Publication MS-2, 6th Edition.” *The Asphalt Institute.* Lexington, KY.

Asphalt Institute. (2001) “Superpave Mix Design. Superpave Series No. 2 (SP-2).” *Asphalt Institute*. Lexington, KY.

Aurilio, V., Pine, W. J. and Lum, P. (2005). “The Bailey Method, Achieving volumetrics and HMA compactability.” *Proceeding of the 50th Annual Canadian Technical Asphalt Association Conference*, Victoria, Canada, pp. 160-183.

Bahia, H. U. Friemel Timothy P., Peterson, Pehr A., Russell, Jeffery S., and Poehnelt, Brian. (1998) “Optimization of Constructibility and Resistance to Traffic: A New Design Approach for HMA Using the Superpave Compactor.” *APT, Journal of the AAPT*, Vol. 67,pp.189-232.

Bahuguna, S., Panoskaltis, V. and Papoulia, K.D. (2006). “Identification and modeling of permanent deformations of asphalt concrete.” *Journal of engineering mechanics,* 231-239.

Bari, J., and Witczak, M. W. (2006). “ Development of a New Revised Version of the Witczak E* Predictive Model for Hot Mix Asphalt Mixtures.” *Journal of the Association of Asphalt Paving Technologists*, Volume 75.

Benson, F. J.,(1970) “Effects of Aggregate Size, Shape, and Surface Texture on the

Properties of Bituminous Mixtures – A Literature Review," *Highway Research Board* Special Report 109, pp. 12-21.

Bernal, J.D., Cherry, I.A., Finney, J.L., and Knight, K.R. (1970). "An optical machine for measuring sphere coordinates in random packings" *Journal of Physics E: Scientific Instruments*, 3: 388-390.

Bhasin, A., Button, J., and A. Chowdhury, (2004) "Evaluation of Simple Performance tests on Hot-Mix Asphalt Mixtures from South Central United States." *Transportation Research Record* 1891, 2004.

Bishop, A. W. (1971). "Shear strength parameters for undisturbed and remolded specimens." *Proceedings of the Roscoe Memorial Symposium*, Cambridge University, Edited by R. H. G. Parry and Foulis, G. T.: 3-58.

Bonaquist, R.F. (2008) "NCHRP report 614: Refining the Simple Performance Tester for Use in Routine Practice." *Transportation Research Board*, National Research Council, Washington, DC.

Bonaquist, R.F. (2008). "NCHRP Report 629: Ruggedness Testing of the Dynamic Modulus and Flow Number Tests with the Simple Performance Tester." *National Cooperative Highway Research Program*, Washington, D.C.

Brian D. Prowell, Jingna Zhang and E. Ray Brown. (2005). "NCHRP 539 report: Aggregate Properties and the Performance of Superpave-Designed Hot Mix Asphalt." *Transportation Research Board (TRB)*, National Research Council, Washington D.C.

Buttlar, W. G., and You, Z. (2001). "Discrete element modeling of asphalt concrete: A micro-fabric approach." *Journal of the Transportation Board*, National Research Council, Washington, D.C., No. 1757, Geomaterials,111–118.

Button, J. W., Perdomo, D., and Lytton, R. L..(1990). "Influence of Aggregate on Rutting of Asphalt Concrete Pavements." *Transportation Research Record 1259*. Transportation Research Board, Washington D.C. pp 141-152.

Carnpen, W. H., Smith, J.R, Erickson, L. G. and Mertz, L. R., (1959) "The Relationships Between Voids, Surface Area, Film Thickness and Stability In Bituminous Paving Mixtures", *Proceedings, AAPT*, Vol. 2S.

Cela, J. J. L. (2002). "Material Identification Procedure for Elastoplastic Drucker-Prager Model." *Journal of Engineering Mechanics*, ASCE, 128(5), pp. 586-591.

Ceylan, H.; Schwartz, C. W.; Kim, S. and Gopalakrishnan, K. (2009). "Accuracy of Predictive Models for Dynamic Modulus of Hot-Mix Asphalt." *Journal of material in Civil Engineering*, 21(6), 286–293.

Chang, C.S. Chao, S. J. and Chang, Y.(1995) "Estimates of Elastic Moduli for Granular

Material with Anisotropic Random Packing Structure" *Inf. J. Solids Structures* 32(14), pp. 1989-2008.

Chen, W.F. and Han, D.J. (1988) "Plasticity for Structural Engineers." *J. Ross Publishing edition*, Springer-Verlag, New York.

Christensen, D.W. and Anderson, D.A. (1992). "Interpretation of dynamic mechanical test data for paving grade asphalt cements." *J. Assoc. Asphalt Paving*. Technol., 61, 1992, pp. 67-116.

Christensen, D.W., Pellinen, T.K., and Bonaquist, R.F. (2003). "Hirsch Model for Estimating the Modulus of Asphalt Concrete." *Journal of the Association of Asphalt Paving Technologists*, Volume 72, Lexington, KY.

Christensen, D. W. et al. (2009). "Draft Final Report to the National Cooperative Highway Research Program (NCHRP) on Project NCHRP 9-33: A Mix Design Manual for Hot Mix Asphalt." *Advanced Asphalt Technologies, LLC.* Sterling, VA.

Cominsky, R. J., Huber, G. A. Kennedy, T. W. and Anderson. R. M. (1994). "The Superpave Mix Design Manual for New Construction and Overlays," *SHRP* Report A-407, Strategic Highway Research Program, Washington, DC

Cominsky, R.J., Killingsworth, B.M. Anderson, D.A. and Crockford, W.M.. (1998) NCHRP Report 409: Quality Control and Acceptance of Superpave-Designed Hot Mix Asphalt. *Transportation Research Board*, National Research Council,

Washington, DC.

Coree,B. J. and Hislop, W. P. (2000). "A laboratory investigation into the effects of aggregate-related factors of critical VMA in asphalt paving mixtures." *Iowa DOT,* Project TR-415, Ames, IA.

Coree, B J and Hislop, W P. (2001) "A Laboratory Investigation Into the Effects of Aggregate-Related Factors on Critical VMA in Asphalt Paving Mixtures" *Asphalt Paving Technology* 2001.

Crawford, C. (1989) "The Rocky Road of Mix Design.", *Hot Mix Asphalt Technology*, National Asphalt Pavement Association, p. 10-13.

Cundall P.A. (1971). "A Computer Model for Simulating Progressive Large Scale Movements in Blocky Rock Systems." *In Proceedings of the Symposium of International Society of Rock Mechanics*, Nancy, France; 1 (II-8).

Cundall, P. A., and Hart. R. (1992) "Numerical Modeling of Discontinua," *J. Engr. Comp.*, 9, 101-113.

Cundall, P.A. and Strack, O.D. (1979). "Discrete Numerical Model for GranularAssemblies." *Geotechnique*, Vol.29(1): 47-65.

Curray, J. R. (1956). "Analysis of two dimensional orientation data." *Journal of Geology*, 64, 117-131.

Deresiewicz, H. (1958). “Mechanics of Granular Matter.” *Advances in Applied Mechanics*, Vol. 5, 233-306.

Drucker, D. C., and Prager, W. (1952). “Soil mechanics and plastic analysis of limit design.” *Quart. Appl. Math*., 10(2), 157-165.

Dukatz, E. L., (1989) “Aggregate Properties Related to Pavement Performance.” *Proceedings of the Association of Asphalt Paving Technologists*. Volume 58.

Eisenmann, J., and Hilmer, A. (1987). “Influence of wheel load and inflation pressure on the rutting effect at asphalt pavements-Experimental and theoretical investigations.” *Proc., 6th Int. Conf. Structural Design of Asphalt Pavement,* Ann Arbor: University of Michigan, 392-403.

Flintsch, G. W., Loulizi A., Diefenderfer S. D., Diefenderfer B. K, and Galal K. A., (2008). “Asphalt Materials Characterization in Support of the Mechanistic -Empirical Pavement Design Guide Implementation Efforts in Virginia.” *Transportation Research Record*, Vol. 2057, 114-125.

Freddy, L. R. Kandhal, P. S. Brown, E. R. Lee D. and Kennedy, T. W. (1996). “Hot Mix Asphalt Materials, Mixture design, and construction.(2nd Edition).” *National Asphalt Pavement Association* Research and Education Foundation.

Garcia, G. and Thompson, M. (2007) “HMA Dynamic Modulus-Temperature Relations”

FHWA- Report ICT-07-006.

Gaudette, B. E., Welke, R. A., (1977). "Investigation of Crushed Aggregates for Bituminous Mixtures." *Michigan Department of State and Highway Transportation.* Report No. TB-58, 1977.

Goh, S.W., You, Z. Williams, R.C. and Li, X. (2011) "Preliminary Dynamic Modulus Criteria of HMA for Field Rutting of Asphalt Pavements: Michigan's Experience," *ASCE Journal of Transportation Engineering*, Vol. 137, No. 1,, pp. 37-45.

Goode, J. F. and Lufsey, L. A.,(1965) "Voids, Permeability, Film Thickness vs. Asphalt Hardening", *Proceedings, AAPT*, Vol. 34.

Griffiths, D.V., and Huang, J. (2009). "Observations on the extended Matsuoka-Nakai failure criterion." *International Journal for Numerical and Analytical Methods in Geomechanics*, 33, 1889-1905.

Gutierrez, M., Ishihara, K., and Touhata, I. (1991). "Noncoaxiality and stress-dilatancy relations for granular materials." *Computer method and advanced in geomechanics*, G. Beer, J. R. Bookeer, and J. P. Carter, eds., Balkema, Rotterdam.

Hajj, E. Y., Ullao, A., Sebaaly, P. E., and R. V. Siddharthan, (2010), "Characteristics of Dynamic Triaxial Testing of Asphalt Mixtures," Draft Final Report, *Federal Highway Administration*.

Hall, K. D., Xiao, D. X., Wang, K. (2010). "Calibration of the MEPDG for Flexible Pavement Design in Arkansas." *Transportation Research Board* CD-ROM, TRB.

Hashin, Z. (1965). "Viscoelastic behaviour of heterogeneous media." *J. Appl. Mech.*, 32(9): 630–636.

Hinrichsen, J.A., and J. Heggen. (1996). "Minimum Voids in Mineral Aggregate in Hot-Mix Asphalt Based on Gradation and Volumetric Properties." *Transportation Research Record*, No. 1545, Washington D.C. 75–79.

Hislop, W. P. Coree. B. J. (2000) "VMA as a Design Parameter in Hot-Mix Asphalt" *Mid-Continent Transportation Symposium 2000*, pp24-29.

Holubec, I., D'Appolonia, E. (1973) "Effect of Particle Shape on the Engineering Properties of Granular Soils," *ASTM* STP 523, pp. 304-318.

Hossain, Z., Indraratna, B., Darve, F., and Thakur, P. K., (2007). "DEM analysis of angular ballast breakage under cyclic loading." Geomechanics and Geoengineering: *An International Journal* Vol. 2(3):175-181.

Howell, D., Behringer, R.P., Veje, C.T. (1999). "Fluctuations in granular flows." *Chaos*, Vol.9 (3): 559–572.

Huang, H., E. Tutumluer, Y. Hashash, and J. Ghaboussi.(2007) "Contact Stiffness Affecting Discrete Element Modeling of Unbound Aggregate Granular Assemblies," *Submitted to the 7th Unbound Aggregates in Roads Symposium*, Nottingham, UK.

Huber, G.A. and Shuler, T.S. (1992). "Providing Sufficient Void Space for Asphalt Cement: Relationship of Mineral Aggregate Voids and Aggregate Gradation." *ASTM* SPT 1147, Philadelphia, PA.

Hudson, S. B. and Davis, R. L.(1962) "Relationship of Aggregate Voidage to Gradation," *Proceedings of the Association of Asphalt Paving Technologists*, Vol. 31.

Kaloush, K.E., (2001). "Simple performance test for permanent deformation of asphalt mixtures." Doctoral Dissertation, *Department of Civil and Environmental Engineering, Arizona State University*, Tempe, Arizona.

Kandhal P. S. and Chakraborty, S. (1996) "Evaluation of voids in the mineral aggregate for AC paving mixtures" *NCAT* Report No. 96-4. Auburn University, Alabama (1996)

Kachanov, L.M. (1986). "Introduction to Continuum Damage Mechanics." *Martinus Nijhoff Publishers*, Dordrecht, The Netherlands.

Kachanov, L.M. (1992). "Effective elastic properties of cracked solids: critical review of some basic concepts." *Applied Mechanics Review*, 45, 304–335.

Karihaloo, B.L., and Fu, D. (1990). "Anisotropic damage model for plain concrete." *Engineering Fracture Mechanics*, 35 (1-3), 205–209.

Kennedy, T.W, Huber, G.A. Harrigan, E.T. Cominsky, R.J. Hughes, C.SQuintus, . H.V.

Moulthrop. J.S. (1994). “Superior Performing Asphalt Pavements (Superpave): The Product of SHRP Asphalt Research Program.” *National Research council*, SI-IRP-A-410.

Kumar, A. and Goetz, W. H.,(1977) “Asphalt Hardening as Affected by Film Thickness, Voids and Permeability in Asphaltic Mixtures”, *Proceedings Association Asphalt Paving Technology*, p. 571-605.

Kuo, C. Y., and Frost, J. D. (1995). “Quantifying the fabric of granular materials-An image analysis approach.” *Report No. GIT-CEE/GEO-95-1*, The Georgia Institute of Technology, Atlanta, GA.

Kvanak et al.(2007). “Statistical development of a flow number predictive equation for the Mechanistic-Empirical Pavement Design Guide.” *TRB* Annual Meeting Paper 07-1000,.

Lade, P.V., and Nelson, R.B. (1987). “Modeling the elastic behavior of granular materials.” *International Journal for Numerical and Analytical Methods in Geomechanics*, 11, 521-542.

Leiva-Villacorta, Fabricil. (2007) “Relationships between Laboratory Measured Characteristics of HMA and Field Compactability.” Auburn University, Thesis of Master Degree.

Li, X. S., and Dafalias, Y. (2002). "Constitutive modeling of inherently anisotropic sand behavior." *Journal of Geotechnical and Geoenvironmental Engineering*, 28(10), 868-880.

Lottman, R. R. and Goetz, W. H., (1956). "Effect of Crushed Gravel Fine Aggregate on the Strength of Asphaltic Surfacing Mixtures." *National Sand and Gravel Association Circular*. No. 63.

Lytton, R. (2000) "Characterizing Asphalt Pavements for Performance." *Transportation Research Record 1723*, Transportation Research Board, National Research Council, Washington, D.C., 5-16.2000.

Lytton, R., Uzan, J., Fernando, E. G., Roque, R., Hiltunen, D., Stoffels, S. M. (1993). "Development and validation of performance prediction models and specifications for asphalt binders and paving mixes." *The Strategic Highway Research Program Report*, No. SHRP-A-357, National Research Council, Washington, DC.

Maire, E., Babout, L., Buffiere, J.-Y., and Fougeres, R. (2001). "Recent results on 3D characterization of microstructure and damage of metal matrix composites and a metallic foam using x-ray tomography." *Journal of Materials Science and Engineering*, A319-321, 216-219.

Mallick, R.B., Buchanan, M.S. Kandhal, P.S. Bradbury, R.L. and McClay, W. (2000) "A

Rational Approach of Specifying the Voids in the Mineral Aggregate for Dense-Graded Hot-Mix Asphalt." *Presented at the 79th Annual Meeting of the Transportation Research Board,* Washington D.C.

Masad, E. (2004). "X-ray computed tomography of aggregates and asphalt mixes." *Mater. Eval. J.*, Am. Soc. Nondestructive Testing, 62, 775 – 783.

Masad, E., D. Little, L. Tashman, S. Saadeh, T. Al-Rousan, and Sukhwani, R. (2003) "Evaluation of Aggregate Characteristics Affecting HMA Concrete Performance." *ICAR* 203-1, 2003

Matsuoka, H. and Nakai, T. (1974). "Stress-deformation and strength characteristics of soil under three different principal stresses." *Proceedings of JSCE*, 232, 59–74.

Matsushima, T. and Saomoto, H. (2002). "Discrete Element Modeling for Irregularly-Shaped Sand Grains." *Proceedings of the 5th European Conference, Numerical Methods in Geotechnical Engineering*, Paris, Fr., Sep. 4-6th, pp. 239-246.

McGennis, R. B. (1997) "Evaluation of Materials from Northeast Texas Using Superpave Mix Design Technology," *Transportation Research Record* 1583, Transportation Research Board, National Research Council, Washington, DC pp. 98–105.

McGennis, R.B. Anderson, R.M. Kennedy, T.W. Solaimanian, M. (1995) "Background of Superpave Asphalt Mixture Design and Analysis." *Federal Highway Administration*,

Report number FHWA-SA-95-003.

McLeod, N.W. (1956) "Relationships between Density, Bitumen Content, and Voids Properties of Compacted Bituminous Paving Mixtures." *Proceedings, Highway Research Board*, Volume 35.

McLeod, N. W. (1959). "Void Requirements for Dense-graded Bituminous Paving Mixtures." *American Society for Testing and Materials (ASTM),* Special Technical Publication (SPT) 252. Philadelphia, PA.

Monismith, C. L. (1970) "Influence of Shape, Size, and Surface Texture on the Stiffness and Fatigue Response of Asphalt Mixtures," *Highway Research Board* Special Report No. 109, pp. 4-11.

Muhunthan, B., Chameau, J., and Masad, E. (1996). "Fabric effects on the yield behavior of soils." *Journal of Soils and Foundations*, 36(3), 85-97.

Murakami, S. (1988). "Mechanical modeling of material damage." *Journal of Applied Mechanics*, 55, 280–286.

Oda, M., and Nakayama, H. (1989). "Yield function for soil with anisotropic fabric." *Journal of Engineering Mechanics*, ASCE, 15(1), 89-104.

Pan,T. (2006) "Investigation of Coarse Aggregate Morphology Affecting Hot Mix Behavior Using Image Analysis" *Doctoral Dissertation of University of Illinois at*

Urbana-Champaign. Champaign, Illinois

Pan, T., Tutumluer, E., and Carpenter, S.H.(2005a). "Investigation of Aggregate Shape Effects on Hot Mix Performance Using an Image Analysis Approach," *The Federal Highway Administration*, UILU-ENG-2005-2003.

Pan, T., Tutumluer, E., and Carpenter, S.H.(2005b) "Effect of Coarse Aggregate Morphology on Resilient Modulus of Hot-Mix Asphalt," *Transportation Research Record (TRB)* No. 1929, National Research Council, Washington, D.C., pp. 1-9.

Panoskaltsis, V. P. and Panneerselvam, D. (2005) "An anisotropic hyperelastic-viscoplastic damage model for asphalt concrete materials and its numerical implementation." *5th GRACM International Congress on Computation Mechanics*, Limassol.

Park, D.W., Chowdhury. A. and Button, J. (2001). "Effects of aggregate gradation and angularity on VMA and rutting resistance." *ICAR*, 201(3F). International Center for Aggregate Research. Austin, TX.

Perzyna, P. (1963). "The Constitutive Equations for Rate Sensitive Plastic Materials," *Quarterly applied Mathematics*, 20, 321-332.

Pietruszczak, S., Krucinski, D. (1989). "Description of anisotropic response of clays using a tensorial measure of structural disorder." *Mechanics of Materials*, 8, 237-249.

PFC^{3D} Manuals. (2008). "General Formation 1-2, verison 4.0". *Itasca Consulting Group Inc. Minneapolis, MI.*

Prithvi S. K. Chakraboily, S.(1996) "Evaluation of Voids in the Mineral Aggregate for AC Paving Mixtures" *NCAT* Report No. 96-4.

Prithvi S. K. Foo, K. Y. Mallick, R. B.. (1998) "A Critical Review of VMA Requirements in Superpave." *NCAT* Report No. 98-1.

Prowell, D. B., Zhang, J., Brown, E. R. (2005) "NCHRP 539 report: Aggregate Properties and the Performance of Superpave-Designed Hot Mix Asphalt.", *Transportation Research Board* (TRB), 2005.

Quintus, H. V. (2010). "NCHRP Project 9-30A, Draft Final Report, Calibration of Rutting Models for HMA Structural and Mixture Design." *National Cooperative Highway Research Program*, Washington, DC, March 2010.

Richardson, C. (1905) "The Modern Asphalt Pavement." *John Wiley & Sons*, New York.

Roberts, F.L., Kandhal, P. S., Brown, E.R., Lee D.Y. and Kennedy, T.W. (1996). "Hot Mix Asphalt Materials, Mixture design, and construction.(2nd Edition)." *NAPA Research and Education Foundation*. Lanham, Maryland.

Rodezno, M. C., Kaloush, K.K. and Corrigan, Matthew R.(2010). "Development of A Flow Number Predictive Model." *Transportation Research Board* CD-ROM, TRB.

Rowe, G. (2009) “Phase angle determination and interrelationships within bituminous materials.” *Advanced Testing and Characterization of Bituminous Materials*, Yaylor & Francis Group, London.

Ruth, B. E. (2000). “Development of Tentative Guidelines for the Selection of Aggregate Gradations for Hot-Mix Asphalt.” *ASTM STP 1412*, ASTM, West Conshohocken, PA., 110–127.

Scarpas, A., Al-Khoury, R., Van Gurp, C., and Erkens, S. M. (1997). “Finite Element Simulation of Damage Development in Asphalt Concrete Pavements.” *Proceedings of 8th International Conference on Asphalt Pavements*, University of Washington, Seattle, WA, 673-692.

Shamsi, K.A. Muhammad, L. Wu, Z. Cooper, S. Abadie, C. (2006) “Compactability and Performance of Superpave Mixtures with Aggregate Structures Designed Using the Bailey Method,” *Journal of the Association of Asphalt Paving Technologists (AAPT*), Vol. 75, pp.91-132.

Shashidhar, N., Gopalakrishnan, K., (2006). “Evaluating the aggregate structure in hot-mix asphalt using three-dimensional computer modeling and particle packing simulations”, *Canada Journal of Civil Engineering*. 33: 945-954.

Shashidhar, N.,Zhong, X., Shenoy, A., and Bastian, E. (2000) "Investigating the role of aggregate structure in asphalt pavement." *In Aggregate, Asphalt Concrete, Bases and Fines: Proceeding of the 8th Annual Symposium of the International Center for Aggregate Research (ICAR)*, Denver, Colo.

Shen, S. and Carpenter, S.H.. (2007). "Development of an Asphalt Fatigue Model Based on Energy Principles", *Journal of the Association of Asphalt Paving Technologists (AAPT)*, in press, Vol.76.

Shen, S., H. Yu, (2011). "Characterize packing of aggregate particles for paving materials: Particle size impact." Construction and building material. Vol. 25, No.3, pp. 1362-1368.

Shen S. and Yu, H. (2010). "Determination of HMA Voids in Mineral Aggregate Based on the Analysis of Aggregate Gradation and Packing." *89th TRB Annual Meeting*, No. 10-0067, Wahington D.C.

Shen, S., and Yu, H. (2011) "Analysis of Aggregate Gradation and Packing for Easy Estimation of Hot-Mix-Asphalt Voids in Mineral Aggregate" *Journal of Material in Civil Engineering*, Vol, 23 No. 5, pp 664-672, 2011.

Shu, X. Huang, B., (2008) "Micromechanics-based dynamic modulus prediction of polymeric asphalt concrete mixtures", *Composites Part B: Engineering*.39, P704-713.

Sobolev, K., Amirjanov, A., (2004). "The development of a simulation model of the dense packing of large particulate assemblies." *Powder Technology* Vol.141 :155-160.

Solaimanian, M., Bonaquist, R. F., Tandon, V. (2007). NCHRP Report 589: Improved Conditioning and Testing Procedures for HMA Moisture Susceptibility, *Transportation Research Board*, National Research Council, Washington, DC

Sousa, J.B. and Weissman, S. L. (1994). "Modeling permanent deformation of asphalt concrete mixtures." *Journal Association of Asphalt Paving Technologists*, 63, 225–257.

Sousa, J. B., and Weissman, S. L. (1995). "Modeling Permanent Deformation of Asphalt Concrete Mixtures." *Journal Association of Asphalt Paving Technologists*, 63, 225-257. 1995.

Sousa, J. B., Weissman, S.L., and Monismith, C. L. (1993). "A nonlinear elastic viscous with damage model to predict permanent deformation of asphalt concrete mixes." *Transportation Research Record*, 1384, 80-93.

Stakston, A.D., Bahia, H. U., (2003). "The Effect of Fine Aggregate Angularity, Asphalt Content and Performance Graded Asphalts on Hot Mix Asphalt Performance." *WisDOT Highway Research Study* 0092-45-98.

Tarefder, R. A., Zaman, M., and Hobson, K., (2003). "A Laboratory and Statistical Evaluation of Factors Affecting Rutting." *International Journal of Pavement Engineering*, 4(1), pp. 59-68.

Tashman, L., Masad, E., Little, D., and Lytton, R. (2004). "Damage evolution in triaxial compression tests of HMA at high temperatures." *J. Assoc. Asphalt Paving Technologists*, 73, 53 - 81.

Tashman, L., Masad, E., Little, D., and Zbib, H. (2005). "A microstructure-based viscoplastic model for asphalt concrete." *International Journal of Plasticity*, 21(2005), 1659-1685.

Tashman, L. and M. A. Elangovan. (2007). Dynamic Modulus Test - Laboratory Investigation and Future Implementation in the State of Washington. Washington State Department of Transportation Final Report. Final Research Report No. WA-RD 704.1.

Tobita, Y. (1989). "Fabric tensors in constitutive equations for granular materials." *Soils and Foundations*, 29(4), 99-104.

Vallerga, B. A., Seed, H. B., Monismith, C. L., and Cooper, R.S., (1957) “Effect of Shape, Size, and Roughness of Aggregate Particles on the Strength of Granular Materials,” *Special Technical Publication*, No.212, ASTM.

Vavrik, W.R. (2000). Doctorate dissertation “Asphalt Mixture Design Concepts to Develop Aggregate Interlock”.*UIUC* P47-50

Vavrik, W. R., Huber, G., Pine, W. J., Carpenter, S. H., and Bailey, R. (2002). "Bailey Method for Gradation Selection in Hot-Mix Asphalt Mixture Design." *Transportation Research E-Circular, Report No: E-C044.*

Vermeer, P.A. and R. de Brost. (1984). “Non-associated Plasticity for Soils, Concrete and Rock.” *Heron*, 29(3), 1-64.

Wang, D. (2007). “Binder Film Thickness Effect on Aggregate Contact Behavior”, Master dissertation of Virginia Polytechnic Institute and State University, Blacksburg, Virginia.

Wang, L. B., Frost, J. D., Voyiadjis, G. Z., and Harman, T. P. (2003). “Quantification of damage parameters using X-Ray tomography images.” *Mechanics of Materials,* 35, 777-790.

Wen, H. and Kim, Y. R. (2002) “Simple performance test for fatigue cracking and validation with WesTrack mixtures.” *Transportation Research Board*, 1789, paper

No. 02-2924.

Willis, J.R., Taylor, A., Tran, N., N., Kvasnak, A., and Copeland, A. (2010) "Correlations Between Flow Number Test Results and Field Performance at the NCAT Pavement Test Track," Paper Submitted to the Transportation Research Board 89th Annual Meeting, 2010, Washington, D.C.

Witczak, M.W. (2007). NCHRP report 580: Specification Criteria for Simple Performance Tests for Rutting. *Transportation Research Board*, National Research Council, Washington, DC.

Witczak, M.W. and Fonseca, O.A. (1996). "Revised Predictive Model for Dynamic (Complex) Modulus of Asphalt Mixtures," Transportation Research Record 1540, 15–23.

Witczak, M.W., Kaloush, K.E. Pellien, T.K. El-Basyouny, M. and Von Quintus H.L. (2002). "NCHRP Report 465: Simple Performance Test for Superpave Mix Design." *Transportation Research Board*, National Research Council, Washington, DC

Yang, Enhui., W. Virgil Ping, Yuan Xiao, Yanjun Qiu, (2011), A Simplified Predictive Model of Dynamic Modulus for Characterizing Florida Hot Mix Asphalt Mixtures, 2011 Transportation Research Board CD-ROM, TRB Paper No. 11-1565.

You, Z., and Buttlar, W. G. (2002). "Stiffness prediction of hot mixture asphalt (HMA) based upon microfabric discrete element modeling (MDEM)." Proc., *4th Int. Conf. on road and airfield pavement technology*, Vol. 1, People's Communications, China, 409–417.

You, Z. and Buttlar, W. G. (2004) "Discrete Element Modeling to predict the modulus of asphalt concrete mixtures." *Journal of material in civil engineering*, Apr.2004, P140-146.

Yu, H., and Shen, S. (2012) "Impact of Aggregate Packing on Dynamic Modulus of Hot Mix Asphalt Mixtures Using Three-Dimensional Discrete Element Method." *Journal of Construction and Building Materials*. Vol. 26, issue 1, pp. 302-309.

Zeghal, M. (2004) "Discrete-Element Method Investigation of the Resilient Behavior of Granular Materials". *Journal of Transportation Engineering*. 08,pp. 503-509.

Zelelew, H.M. (2008). "Simulation of the permanent deformation of asphalt concrete mixtures using discrete element method (DEM)." Doctoral Dissertation, Washington State University, Pullman, WA.

APPENDIX A: LIST OF ABBREVIATIONS

AC: Hot Mix Asphalt
VMA: Voids in Mineral Aggregates
VFA: Voids Filled with Asphalt
CMD: Continuous Maximum Density
DEM: Discrete Element Modeling
MDL: Maximum Density Line
FM: Fineness Modulus
CAPC: Coarse Aggregate Percent Crushed
FAPC: Fine Aggregate Percent Crushed
NMPS: Nominal Maximum Particle Size
PCS: Primary Control Sieve
SCS: Secondary Control Sieve
TCS: Tertiary Control Sieve
CUW: Chosen Unit Weight
LUW: Loose Unit Weight
RUW: Rodded Unit Weight
CUW: Chosen Unit Weight
RAP: Reclaimed Asphalt Pavement

APPENDIX B: EFFECTS OF SIEVE SIZE ON DYNAMIC MODULUS

Effect of percent of aggregates passing individual sieve size on dynamic modulus at different temperatures.

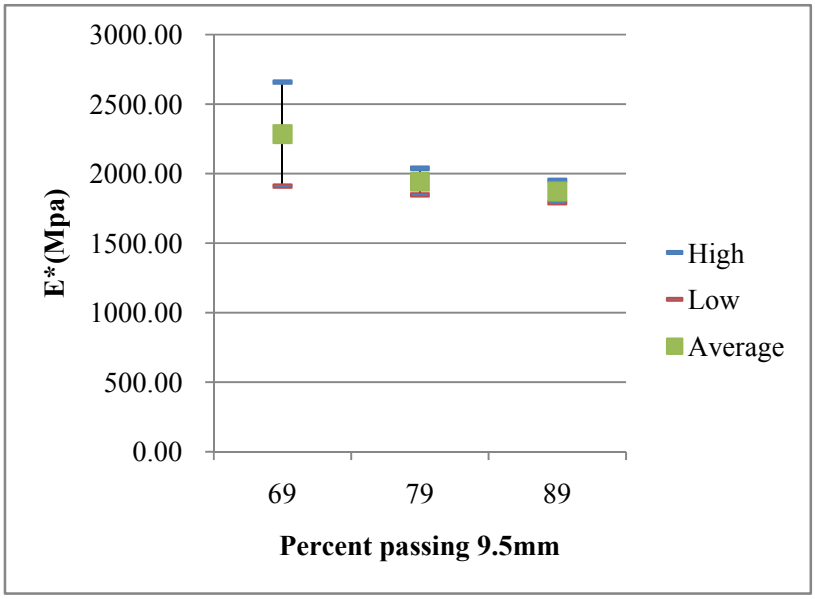

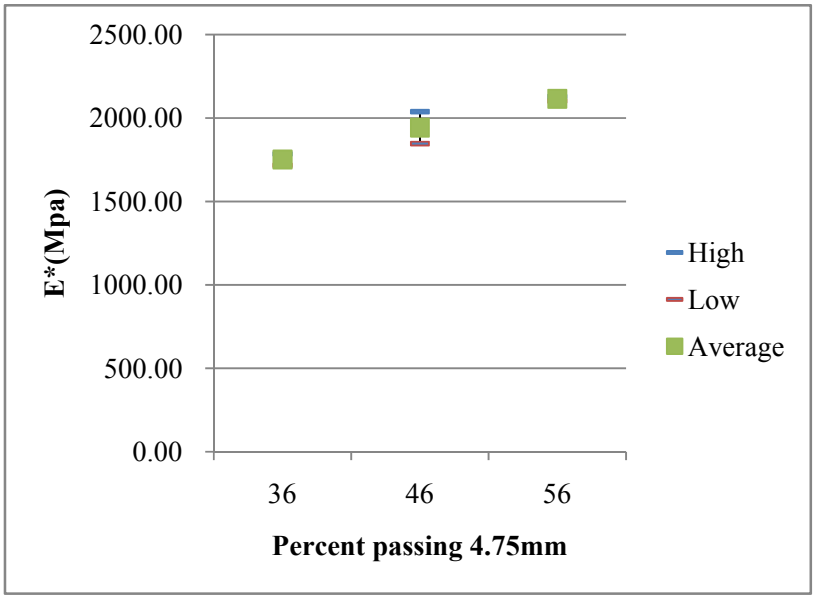

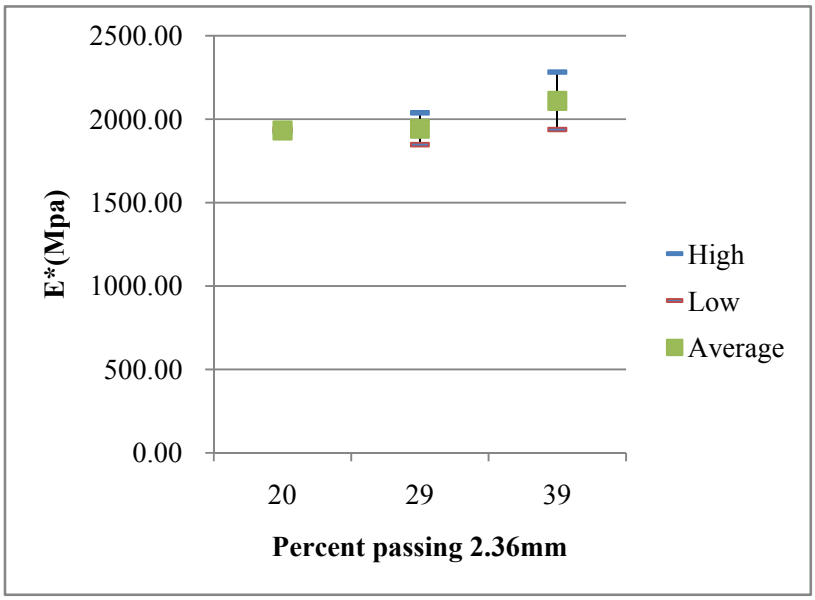

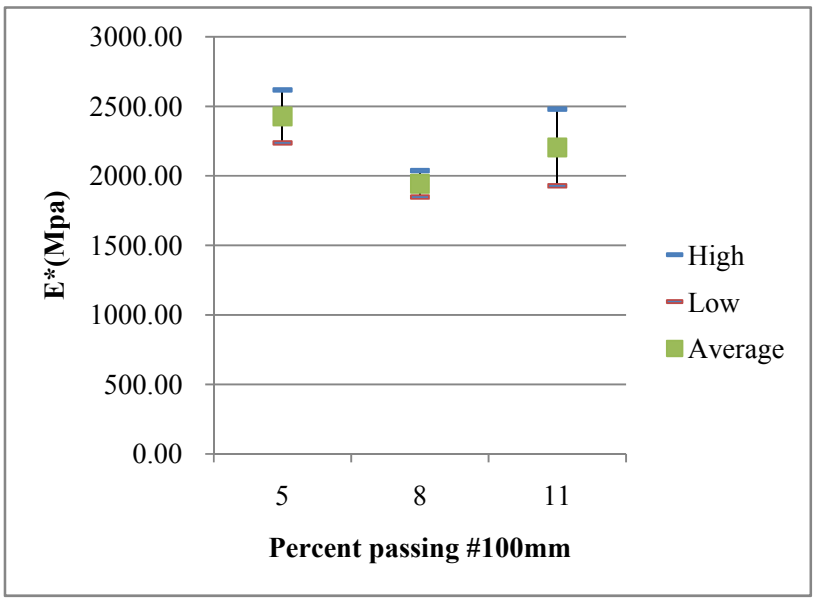

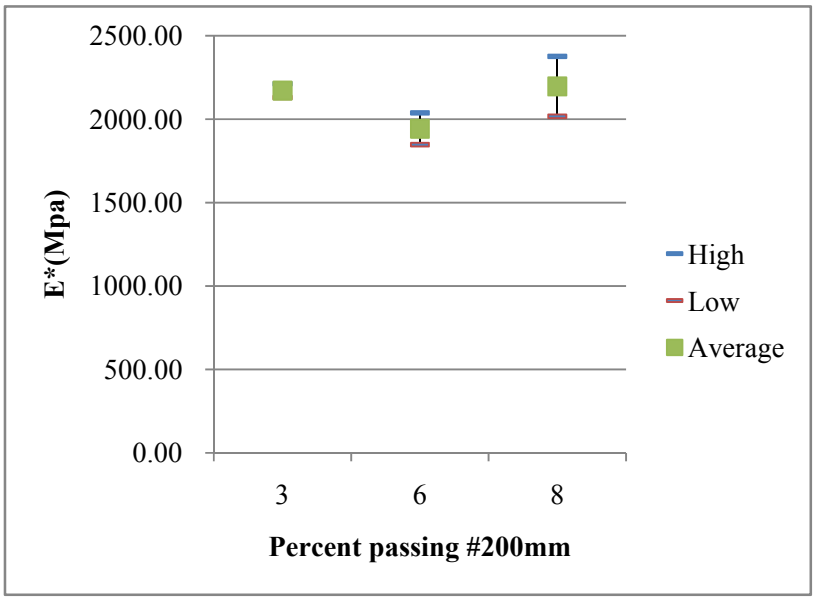

Figure 1. E* changes with the change of each sieve size (21.1°C)

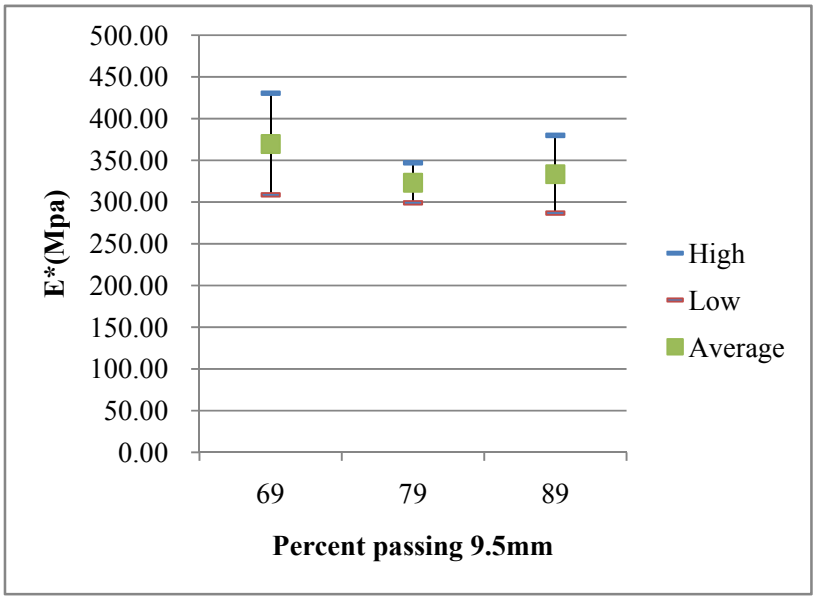

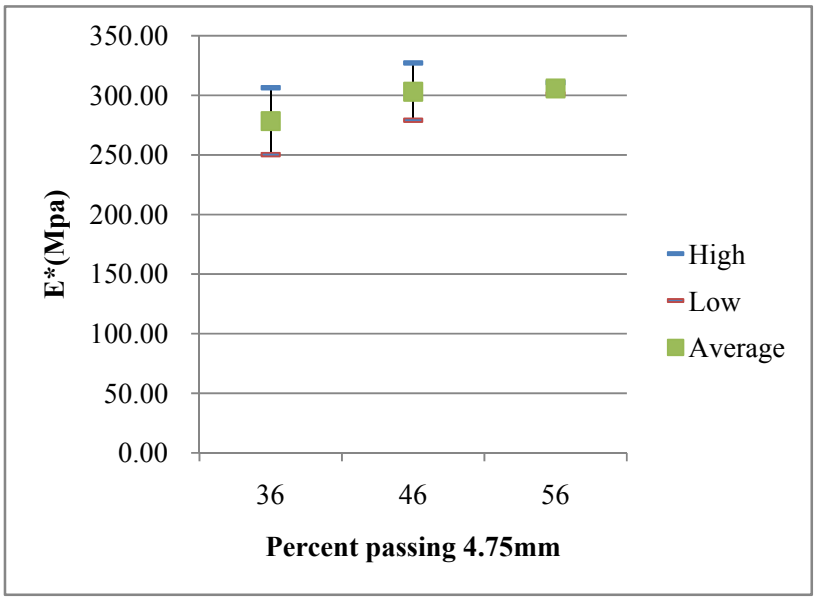

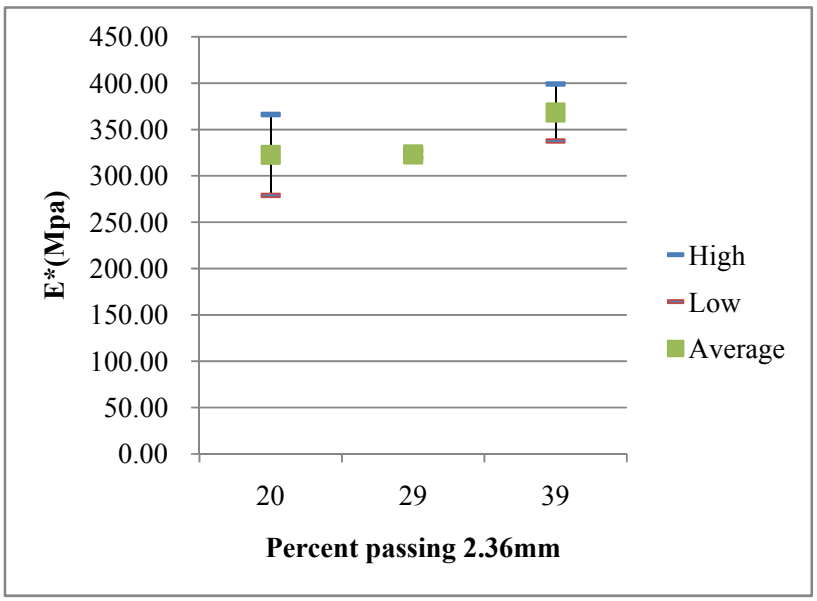

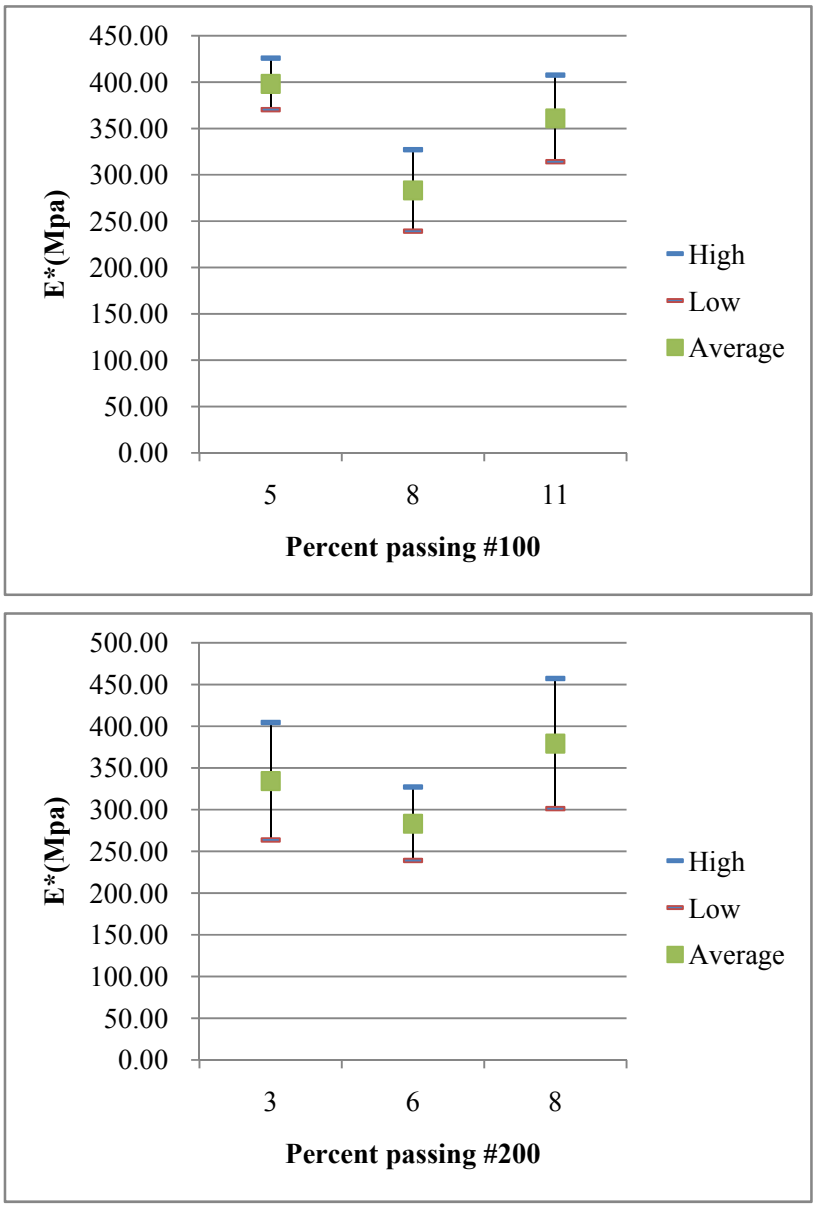

Figure 2. E* changes with the change of each sieve size (37.8°C)

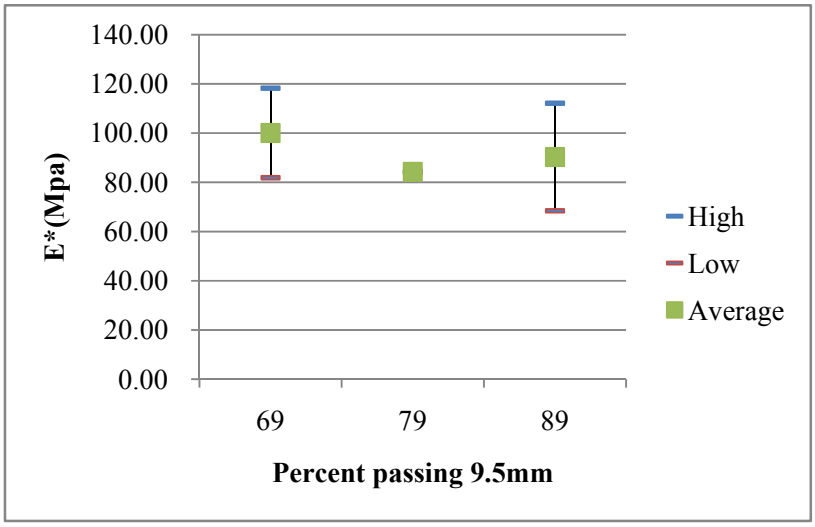

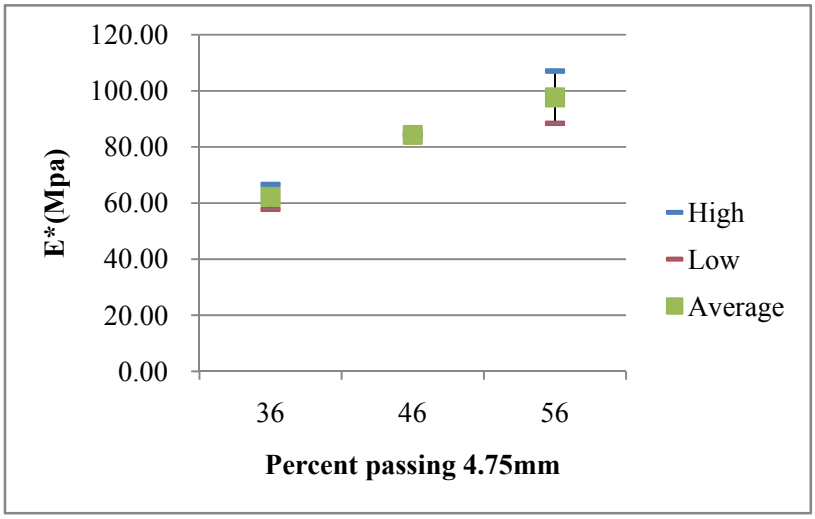

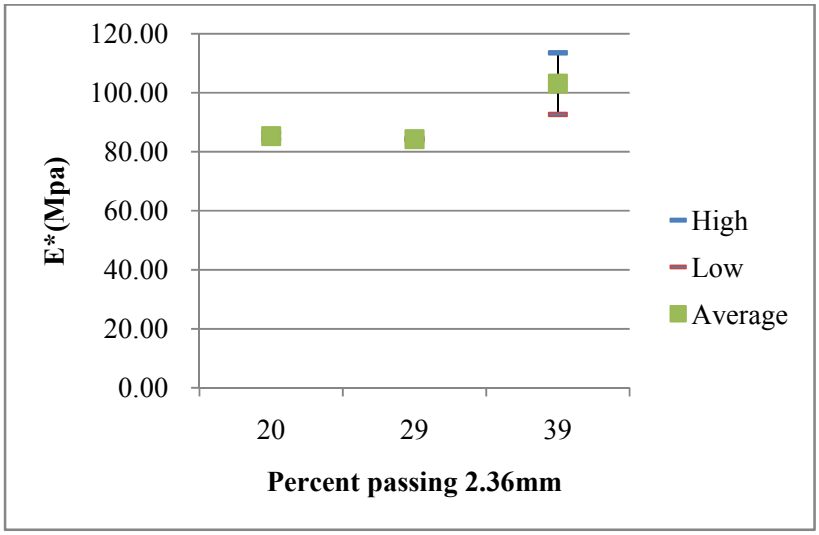

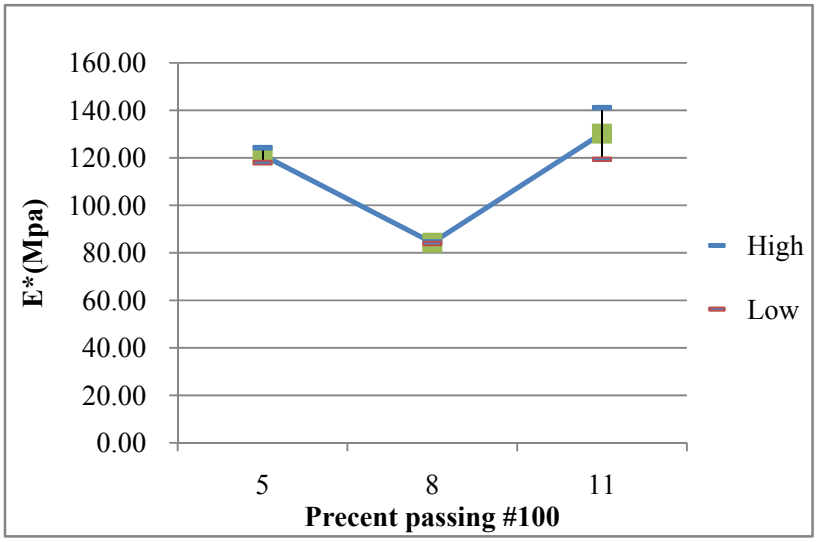

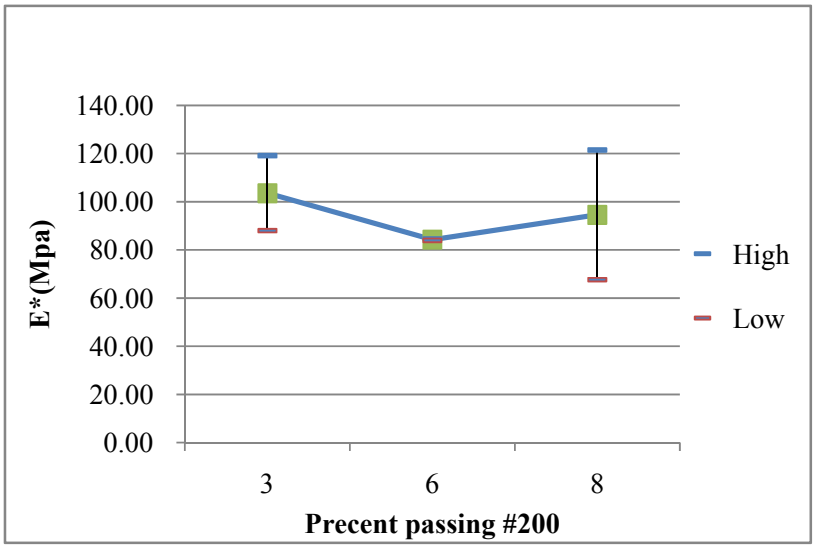

Figure 3. E* changes with the change of each sieve size (54.4°C)

APPENDIX C: DESIGN EXAMPLE

By using the volumetric properties of the asphalt mixture such as the VMA to link the mix's composition (aggregate and asphalt binder) to the engineering performance, this design approach provides a step-by-step procedure to guide gradation design and help the selection of asphalt binder content at the early stage of the mix design. A dense-graded asphalt mixture is used in this section as an example to describe the procedure details which consists of six steps. An aggregate sample of three stockpiles (X, Y, and Z) and nominal maximum size of 12.5 mm and a binder of PG 64-28 are pre-selected according to the project description.

C.1 STEP 1: SELECTION OF A TRIAL GRADATION

An initial trial aggregate gradation is first selected based on past experience. It should in general satisfy the existing Superpave control points criteria and have a continuous gradation curve as normally seen for a dense graded mixture. Table C-1 shows the calculation of the first trial blending with 30%, 50%, and 20% proportions for stockpile X, Y, and Z. The gradation curve of the first trial blending is plotted in Figure C-1, denoted as gradation before adjustment.

C.2 STEP 2: SELECTION/IDENTIFICATION OF A DESIGN GRADATION TYPE

The second step is to determine the gradation type for the selected trial blend. Following Equations (1)-(2), the deviation value $P_d(d)$ for each sieve size is calculated and shown in Table C-2.

$$P_d(d)=P(d)- P_{Dens.} \quad (1)$$

$$P_{Dens.} = \left(\frac{d}{D_{\max}}\right)^{0.45} \times 100\% \quad (2)$$

Where

$P_d(d)$: the percent of aggregates (size d) deviating from the maximum density line.

$P(d)$: Percent of aggregates passing sieve size d for a specific gradation (%);

$P_{Dens.}$: Percent of aggregates passing the maximum density line (%), which can be calculated from Equation (2);

d: sieve size (mm);

D_{max}: maximum sieve size for that gradation (mm).

For the gradation with NMPS of 12.5mm, the selected four critical sieve sizes are 9.5mm, 4.75mm, 2.36mm, and 1.18mm. By summing the $P_d(d)$ values for these four sieves, a critical deviation value (P_{dc}) of -17 is obtained. According to Table 8-1, this gradation is categorized as a coarse-graded gradation.

Table C-1. Stockpile gradations and trial blending

	Stockpile X		Stockpile Y		Stockpile Z		Combined gradation
Sieve Size(mm)	% Passing	Proportion 30%	% Passing	Proportion 50%	% Passing	Proportion 20%	% Passing
19	100	30	100	50	100	20	100
12.5	99	29.7	100	50	98	19.6	96
9.5	60	18	98	49	90	18	85
4.75	2.8	0.8	62	31	66	13.2	45
2.36	1.8	0.5	38	19	48	9.6	29
1.18	1.6	0.5	24	12	33	6.6	19
0.6	1.5	0.5	17	8.5	23	4.6	14
0.3	1.4	0.4	12	6	16	3.2	10
0.15	1.3	0.4	9	4.5	12	2.4	7
0.075	1.1	0.3	6.9	3.5	9.8	2	5.8

Table C-2. The percent passing of maximum density line

Sieve size	19	12.5	9.5	4.75	2.36	1.18	0.6	0.3	0.15	0.075
P(d)	100	96	***85***	***45***	***29***	***19***	14	10	7	5.9
$P_{Dens.}$	100	83	***73***	***54***	***39***	***29***	21	16	11	8.3

$P_d(d)$	0	13	***12***	***-9***	***-10***	***-10***	-7	-6	-4	-2.4
P_{dc}			***-17***							

C.3 Step 3: Gradation Adjustment Based on Estimated VMA

Table C-3. f_v values for coarse-graded gradations with NMPS=12.5mm

Sieve size	f_v
19	0.411
12.5	0.411
9.5	0.411
4.75	0.410
2.36	0.169
1.18	-0.366
0.6	-0.366
0.3	-0.366
0.15	-0.536
0.075	-0.952

Once the gradation type is determined, Equation 18 can be used for estimating the VMA for the trial gradation. Table C-3 should be used for the f_v values of coarse-graded gradations. Table C-4 presents an example of engineering work sheet for the VMA calculation. As shown, the estimated VMA for the trial gradation is 16.9%.

$$p = \frac{\sum_{i=1}^{n} f_{vi} V_{ai}}{1 + \sum_{i=1}^{n} f_{vi} V_{ai}} \quad (3)$$

Where,

$f_{vi}$is the $f_v$value for ith sieve size of the gradation. For coarse-graded gradations with NMPS of 12.5mm, the suggested f_v values are given in Table C-3.

V_{ai} is the percent of aggregates by volume retained in the ith sieve size, which is corresponding to the percent of aggregates by weight retained on each sieve size.

p is the porosity or VMA of the aggregate structure.

It is very possible this trial design will not give a VMA as desired. As for this example, the calculated VMA (16.9%) is greater than the target VMA (14-16%), and the gradation proportions have to be adjusted to first satisfy the volumetric requirement.

Finer aggregates tend to fill the voids while coarser aggregates tend to create voids. If the desired VMA is lower than the predicted VMA, increase the proportion of stockpile with more fine aggregates and decrease the proportion of stockpile with more coarse aggregates should be the direction of adjustment. In this case, because the initial VMA for trial gradation is 0.8% higher than the target VMA, by increasing stockpile Y at the same time decreasing stockpile X in the excel spreadsheet, the gradation may be adjusted. The final results are shown in Table C-5and Table C-6. All these changes can be simultaneously visualized in the excel spreadsheet to ensure all gradations are

conforming to the Superpave control points requirement (Figure C-1).

Table C-4. VMA prediction process for initial trial blend

Sieve size(mm)	Passing(%)	Cumulative Retained(%)	Retained(%)	f_v	
A	***B***	***C***	***D***	***E***	***D*E***
19	100	0			
12.5	96	4	4	0.411	1.64
9.5	85	11	11	0.411	4.52
4.75	45	55	40	0.411	16.44
2.36	29	71	16	0.410	6.56
1.18	19	81	10	0.169	1.69
0.6	14	86	6	-0.366	-1.83
0.3	10	90	4	-0.366	-1.46
0.15	7	93	2	-0.366	-1.10
0.075	5.9	94.1	1.6	-0.536	-0.59
Pan		100.0	5.7	-0.952	-5.62
				Sum of *E*	20.3

VMA=Sum/(100+Sum)	16.9

It is noted that errors may still exist when compared with the measured VMA due to many factors such as the angularity and shape of the aggregates and the experimental errors. This study found the prediction accuracy is approximately within ±1% when compared to the measured VMA.

Table C-5. Final combined gradation

	Stockpile X		Stockpile Y		Stockpile Z		Combined gradation
Sieve Size(mm)	% Passing	Proportion 20%	% Passing	Proportion 60%	% Passing	Proportion 20%	% Passing
19	100	30	100	50	100	20	100
12.5	96	29.7	96	50	98	19.6	96
9.5	67	18	94	49	90	18	81
4.75	73	0.8	20	31	66	13.2	53
2.36	32	0.5	20	19	48	9.6	31
1.18	19	0.5	13	12	33	6.6	20
0.6	13	0.5	10	8.5	23	4.6	14
0.3	14	0.4	5	6	16	3.2	11

0.15	9	0.4	4	4.5	12	2.4	8
0.075	6.6	0.3	3.9	3.5	9.8	2	6.3

Table C-6. VMA prediction for final gradation

Sieve size(mm)	Passing(%)	Cumulative Retained(%)	Retained(%)	f_v	
A	***B***	***C***	***D***	***E***	***D*E***
19	100	0			
12.5	96	4	4	0.411	1.64
9.5	81	19	15	0.411	6.17
4.75	53	47	28	0.411	11.51
2.36	31	69	22	0.410	9.02
1.18	20	80	11	0.169	1.86
0.6	14	86	6	-0.366	-2.20
0.3	11	89	3	-0.366	-1.10
0.15	8	92	3	-0.366	-1.10

0.075	6.3	93.7	1.7	-0.536	-0.91
Pan		100.0	6.3	-0.952	-6.00
				Sum of *E*	18.9
				Sum/(100+Sum)	15.9

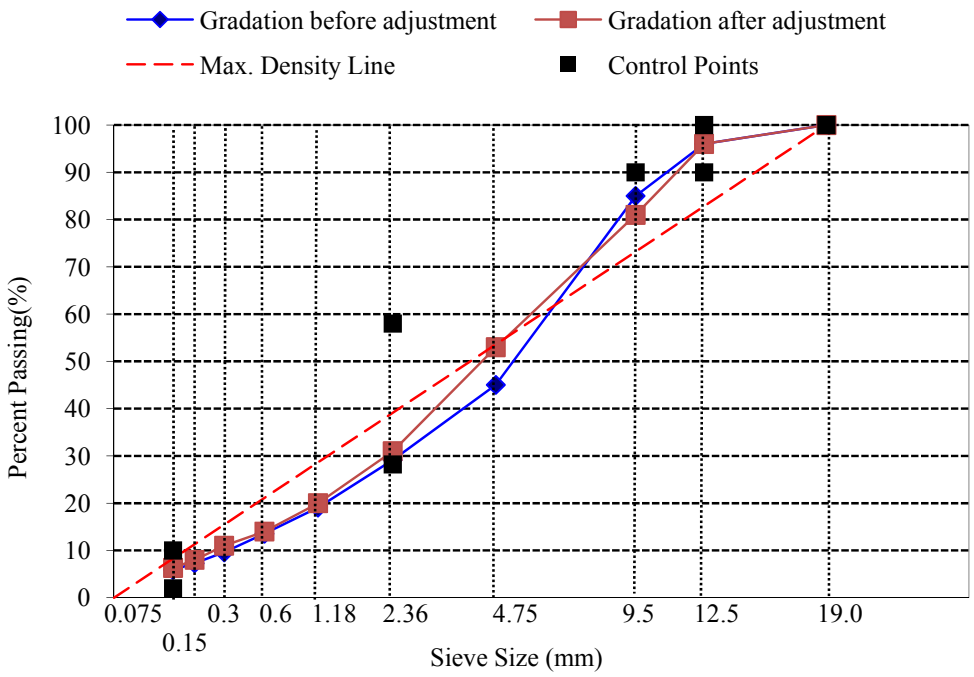

Figure C-1. Gradation plots for design examples (before and after adjustment)

C.4 STEP 4: SELECTION OF ASPHALT BINDER CONTENT

Based on the design air voids of 4% as specified in the Superpave specifications and the estimated VMA, the VFA can be calculated using Equation (4).

$$VFA=100*(1-Va/VMA) \quad (4)$$

Consequently, the effective asphalt content is calculated using Equation (5),

$$P_{be}=(VMA-V_a)* G_b/G_{sb} \quad (5)$$

For given types of aggregate and asphalt binder, the absorption rate of asphalt binder should be relatively consistent. Therefore, the design asphalt content required to produce a mix with known VMA and AV can be estimated, as shown in Equation (6).

$$P_b = P_{be} + \frac{P_{ba}}{100} \times P_s \quad (6)$$

Where,

P_{ba} is the asphalt absorption rate by weight of total aggregates, and

Ps is the amount of aggregates by weight.

Still using the same example shown above, along with other known information (predicted VMA of 15.9%, design air voids of 4%, specific gravity of asphalt (G_b) of 1.02, and the bulk specific gravity of aggregate (G_{sb}) of 2.680), the estimated effective asphalt binder content can be calculated as:

$$P_{be}= (15.9-4) * 1.02 / 2.680=4.53\% \quad (7)$$

Using the asphalt absorption rate of 1% as determined from previous experiments, the design asphalt content is determined as:

$$P_b= 4.53 + (100-4.53) *1.0\%=5.48\% \quad (8)$$

C.5 STEP 5: DYNAMIC MODULUS PREDICTION

Till step 4, a mix design that satisfies the existing Superpave volumetric requirements has been identified. However, it is still not clear the mechanical properties of the mix and the mix may still lead to unsatisfactory engineering performance. In the new mix design method, the dynamic modulus is used as a key mechanical property for the evaluation of the future performance of the mix. The modified Hirsch model, as recommended in this study, is presented in Equation (9) for estimating the dynamic modulus at design stage.

$$\left|E^*\right| = Pc\left[4.8E6\left(1-\frac{VMA}{100}\right)+3\left|G_b^*\right|\left(\frac{VFA\cdot VMA}{10,000}\right)\right] + (1-Pc)\left[\frac{1-\frac{VMA}{100}}{4.8E6}+\frac{VMA}{3VFA\cdot\left|G_b^*\right|}\right]^{-1} \quad (9)$$

Where,

|E*| = dynamic modulus, psi

|G*|binder = binder dynamic modulus, psi

VMA= voids in the mineral aggregate, %

VFA = voids filled with asphalt, %

Pc = aggregate contact factor.

$$Pc = \frac{\left(0.2 + \frac{3VFA \cdot |G_b^*|}{VMA}\right)^{0.56}}{600 + \left(\frac{3VFA \cdot |G_b^*|}{VMA}\right)^{0.56}} \quad (10)$$

It should be noted that the VMA value used in the equation should be the actual VMA corresponding to the E* specimens. In case the dynamic modulus (E*) is tested at 7% air voids, the estimated VMA which is corresponding to the design air voids of 4% should be corrected. Based on an evaluation of 11 different mixtures from Washington State, it is found that the VMA difference for the mix with the same mix design but compacted to different air voids (4% and 7%) is approximately 2.5%. Therefore, this paper recommends adding 2.5% to the originally estimated VMA (corresponding to 4% air voids) to obtain the VMA for E* specimens (7% air voids). For the design example, a VMA value of 17.5% (15%+2.5%) should be used in the prediction equation.

Besides the volumetric properties (VMA and VFA) that can be estimated, the only information required is the binder's dynamic shear modulus (G*) which can be measured using the dynamic shear rheometer (DSR). A G* master curve for rotational thin film oven (RTFO) aged binder can be developed so that the G* information corresponding to the temperature and loading frequency of the mixture's dynamic modulus can be extracted. Equation 22 and 23 are thus used for determining the dynamic modulus of the

mixture.

This predicted dynamic modulus (E*) can be integrated into the DARWin ME (MEPDG) design program to determine the expected field performance; or it can be used by the state agencies as mixture screening criteria for the field performance, as suggested in the Michigan practice (Goh et al. 2011). If the designed mixture cannot produce satisfactory predicted E*, steps 2-5 should be repeated until a mixture which satisfies both the volumetric requirement and the dynamic modulus requirement could be identified. Because all these steps are conducted in the computer, an excel spreadsheet can be used to find a solution in a timely manner.

C.6 Step 6: Mix Design Verification

Once the target design including both gradation and the design asphalt content has been identified, two gyratory specimens will be compacted to verify the design. The volumetrics of the specimens will be determined to be compared with the Superpave specifications. Slight adjustment for asphalt content may be needed to obtain a mix with 4% air voids. In addition, it is suggested two more gyratory specimens being compacted to measure the dynamic modulus and to be compared with the predicted dynamic modulus values. If necessary, the parameters of the modified Hirsch model should be calibrated for local mixtures.

For the example showed above, using the design gradation shown in Table C-6 and the estimated design asphalt content of 5.48%, two gyratory samples (T-1 and T-2) were compacted to design number of gyrations. Their measured volumetric properties were compared with the predicted values and summarized in Table C-7. As shown, the prediction and the experimental results are very close.

Two more gyratory samples were prepared to a target air void of 7% to conduct dynamic modulus test following the AASHTO TP79 specification. The results were compared with the predictions, shown in Figure C-2. The results followed the line of equality well, indicating a good prediction. The obtained dynamic modulus value can be either used in the MEPDG for pavement design, or be used by the local agencies for the material screening.

Until now, the mix design has completed because both the volumetric properties and the dynamic modulus have been verified to be satisfactory. If large discrepancies are found between the experiments and the prediction, steps 2-6 need to be repeated and the models may need to be recalibrated.

Table C-7. VMA prediction for two samples

	Air voids(%)		VMA(%)		VFA(%)	
Sample	Target	Measured	Predicted	Measured	Predicted	Measured
T-1	4.0	4.3	15.9	15.3	74.8	71.9
T-2	4.0	4.5	15.9	15.7	70.7	71.3

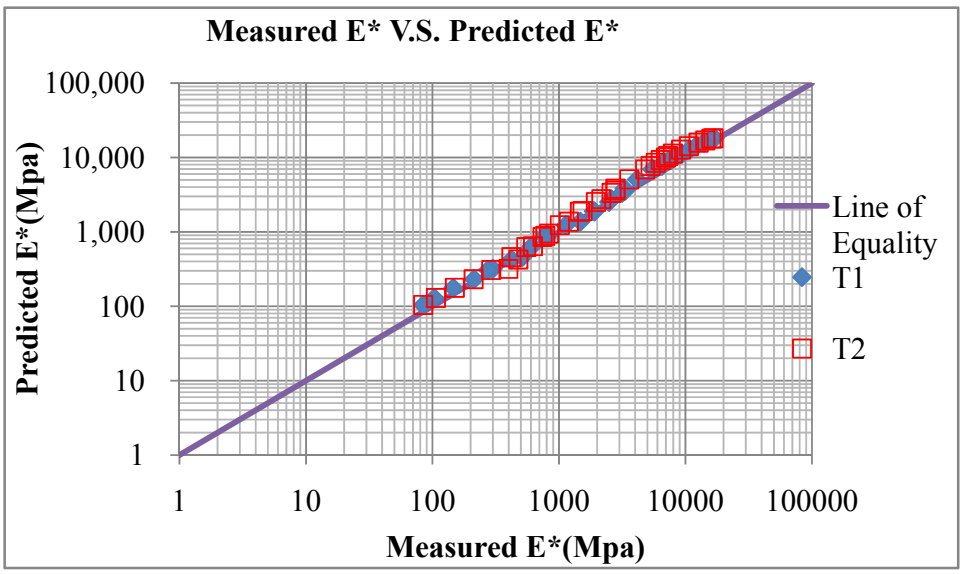

Figure C-2. Predicted dynamic modulus and measured dynamic modulus.

APPENDIX D: G* information for all binders

Three sections of information are included in Appendix D: (1) G* of Asphalt binders; (2) Summary of dust proportions of each mix design; and (3) G* of mastics.

D.1 G* OF ASPHALT BINDERS

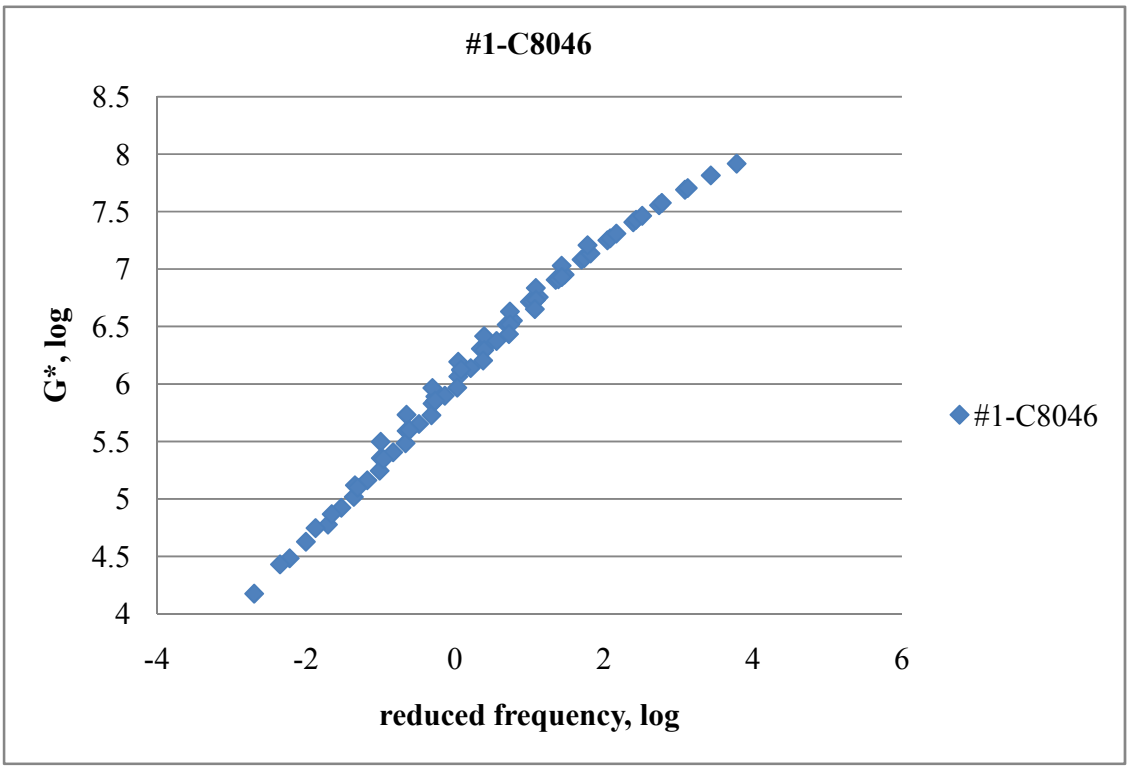

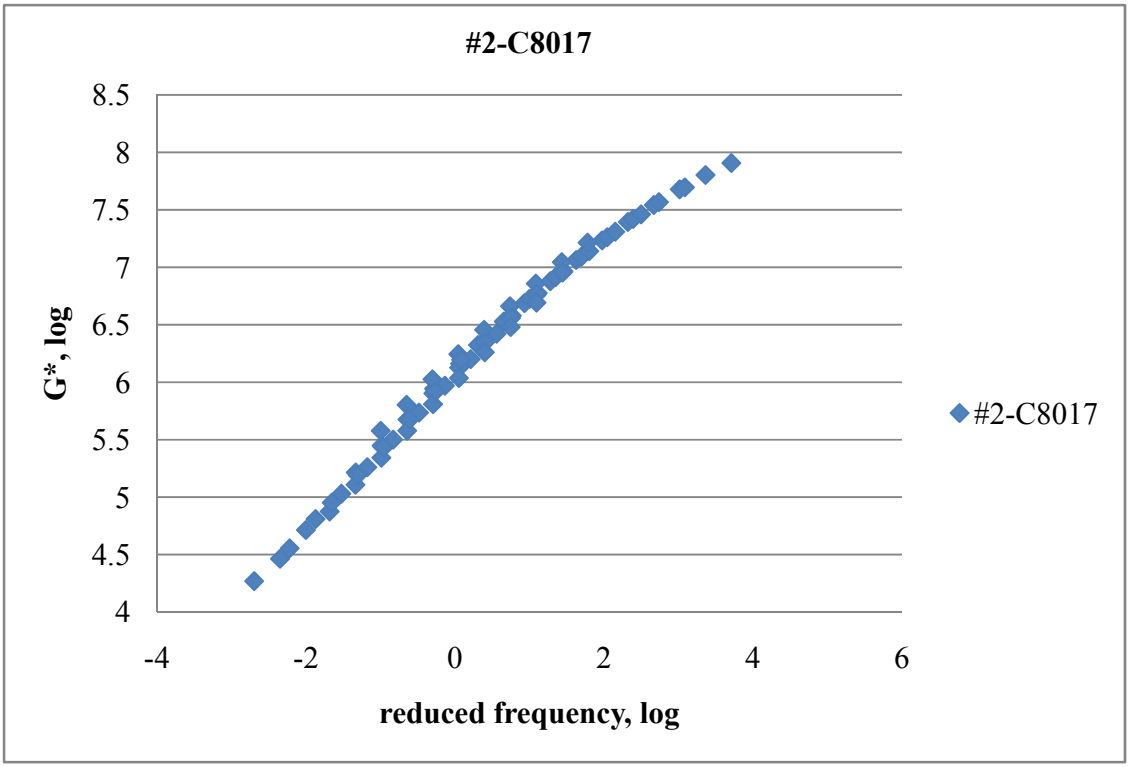

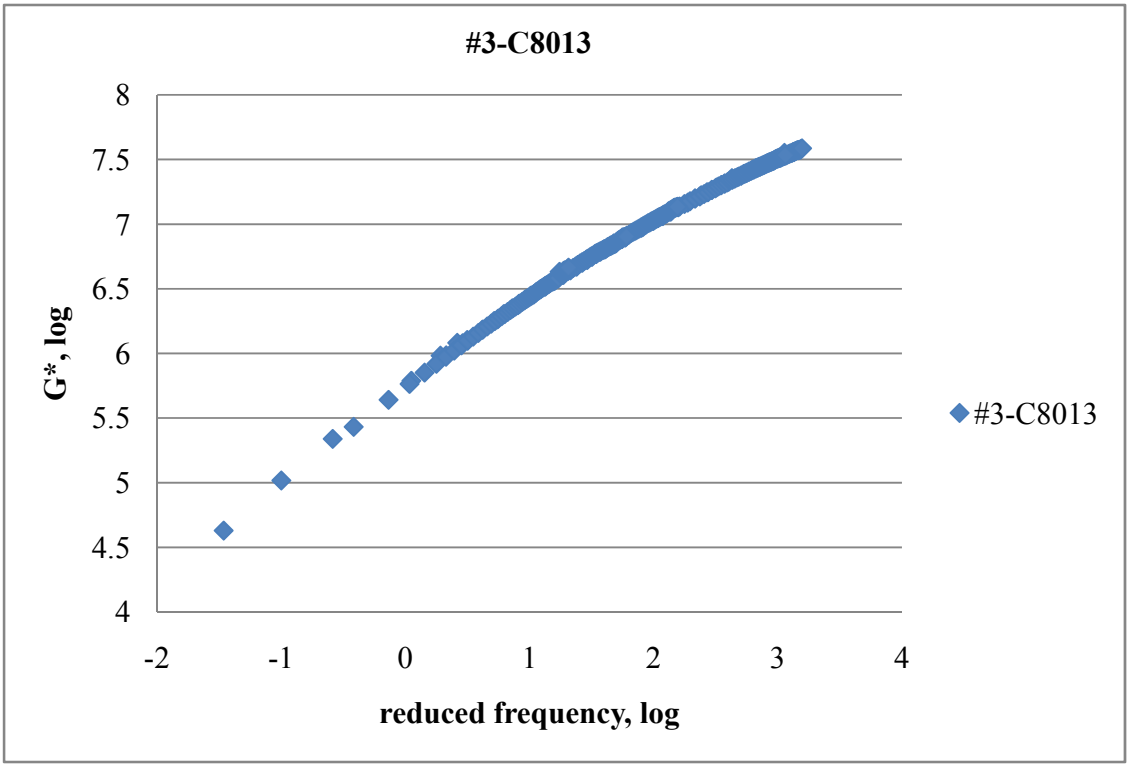

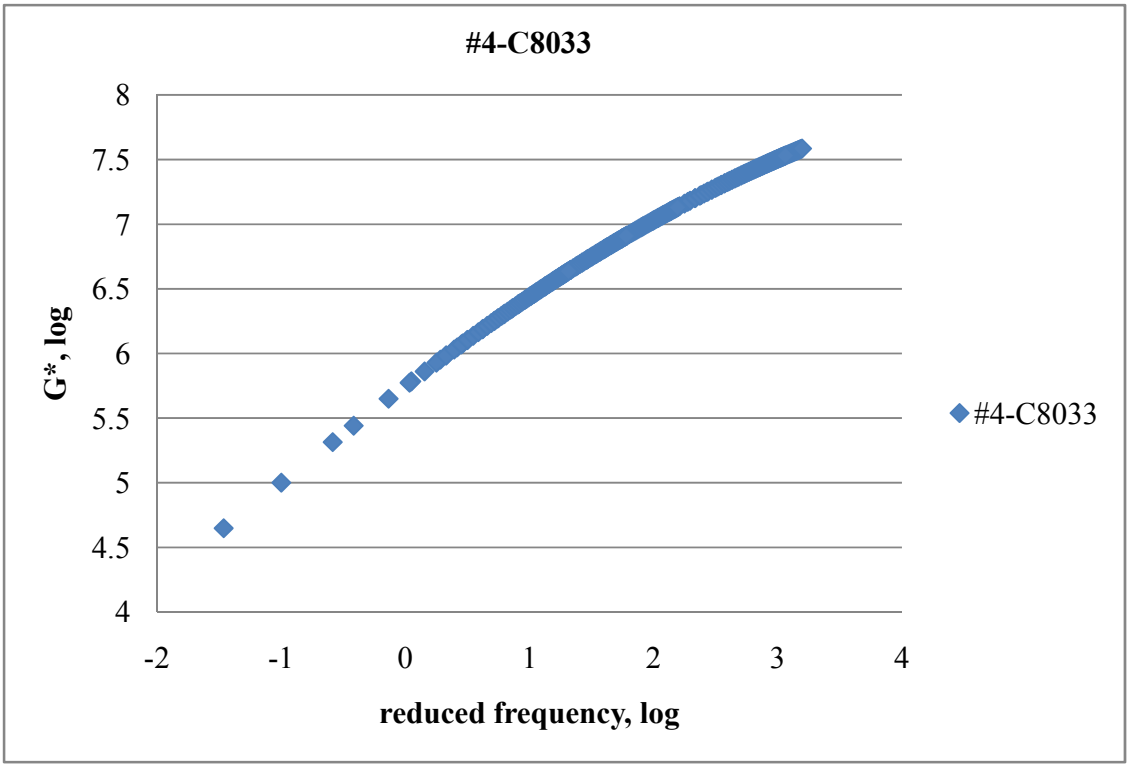

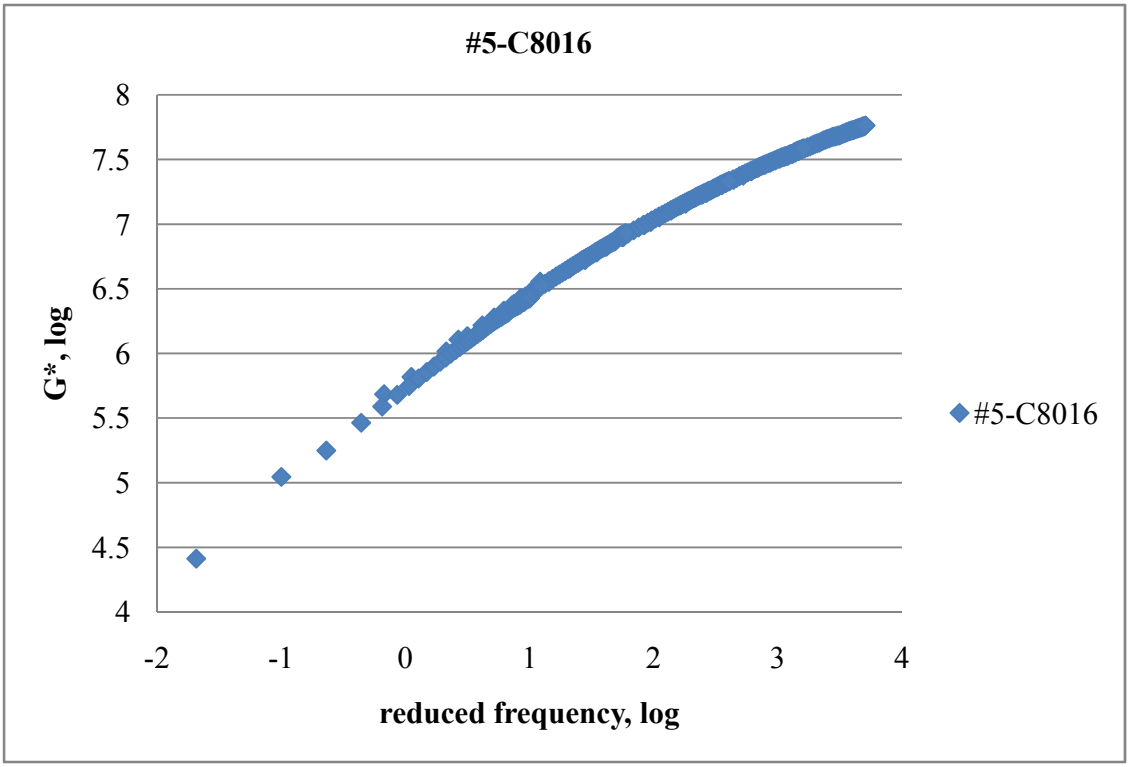

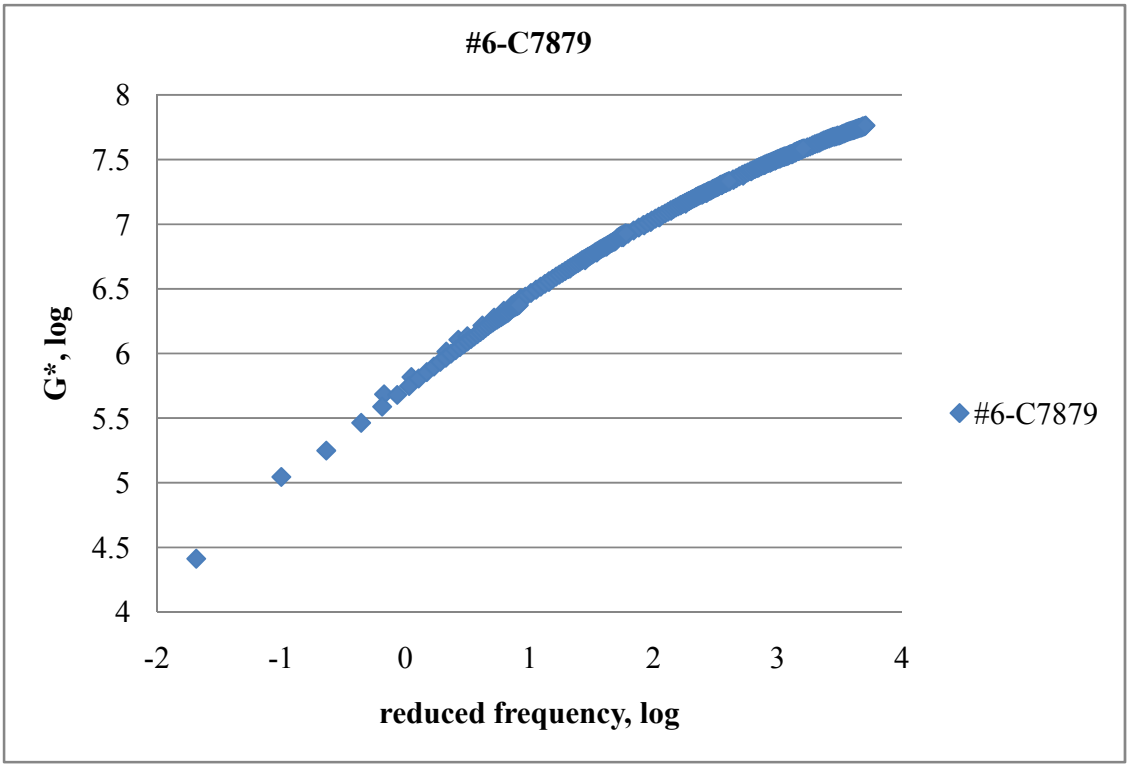

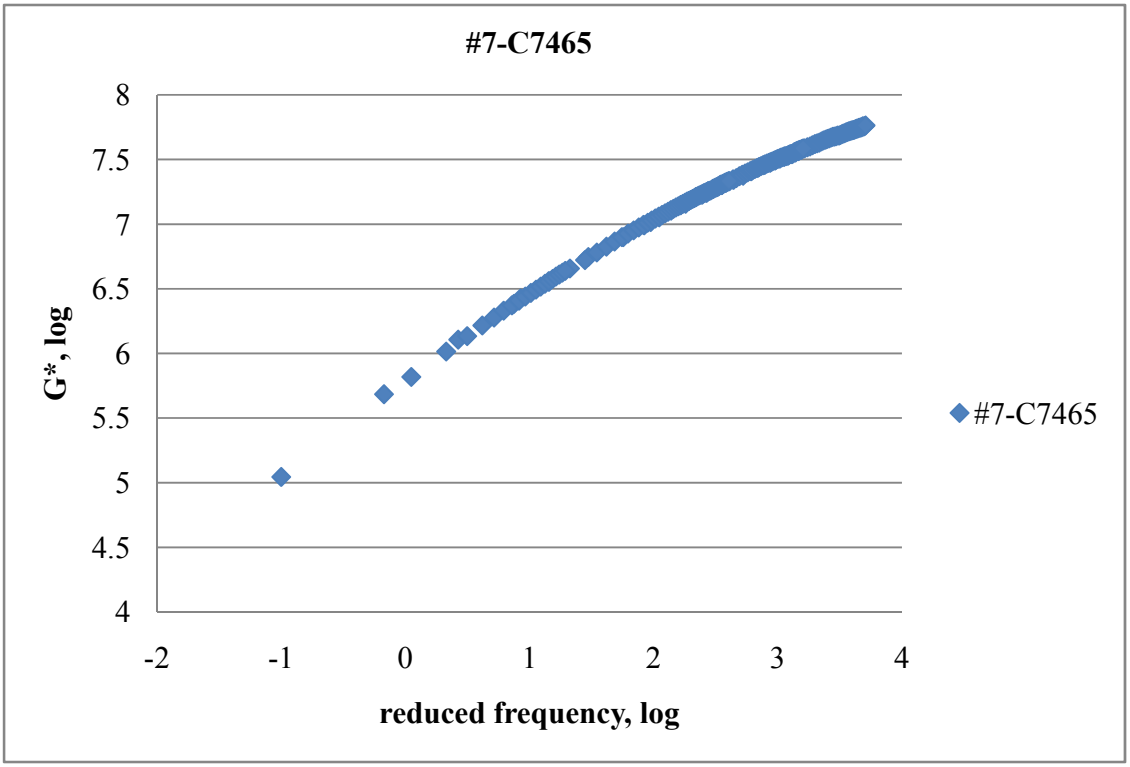

D.2 DUST PROPORTION

Project No.	Contract No.	Asphalt Content (%)	Pbe(%)	Dust(%)	A/D
#1	C8046	5.4	5.1	6.3	0.81
#2	C8017	5.7	4.6	6.3	0.73
#3	C8013	5.2	4.1	5.7	0.72
#4	C8033	5.2	4.6	5.5	0.84
#5	C8016	5.3	4.6	5.1	0.90
#6	C7879	5.4	4.7	6	0.78
#7	C7465	5.6	4.9	4.9	1.00

D.3 G* OF MASTICS